

TESIS DOCTORAL

Impacto de la variabilidad ambiental en zonas acuáticas someras: Efecto sobre el metabolismo neto y flujos sedimento-agua en la zona intermareal.

Impact of environmental variability in shallow marine areas: effect on net metabolism and sediment-water fluxes in the intertidal zone.

Valle Pérez Rodríguez

Universidad de Cádiz

Facultad de Ciencias del Mar y Ambientales

Departamento de Biología. Área de Ecología

Laboratorio de Ecología Microbiana y Biogeoquímica

2025

Impacto de la variabilidad ambiental en zonas acuáticas someras: Efecto sobre el metabolismo neto y flujos sedimento-agua en la zona intermareal.

Memoria presentada por Valle Pérez Rodríguez para optar al Grado de Doctor en Ciencias y Tecnologías Marinas por la Universidad de Cádiz con mención de Doctorado Internacional

PEREZ RODRIGUEZ VALLE - 71173110R

Firmado digitalmente por PEREZ RODRIGUEZ VALLE - 71173110R
Fecha: 2025.05.07 21:16:06 +02'00'

Fdo. Valle Pérez Rodríguez

Los directores Dr. D. Alfonso Corzo Rodríguez, Catedrático del Área de Ecología de la Universidad de Cádiz y **Dr. D. Emilio Guillermo García Robledo,** Contratado Doctor del Área de Ecología de la Universidad de Cádiz

CERTIFICAN:

Que la presente memoria titulada **"Impacto de la variabilidad ambiental en zonas acuáticas someras: Efecto sobre el metabolismo neto y flujos sedimento-agua en la zona intermareal."** Presentada por Valle Pérez Rodríguez, ha sido realizada bajo su dirección y autorizan su presentación y defensa, para optar al Grado de Doctor por la Universidad de Cádiz.

Y para que así conste y surta los efectos oportunos, firman los presentes en Puerto Real (Cádiz) a 7 de mayo de dos mil veinticinco.

CORZO RODRIGUEZ ALFONSO - 24888026W

Firmado digitalmente por CORZO RODRIGUEZ ALFONSO - 24888026W
DN: C=ES, SERIALNUMBER=IDCES-24888026W, G=ALFONSO, SN=CORZO RODRIGUEZ, CN=CORZO RODRIGUEZ ALFONSO - 24888026W
Razón: Soy el autor de este documento
Ubicación: la ubicación de su firma aquí
Fecha: 2025-05-07 17:11:30
Foxit Reader Versión: 9.7.0

Dr. D. Alfonso Corzo Rodríguez

GARCIA ROBLEDO EMILIO GUILLERMO - 70813439G

Firmado digitalmente por GARCIA ROBLEDO EMILIO GUILLERMO - 70813439G
Fecha: 2025.05.07 19:01:26 +02'00'

Dr. D. Emilio Guillermo García Robledo

Para la realización de esta Tesis Doctoral, Valle Pérez Rodríguez ha disfrutado de una beca de postgrado del Programa de Formación de Personal Investigador (FPI) del Plan Propio de Investigación 2018 de la Universidad de Cádiz (2018-009 / PU / EPIF-FPI-CT / CP) adscrita al proyecto del Plan Nacional de I+D+i "Ecología microbiana y biogeoquímica de los sedimentos intermareales: las mareas, el fotoperiodo y los eventos climáticos externos.". (MICROBAHIA2, CTM2017-82274-R). Su actividad investigadora se ha realizado como miembro del grupo de investigación RNM944-Ecología Microbiana y Biogeoquímica en el laboratorio de Ecología Microbiana y Biogeoquímica bajo la supervisión del Pr. Dr. Alfonso Corzo y del Dr. Emilio Guillermo García Robledo. Parte de la investigación de esta tesis se ha llevado a cabo durante una estancia de investigación de 3 meses financiada mediante una ayuda del Plan Propio UCA 2022-2023 de apoyo y estímulo a la investigación y transferencia. La estancia se realizó en el *NIOZ, the Royal Netherlands Institute for Sea Research, Department of Estuarine & Delta Systems* bajo la supervisión de Karline Soetaert. Previamente, Valle Pérez Rodríguez asistió a un curso de reconocido prestigio internacional como apoyo a su formación y a los diferentes trabajos realizados durante su tesis cuyo título era *"Aquatic Microbial and Molecular Ecology"* y se impartió por los profesores Dr. Erik Kristensen, Ronnie N. Glud y Alexander H. Treusch en la University of South Denmark.

Por otro lado, como formación complementaria ha participado en varios congresos internacionales y nacionales:

- V Simposio Científico de Alumnos de Ciencias del Mar y Ambientales (10 y 17 de mayo de 2019, Cádiz). Comunicación oral: "Impacto de las olas de calor en sistemas acuáticos someros: alteración del metabolismo neto y de flujos de gases de efecto invernadero en Río San Pedro (Bahía de Cádiz)."
- II Congreso Internacional de Jóvenes Investigadores del Mar (1 al 4 de octubre del 2019, Málaga). Póster: "Impact of heat-waves in shallow aquatic systems: changes in O_2, N_2O and CH_4 fluxes in the sediment-water interface."
- VII International Symposium on Marine Sciences - XX Seminario Ibérico de Química Marina (1 al 3 de Julio del 2020, Barcelona). Comunicación oral: "How heat waves affect the sediment-water interface in shallow aquatic areas?"
- III Congreso internacional de Investigadores dle Mar (6 al 9 de septiembre del 2021, Motril, Granada). Comunicación oral: "Impact of a wind storm on the intertidal areas of Cadiz Bay: Effects on the distribution and net metabolism of micriphytobenthos."
- 10th Scientific Conference of the Hellenic Ecological Society «HELECOS 10 – Ecology and the Conservation of Nature: Advances and Retreats in an Age of Crisis» (14 al 17 de octubre, 2021, Ioánina, Grecia). "Heat waves in shallow

coastal systems increase anaerobic metabolism and greenhouse gases fluxes."

- Estuarine & Coastal Sciences Association (ECSA) 59 - Using the best scientific knowledge for the sustainable management of estuaries and coastal seas (5 al 8 de septiembre, 2022, Kursaal, San Sebastián, España). Comunicación oral: "The role of intertidal sediments in the carbon and nutrients dynamics of the Guadalquivir Estuary (South of Spain)."
- ASLO AQUATIC SCIENCES MEETING 2023 - Resilience and recovery in aquatic systems (4 al 9 de 2023, Palma de Mallorca, España). Póster: "Effects of wind storms on the abundance and net metabolism of intertidal microphytobenthic communities."

Parte de los resultados presentados en esta memoria de Tesis Doctoral han sido publicados en revistas internacionales indexadas JCR (Capítulo 2 en *Frontiers in Marine Science*) o bien se encuentran en preparación para su publicación (Capítulos 3 y 4).

"From sprinkler splashes to fireplace ashes
***I gave my blood, sweat, and tears for this**."*

- Taylor Alison Swift

"Bajo la lluvia y el chaparrón
no aceptes copia ni imitación.
Sangre y sudor.
Antes ser cabeza de ratón
a ser la cola de otro león,
la leyenda como Camarón.
***Sangre y sudor**."*

- Jorge Escorial Moreno

Agradecimientos:

Después de mucho tiempo aquí estamos. El tiempo que ha transcurrido desde que empecé el doctorado ha sido bastante caótico, pasando por una pandemia mundial, olas de calor récord en Europa, invasiones y guerras… Personalmente, al igual que generalmente hablando, han sido unos años duros, pero eso no quita que ha sido muy gratificante. De todos estos años me quedo con toda la experiencia, todos los conocimientos, y las herramientas adquiridas, tanto laborales como personales.

En primer lugar, agradecer a mis directores de tesis, Alfonso y Emilio, toda la paciencia, tiempo y dedicación que han tenido hacia los proyectos, artículos, y más directamente hacia mí. Entiendo que soy una persona compleja y que, por suerte o desgracia, tenemos puntos de vista diferentes frente a alguna que otra cosa, pero valoro enormemente todos los conocimientos y consejos que me habéis dado. Habéis conseguido formar, junto a Sokratis -al que también le agradezco muchísimo y debo reconocer una dedicación plena-, un laboratorio espectacular de Ecología microbiana y Biogeoquímica que muchas universidades envidian. Todos los muestreos, preparaciones de material, experimentos en la sala húmeda, análisis de amonio -que tuve que repetir de media 4 veces cada-, microperfiles, interpretaciones de los datos… Lot, Sandra -mi castellana favorita-, Irene, Marika, encontraros de manera tan fortuita fue un regalo. También a nuestro oráculo del doctorado, Lola, gracias por atender a todas las dudas -relacionadas con el doctorado y no- que nos han surgido a Ana y a mí durante todos estos años.

Después, a toda la gente que ha aportado a mi conocimiento y crecimiento laboral. Aprender de modelaje biogeoquímico no es sencillo para nada, pero Karline Soetaert, aun siendo de las mayores expertas en el tema, no perdió un segundo en explicarme las cosas paso por paso. Enseñándome gran infinidad y posibilidad de ajustes y análisis muy útiles. Al laboratorio BioEcoFunc, que no dudó en abrirme las puertas y acogerme de una manera que nunca hubiese esperado. Gracias a Iván y Nacho, por ser unos profesionales como la copa de un pino, crear de cero un laboratorio tan bueno y dejarme formar parte de él. A Triana por estos últimos años, estar al pie del cañón y darme tantísimo apoyo. Vales oro. Te quiero, amiga.

A mis oceanógrafas favoritas. En general ya con el añito de máster quedó claro que lo que habíamos construido en un año iba a ir para adelante. Rut -la única onubense con la que me relaciono- nuestro viaje a Brasil nos lo llevamos con nosotras a la tumba. Gracias por no matarme en esas semanitas. A ti también Leti, por enseñarnos Brasil desde tu prisma y por hacernos partícipe de tu boda. Arrate, mi nezka aizkolari favorita, haber presenciado a Taylor Swift en directo... Ojo. El vínculo que tengo con Arrate es algo que difícilmente la gente podrá entender, pero es muy muy fuerte, nos separan cerca de 1.200 km, pero siempre voy a poder contar con ella. Destacar también a mis amigas, que siempre han

estado para mí desde el instituto, aunque alguna algo más -Ana lleva conmigo desde preescolar-. Me voy a permitir, ya que es mi escrito, destacar a Lucía y a Ana en especial. Aun así, para todas, amigas, gracias por demostrarme que la distancia no significa absolutamente nada. Por el cariño, el amor, y el respeto incondicional que me habéis demostrado todos estos años. Por la paciencia y el apoyo. Me alegro de poder seguir creciendo a vuestra vera. Os quiero y valoro mucho.

Desde el comienzo de los tiempos de este doctorado tengo a cuatro personas que me guían, me aconsejan y ayudan cada vez que lo necesito. La primera es la Dra. Ana Magro, que empezó conmigo mano a mano, y, que, aunque esté obsesionada con los peces y la piscina, siempre ha sido un apoyo y un ejemplo. Sufrimiento, películas a horas intempestivas, Pedro Pascal, tanto tiempo y momentos - aunque no te guste el techno-. La segunda es la Dra. Isabel Casal Porras, dueña de Bruno y fiel defensora del sentimiento de la felicidad. Isa, quien la conozca lo sabe, es como la madre de todos, está siempre disponible para ayudar. De pies a cabeza un ejemplo a seguir, tanto en lo laboral como en lo personal. Gracias a Isa conocí a Alba, que es una persona espectacular también. Las dos siempre me han animado muchísimo y me han hecho disfrutar incluso en un pueblo perdido de la mano de Dios en Córdoba. Eternamente agradecida por esta amistad tan bonita que enseñáis al mundo y por dejarme ser partícipe de ella.

Ya me parecía que iba tocando un punto y aparte, perdón. Las otras dos personas ya se han mencionado previamente, son Olga y María. Olga es muy miope y tiene un perro majísimo que se llama Nilo; María, a su vez, tiene una mano increíble con la cerámica y rastas. Ambas están haciendo sus respectivos doctorados en física de la Antártida y en ecología de PUFAs PUAs, etc. Intuyo que al igual que yo, no entendáis nada de esta última frase. Ambas son de las personas más capaces y buenas con las que me he cruzado en la vida. Nunca me han dejado atrás y siempre han mirado por mí. Han sido capaces de dedicarme tiempo, aunque para ellas ni siquiera tuvieran, y no han dudado ni una sola vez en decirme las cosas tal y como son. Llevan en mi vida desde hace unos años, pero siento que las conozco de toda la vida.

A las cuatro, gracias por toda la paciencia y por tirar de mí muchas veces que yo quería echar por la borda todo lo conseguido en todo este tiempo. Gracias a vosotras he crecido y conseguido ser quien soy a día de hoy. Os adoro.

Al venir a Cádiz me apunté a rugby, y, pese haber perdido un ligamento cruzado anterior por el camino, no me arrepiento ni un poco de la decisión. Si tengo que hacer una mención especial a gente que me ha dado el rugby, me quedaría con Diana, Agrela, y Tuchi, aunque Bea e Irene también me han ayudado mucho en esta última etapa. Diana es muy sevillana, muy bruta, y muy buena, pero ha aguantado carros y carretas por mi parte. Agrela, es un

ser de luz, siempre ha tenido sus brazos abiertos para calmarme y darme su punto de vista de las cosas -suele ser bastante más positivo que el mío-; y con Tuchi, la madre tierra, que me demuestra que da igual las situaciones que existan, que son totalmente asequibles. Las tres me han enseñado muchas cosas, y lo que es el amor entre compañeras.

Pero lo que mejor me ha dado el rugby es a mi María. Una persona francamente maravillosa y capaz. Es súper inteligente y resolutiva. Como buena profesional, es profesora de matemáticas, tiene muy buen control de la paciencia y calcula a la perfección sus palabras -spoiler: no siempre-. El tiempo pasa muy rápido y, por suerte o por desgracia, se ha tenido que comer la última fase del doctorado, que las malas lenguas dicen que es la más complicada. Sinceramente, lo que más agradezco es el apoyo incondicional, lo que me ayuda a relativizar las cosas y que ella consigue valorarme lo que yo nunca haré. Que ha habido momentos que no he tenido ganas de absolutamente nada y, pum, llegaba María y todo mejoraba. Te quiero mucho. Gracias por tener tantísima paciencia.

Siento si me dejo a alguien por el camino, pero siempre me han dicho que lo mejor se deja para el final. Mi familia. Ellos siempre han creído en mí y me han animado. Mis tíos -en especial mi madrina, que siempre ha estado súper orgullosa de mí-, mis primos, todos. Yo siempre he encontrado un ejemplo a seguir en mi padre, mi madre y mi hermana. Cada uno son de una manera, pero eso también ha hecho que mi personalidad se afine. No podría pedir una familia más comprensiva y real que la que tengo. Somos muy sentidos y siempre vamos de cara. A mis padres les quiero una barbaridad y les debo que me hayan permitido formarme en lo que yo quería y seguir haciendo mi vida pese a todo. Ambos son muy diferentes, pero se complementan que da gusto. Ni un día han dejado de animarme para que siga en pie. A Marina no sé ni qué decirle porque me pongo a llorar cada vez que pienso en lo muchísimo que la quiero -y eso que somos polos opuestos-. La tengo de referencia para literalmente todo. Gracias por todo. No os puedo querer más y no podría tener una familia mejor. Sois el pilar fundamental de mi vida. Gracias.

Por último, a mi Rukia, que me alegra todos y cada uno de mis días.

ABSTRACT:

Environmental variability, from seasonal cycles to extreme events such as heatwaves and windstorms, profoundly affects the biogeochemistry of shallow, intertidal sediments. This thesis integrates three complementary studies to evaluate how physical factors control net metabolism and sediment–water fluxes in intertidal zones of southwestern Spain.

In the first study, benthic primary production and nitrogen dynamics were evaluated in intertidal sediments of the Guadalquivir River estuary, a highly turbid and nutrified system, over an annual cycle. Sediment–water oxygen and dissolved inorganic nitrogen fluxes, together with vertical profiles of photosynthetic pigments, organic carbon, and porewater nutrients, showed that microphytobenthos maintains net autotrophic sediments at both the estuary mouth and mid-estuary sites, with winter production peaks despite higher summer irradiance. Microphytobenthos Ammonium uptake accounted for almost all ammonium removal, while persistent nitrate consumption sustained elevated denitrification rates. Thus, denitrification far exceeded iron and sulfate-reduction as the main anaerobic mineralization pathway, although it was surpassed by nitrogen uptake from microphytobenthos, underscoring the central role of benthic microalgae in estuarine nutrient recycling.

In a second study, we analyzed the effects of extreme temperatures, simulating a heatwave (10-42 °C), on net metabolism, nutrient cycling, and greenhouse-gas exchange through sediment-core incubations and oxygen microprofiling in sediments from the Bay of Cadiz. Prolonged exposure to high temperatures accelerated respiration and altered the nitrogen cycle. Moderate warming enhanced nitrification and nitrite flux to the overlying water, whereas temperatures above 34 °C favored anaerobic processes such as denitrification or DNRA. Metagenomic analyses revealed an increase of denitrification genes and thermotolerant methanogens under the highest-temperature treatments. Consequently, nitrous oxide flux peaked at intermediate temperatures before declining, while methane emissions increased exponentially with rising temperature. These results suggest that more intense and prolonged heatwaves could transform shallow sediments from carbon dioxide, nitrous oxide and methane sinks into net sources.

Finally, we investigated the biogeochemical response to environmental variability caused by a major windstorm in the inner Bay of Cádiz. Samples were taken before,

during, and after the storm at two sites, one sandy, one muddy, within the inner bay. These surveys revealed transient peaks in total suspended solids (TSS), chlorophyll-a, and dissolved nutrients in the water column, demonstrating benthic-pelagic coupling. Concurrently, oxygen penetration, net metabolism, and pore-water nutrients showed significant alterations, reflecting sediment resuspension and hydrodynamic changes. Satellite imagery confirmed spatial heterogeneity in material and nutrient export, with up to a 3.6-fold increase in export to adjacent coastal waters.

These studies demonstrate that shallow intertidal sediments exhibit very dynamic, tightly coupled carbon, nitrogen, and oxygen fluxes, regulated by both gradual disturbances and abrupt events. By integrating laboratory experiments, year-round field observations, molecular biology, and remote sensing, this thesis makes a substantial contribution to our understanding of how climatic variability and anthropogenic pressures modulate coastal ecosystem function and greenhouse-gas balances.

RESUMEN:

La variabilidad ambiental que se produce a distintas escalas temporales, desde ciclos estacionales hasta eventos extremos como olas de calor y temporales de viento, condiciona ampliamente la biogeoquímica de los sedimentos someros e intermareales. Esta tesis integra tres estudios complementarios para evaluar cómo los factores físicos controlan el metabolismo neto y los flujos sedimento-agua en ecosistemas costeros someros del suroeste de España.

En un primer estudio, se evaluó la producción primaria bentónica y la dinámica del nitrógeno en sedimentos intermareales del estuario del río Guadalquivir, sistema con gran turbidez y elevada carga de nitrato, a lo largo de un ciclo anual. Los flujos sedimento-columna de agua de oxígeno y nitrógeno inorgánico disuelto (amonio, nitrato y nitrito), junto a perfiles verticales de concentración de pigmentos fotosintéticos, carbono orgánico y concentración de nutrientes en el agua intersticial, mostraron que el microfitobentos mantiene los sedimentos intermareales de la desembocadura y del tramo medio con un metabolismo neto autotrófico, con picos de producción invernales a pesar de observarse una mayor irradiancia en verano. La demanda de amonio por parte del microfitobentos explicó su alta captación, mientras que la absorción de nitrato se debe posiblemente a altas tasas de desnitrificación. Así, la desnitrificación superó en gran manera la reducción de hierro y sulfato como vía principal de mineralización anaerobia, aunque este se vio sobrepasado por la captación de nitrógeno del microfitobentos, subrayando el papel central de las microalgas bentónicas en el reciclaje de nutrientes estuarinos.

En un segundo estudio, se analizaron los efectos de temperaturas extremas, simulando una ola de calor (10-42ºC) sobre el metabolismo neto, el ciclo de nutrientes y el intercambio de gases de efecto invernadero mediante incubaciones de testigos de sedimento y microperfiles de oxígeno en sedimentos de la zona de la Bahía de Cádiz. La exposición prolongada a altas temperaturas aceleró la respiración y alteró el ciclo del nitrógeno. Mientras que un incremento moderado de temperatura potenció la nitrificación y el flujo de nitrito hacia la columna de agua, temperaturas superiores a 34ºC favorecieron procesos anaerobios como desnitrificación o DNRA. Los análisis metagenómicos mostraron un aumento de genes de desnitrificación y de metanógenos termotolerantes en los tratamientos de mayor temperatura. El flujo de óxido nitroso hacia la columna de agua alcanzó su máximo a temperaturas intermedias, disminuyendo en temperaturas superiores,

mientras que las emisiones de metano aumentaron de manera exponencial con la exposición a temperaturas ascendentes. Estos resultados sugieren que olas de calor de mayor magnitud y más prolongadas en el tiempo pueden cambiar la naturaleza de los sedimentos someros, invirtiendo su comportamiento como sumidero de dióxido de carbono, óxido nitroso y metano, convirtiéndolos zonas de gran emisión de estos gases.

En un último estudio, investigamos la respuesta biogeoquímica a la variabilidad ambiental causada por un fuerte temporal de viento en la parte interna de la Bahía de Cádiz. Se hicieron muestreos antes, durante y después al evento extremo de viento en varios puntos del saco interno de la Bahía, uno con fondo más arenoso y otro más fangoso. Los datos revelaron picos transitorios de sólidos totales en suspensión, clorofila-a y nutrientes disueltos en la columna de agua, demostrando un acoplamiento en los compartimentos bentónico y pelágico. Paralelamente, la penetración de oxígeno, el metabolismo neto y las concentraciones de nutrientes en el agua intersticial mostraron alteraciones significativas, reflejando así procesos de resuspensión y cambios hidrodinámicos. Además, las imágenes de satélite confirmaron heterogeneidad espacial en la exportación de material y nutrientes, con incrementos de hasta 3.6 veces la exportación hacia aguas costeras adyacentes.

Estos estudios demuestran que los sedimentos intermareales someros presentan flujos de carbono, nitrógeno y oxígeno muy dinámicos y acoplados, regulados tanto por perturbaciones graduales como por eventos bruscos. Al integrar experimentos de laboratorio, observaciones de campo anuales, biología molecular y teledetección, esta tesis aporta un avance sustancial en la comprensión de cómo la variabilidad climática y las presiones antropogénicas modulan la función de los ecosistemas costeros y sus balances de gases de efecto invernadero.

Contents

Chapter 1:

General introduction

1.1. Importance of shallow coastal zones: Intertidal sediments as ecologically significant and dynamic ecosystems. 2

1.2. Importance of microphytobenthos in the dynamics of intertidal ecosystems 4

1.3. Impact of climate change on shallow coastal environments 8

1.3.1. Heat waves 10

1.3.2. Extreme wind conditions 12

1.4. Areas of study: intertidal zones of the Cadiz region. 13

1.4.1. Bay of Cadiz 13

1.4.2. Guadalquivir Estuary 15

1.5. Aims of study 16

1.5. Objetivos del estudio 18

Chapter 2:

Benthic metabolism and nutrient dynamics of a hyperturbid and hypernutrified estuary 27

1. Introduction 29

2. Material and Methods 31

2. 1. Study site and sampling 31

2. 2. Total suspended solids and inorganic nutrients in the water column 32

2. 3. Sediment-water fluxes of oxygen and inorganic nitrogen 33

2. 4. Inorganic nitrogen, iron, sulfate and dissolved inorganic carbon in the porewater 34

2. 5. Organic matter, organic carbon, total nitrogen and chlorophyll in the sediment 35

2. 6. Statistical analysis 35

3. Results 36

3. 1. Organic carbon and total nitrogen content in the sediment 36

3. 2. Photosynthetic pigments content in the sediment 38

3. 3. Oxygen fluxes at the sediment-water interface 38

3. 4. Inorganic nutrients in the water column and sediment porewater 39

3. 5. Dissolved inorganic carbon, iron and sulphate in the sediment porewater. 41

3. 6. Fluxes of inorganic nitrogen at the sediment-water interphase 41

3. 7. Net production rates of DIC, NH_4^+ and Fe^{2+} and net consumption rate of SO_4^{2-} within the sediment 43

4. Discussion 44

4. 1. Organic carbon and total nitrogen 44

4. 2. Microphytobenthic biomass seasonal dynamics 46

4. 3. Net metabolism in the Guadalquivir intertidal sediments 47

4. 4. Inorganic nitrogen concentration in the water column and sediment 48

4. 5. Fluxes of inorganic nitrogen at sediment-water interface 49

4. 6. Iron and sulfate as alternative electrons acceptors 51

4. 7. Mineralization of organic matter in the sediment 52

5. Conclusions 55

Chapter 3:

Impact of heatwaves on net metabolism, nutrient and greenhouse gases fluxes at the sediment water interphase of a shallow coastal ecosystems 77

1. Introduction 78

2. Material and Methods 80

2. 1. Study site and sampling 80

2. 2. Sediment-water fluxes 81

2. 3. Organic matter, DIC and nutrients profiles in the sediment 83

2. 4. Apparent activation energy and Q10 calculation 83

2. 5. DNA extraction, PCR and sequencing of 16S rRNA 84

2. 6. Bioinformatics analysis 84

2.7. Quantitative PCR 85

2.8. Statistical analysis 86

3. Results 87

3. 1. Diffusive and total oxygen fluxes at the sediment-water interface 88

3. 2. Dissolved inorganic carbon and nitrogen profiles 89

3.3. DIC and DIN fluxes at the sediment-water interface 90

3. 4. N_2O and CH_4 fluxes 94

3. 5. Organic carbon and total nitrogen content 95

3.6. Quantitative PCR 96

3.7. Taxonomic responses of Archaea and Bacteria to heat treatments 97

3. 8. Richness, diversity and community responses of Bacteria to heat treatments 99

3. 9. Reconstructed functional analysis using PiCrust2 99

4. Discussion 100

4. 1. Effect of temperature increase on total sediment metabolism 100

4. 2. Nitrogen cycling processes 102

4. 3. Production of greenhouse gases 104

Chapter 4

Wind storms increase benthic-pelagic coupling and nutrient outwelling from shallow coastal wetlands 124

1. Introduction 126

2. Material and methods 128

2.1. Study site description and sampling 128

2.2. Oxygen microprofiles and net metabolism at the sediment water interface 129

2.3. Total suspended solids, photosynthetic pigments and nutrients content in the water column 130

2.4. Organic matter, nutrients and chlorophyll content in sediment 131

2.5. Chlorophyll-a and suspended particulate matter using Sentinel-2 imagery 131

2.6. Statistical analysis 132

3. Results 133

3.1. Meteorological conditions during the studied windstorm 133

3.2. In situ total suspended solids and chlorophyll-a in the water column 133

3.3. Remote sensing of chlorophyll and suspended particulate matter 134

3.4 Chlorophyll-a, organic carbon and total nitrogen in the sediment 135

3. 5. Oxygen profiles at the sediment surface and net production and respiration rates 137

3.6. Nutrient concentrations in the water column and sediment 137

3.7 Multivariate analysis 139

4. Discussion 141

4.1. Sediment and MPB resuspension induced by a windstorm event 141

4.2 Influence of the WSE in the sediment chlorophyll, organic carbon and nitrogen 142

4.3. Effects of WSE on net metabolism at the sediment-water interface 144

4.4. Exchange of nutrients between the sediment and the water column 147

4.5. WSE-induced shift in ecosystem state and outwelling to coastal waters 149

5. Conclusions 151

Chapter 5:

General discussion and conclusions 165

1.1. Contribution of microphytobenthos to sediment biogeochemistry in the Guadalquivir Estuary 166

1.2. Effect of heat waves on intertidal sediment biogeochemical processes 168

1.3. Windstorm-generated turbulence affects the dynamics of shallow coastal ecosystems 170

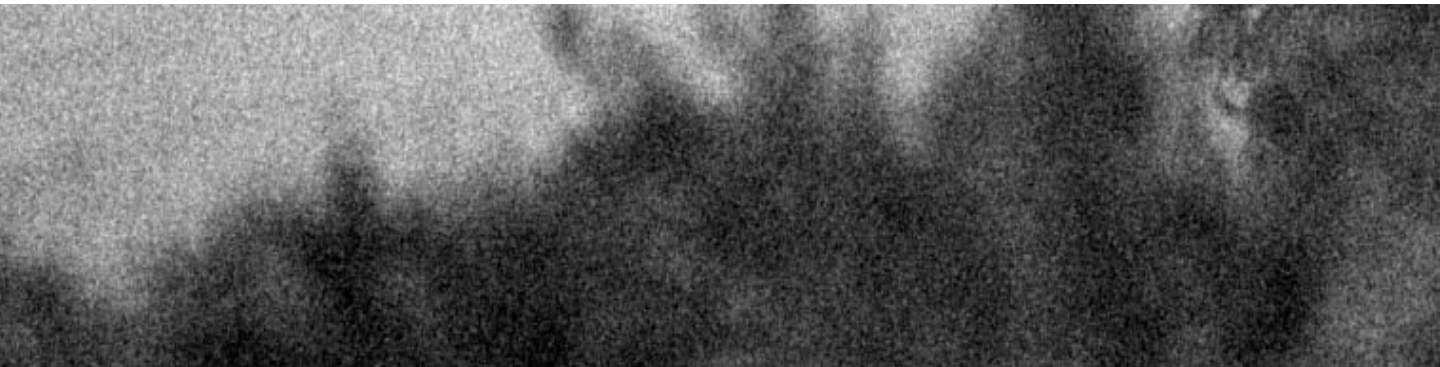
1.4. General conclusions 180

1.4. Conclusiones generales 182



Chapter 1:

General introduction and objectives



1.1. Importance of shallow coastal zones: Intertidal sediments as ecologically significant and dynamic ecosystems.

Coastal wetlands, as defined by Ramsar Convention on Wetlands, are water bodies, whether natural or man-made, permanent or seasonal containing still or running water that may be fresh, brackish or saline, together with coastal marine zones whose depth at low tide does not exceed six meters. These ecosystems are highly productive, represent biodiversity "hot spots" and provide essential services like food supply, waste remediation, water purification, carbon storage and erosion control. These functions contribute to mitigating environmental problems, such as climate change, by capturing and storing carbon, reducing greenhouse gases emissions and protecting coastal areas from storms and flooding (Canfield, 2005; Hopkinson et al., 2019; Li et al., 2020; Schutte et al., 2019). Tidal saltmarshes, one of the most common forms of coastal wetland in the temperate zone (Hopkinson et al., 2019), in addition to their importance as reservoir of biodiversity, are key players in biogeochemical cycles, acting as buffers that facilitate the exchange of energy and matter between terrestrial, marine and atmospheric systems (Canfield, 2005; Underwood & Kromkamp, 1999). They contribute significantly to coastal productivity, host high rates of mineralization and burial of organic matter, and contribute to the regeneration of inorganic nutrients, being these processes highly coupled to high rates of primary and secondary productivity (Froneman, 2005; Schutte et al., 2019). A fraction of the saltmarshes productivity, in the form of particulate and dissolved organic carbon and regenerated nutrients, is exported to coastal waters (outwelling) stimulating coastal productivity, including species of economics interest. Global distribution of tidal saltmarshes is widely heterogeneous and they tend to be more common in the temperate zone of Northern hemisphere (Figure 1).

Saltmarshes present a characteristic zonation of plant communities that thrive in different sea level ranges, that affect emersion/immersion time, changes in salinity and different biogeochemical characteristics. The present PhD Thesis focus in the study of net metabolism and biogeochemistry of bare intertidal flats, located between the high and low tide marks. These ecotopes generally lack rooted vegetation and have a high surface-to-volume ratio, which facilitates the exchange of matter between the sediment and the water column. This favors the decomposition of organic matter and nutrient cycling, and makes these areas

extremely productive ecosystems, outperforming shelf areas by as much as 10-15 times despite covering only 10 % of global coastal areas (Paterson et al., 2019; Schutte et al., 2019). These sediments harbor dense microbial and metazoan populations that process organic matter more efficiently than the water column (Glud, 2008).

Intertidal flats are constantly reworked by dynamic sediment transport processes,

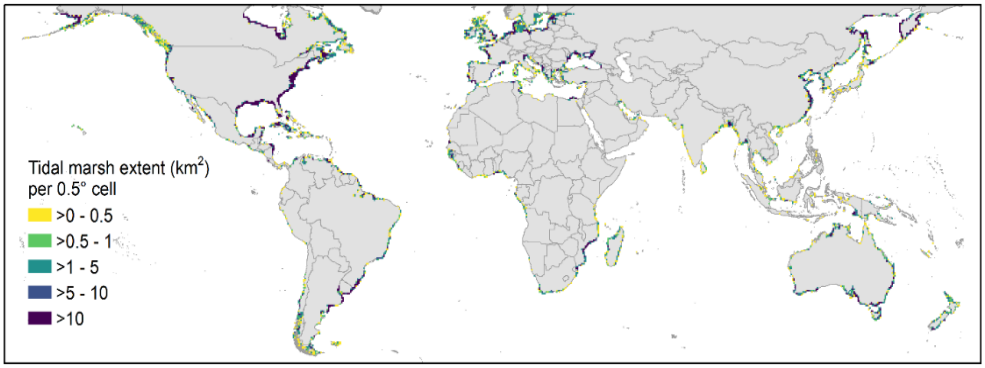


Figure 1. Tidal marshes in 2020, greater extension represents with darker colors (km^2) within a 0.5° grid cell. © (Worthington et al., 2024)

such as erosion, deposition and consolidation, which modify their landscape over time and make them environments very sensible to climatic events (Tolhurst et al., 2006). Intertidal flats experience regular cycles of different periods of tidal immersion and emersion depending on their position on the intertidal gradient, which generates a zonation of species adapted to different niches with unique physiological and behavioral strategies. The biological communities inhabiting these areas face physical pressures such as wind and waves, biotic pressures such as predation and grazing, and physiological challenges such as resistance to desiccation and tolerance to salinity and temperature fluctuations (Paterson et al., 2019). In this context, the specific physical and geomorphological characteristics of these ecotopes, make them very sensitive to different effects of climate change, like the increase in the frequency and intensity of different types of extreme climatic events like wind storms, heat waves, etc. These changes are likely to affect their high productivity and their ecosystems functions and services.

1.2. Importance of microphytobenthos in the dynamics of intertidal ecosystems

Intertidal mudflats are highly dynamic and vulnerable ecosystems, characterized by rapid changes in environmental conditions. Factors such as tides and sunlight variations generate constant fluctuations in key parameters such as irradiance, salinity, temperature, water content and oxygen, among others (Kromkamp, 2006).These areas present a high surface-volume range, where the thin water column is unable to effectively buffer environmental changes, increasing its sensitivity to perturbations. Nonetheless, intertidal unvegetated (bare) sediments provide an habitat for many species, from microorganisms to meio- and macrofauna (Paterson et al., 2019).



Figure 2. (**A**)**.** Intertidal sediment colonized by MPB in the Guadalquivir Estuary (**B**)**.** Zoom in at the sediment cores before they were pulled out from the sediment (**C**)**.** Sediment cores in the laboratory collected from Cadiz Bay tidal flats.

Microbial benthic primary producers constitute a community of photoautotrophs generally dominated by diatoms and cyanobacteria, with a less important presence of other taxonomic groups such as green microalgae and euglenophytes (Kromkamp, 2006; MacIntyre et al., 1996). This community of microbial photoautotrophs, commonly named microphytobenthos (MPB), can be visible to the naked eye as green or golden-brown biofilm when present in high abundance (**Figure 2. A, B, C**). The vertical distribution of MPB is limited by light penetration, both in its presence in intertidal and shallow subtidal zones along the sea level gradient, and in its vertical distribution within the sediment. Irradiance decreases exponentially within the sediment, restricting the photic or productive zone to a very

thin layer of several mm in muddy sediments (Cartaxana et al., 2016; Haro et al., 2019; Kühl et al., 1994).

MPB plays pivotal biogeochemical and ecological roles in tidal flats and other shallow aquatic ecosystems, contributing to carbon fixation, nutrient recycling, and sediment stabilization (Haro et al., 2019; Kromkamp, 2006; Sundbäck & Granéli, 1988; Sundbäck & Miles, 2002; Underwood & Paterson, 1993). MPB photosynthesis supports food webs, providing energy to marine meiofauna and macrofauna (Middelburg et al., 2000) and to heterotrophic bacteria through the production of exopolymers (Bohórquez et al., 2017). In addition, these exopolymers enhance sediment cohesion and stability, thereby improving water quality (Tolhurst et al., 2002). Furthermore, daily photosynthetic oxygen production by microphytobenthos (MPB) drives aerobic organic matter decomposition in sediments, sustaining nutrient cycling and improving the ecosystem health in shallow coastal areas (Haro et al., 2019; MacIntyre et al., 1996; Sundbäck & Miles, 2002; Underwood & Kromkamp, 1999).

The first record on microphytobenthic primary production was published in 1950 by Aleem and colleagues, in which they studied how the light and tides might affect some diatoms in England mudflats. Today, several methods are available for measuring the MPB productivity such as core and benthic chambers incubations for measuring the O_2 exchange between the sediment and the water, oxygen microelectrode and optodes techniques, ^{14}C based techniques or variable fluorescence techniques such as pulse amplitude modulated (PAM) that can be used in the laboratory or in situ (Kromkamp, 2006). In the present thesis we have used two of these techniques for the study of MPB primary production and the net metabolism of the benthic compartment: sediment core incubations and microsensor profiling.

O_2 microsensors provide a detailed information on oxygen concentration at the sediment-water interface on a micrometer scale (Revsbech & Jørgensen, 1986). Microsensors are used normally for measuring the vertical oxygen concentration at the sediment-water interface at microscale with a resolution in the range of tens of microns (**Figure 3.**). MPB photosynthesis activity, determined by irradiance and photoperiod, largely regulates the availability of O_2 in sediments, including maximum O_2 penetration depth (Z_{ox}). In fine sediments, the exchange of O_2, CO_2, and other solutes with the overlying water occurs via molecular diffusion through

the diffusive boundary layer (DBL), with the thickness of this layer playing a key role in regulating solute transport (Jørgensen & Revsbech, 1985). During MPB photosynthesis, oxygen concentrations increase just below the sediment surface, diffusing both upward into the upper sediment layers and the water column (J_{Up}) or downward into deeper sediment layers (J_{Down}) (Figure 3.). This enhanced diffusion of oxygen into deeper sediment layers in light extends the oxygen penetration depth (Z_{ox}) with respect to the dark conditions. Therefore extending the oxic sediment layer, where oxygen is available for microbial aerobic respiration and the oxidation of organic matter (Glud, 2008).

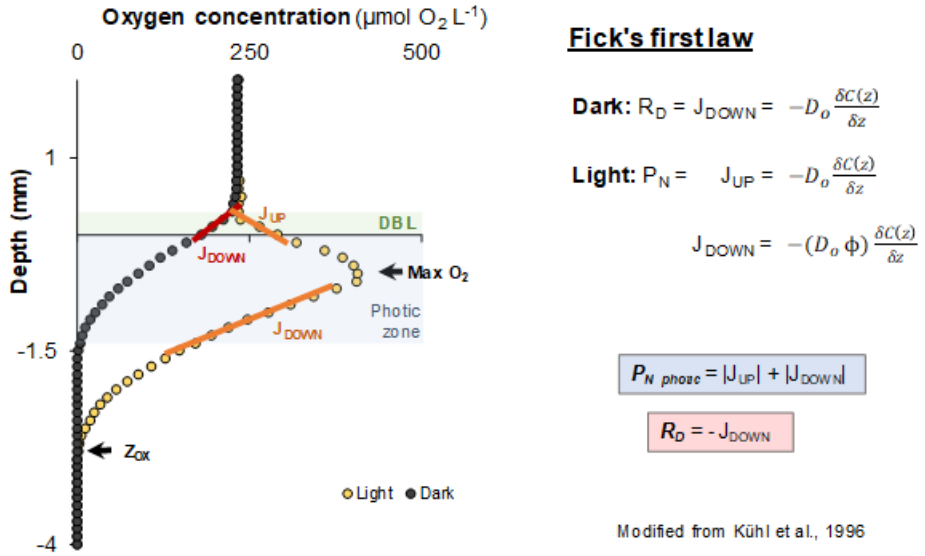


Figure 3. Scheme of vertical oxygen concentration profiles made by microelectrodes. 0 depth represents the sediment surface. Dark blue dots represent oxygen concentration measurements made in dark conditions and yellow ones in light condition. Max O_2 represents the maximum O_2 concentration in light, Z_{ox} the maximum O_2 penetration depth, J represents the O_2 flux (up if its upwards or down if its downwards), D_o is the diffusion coefficient in seawater, ϕ, sediment porosity. P_N represents net production in the sediment and $P_{N\ photic}$, the net production for the photic zone, R_D is respiration rate in darkness.

Since oxygen transport in non-permeable sediments occurs by molecular diffusion, Fick's first law is used to estimate net production and respiration rates. These rates are derived from the slopes of oxygen concentration profiles, based on the molecular diffusion coefficient of oxygen and the porosity of the sediment (Glud, 2008; Schutte et al., 2019). Net primary production for the whole sediment community can be determined by J_{up} at the DBL, while net primary production for

the photic layer can be calculated by accounting for both J_{Up} and J_{Down} in light conditions (Figure 3). Respiration in dark conditions (R_D) is determined from J_{Down} in dark conditions. Within the climate change scenario, temperature can affect to this diffusion coefficient and to the solubility of the oxygen, altering rates of net production, respiration and other chemical and biological processes (Kristensen, 2000; Price & Sowers, 2004), in addition to more specific effect of temperature on the physiological response of MPB and heterotrophic organisms (Laviale et al., 2015; Morris & Kromkamp, 2003).

Light is a critical factor for MPB, as it carries out photosynthesis in the photic layer of the sediment, a very thin layer that also varies depending on sediment grain size and biomass density (Cartaxana et al., 2016; Kühl et al., 1994). An increase in water column turbidity can reduce the incident irradiance and the extent of the photic layer, consequently decreasing MPB productivity (Irigoien & Castel, 1997; Migné et al., 2009; Pivato et al., 2019). In areas with shallower water columns, MPB biomass tends to be higher with higher light exposure (Van Der Wal et al., 2010), exhibiting daily fluctuations in the biomass located at the surface due to light-regulated circadian migration (Haro et al., 2019; Kromkamp, 2006), adjusting to the irradiance levels necessary to maintain their vital functions and avoiding processes such as photoinhibition. These changes in irradiance associated with both the tides and the daily light cycle, affect the production and respiration rates of the MPB.

The relationship of MPB with nutrients varies according to local conditions. While in marine systems the limitation is usually associated with nitrogen and in freshwater systems with phosphorus, in cohesive sediments rich in organic matter, bacterial mineralization generates high concentrations of dissolved nutrients, while more oligotrophic sediments may limit their availability (Admiraal, 1984). In nutrient-poor systems, MPB can effectively reduce the release of nutrients from the sediment into the water column, being more relevant in the presence of light, as occurs in micromareal systems (Sundbäck et al., 2000). The inorganic nutrient demand of MPB can affect other microbial processes by competition for specific substrates, such as nitrification-denitrification at the sediment-water interface (Risgaard-Petersen, 2003), affecting the mineralization of organic matter mineralization as well.

1.3. Impact of climate change on shallow coastal environments

The acceleration of greenhouse gas emissions due to human activities is intensifying global warming, with severe impacts across marine, terrestrial, freshwater and polar ecosystems (Cooley et al., 2023; Parmesan et al., 2022; Parmesan & Yohe, 2003). The steady rise in global average temperatures is associated with an increased frequency, intensity, and duration of extreme climatic events (ECE), such as heat waves, windstorms, and hurricanes (Feser et al., 2015; Parmesan et al., 2022; Perkins-Kirkpatrick & Lewis, 2020). ECE are defined as weather events with magnitudes that deviate significantly from local averages, exceeding upper or lower thresholds. These events, coupled with rising air and sea temperatures, are driving sea level rise, melting ice, and altering atmospheric and oceanic circulation patterns (Perkins-Kirkpatrick & Lewis, 2020).

The ecological consequences of climate change and ECE on coastal and estuarine ecosystems are profound, leading to shifts in species distributions, population abundances, and local and global extinctions, with potentially irreversible ecosystem alterations (Cooley et al., 2023; Easterling et al., 2000, 2000; Frölicher & Laufkötter, 2018; Parmesan et al., 2022; Ummenhofer & Meehl, 2017). Coastal and estuarine ecosystems, which provide critical services such as habitat protection, erosion control, carbon storage, and nutrient cycling, are particularly vulnerable to ECE. Events like storms and intense rainfall disrupt freshwater inflows, introducing excess nutrients and organic matter that trigger phytoplankton blooms, disrupt food webs, and cause significant biogeochemical changes (Paerl & Paul, 2012; Voynova et al., 2017). In shallow and intertidal systems, heatwaves (Figure 4B) alter metabolic processes, disrupting carbon and nitrogen cycling, while windstorms (Figure 4C) resuspend sediments, driving additional nutrient exchange, MPB redistribution, and sediment transport, further compounding these impacts (Haro et al., 2019; Hope et al., 2020). Together, these events disrupt ecosystem processes, highlighting the importance of understanding their effects on sediment dynamics and biogeochemical cycles.

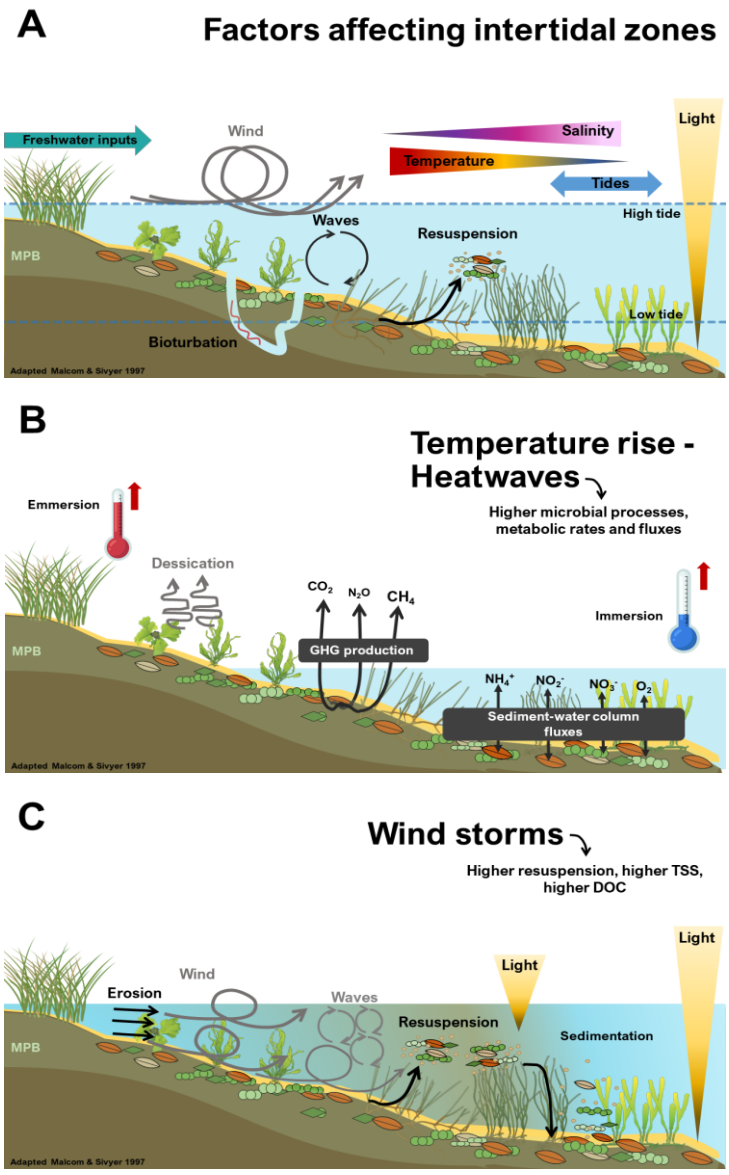


Figure 4. A. Factors affecting intertidal zones in standard conditions. Below, different scenarios illustrate the anticipated outcomes in our system when a significant extreme climatic event (ECE) occurs: B. Under heatwave exposition, and, C. under wind-storm.

1.3.1. Heat waves

Analyzing the climate data collected since 1950 until 2018 by the Spanish Meteorological Agency (AEMET), changes in temperature can be observed, both in average values and in the frequency and magnitude of extreme conditions, such as heat waves (defined here as number of days with maximum temperatures >35ºC) (Figure 5A). In some meteorological stations in the Andalusian capitals, a significant increase in the mean annual temperature of between 0.1 and 0.44 ºC every ten years has been quantified, as in Seville, near to Lebrija, where the change was about 0.30 ºC or in the Bay of Cadiz, a temperature increase of between 0.17ºC and 0.23ºC in ten years has been observed (Figure 5B,C).

Global warming intensifies greenhouse gas (GHG) emissions from shallow coastal sediments. Increased metabolic activity of microorganisms and macrofauna due to higher temperatures accelerates the decomposition of organic matter, which releases CO_2, CH_4 and N_2O into the atmosphere (Canfield, 2005; Parmesan et al., 2022; Schutte et al., 2019). Heat waves and elevated rising water temperatures may drive three interconnected effects: gases diffuse more rapidly due to lower water viscosity and higher molecular motion; oxygen solubility declines; and organic carbon and nitrogen mineralization are intensified (Apple et al., 2006; Hicks et al., 2018). In particular, it is estimated that CH_4 emissions in freshwater and estuarine systems could increase by 6-20% for every 1 °C increase in temperature, with more marked effects in shallow, nutrient-rich waters (Parmesan et al., 2022; Ummenhofer & Meehl, 2017).

Increasing temperature has a direct impact on in many sedimentary processes by influencing the metabolic rates of microorganisms and chemical reactions in the sediment (Apple et al., 2006; Hicks et al., 2018; Kauppi & Villnäs, 2022; Price & Sowers, 2004). In intertidal sediments, temperature swings during emersion and immersion cycles disrupting net metabolism by affecting both photosynthesis and respiration (Blanchard et al., 1996). Photosynthesis is inhibited due to damage to photosystem II at temperatures exceeding 30 ºC, whereas respiration increases up to ca. 35 ºC before declining as enzymes denaturalize (Morris & Kromkamp, 2003). Additionally, heat waves lead to more frequent drying and rewetting cycles, which change redox conditions by creating surface crusts that limit oxygen supply. These changes slow down important nitrogen cycle processes, such as denitrification and

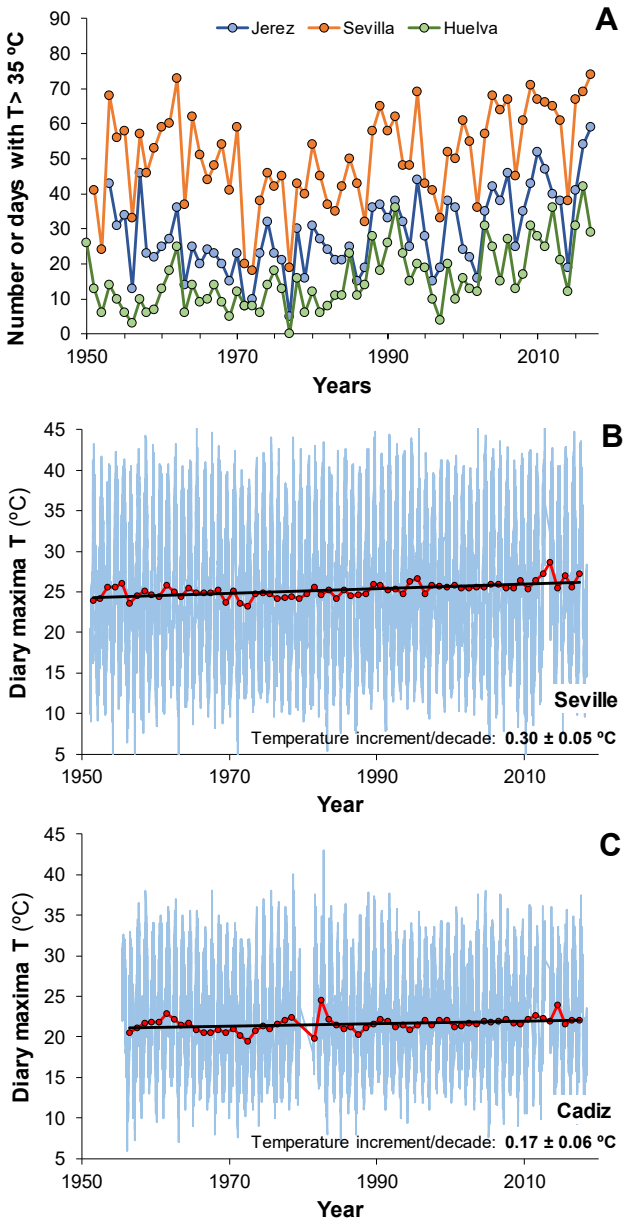


Figure 5. A. Time evolution of the number of days per year with a temperature above 35ºC in three important capitals from Andalusia, Cadiz is not represented as the Atlantic Ocean makes the temperature much milder. **B, C.** Daily evolution of the maximum daily temperature (in blue line) measured at AEMET stations in Seville and Cadiz. In red is represented the evolution of the mean annual temperature, with which the linear temperature increase per decade has been calculated (black line). The linear increase in temperature is statistically significant in all the data.

dissimilatory nitrate reduction to ammonium, because anaerobic enzymes are inhibited when oxygen levels temporarily rise conditions (Rahman et al., 2019). The thermal sensitivity of these processes, is usually estimated by the Q_{10} coefficient, which reflects how the rates of chemical and biological reactions increase with an increase of 10º C (Hancke & Glud, 2004; Kwon et al., 2020). The Q_{10} is a dimensionless number that reflects the ratio of reaction rates at two temperatures separated by 10°C. In ecology, it ranges normally between 2-3, indicating high thermal sensitivity (increase of 2x-3x the velocity of the reaction per each 10º C) (Duff & Teal, 1965; Fierer et al., 2006; Thamdrup et al., 1998), although anaerobic processes like methanogenesis can exhibit $Q_{10} > 3$. A Q_{10} of 1 indicates that the study process is independent of the temperature, whereas higher values reflect higher thermal sensitivity. This parameter helps model global warming impacts on biogeochemical cycles, although its accuracy is limited by the additional control of other factors such as the oxygen availability, substrate quality (depending of labile/recalcitrant organic matter) and microbial community composition (Fierer et al., 2006).

1.3.2. Extreme wind conditions

The Bay of Cadiz, due to its geographic position, is partially shielded from northern and eastern winds, but it is vulnerable to western and southern winds. Westerly winds from the Atlantic bring cooler temperatures, while easterly winds from the Mediterranean raise temperatures (Vargas et al., 2003). The North Atlantic and Western Europe, especially the Iberian Peninsula, are expected to experience increasingly intense winter storms, higher frequencies of windy days, and more severe heat waves, resulting in heightened seasonal shifts and drier conditions (Feser et al., 2015).

Wind storms can have strong influence on the sediment dynamics in shallow aquatic environments (Figure 4). They erode sediment and redistribute it within the basin and transport it offshore with tides, counteracting the gradual sediment accumulation during calm periods. Storm-induced erosion reduces surface mud and MPB cover, lowering the erosion threshold, whereas tranquil periods promote mud accumulation and sediment stability (Dyer et al., 2000; Green & Coco, 2014). The resuspension of particles caused by strong winds increases water turbidity,

reducing light penetration and negatively impacting benthic communities (Savelli et al., 2019; Ubertini et al., 2012). This resuspension can physically harm benthic organisms, but simultaneously introduces resuspended nutrients into the water column, supporting local food webs. Wind-induced shear stress generates waves and sediment movement, redistributing particulate matter, nutrients and MPB cells, occasionally transferring them to adjacent areas (Ha et al., 2020; Jiménez-Arias et al., 2020; Zhang & Blomquist, 2018). These processes also alter the spatial distribution of sediment and associated biological activity. Storms thus impact MPB biomass, productivity, and microbial activity at the sediment surface, shifting the balance between biostabilizing processes, linked to MPB growth and exopolymer production, and destabilizing abiotic processes, thus reshaping sedimentary and ecological equilibrium (Ha et al., 2020; Zhang & Blomquist, 2018).

1.4. Areas of study: intertidal zones of the Cadiz region.

Shallow coastal aquatic zones, such as Cadiz Bay saltmarshes and Guadalquivir estuary, are biogeochemical hot-spots, where organic matter can undergo substantial biogeochemical transformations and inorganic nutrients are regenerated (Barbier et al., 2011; Corzo et al., 2009; Garcia-Robledo et al., 2016; Haro et al., 2020; Liu et al., 2021; Ribas-Ribas, 2011). These areas are of great ecological value in southeastern Spain, the natural park of the Bay of Cadiz, a protected natural area since 1989 (UICN IV category), and the Guadalquivir estuary, part of the Doñana nature reserve (UNESCO), being both highly exposed to environmental disruptions such as heatwaves and wind storms, with yet unknown consequences in these relevant ecosystems.

1.4.1. Bay of Cadiz

The inner Bay of Cadiz is a shallow basin characterized by an average depth under 3 meters. It includes an extensive intertidal zone (about 60% of its area, ~9 km x 5km) dominated by muddy sediments (grain size < 63 µm), with localized zones of sands and sand-mud mixtures (Haro et al., 2020). The bay experiences semidiurnal tides, with levels fluctuating between a high of 1.75 m and a low of -1.5 m relative to the mean sea level. The shallow coastal ecosystem of the Bay of Cadiz has large extensions of intertidal sediments (Figure 6A) that host a complex microbial

community which is at the base of the food webs and affects both local biogeochemical cycles and ecosystem productivity (Garcia-Robledo et al., 2016; Haro et al., 2020). In this thesis, we focused on distinct zones within the inner Bay of Cadiz. These included the muddy areas of the tidal channel of the San Pedro River, the sandier western part of the inner bay, and the eastern region near Puerto Real, where marshes form in a muddier and more exposed environment.

Sandy systems, shaped by strong hydrodynamic forces that remove finer grains, create habitats with large interstitial spaces. These voids facilitate oxygen penetration through advective transport, influencing organic matter breakdown and nutrient cycling (Paterson et al., 2019), as occurs in the western part of the inner Bay of Cadiz. Traditionally viewed as low in productivity, recent studies show that sandy sediments allow deeper light penetration, enabling deeper microphytobenthic photosynthesis layer even when submerged, contrasting with mudflats, where turbidity restricts incident light and light penetration within the sediment is lower as well.

Muddy environments, such as most of the inner Cadiz Bay, are richer in organic matter, from both local production and external sources, especially in low-energy settings that favor fine particles sedimentation (Nybakken & Bertness, 2005). The dense particle structure restricts oxygen to surface layers, leading to steep chemical gradients and active organic recycling (Aspden et al., 2004). These areas support thriving surface microphytobenthos communities (Consalvey et al., 2004), making these systems crucial contributors to coastal primary productivity (Underwood & Kromkamp, 1999).



Figure 6. High amount of total suspended solids (TSS) can be seen in the turbidity of the water of the Bay of Cadiz after a wind-storm event (**A**), and also discharged from the Guadalquivir River to the Atlantic Ocean (**B**) (NASA AQUA satellite image taken in 2012 for the Sen2Coast project.)

1.4.2. Guadalquivir Estuary

In southeastern Europe, the most important estuary is the Guadalquivir, included within the Doñana Nature Reserve, whose marshes are a protected area due to their great importance in terms of primary production and biodiversity within Europe. It was declared a biosphere reserve in 1981 and awarded the Council of Europe Diploma for Conservation four years later in 1985 and became a UNESCO World Heritage Site in 1994. Doñana is part of the Natura 2000 Network, the RAMSAR Convention and the European Charter for Sustainable Tourism (Rodríguez-Ramírez et al., 2019; Ruiz et al., 2015).

The Guadalquivir Estuary is crucial for both human and ecological functions, largely shaped by tidal forces, freshwater inputs, and wind (Ruiz et al., 2015). Characterized by mesotidal fluctuations of up to 3.5 meters and peak tidal currents near 1 m/s, the estuary experiences high concentration of total suspended solids (TSS) due to geomorphological conditions, relatively low freshwater flow and land use in its watershed (Flecha et al., 2015). These factors lead to prolonged water residence times and extensive sediment plumes (Figure 6B) into the Gulf of Cadiz (Barbier et al., 2011; Gomiz-Pascual et al., 2021). This high TSS concentration restricts light penetration, limiting primary production by phytoplankton and creating an oxygen-deficient water column dominated by respiration (Díez-Minguito & De Swart, 2020; Miró et al., 2022).

The inputs of nutrients to the Guadalquivir estuary, which come from intensive agriculture (due to fertilizers use (Ribas-Ribas et al., 2013) and/or urban runoff, drive autotrophic microbial activity. This increased activity consumes dissolved oxygen, creating anoxic conditions that promote denitrification, a key pathway for N_2O production (Sánchez-Rodríguez et al., 2022; Sánchez-Rodríguez et al., 2024). Climatic variables such as temperature or humidity modulate these processes, thus affecting oxygen availability. As a result, the estuary shows a negative net metabolic balance characterized by elevated CO_2 levels (Flecha et al., 2015; Sánchez-Rodríguez et al., 2022; Sánchez-Rodríguez et al., 2024b). So far, the study of this O_2-CO_2 balance in the estuary has never considered the effect of the microphytobenthic community's metabolism present in the shores of the estuary.

1.5. Aims of study

The general aim of this Ph. D. Thesis was to investigate the impact of extreme weather events (heat waves and wind storms) on the microbial ecology and biogeochemistry of intertidal flats sediments of Cadiz Bay, and to study the seasonal dynamics of microphytobenthos and the mineralization of organic matter in tidal flats of the Guadalquivir Estuary, as contrasting models of shallow coastal environments in the South of Europe. In this work we aimed to elucidate how heatwaves induce significant biogeochemical shifts, altering net metabolism, nutrient fluxes, and greenhouse gas dynamics of shallow sediments of the Bay of Cadiz. This study shows the vulnerability of these ecosystems to rising temperatures and highlights the complex responses of biogeochemical processes under thermal stress. In addition, we also explored the effects of windstorms on intertidal microbial communities, dominated by microphytobenthos, revealing the changes induced by the turbulent conditions in their functioning and the biogeochemical impacts occurring at the whole Bay caused by the sediment resuspension. Finally, we investigated the role of microphytobenthos, the benthic metabolism and nutrient dynamics in intertidal flats of the hyperturbid and hypernutrified Guadalquivir Estuary. Specifically, the interactions between the autochthonous production by MPB and the mineralization of organic matter and nutrient cycling in this estuarine environment. Our findings showed for the first time the role of intertidal sediment of the estuary's as biogeochemical hotspots, where sediment-water exchanges play a pivotal role in nutrient cycling and ecosystem productivity. The study highlighted the crucial contribution of MPB primary production for overall productivity of the Guadalquivir Estuary. Together, these interconnected studies provide a comprehensive understanding of how shallow coastal ecosystems respond to and recover from environmental stresses imposed by both extreme weather events and estuarine dynamics.

The present thesis was developed around two main hypotheses:

Hypothesis 1: Microbial processes and biogeochemistry of intertidal sediments are strongly affected by extreme climatic events such as heat waves and windstorms that impact coastal ecosystems such as the Bay of Cadiz with increasing frequency.

Hypothesis 2: Microphytobenthos communities inhabiting the sediment of the Guadalquivir River estuary play a key role in the primary production and nutrient

recycling of the estuary, significantly influencing the biogeochemistry of the system and exhibiting a seasonal pattern.

To validate these hypotheses, the following objectives were established:

Objective 1: To evaluate the effects of two types of extreme climatic events (windstorms and heat waves) on the ecological and biogeochemical characteristics of intertidal sediments and the water column in the Bay of Cadiz

Specific objective I: To investigate the effect of prolonged high temperature exposure on net metabolism, nutrient dynamics, production and/or release of greenhouse gases in the intertidal sediments of the Bay of Cadiz.

Specific objective II: To evaluate the effect of windstorms on resuspension, net metabolism, microphytobenthic biomass in the intertidal zone and on nutrient dynamics in the sediment and water column of the Bay of Cadiz.

Objective 2: To monitor seasonal and spatial variations in MPB biomass and net metabolism, nutrient concentrations and sediment-water fluxes to assess the ecological and biogeochemical roles of intertidal sediments in the Guadalquivir River estuary.

Specific objective III: To investigate and assess seasonally the changes in biogeochemistry and nutrient dynamics in the intertidal mudflats of the Guadalquivir Estuary.

Specific objective IV: To investigate and assess seasonally the relevance of the microphytobenthic community in the intertidal mudflats of the Guadalquivir Estuary.

1.5. Objetivos del estudio

El objetivo general de esta Tesis Doctoral fue investigar el impacto de eventos climáticos extremos (olas de calor y temporales de viento) sobre la ecología microbiana y la biogeoquímica de los sedimentos de las llanuras intermareales de la Bahía de Cádiz, así como estudiar la dinámica estacional del microfitobentos y la mineralización de la materia orgánica en las llanuras mareales del estuario del Guadalquivir, como modelos contrastados de ambientes costeros someros del Sur de Europa. En este trabajo pretendemos dilucidar cómo las olas de calor inducen cambios biogeoquímicos significativos, alterando el metabolismo neto, los flujos de nutrientes y la dinámica de gases de efecto invernadero de los sedimentos someros de la Bahía de Cádiz. Este estudio muestra la vulnerabilidad de estos ecosistemas al aumento de temperaturas y pone de manifiesto las complejas respuestas de los procesos biogeoquímicos bajo estrés térmico. Además, también exploramos los efectos de los temporales de viento sobre las comunidades microbianas intermareales, dominadas por microfitobentos, revelando los cambios inducidos por las condiciones turbulentas en su funcionamiento y los impactos biogeoquímicos que se producen en toda la Bahía causados por la resuspensión de sedimentos. Finalmente, investigamos el papel del microfitobentos, el metabolismo bentónico y la dinámica de nutrientes en las planicies intermareales del estuario hiperturbio e hipernutrido del Guadalquivir. En concreto, las interacciones entre la producción autóctona por MPB y la mineralización de la materia orgánica y el ciclo de nutrientes en este ambiente estuarino. Los resultados mostraron por primera vez el papel de los sedimentos intermareales del estuario como puntos calientes biogeoquímicos, donde los intercambios sedimento-agua juegan un papel fundamental en el ciclo de nutrientes y la productividad del ecosistema. El estudio destacó la contribución crucial de la producción primaria de MPB para la productividad global del estuario del Guadalquivir. En conjunto, estos estudios interconectados proporcionan una comprensión global de cómo los ecosistemas costeros poco profundos responden y se recuperan de las tensiones ambientales impuestas tanto por los fenómenos meteorológicos extremos como por la dinámica estuarina.

La presente tesis se ha desarrollado en torno a dos hipótesis principales:

Hipótesis 1: Los procesos microbianos y la biogeoquímica de los sedimentos intermareales se ven fuertemente afectados por eventos climáticos extremos como olas de calor y temporales de viento que impactan con creciente frecuencia en ecosistemas costeros como la Bahía de Cádiz.

Hipótesis 2: Las comunidades de microfitobentos que habitan el sedimento del estuario del río Guadalquivir juegan un papel clave en la producción primaria y el reciclaje de nutrientes del estuario, influyendo significativamente en la biogeoquímica del sistema y mostrando un patrón estacional.

Para validar estas hipótesis, se establecieron los siguientes objetivos:

Objetivo 1: Evaluar los efectos de dos tipos de eventos climáticos extremos (temporales de viento y olas de calor) sobre las características ecológicas y biogeoquímicas de los sedimentos intermareales y la columna de agua de la Bahía de Cádiz.

Objetivo específico I: Investigar el efecto de la exposición prolongada a altas temperaturas sobre el metabolismo neto, la dinámica de nutrientes, la producción y/o liberación de invernadero en los sedimentos intermareales de la Bahía de Cádiz.

Objetivo específico II: Evaluar el efecto de los temporales de viento sobre la resuspensión, el metabolismo neto, la biomasa microfitobentónica en la zona intermareal y sobre la dinámica de nutrientes en el sedimento y la columna de agua de la Bahía de Cádiz.

Objetivo 2: Monitorizar las variaciones estacionales y espaciales en la biomasa y metabolismo neto de MPB, concentraciones de nutrientes y flujos sedimento-agua para evaluar el papel ecológico y biogeoquímico de los sedimentos intermareales en el estuario del Guadalquivir.

Objetivo específico III: Investigar y evaluar estacionalmente los cambios en la biogeoquímica y la dinámica de nutrientes en las marismas intermareales del estuario del Guadalquivir.

Objetivo específico IV: Investigar y evaluar estacionalmente la relevancia de la comunidad microfitobentónica en las marismas intermareales del estuario del Guadalquivir.

References

Admiraal, W. (1984). *The ecology of estuarine sediment-inhabiting diatoms*. *3*, 269-322.

Aleem, A. A. (1950). The diatom community inhabiting the mud-flats at Whitstable. *New Phytologist*, *49*(2), 174-188. https://doi.org/10.1111/j.1469-8137.1950.tb07503.x

Apple, J., Del Giorgio, P., & Kemp, W. (2006). Temperature regulation of bacterial production, respiration, and growth efficiency in a temperate salt-marsh estuary. *Aquatic Microbial Ecology*, *43*, 243-254. https://doi.org/10.3354/ame043243

Aspden, R. J., Vardy, S., & Paterson, D. M. (2004). Salt Marsh Microbial Ecology: Microbes, Benthic Mats and Sediment Movement. En S. Fagherazzi, M. Marani, & L. K. Blum (Eds.), *Coastal and Estuarine Studies* (pp. 115-136). American Geophysical Union. https://doi.org/10.1029/CE059p0115

Barbier, E. B., Hacker, S. D., Kennedy, C., Koch, E. W., Stier, A. C., & Silliman, B. R. (2011). The value of estuarine and coastal ecosystem services. *Ecological Monographs*, *81*(2), 169-193. https://doi.org/10.1890/10-1510.1

Blanchard, G., Guarini, J., Richard, P., Gros, P., & Mornet, F. (1996). Quantifying the short-term temperature effect on light-saturated photosynthesis of intertidal microphytobenthos. *Marine Ecology Progress Series*, *134*, 309-313. https://doi.org/10.3354/meps134309

Bohórquez, J., McGenity, T. J., Papaspyrou, S., García-Robledo, E., Corzo, A., & Underwood, G. J. C. (2017). Different Types of Diatom-Derived Extracellular Polymeric Substances Drive Changes in Heterotrophic Bacterial Communities from Intertidal Sediments. *Frontiers in Microbiology*, *8*. https://doi.org/10.3389/fmicb.2017.00245

Canfield, D. E. (2005). *Aquatic geomicrobiology*. Elsevier.

Cartaxana, P., Cruz, S., Gameiro, C., & Kühl, M. (2016). Regulation of Intertidal Microphytobenthos Photosynthesis Over a Diel Emersion Period Is Strongly Affected by Diatom Migration Patterns. *Frontiers in Microbiology*, *7*. https://doi.org/10.3389/fmicb.2016.00872

Consalvey, M., Paterson, D. M., & Underwood, G. J. C. (2004). The ups and downs of life in a benthic biofilm: Migration of benthic diatoms. *Diatom Research*, *19*(2), 181-202. https://doi.org/10.1080/0269249X.2004.9705870

Cooley, Schoeman, D., Bopp, L., Boyd, P., Donner, S., Ghebrehiwet, D. Y., Ito, S.-I., Kiessling, W., Martinetto, P., Ojea, E., Racault, M.-F., Rost, B., & Skern-Mauritzen, M. (2023). Oceans and Coastal Ecosystems and Their Services. En *Climate Change 2022 – Impacts, Adaptation and Vulnerability: Working Group II Contribution to the Sixth Assessment Report of the Intergovernmental Panel on Climate Change* (1.ª ed.). Cambridge University Press. https://doi.org/10.1017/9781009325844

Corzo, A., Van Bergeijk, S., & García-Robledo, E. (2009). Effects of green macroalgal blooms on intertidal sediments: Net metabolism and carbon and nitrogen contents. *Marine Ecology Progress Series*, *380*, 81-93. https://doi.org/10.3354/meps07923

Díez-Minguito, M., & De Swart, H. E. (2020). Relationships Between Chlorophyll-a and Suspended Sediment Concentration in a High-Nutrient Load Estuary: An Observational and Idealized Modeling Approach. *Journal of Geophysical Research: Oceans*, *125*(3), e2019JC015188. https://doi.org/10.1029/2019JC015188

Duff, S., & Teal, J. M. (1965). Temperature change and gas exchange in Nova Scotia and Georgia salt-marsh muds. *Limnology and Oceanography*, *10*(1), 67-73. https://doi.org/10.4319/lo.1965.10.1.0067

Dyer, K. R., Christie, M. C., Feates, N., Fennessy, M. J., Pejrup, M., & Van Der Lee, W. (2000). An Investigation into Processes Influencing the Morphodynamics of an Intertidal Mudflat, the Dollard Estuary, The Netherlands: I. Hydrodynamics and Suspended Sediment. *Estuarine, Coastal and Shelf Science*, *50*(5), 607-625. https://doi.org/10.1006/ecss.1999.0596

Easterling, D. R., Meehl, G. A., Parmesan, C., Changnon, S. A., Karl, T. R., & Mearns, L. O. (2000). Climate Extremes: Observations, Modeling, and Impacts. *Science*, *289*(5487), 2068-2074. https://doi.org/10.1126/science.289.5487.2068

Feser, F., Barcikowska, M., Krueger, O., Schenk, F., Weisse, R., & Xia, L. (2015). Storminess over the North Atlantic and northwestern Europe—A review. *Quarterly Journal of the Royal Meteorological Society*, *141*(687), 350-382. https://doi.org/10.1002/qj.2364

Fierer, N., Colman, B. P., Schimel, J. P., & Jackson, R. B. (2006). Predicting the temperature dependence of microbial respiration in soil: A continental-scale analysis. *Global Biogeochemical Cycles*, *20*(3), 2005GB002644. https://doi.org/10.1029/2005GB002644

Flecha, S., Huertas, I. E., Navarro, G., Morris, E. P., & Ruiz, J. (2015). Air–Water CO2 Fluxes in a Highly Heterotrophic Estuary. *Estuaries and Coasts*, *38*(6), 2295-2309. https://doi.org/10.1007/s12237-014-9923-1

Frölicher, T. L., & Laufkötter, C. (2018). Emerging risks from marine heat waves. *Nature Communications*, *9*(1), 650. https://doi.org/10.1038/s41467-018-03163-6

Froneman, P. W. (2005). Biogeochemistry of Marine Systems. *African Journal of Aquatic Science*, *30*(1), 91-91. https://doi.org/10.2989/16085910509503840

Garcia-Robledo, E., Bohorquez, J., Corzo, A., Jimenez-Arias, J. L., & Papaspyrou, S. (2016). Dynamics of Inorganic Nutrients in Intertidal Sediments: Porewater, Exchangeable, and Intracellular Pools. *Frontiers in Microbiology*, *7*. https://doi.org/10.3389/fmicb.2016.00761

Glud, R. N. (2008). Oxygen dynamics of marine sediments. *Marine Biology Research*, *4*(4), 243-289. https://doi.org/10.1080/17451000801888726

Gomiz-Pascual, J. J., Bolado-Penagos, M., Gonzalez, C. J., Vazquez, A., Buonocore, C., Romero-Cozar, J., Perez-Cayeiro, M. L., Izquierdo, A., Alvarez, O., Mañanes, R., & Bruno, M. (2021). The fate of Guadalquivir River discharges in the coastal strip of the Gulf of Cádiz. A study based on the linking of watershed catchment and hydrodynamic models. *Science of The Total Environment*, *795*, 148740. https://doi.org/10.1016/j.scitotenv.2021.148740

Ha, H. J., Kim, H., Kwon, B.-O., Khim, J. S., & Ha, H. K. (2020). Influence of tidal forcings on microphytobenthic resuspension dynamics and sediment fluxes in a disturbed coastal environment. *Environment International*, *139*, 105743. https://doi.org/10.1016/j.envint.2020.105743

Hancke, K., & Glud, R. (2004). Temperature effects on respiration and photosynthesis in three diatom-dominated benthic communities. *Aquatic Microbial Ecology*, *37*, 265-281. https://doi.org/10.3354/ame037265

Haro, S., Bohórquez, J., Lara, M., Garcia-Robledo, E., González, C. J., Crespo, J. M., Papaspyrou, S., & Corzo, A. (2019). Diel patterns of microphytobenthic primary production in intertidal sediments: The role of photoperiod on the vertical migration circadian rhythm. *Scientific Reports*, *9*(1), 13376. https://doi.org/10.1038/s41598-019-49971-8

Haro, S., Lara, M., Laiz, I., González, C. J., Bohórquez, J., Garcia-Robledo, E., Corzo, A., & Papaspyrou, S. (2020). Microbenthic Net Metabolism Along Intertidal Gradients (Cadiz Bay, SW Spain): Spatio-Temporal Patterns and Environmental Factors. *Frontiers in Marine Science*, *7*, 39. https://doi.org/10.3389/fmars.2020.00039

Hicks, N., Liu, X., Gregory, R., Kenny, J., Lucaci, A., Lenzi, L., Paterson, D. M., & Duncan, K. R. (2018). Temperature Driven Changes in Benthic Bacterial Diversity Influences Biogeochemical Cycling in Coastal Sediments. *Frontiers in Microbiology*, *9*, 1730. https://doi.org/10.3389/fmicb.2018.01730

Hope, J. A., Paterson, D. M., & Thrush, S. F. (2020). The role of microphytobenthos in soft-sediment ecological networks and their contribution to the delivery of multiple ecosystem services. *Journal of Ecology*, *108*(3), 815-830. https://doi.org/10.1111/1365-2745.13322

Hopkinson, C. S., Wolanski, E., Cahoon, D. R., Perillo, G. M. E., & Brinson, M. M. (2019). Coastal Wetlands. En *Coastal Wetlands* (pp. 1-75). Elsevier. https://doi.org/10.1016/B978-0-444-63893-9.00001-0

Irigoien, X., & Castel, J. (1997). Light Limitation and Distribution of Chlorophyll Pigments in a Highly Turbid Estuary: The Gironde (SW France). *Estuarine, Coastal and Shelf Science*, *44*, 507-517.

Jiménez-Arias, J. L., Morris, E., Rubio-de-Inglés, M. J., Peralta, G., García-Robledo, E., Corzo, A., & Papaspyrou, S. (2020). Tidal elevation is the key factor modulating burial rates and composition of organic matter in a coastal wetland with multiple habitats. *Science of The Total Environment*, *724*, 138205. https://doi.org/10.1016/j.scitotenv.2020.138205

Jørgensen, B. B., & Revsbech, N. P. (1985). Diffusive boundary layers and the oxygen uptake of sediments and detritus1. *Limnology and Oceanography*, *30*(1), 111-122. https://doi.org/10.4319/lo.1985.30.1.0111

Kauppi, L., & Villnäs, A. (2022). Marine heatwaves of differing intensities lead to distinct patterns in seafloor functioning. *Proceedings of the Royal Society B: Biological Sciences*, *289*(1986), 20221159. https://doi.org/10.1098/rspb.2022.1159

Kristensen, E. (2000). Organic matter diagenesis at the oxic/anoxic interface in coastal marine sediments, with emphasis on the role of burrowing animals. En G. Liebezeit, S. Dittmann, & I. Kröncke (Eds.), *Life at Interfaces and Under Extreme Conditions* (pp. 1-24). Springer Netherlands. https://doi.org/10.1007/978-94-011-4148-2_1

Kromkamp, J. (Ed.). (2006). *Functioning of microphytobenthos in estuaries*. Royal Netherlands Academy of Arts and Sciences.

Kühl, M., Lassen, C., & Jorgensen, B. (1994). Light penetration and light intensity in sandy marine sediments measured with irradiance and scalar irradiance fiber-optic microprobes. *Marine Ecology Progress Series*, *105*, 139-148. https://doi.org/10.3354/meps105139

Kwon, B.-O., Kim, H., Noh, J., Lee, S. Y., Nam, J., & Khim, J. S. (2020). Spatiotemporal variability in microphytobenthic primary production across bare intertidal flat, saltmarsh, and mangrove forest of Asia and Australia. *Marine Pollution Bulletin*, *151*, 110707. https://doi.org/10.1016/j.marpolbul.2019.110707

Laviale, M., Barnett, A., Ezequiel, J., Lepetit, B., Frankenbach, S., Méléder, V., Serôdio, J., & Lavaud, J. (2015). Response of intertidal benthic microalgal biofilms to a coupled light–temperature stress: Evidence for latitudinal adaptation along the A tlantic coast of S outhern E urope. *Environmental Microbiology*, *17*(10), 3662-3677. https://doi.org/10.1111/1462-2920.12728

Li, J., Qu, W., Han, G., Lu, F., Zhou, Y., Song, W., Xie, B., & Eller, F. (2020). Effects of Drying-Rewetting Frequency on Vertical and Lateral Loss of Soil Organic Carbon in a Tidal Salt Marsh. *Wetlands*, *40*(5), 1433-1443. https://doi.org/10.1007/s13157-020-01286-5

Liu, K., Xiao, X., Zhang, D., Ding, Y., Li, L., & Zhao, M. (2021). Quantitative estimates of organic carbon contributions to the river-estuary-marine system in the Jiaozhou Bay, China. *Ecological Indicators*, *129*, 107929. https://doi.org/10.1016/j.ecolind.2021.107929

MacIntyre, H. L., Geider, R. J., & Miller, D. C. (1996). Microphytobenthos: The Ecological Role of the «Secret Garden» of Unvegetated, Shallow-Water Marine Habitats. I. Distribution, Abundance and Primary Production. *Estuaries*, *19*(2), 186. https://doi.org/10.2307/1352224

Middelburg, J. J., Barranguet, C., Boschker, H. T. S., Herman, P. M. J., Moens, T., & Heip, C. H. R. (2000). The fate of intertidal microphytobenthos carbon: An in situ ^{13}C-labeling study. *Limnology and Oceanography*, *45*(6), 1224-1234. https://doi.org/10.4319/lo.2000.45.6.1224

Migné, A., Spilmont, N., Boucher, G., Denis, L., Hubas, C., Janquin, M.-A., Rauch, M., & Davoult, D. (2009). Annual budget of benthic production in Mont Saint-Michel Bay considering cloudiness, microphytobenthos migration, and variability of respiration rates with tidal conditions. *Continental Shelf Research*, *29*(19), 2280-2285. https://doi.org/10.1016/j.csr.2009.09.004

Miró, J. M., Megina, C., Donázar-Aramendía, I., & García-Gómez, J. C. (2022). Effects of maintenance dredging on the macrofauna of the water column in a turbid estuary. *Science of The Total Environment*, *806*, 151304. https://doi.org/10.1016/j.scitotenv.2021.151304

Morris, E. P., & Kromkamp, J. C. (2003). Influence of temperature on the relationship between oxygen- and fluorescence-based estimates of photosynthetic parameters in a marine benthic diatom *(Cylindrotheca closterium)*. *European Journal of Phycology*, *38*(2), 133-142. https://doi.org/10.1080/0967026031000085832

Nybakken, J. W., & Bertness, M. D. (2005). *Marine biology: An ecological approach* (6. ed., [student's ed.], [Nachdr.]). Pearson/Benjamin Cummings.

Paerl, H. W., & Paul, V. J. (2012). Climate change: Links to global expansion of harmful cyanobacteria. *Water Research*, *46*(5), 1349-1363. https://doi.org/10.1016/j.watres.2011.08.002

Parmesan, C., Morecroft, M. D., & Trisurat, Y. (2022). *Climate Change 2022:Impacts, Adaptation and Vulnerability*.

Parmesan, C., & Yohe, G. (2003). A globally coherent fingerprint of climate change impacts across natural systems. *Nature*, *421*(6918), 37-42. https://doi.org/10.1038/nature01286

Paterson, D. M., Fortune, I., Aspden, R. J., & Black, K. S. (2019). Intertidal Flats. En *Coastal Wetlands* (pp. 383-406). Elsevier. https://doi.org/10.1016/B978-0-444-63893-9.00011-3

Perkins-Kirkpatrick, S. E., & Lewis, S. C. (2020). Increasing trends in regional heatwaves. *Nature Communications*, *11*(1), 3357. https://doi.org/10.1038/s41467-020-16970-7

Pivato, M., Carniello, L., Moro, I., & D'Odorico, P. (2019). On the feedback between water turbidity and microphytobenthos growth in shallow tidal environments. *Earth Surface Processes and Landforms*, *44*(5), 1192-1206. https://doi.org/10.1002/esp.4567

Price, P. B., & Sowers, T. (2004). Temperature dependence of metabolic rates for microbial growth, maintenance, and survival. *Proceedings of the National Academy of Sciences*, *101*(13), 4631-4636. https://doi.org/10.1073/pnas.0400522101

Rahman, M., Grace, M. R., Roberts, K. L., Kessler, A. J., & Cook, P. L. M. (2019). Effect of temperature and drying-rewetting of sediments on the partitioning between denitrification and DNRA in constructed urban stormwater wetlands. *Ecological Engineering*, *140*, 105586. https://doi.org/10.1016/j.ecoleng.2019.105586

Revsbech, N. P., & Jørgensen, B. B. (1986). Microelectrodes: Their Use in Microbial Ecology. En K. C. Marshall (Ed.), *Advances in Microbial Ecology* (Vol. 9, pp. 293-352). Springer US. https://doi.org/10.1007/978-1-4757-0611-6_7

Ribas-Ribas, M. (2011). Spatio-temporal variability of the dissolved organic carbon and nitrogen in a coastal area affected by river input: The north eastern shelf of the Gulf of Cádiz (SW Iberian Peninsula). *Marine Chemistry*.

Ribas-Ribas, M., Anfuso, E., Gómez-Parra, A., & Forja, J. M. (2013). Tidal and seasonal carbon and nutrient dynamics of the Guadalquivir estuary and the Bay of Cádiz (SW Iberian Peninsula). *Biogeosciences*, *10*(7), 4481-4491. https://doi.org/10.5194/bg-10-4481-2013

Risgaard-Petersen, N. (2003). Coupled nitrification-denitrification in autotrophic and heterotrophic estuarine sediments: On the influence of benthic microalgae. *Limnology and Oceanography*, *48*(1), 93-105. https://doi.org/10.4319/lo.2003.48.1.0093

Rodríguez-Ramírez, A., Villarías-Robles, J. J. R., Pérez-Asensio, J. N., & Celestino-Pérez, S. (2019). The Guadalquivir Estuary: Spits and Marshes. En J. A. Morales (Ed.), *The Spanish Coastal Systems* (pp. 517-541). Springer International Publishing. https://doi.org/10.1007/978-3-319-93169-2_22

Ruiz, J., Polo, M. J., Díez-Minguito, M., Navarro, G., Morris, E. P., Huertas, E., Caballero, I., Contreras, E., & Losada, M. A. (2015). The Guadalquivir Estuary: A Hot Spot for Environmental and Human Conflicts. En C. W. Finkl & C. Makowski (Eds.), *Environmental Management and Governance* (Vol. 8, pp. 199-232). Springer International Publishing. https://doi.org/10.1007/978-3-319-06305-8_8

Sánchez-Rodríguez, J., Sierra, A., Jiménez-López, D., Ortega, T., Gómez-Parra, A., & Forja, J. (2022). Dynamic of CO2, CH4 and N2O in the Guadalquivir estuary. *Science of The Total Environment*, *805*, 150193. https://doi.org/10.1016/j.scitotenv.2021.150193

Sánchez-Rodríguez, J., Sierra, A., Moreno, S., Forja, J., & Ortega, T. (2024). Nitrous oxide variability along an estuary influenced by agricultural land use (Guadalquivir estuary, SW Spain). *Marine Chemistry*, *267*, 104467. https://doi.org/10.1016/j.marchem.2024.104467

Sánchez-Rodríguez, J., Sirviente, S., Sierra, A., Gómiz-Pascual, J. J., Bolado-Penagos, M., Bruno, M., Forja, J., & Ortega, T. (2024). Buffer properties in the Guadalquivir Estuary (SW Iberian Peninsula). *Estuarine, Coastal and Shelf Science*, *309*, 108983. https://doi.org/10.1016/j.ecss.2024.108983

Savelli, R., Bertin, X., Orvain, F., Gernez, P., Dale, A., Coulombier, T., Pineau, P., Lachaussée, N., Polsenaere, P., Dupuy, C., & Le Fouest, V. (2019). Impact of Chronic and Massive Resuspension Mechanisms on the Microphytobenthos Dynamics in a Temperate Intertidal Mudflat. *Journal of Geophysical Research: Biogeosciences*, *124*(12), 3752-3777. https://doi.org/10.1029/2019JG005369

Schutte, C. A., Ahmerkamp, S., Wu, C. S., Seidel, M., De Beer, D., Cook, P. L. M., & Joye, S. B. (2019). Biogeochemical Dynamics of Coastal Tidal Flats. En *Coastal Wetlands* (pp. 407-440). Elsevier. https://doi.org/10.1016/B978-0-444-63893-9.00012-5

Sundbäck, K., & Granéli, W. (1988). Influence of microphytobenthos on the nutrient flux between sediment and water- a laboratory study. *Marine Ecology Progress Series*, *43*, 63-69. https://doi.org/10.3354/meps043063

Sundbäck, K., & Miles, A. (2002). Role of microphytobenthos and denitrification for nutrient turnover in embayments with floating macroalgal mats: A spring situation. *Aquatic Microbial Ecology*, *30*, 91-101. https://doi.org/10.3354/ame030091

Sundbäck, K., Miles, A., & Göransson, E. (2000). Nitrogen fluxes, denitrification and the role of microphytobenthos in microtidal shallow-water sediments:an annual study. *Marine Ecology Progress Series*, *200*, 59-76. https://doi.org/10.3354/meps200059

Thamdrup, B., Hansen, J. W., & JÃ¸rgensen, B. B. (1998). Temperature dependence of aerobic respiration in a coastal sediment. *FEMS Microbiology Ecology*, *25*(2), 189-200. https://doi.org/10.1111/j.1574-6941.1998.tb00472.x

Tolhurst, T. J., Friend, P. L., Watts, C., Wakefield, R., Black, K. S., & Paterson, D. M. (2006). The effects of rain on the erosion threshold of intertidal cohesive sediments. *Aquatic Ecology*, *40*(4), 533-541. https://doi.org/10.1007/s10452-004-8058-z

Tolhurst, T. J., Gust, G., & Paterson, D. M. (2002). The influence of an extracellular polymeric substance (EPS) on cohesive sediment stability. En *Proceedings in Marine Science* (Vol. 5, pp. 409-425). Elsevier. https://doi.org/10.1016/S1568-2692(02)80030-4

Ubertini, M., Lefebvre, S., Gangnery, A., Grangeré, K., Le Gendre, R., & Orvain, F. (2012). Spatial Variability of Benthic-Pelagic Coupling in an Estuary Ecosystem: Consequences for Microphytobenthos Resuspension Phenomenon. *PLoS ONE*, *7*(8), e44155. https://doi.org/10.1371/journal.pone.0044155

Ummenhofer, C. C., & Meehl, G. A. (2017). Extreme weather and climate events with ecological relevance: A review. *Philosophical Transactions of the Royal Society B: Biological Sciences*, *372*(1723), 20160135. https://doi.org/10.1098/rstb.2016.0135

Underwood, G. J. C., & Kromkamp, J. (1999). Primary Production by Phytoplankton and Microphytobenthos in Estuaries. En *Advances in Ecological Research* (Vol. 29, pp. 93-153). Elsevier. https://doi.org/10.1016/S0065-2504(08)60192-0

Underwood, G. J. C., & Paterson, D. M. (1993). *Seasonal changes in diatom biomass, sediment stability and biogenic stabilization in the Severn Estuary*. *73*, 871-887.

Van Der Wal, D., Wielemaker-van Den Dool, A., & Herman, P. M. J. (2010). Spatial Synchrony in Intertidal Benthic Algal Biomass in Temperate Coastal and Estuarine Ecosystems. *Ecosystems*, *13*(2), 338-351. https://doi.org/10.1007/s10021-010-9322-9

Vargas, J. M., Garćia-Lafuente, J., Delgado, J., & Criado, F. (2003). Seasonal and wind-induced variability of Sea Surface Temperature patterns in the Gulf of Cádiz. *Journal of Marine Systems*, *38*(3-4), 205-219. https://doi.org/10.1016/S0924-7963(02)00240-3

Voynova, Y. G., Brix, H., Petersen, W., Weigelt-Krenz, S., & Scharfe, M. (2017). Extreme flood impact on estuarine and coastal biogeochemistry: The 2013 Elbe flood. *Biogeosciences*, *14*(3), 541-557. https://doi.org/10.5194/bg-14-541-2017

Zhang, Q., & Blomquist, J. D. (2018). Watershed export of fine sediment, organic carbon, and chlorophyll-a to Chesapeake Bay: Spatial and temporal patterns in 1984–2016. *Science of The Total Environment*, *619-620*, 1066-1078. https://doi.org/10.1016/j.scitotenv.2017.10.279



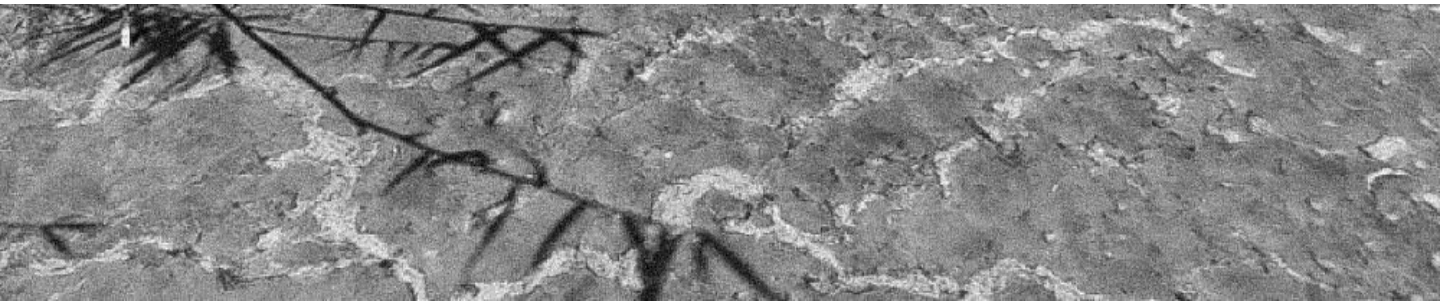
Chapter 2:

Benthic metabolism and nutrient dynamics of a hyperturbid and hypernutrified estuary

Published in Frontiers in Marine Science 26 July 2024

Front. Mar. Sci. 11:1389673.

doi: 10.3389/fmars.2024.138967



Benthic metabolism and nutrient dynamics of an hyperturbid and hypernutrified estuary

Valle Perez-Rodriguez[1,2*], Alfonso Corzo[1,2], Sokratis Papaspyrou[1,2], Stefanie Anne van Bergeijk[3], Cesar Vilas[3], Pedro Cañavate[3], Emilio Garcia-Robledo[1,2]

[1]Microbial Ecology and Biogeochemistry laboratory, Department of Biology, Faculty of Marine and Environmental Science, University of Cadiz, Pol. Río San Pedro s/n, Puerto Real, Spain

[2]Instituto Universitario de Investigación Marina (INMAR), Campus Universitario de Puerto Real, 11510, Cadiz, Spain

[3]IFAPA Centro El Toruño Ctra. N IV Madrid-Cádiz, km 654a Camino de Tiro Pichón, 11500 El Puerto de Santa María, Spain

Keywords: Guadalquivir estuary, Hyperturbid estuary, Seasonal variations, Microphytobenthos, Nutrients uptake, Sediment-water column fluxes

Abstract

The biogeochemical role of the sediments in the Guadalquivir River estuary, a vital region in the SW Iberian Peninsula, has been considerably neglected. The benthic microalgae (microphytobenthos, MPB) inhabiting the sediment surface could contribute to the autochthonous primary production and influence nutrient recycling in this hyper-turbid and hypernutrified estuary. Sediment-water column fluxes of O_2 and dissolved inorganic nitrogen species (DIN=NH_4^++NO_3^-+NO_2^-) were assessed in laboratory incubations of sediment cores from Bonanza (mouth) and Lebrija (middle) during a one-year study. Vertical profiles down to 10 cm depth of photosynthetic pigments, organic C, total nitrogen, DIN, Fe^{2+}, SO_4^{2-}, and dissolved inorganic carbon (DIC) were also measured. Chlorophyll *a* in the sediment surface was higher at the estuarine mouth, exhibiting a seasonal pattern at both sites with highest values in winter and lowest in summer. Net community production (NCP) was higher in Bonanza compared to Lebrija and showed positive values most of the year, indicating that MPB contributed to the overall autochthonous primary production of the estuary. Seasonal changes in chlorophyll *a* and NCP were not parallel, suggesting different ecological controls. The sediment was generally a net sink of NO_3^- and NH_4^+ in both sites, with several fold higher rates for NO_3^- uptake. MPB N-demand could account for the entire sediment DIN uptake in Bonanza and 21% in Lebrija. The remaining high NO_3^- uptake rates indicate that they sustain elevated sediment denitrification rates. In contrast, rates of anaerobic oxidation of organic matter by Fe-reduction and SO_4^{2-}-reduction, estimated from Fe^{2+} and SO_4^{2-} vertical concentration profiles, were several orders of magnitude lower than the estimated water column-dependent denitrification rates. Overall, this study shows

the importance of MPB in the Guadalquivir Estuary and the potential dominant role of denitrification in the anaerobic mineralization of organic matter.

1. Introduction

Coastal systems play a pivotal role in global biogeochemical cycles, buffering the exchange of matter and energy across terrestrial, oceanic, and atmospheric compartments. Among these systems, estuarine regions are renowned for their elevated productivity, driven by the influx of organic and inorganic matter from rivers and the autochthonous primary productivity of diverse organisms (Underwood & Kromkamp, 1999). The Guadalquivir Estuary, located in the Gulf of Cadiz (southwestern Spain), extends approximately 110 kilometers from its mouth to the Alcalá del Río dam, Seville. It is one of the region's most ecologically and economically important estuaries, despite undergoing significant anthropogenic alterations since historical times. Such activities include urban and agricultural waste and recurrent dredging, which result in elevated turbidity and very high nutrient concentrations in the water column (Díez-Minguito & de Swart, 2020; Miró et al., 2022; Ruiz et al., 2017). Nitrate concentrations higher than 500 µM are frequently recorded at the head of Guadalquivir Estuary (Flecha et al., 2015; Mendiguchía et al., 2007). High concentration of suspended particulate matter is been also frequently observed (> 500 mg L^{-1}) reaching up to 30 g L^{-1} during an extreme turbidity event (Megina et al., 2023). This high turbidity affects various component of the biological community such as the macrofauna and small fishes (Donázar-Aramendía et al., 2019; Miró et al., 2020, 2022). In addition, the very high turbidity, which significantly reduces the photic layer, limits autochthonous phytoplankton primary production resulting in a net heterotrophic water column (Flecha et al., 2015; Huertas et al., 2018; Ruiz et al., 2017; Soetaert et al., 2006). However, the intertidal sediments in the Guadalquivir River banks are inhabited by a conspicuous benthic microalgal community known as microphytobenthos (MPB), which might contribute significantly to the autochthonous primary production within the estuary explaining part of its high productivity (Díez-Minguito & de Swart, 2020; Donázar-Aramendía et al., 2019; Miró et al., 2020; Schutte et al., 2018).

The MPB community, generally dominated by diatoms, includes cyanobacteria and other microalgal taxa (Underwood & Kromkamp, 1999). MPB plays a significant ecological and biogeochemical role in estuarine ecosystems in addition to their

contribution to the total C fixation as primary producers (Haro et al., 2019; Sundbäck & Miles, 2002; Underwood & Kromkamp, 1999). MPB is an important food source both directly for marine meiofauna and macrofauna (Middelburg et al., 2000) and indirectly due to the production of exopolymers that serve as a carbon source for heterotrophic bacteria (Bohórquez et al., 2017). In addition, these exopolymers promote sediment cohesion and stabilization, and enhance water quality, as well (Paterson, 1989; Yallop et al., 1994). Furthermore, MPB plays a crucial role in the mineralization of organic matter and nutrient recycling by influencing sediment oxygen levels, organic matter lability, and the exchange of nutrients between the sediment and water column. The rate and pathways of organic matter mineralization, as well as the partitioning between aerobic and anaerobic metabolism, such as denitrification and sulfate- and iron reduction, can be strongly influenced directly and indirectly by MPB activity due to oxygen production during daytime photosynthesis. Nitrogen demand by MPB can also affect coupled nitrification-denitrification in estuarine sediments and therefore nitrogen speciation and exchange rate across the sediment-water interface (Høgslund et al., 2023; Rios-Yunes et al., 2023; Risgaard-Petersen, 2003; Schutte et al., 2018; Soetaert et al., 2006).

Despite the evident presence of MPB in the Guadalquivir intertidal riverbanks, there is no information on its role as a potential contributor to total autochthonous primary production and biogeochemical cycling at the sediment –water interface in this important and very turbid temperate estuary. Therefore, the main objective of this study was to investigate the seasonal variations in MPB biomass and net metabolism, to analyze the spatio-temporal changes in nutrient concentrations, and to assess the fluxes of inorganic nutrients between the sediment and the water column. To the best of our knowledge, this is the first study that describes the main biogeochemical characteristics of the Guadalquivir Estuary intertidal sediments and evaluates the potential role of MPB, complementing the better-studied water column. These data contribute to obtaining a more integrated view of the biogeochemical and ecological characteristics of the system.

2. Material and Methods

2. 1. Study site and sampling

The Guadalquivir estuary (Fig. 1), located in southwest coast of the Iberian Peninsula, is about 110 km long and 150-800 m wide (Navarro et al., 2011). It is affected by a semidiurnal tidal cycle, with a maximum spring tidal range of 3.5 m (Díez-Minguito et al., 2012). The watershed is in a warm-temperate climate area with hot and dry summers and irregular rainfall characterised by oceanic storms. However, the river discharge is controlled by the net of dams in the watershed and ultimately by the Alcalá del Río dam (Fig. S1), located in the upper section (not shown in the map of Fig. 1). Two sampling sites were selected along the estuary to cover a wide range of salinity: (i) Lebrija (36°57'27.9"N 6°10'36.7"W), with low salinity range (from 1 to 7 PSU), and (ii) Bonanza (36°52'33.2"N 6°20'58.2"W), near the mouth of the estuary, with higher salinity values (from 10 to 23 PSU). At each sampling site, five sediment cores (5 cm Ø, 30 cm length) and in situ water (30 L) were collected on new moon quarterly (November 2018, February, May, August, and November 2019). Sediment samples were collected in the bare muddy

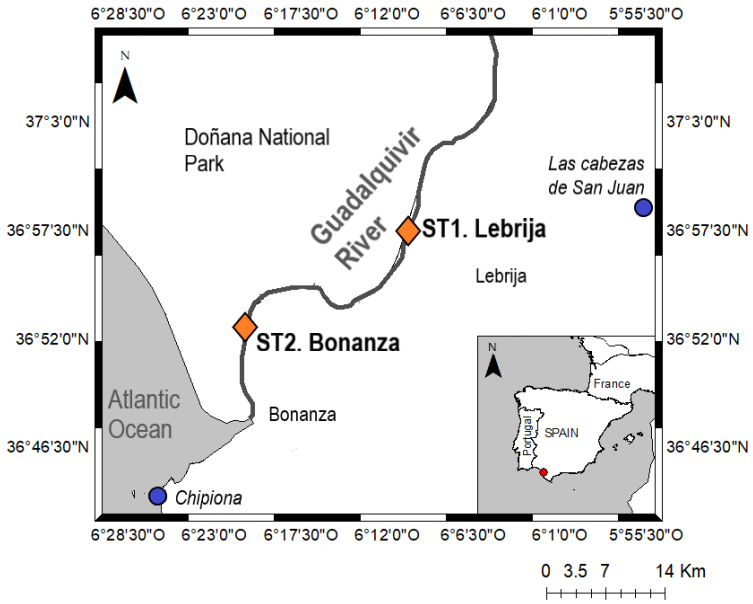


Fig. 1. Map of the lower Guadalquivir estuary indicating the location of the two sampling sites (orange rhombs). The locations of the closest weather stations (blue dots) are also shown.

intertidal zone along the riverbanks during emersion. Samples were collected from an area of about 2 m^2 in each site, avoiding fragments of vegetation or leaves in the collected samples in a time range of ± 50 min from low tide. Tidal amplitudes throughout the sampling period did not change in Bonanza (~1.1m), while in Lebrija were 1.1m in November 2018, 0.8m in February and November, and 1m in May and August 2019. Water samples were collected as close as possible to the sediment cores (a few meters). Sediment cores and *in situ* water were immediately transported to the laboratory, where the cores were placed in two 12 L aquaria (one for Bonanza and the other for Lebrija) filled with *in situ* water and maintained in a temperature-controlled room at 18ºC. Sediment cores were illuminated with white LED lamps (Lince 6M Verso, Light Environment Control S. L.) at an irradiance of 1300 µmol photons m^{-2} s^{-1} measured at the water interface.

2. 2. Total suspended solids and inorganic nutrients in the water column

Monthly samplings of some water column variables were done at new moon at the same sampling sites, Lebrija and Bonanza, from a boat with a multiparameter probe (EXO2, YSI), anchored at about 10 m from the shore and at the same time range from low tide (data in Table 1). Surface water samples were taken for the measurement of total suspended solids (TSS) and inorganic nutrients during the sediment sampling period, from November 2018 to November 2019. For TSS, the water samples were filtered over pre-weighed GF/F filters and weighed again after drying at 60 °C. The filtered water was collected for the measurement of inorganic nutrients. In addition, coinciding with the sediment sampling dates (every three months), water column samples were collected to measure only inorganic nitrogen

Table 1. Monthly averages ± SD of temperature (ºC), salinity (PSU), total suspended solids (TSS, mg L^{-1}) and inorganic nutrients (DIN=NO_3^-+ NO_2^- +NH_4^+, PO_4^{3-} and SiO_4^{4-}, µmol L^{-1}) in the water column at low tide, from November 2018 to November 2019 (n=14), in Bonanza and Lebrija, in the Guadalquivir estuary.

	T	*Salinity*	*TSS*	*DIN*	*PO_4^{3-}*	*SiO_4^{4-}*
Lebrija	19.5 ± 5.3	5.3 ± 3.1	325.4 ± 188.7	341.6 ± 148.2	2.9 ± 0.9	81.4 ± 137.4
Bonanza	19.2 ± 5.2	15.9 ± 6.0	91.8 ± 63.0	246.0 ± 111.5	2.4 ± 0.9	59.1 ± 105.8

species, close to the sediment core sampling sites. All water samples were immediately filtered through a GF/G filter and stored frozen (−20ºC) until analysis. Inorganic nitrogen nutrient concentrations were measured spectrophotometrically on a microplate reader (Multiskan GO, Thermo Scientific), following methods described by Bower *et al.* (1980) for NH_4^+ and García-Robledo *et al.* (2014) for NO_3^- and NO_2^-. PO_4^{3-} and SiO_4^{4-} were determined following Grasshoff, *et al*. (1999).

2. 3. Sediment-water fluxes of oxygen and inorganic nitrogen

Sediment-water fluxes were measured the day after sampling by whole-core incubations in light and dark conditions. Light and dark incubations were performed sequentially in the same sediment cores after a minimum of 1 hour of pre-incubation at the same light condition. For the incubations, sediment cores (n = 5, circa 20 cm of sediment and 10 cm of water column) were closed with transparent Plexiglas lids and kept closed for 2-7 hours depending on season. The duration of incubations was adjusted to avoid oxygen variations of more than 20%.

Inorganic nitrogen (NH_4^+, NO_3^-, NO_2^-) concentrations were measured in water samples collected in the water column of the cores before and after the incubations. All water samples were immediately filtered through a GF/G filter and stored frozen (−20ºC) until analysis as already described. Sediment-water fluxes (J, mmol m^{-2} h^{-1}) of inorganic nitrogen species were calculated as the difference between the initial and final concentrations during the incubation according to the following equation (Eq. 1):

$$\mathrm{J} = \frac{(\mathrm{C_{final}} - \mathrm{C_{initial}})}{\Delta \mathrm{t}} \times \frac{V}{A} \qquad (1)$$

where, C is the concentration of the solute (mmol/m^3), V represents the volume of the water column in the core (m^3), A represents the area of the sediment core (m^2), and Δt the incubation time interval (hours). Positive and negative fluxes represent nutrient efflux from the sediment and sediment net uptake, respectively.

To measure O_2 fluxes, changes in O_2 concentration during the incubations were measured every 30 seconds in each core by using optical oxygen sensors (OXSP5, PyroScience®). Oxygen fluxes at sediment water interface (net community production, NCP, fluxes measured in light conditions; and dark respiration, R_{dark}, fluxes measured in dark condition) expressed by unit of surface (mmol O_2 m^{-2} h^{-1})

were calculated as the slope of the changes in oxygen concentration with time (mmol O_2 m^{-3} h^{-1}) and normalized to the area and volume of the water column during the incubation similarly to Eq.1, except that $\Delta[O_2]/\Delta t$, was obtained from the slope of continuous changes in O_2 concentration over time.

Daily net community production (DNCP) was calculated from NCP and R_{dark}, taking into account the seasonal changes in the local daylight (t_L) and night (t_D) periods, according to DNCP= NCP×t_L - R_D×t_D.

2. 4. Inorganic nitrogen, iron, sulfate and dissolved inorganic carbon in the porewater

Once the incubations were completed, the five sediment cores were sliced into 1 cm thick slices down to 10 cm depth. The sediment was centrifuged at 4700 ×g for 20 min at 4ºC to extract the porewater. The sediment pellet was freeze-dried and preserved in darkness for further analyses (chlorophyll, organic carbon and total nitrogen, see following section).

For inorganic nitrogen (NH_4^+, NO_3^- and NO_2^-), porewater samples collected were preserved and analyzed as described above for the water column. For Fe^{2+} analysis, 0.4 mL of porewater was transferred to Eppendorf tubes with 0.1 mL of HCl 2N to avoid oxidation. Fe^{2+} was measured following Viollier *et al.* method (2000). Sulphate (SO_4^{2-}) was analyzed by ion chromatography in aqueous matrices (METROHM:858-Professional Sample processor) (INMAR Peripheral Services).

For dissolved inorganic carbon (DIC) analysis, 1 mL of porewater was transferred to 3 mL Exetainers (Labco, UK) with 2 mL of MQ water and preserved with 0.1 mL of 37% formalin. DIC in the porewater was determined by a colorimetric method (Sarazin et al., 1999). Calibration was performed with standards spiked with the same amount of formalin as the samples.

Production/consumption rates of NH_4^+, Fe^{2+}, SO_4^{2-} and DIC were calculated from their concentration profiles within the sediment using the software PROFILE (Berg *et al.* 1998). The porosity used in calculation was an average of the porosity measured in the samples (0.75). Irrigation and bio-diffusivity was considered negligible. The diffusion coefficients were extracted from Li & Gregory (1974).

2. 5. Organic matter, organic carbon, total nitrogen and chlorophyll in the sediment

Organic carbon (C_{org}) was determined as the difference between the total carbon measured in the freeze-dried sediment samples and inorganic carbon measured on a replicate previously combusted at 550ºC for 4 h. Total Nitrogen was measured in the freeze-dried sediment samples. Both samples were analyzed on an elemental analyzer (LECO CHNS 932) at the Central Services of the University of A Coruña, Spain.

Photosynthetic pigments were extracted from freeze-dried sediment (circa 1.5 g) in 100% methanol buffered with $MgCO_3$. After 18 h in darkness at 4ºC, absorbance spectra of the extracts were measured on a microplate reader (Multiskan GO; Thermo Scientific) before and after acidifying with 100 µL of 1 N HCl. Chlorophyll *a* (Chla) and phaeophytin *a* (Phaeoa) were measured according to Stal *et al*. (1984). Active chlorophyll was estimated as the ratio between Chla and Phaeoa (Chla/Phaeoa) in each sample.

2. 6. Statistical analysis

In order to explore statistical differences in our data, variables were first graphically checked for extreme values or skewed distributions (Zuur et al., 2010). Sediment Fe^{2+}, NO_3^-, NO_2^-, Chla, and Phaeoa were ln(x+1) transformed. Analysis was performed on each variable individually by PERMANOVA in PRIMER 6.0 (PRIMER-e Ltd) using a Euclidean distance similarity index and 1000 permutations. When permutations were low, a Monte Carlo approximation was used to obtain the p values (Anderson et al., 2008). Post hoc tests were performed when a significant effect was found. If a significant interaction was observed, post hoc tests were performed within the other factor.

Differences in water column concentrations were tested for the effects of time and location. Sediment-water fluxes were analysed separately for light and in darkness with time and location and their interaction as fixed factors. In order to test whether a difference existed in the magnitude of nutrients fluxes between light and darkness, an analysis was performed using the paired difference for each core between light and dark incubation. For the sediment column variables, i.e. solid phase and porewater solutes, time, location, and depth were tested as fixed factors. Since

depth intervals within cores are not independent, core identity was introduced as a random factor nested within site and time. The interactions of time by location, and depth by location were also included in the model. Correlations between variables were tested with a Spearman rank correlation coefficient.

Statistical significance was established at $p<0.05$. All the results were expressed as mean ± SE unless otherwise stated. All results are interpreted through the "lens of statistical clarity" sensu (Dushoff et al., 2019).

3. Results

3. 1. Organic carbon and total nitrogen content in the sediment

The organic carbon content in the sediment (C_{org}) in both sites showed a slight trend to decrease with depth (**Fig. 2A**) ($p <0.0001$; **Table S2**). C_{org} was generally higher in Bonanza (5.29-11.72 mg cm^{-3}) than in Lebrija (4.93-8.85 mg cm^{-3}) (**Fig. S2**, **Fig. 2A**), although the difference was statistically clear only in July and November 2019 (post-hoc test, $p<0.05$**; Table S5**). C_{org} changed along the year within each site with differences being clear in some of the months (post-hoc, $p<0.05$**; Table S5**), but seasonal changes were not synchronous in both sites (**Fig. 2A**).

Total Nitrogen (N_T) content range was similar in Bonanza and Lebrija (0.35-0.91 mg cm^{-3} and 0.31-0.75 mg cm^{-3}, respectively) although statistically clear interactions were observed between site and depth and site and date ($p <0.0001$; **Table S2**). At both sites, values showed differences with sediment depth (post-hoc, $p <0.05$; **Table S5**) with highest values observed near the surface (**Fig. S2B, Fig. 2B**). N_T showed clear differences with time in both sites. N_T showed clearly lowest values in November 2018 and February in Bonanza, while in Lebrija statistically clearly higher values were observed in February compared to the rest of months (**Fig. 2B**) (post-hoc, $p <0.045$; **Table S5**).

The molar ratio of C_{org} to N_T (C:N) (**Fig. S2C**) was usually higher in Bonanza than in Lebrija, although only in August and November 2019 was this difference statistically clear (post-hoc, $p <0.026$; **Table S5**). The mean C:N ratio measured in Bonanza was 15.48 ± 0.98 mol/mol and 12.25 ± 0.35 mol/mol in Lebrija.

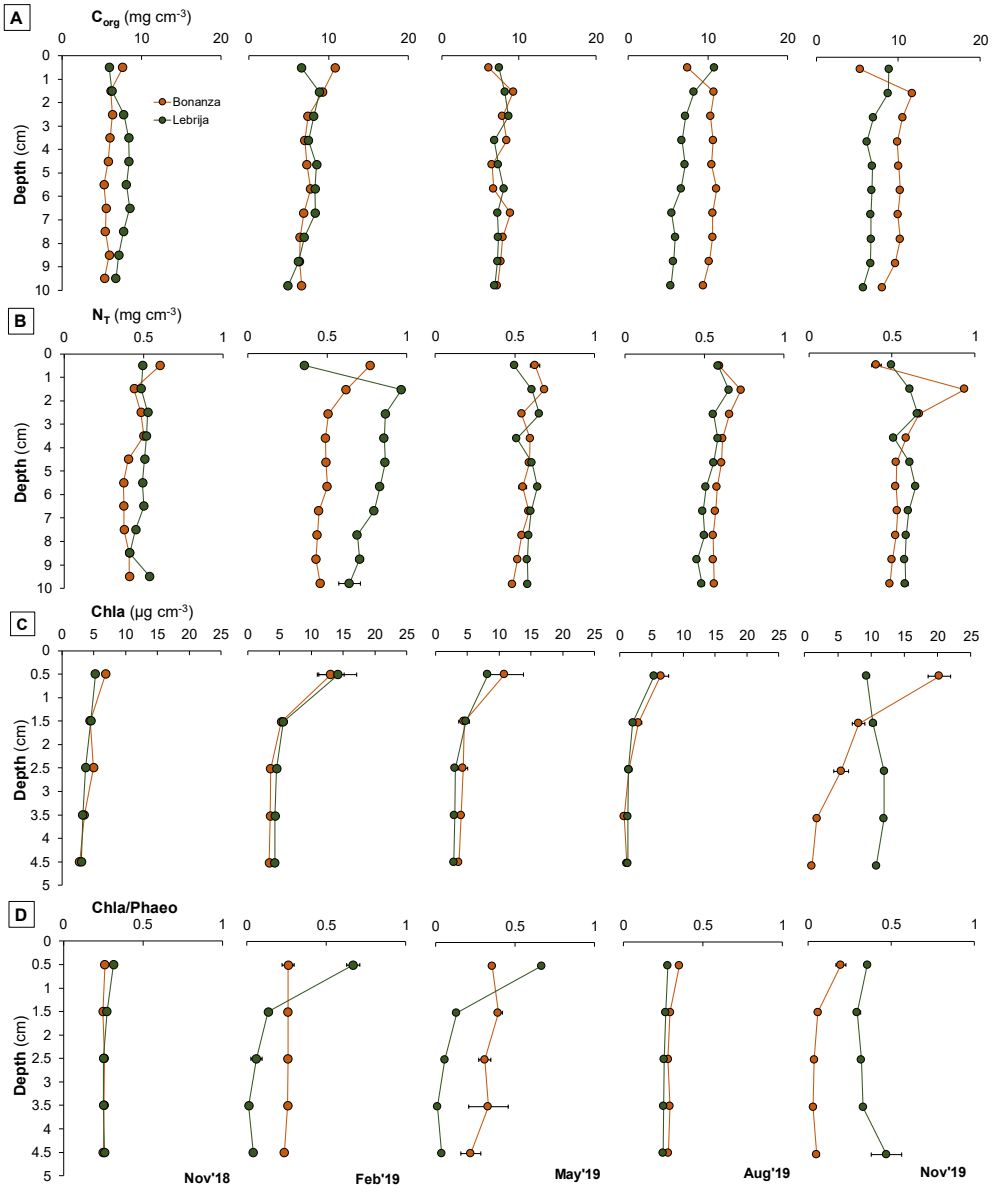


Fig. 2. Seasonal changes in sediment (**A**) organic carbon (C_{Org}), (**B**) total nitrogen (N_T), (**C**) chlorophyll-a (Chla) contents and (**D**) in Chlorophyll-a:Phaeophytin-a ratio in the first 10 cm in Bonanza (orange dots and lines) and Lebrija (green dots and lines) along the Guadalquivir estuary, from November 2018 to November 2019. Data points represent means ± SE (n=3).

3. 2. Photosynthetic pigments content in the sediment

Chla concentrations in the sediment were highest at the sediment surface, decreasing exponentially with depth (Fig. 2C, S2D) (post-hoc, $p<0.05$; Table S5). The annual mean Chla concentration in the upper 1 cm sediment layer was higher in Bonanza than in Lebrija, being 11.48 ± 1.45 μg cm^{-3} and 8.48 ± 0.94 μg cm^{-3}, respectively. Chla showed clear differences with season at both sites (post-hoc, $p<0.05$; Table S5). The highest concentrations were measured in February and November 2019, reaching up to 13.00 ± 2.73 and 20.25 ± 2.16 μg cm^{-3} in Bonanza and 14.16 ± 3.85 μg cm^{-3} and 9.33 ± 0.26 μg cm^{-3} in Lebrija, respectively. The lowest values were found in August, being 6.44 ± 1.62 μg cm^{-3} and 5.40 ± 0.70 μg cm^{-3} in Bonanza and Lebrija, respectively.

The ratio between Chla and Phaeoa (Chla:Phaeoa) was not clearly different between Bonanza (range from 0.01 ± 0.02 to 0.67 ± 0.09) and Lebrija (from 0.03 ± 0.01 to 0.47 ± 0.20) although a significant interaction was found ($p < 0.001$; Table S2). The seasonal changes of Chla:Phaeoa followed a similar spatio-temporal evolution to that of Chla, with some exceptions. In Bonanza, the highest values of Chla:Phaeoa were observed at August at the sediment surface, whereas in Lebrija, this occurred in November at the deepest sediment layer (Fig. 2D).

3. 3. Oxygen fluxes at the sediment-water interface

The microbenthic community from both sampling sites were photosynthetically active in light conditions (Fig. 3A). Net community production during light (NCP) was clearly higher in Bonanza than Lebrija (post-hoc, $p<0.019$; Table S5), with the exception of February, with mean values of 5.42 ± 3.58 and 1.54 ± 2.24 mmol m^{-2} h^{-1}, respectively (Fig. 3A). Respiration rates in darkness (R_{dark}) were 2.38 ± 0.14 mmol m^{-2} h^{-1} in Bonanza, being on average 1.8 times higher than those measured in Lebrija (1.31 ± 0.49 mmol m^{-2} h^{-1}) (Fig.3B). Highest values of NCP were observed in August in Bonanza (post-hoc, $p<0.003$; Table S5), and in February in Lebrija (post-hoc, $p<0.001$; Table S5). R_{dark} covaried in both sampling sites along the seasonal cycle and was highest in May, followed by August. Differences between months were clearly higher in Bonanza than Lebrija. In both Bonanza, DNCP was always positive ranging from 21.4 to 129.8 mmol O_2 m^{-2} d^{-1} in November 2019 and

August, respectively. In Lebrija, it ranged from -23.3 to 43.9 mmol O_2 m^{-2} d^{-1}, showing positives values only in February and August.

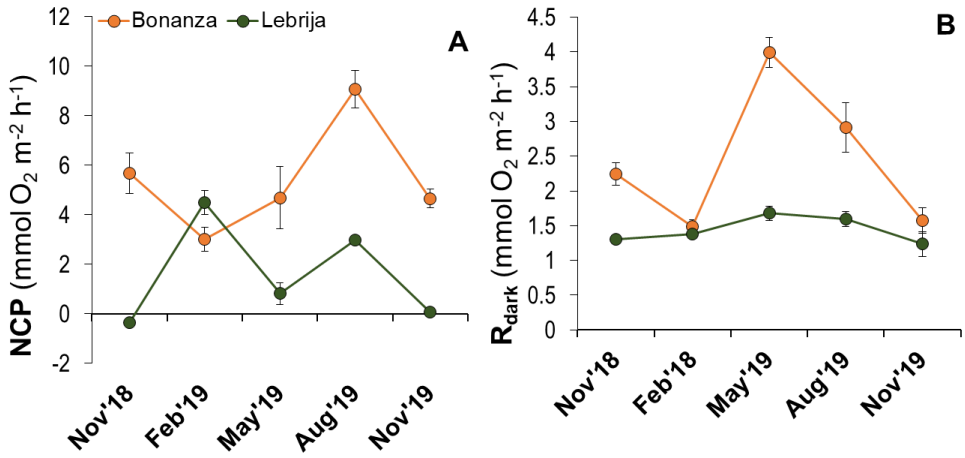


Fig. 3. Seasonal changes in (A) net community production in light and (B) dark respiration estimated from the O_2 fluxes across the sediment-water column interface in Bonanza (orange) and Lebrija (green) along the Guadalquivir estuary during the sampling period, from November 2018 to November 2019. Data points represent means ± SE (n=5).

3. 4. Inorganic nutrients in the water column and sediment porewater

Dissolved inorganic nitrogen (DIN) was the dominant nutrient in the Guadalquivir water column in Bonanza and Lebrija during the studied period (Table 1). The most abundant inorganic nitrogen nutrient in the water of Guadalquivir River was nitrate (90 - 99.7 % of DIN). Nitrate concentrations in the water column showed statistically clear seasonal changes between all months in Lebrija and the majority in Bonanza (post-hoc, p-value<0.039; Table S5) (Fig. 4A). Seasonal maximum nitrate concentration was found in February 2019 with values up to 395 and 639 µM in Bonanza and Lebrija, respectively. Minimum nitrate concentration was measured in August (30 - 40 µM), 10 times lower than the maximum measured in February. Concentrations increased again in November 2019 up to 93 and 257 µM in Bonanza and Lebrija, respectively (Fig. 4A). Nitrite concentrations were close to detection limits never exceeding 2 µM (Fig. 4B). Ammonium concentration in the water column ranged from 0.15 to 10.7 µM, with two peaks in May and November

2019 (Fig. 4C). Water column ammonium was similar in both sampling sites except in February and May, when higher concentrations were measured in Bonanza but these were not statistically clear ($p>0.05$, Table S5). PO_4^{3-} concentrations were about 2-3 µM in both sites, the N:P stoichiometric ratio was much higher than the typical one for phytoplankton (16). Mean dissolved SiO_4^{4-} concentration was 81.4 ± 137.4 and 59.1 ± 105.8 (mean ±SD), in Lebrija and Bonanza, respectively, but dropped to 26.2±7.8 and 16.7 ± 6.9 µM when the very high concentrations (up to 474.5 µM and 362.9 µM measured in November and December 2018, respectively) were excluded from annual averages (Table 1). Porewater NH_4^+ levels greatly exceeded those in the water column, increasing significantly with depth at both stations. Concentrations ranged from 2 - 35 µM in the top centimeter to maximum values of 390 - 490 µM at 10 cm depth. Differences were statistically clear down to 4.5 cm in Lebrija, whereas in Bonanza they were even deeper (post-hoc, $p<0.019$; Table S5) (Fig S2, Fig. 5A). Clear seasonal differences were observed mainly with in February compared to the rest of the months in Lebrija and February and November 2019 for Bonanza (post hoc, $p<0.05$; Table S5). While high values were recorded with depth in both sites in August, in February concentrations were high in Bonanza but low in Lebrija (Fig. 5A). Porewater NO_3^- and NO_2^- were detected in the top two centimeters of sediment, rapidly decreasing with depth (Fig. S2, Fig. 5). Concentration of NO_3^- and NO_2^- in the sediment varied over time, with different patterns at each station. However, the lowest concentrations were observed at both sites in August (Fig. 5B, C).

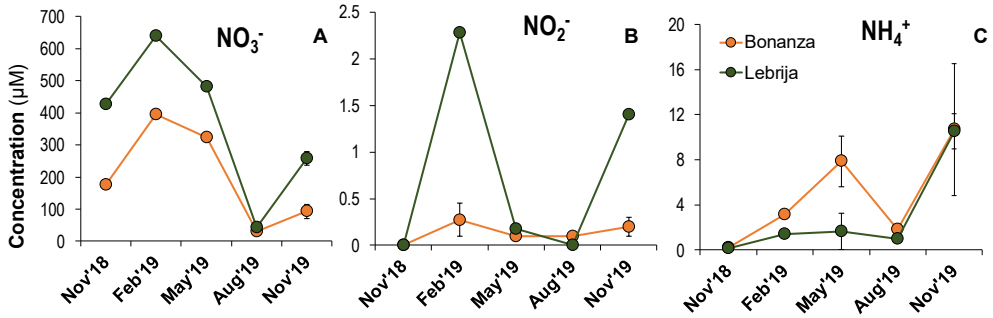


Fig. 4. Seasonal changes in (A) NO_3^-, (B) NO_2^- and (C) NH_4^+ concentration in the water column in Bonanza and Lebrija along the Guadalquivir estuary during the sampling period, from November 2018 to November 2019. Data points represent means ± SE (n=3).

3. 5. Dissolved inorganic carbon, iron and sulphate in the sediment porewater.

The concentrations of dissolved inorganic carbon in the sediment (DIC) showed a similar range in Bonanza and Lebrija (4.47 - 12.10 mM and 2.29 - 11.97 mM, respectively) but was clearly different between sites (post hoc, $p<0.016$; Table S5) with the exception of February and August. In both sites, DIC increased with depth (Fig. S2K, Fig. 6A) with the exception of the bottom samples in Bonanza (post hoc, $p<0.001$; Table S5). In addition, for most dates average values with depth DIC varied throughout the year at both sites although out of phase (post hoc, $p<0.05$; Table S5) (Fig. 6A).

Porewater Fe^{2+} concentrations ranged from 0.05 to 416 µM in Lebrija and up to 826 µM in Bonanza (Fig. 6B), showing clear differences between sites with the exception of August (post hoc, $p<0.05$; Table S5). The Fe^{2+} profiles observed at both Lebrija and Bonanza remained relatively stable throughout the year, showing consistent and similar initial concentrations down to a depth of approximately 2.5 centimeters where the iron concentration gradually increased for a few centimeters before decreasing again. For both sites, the highest average Fe^{2+} concentration was recorded in August, with Bonanza twice as high as Lebrija Differences between depths were more clear in Bonanza than in Lebrija (post hoc, $p<0.05$; Table S5). SO_4^{2-} porewater content ranged from 9.23 ± 1.27 mM to 11.85 ± 1.72 mM at Bonanza and between 4.40 ± 0.50 mM to 5.48 ± 0.54 mM at Lebrija, showing statistically clear differences between the two sampling sites ($p< 0.001$) (Fig. 6C).

3. 6. Fluxes of inorganic nitrogen at the sediment-water interphase

Net NH_4^+ fluxes across the sediment-water interface measured by whole core incubations were generally negative throughout the measured period (-0.96 to 0.32 mmol m^{-2} h^{-1}), indicating net consumption rates by the sediment at both locations (Fig. 7A). NH_4^+ fluxes in Lebrija were generally lower than in Bonanza with no changes in the direction or magnitude between light and dark fluxes ($p>0.05$). In contrast, in Bonanza, differences between light and dark fluxes were statistically clear (post-hoc, $p<0.05$; Table S5) with the exception of February.

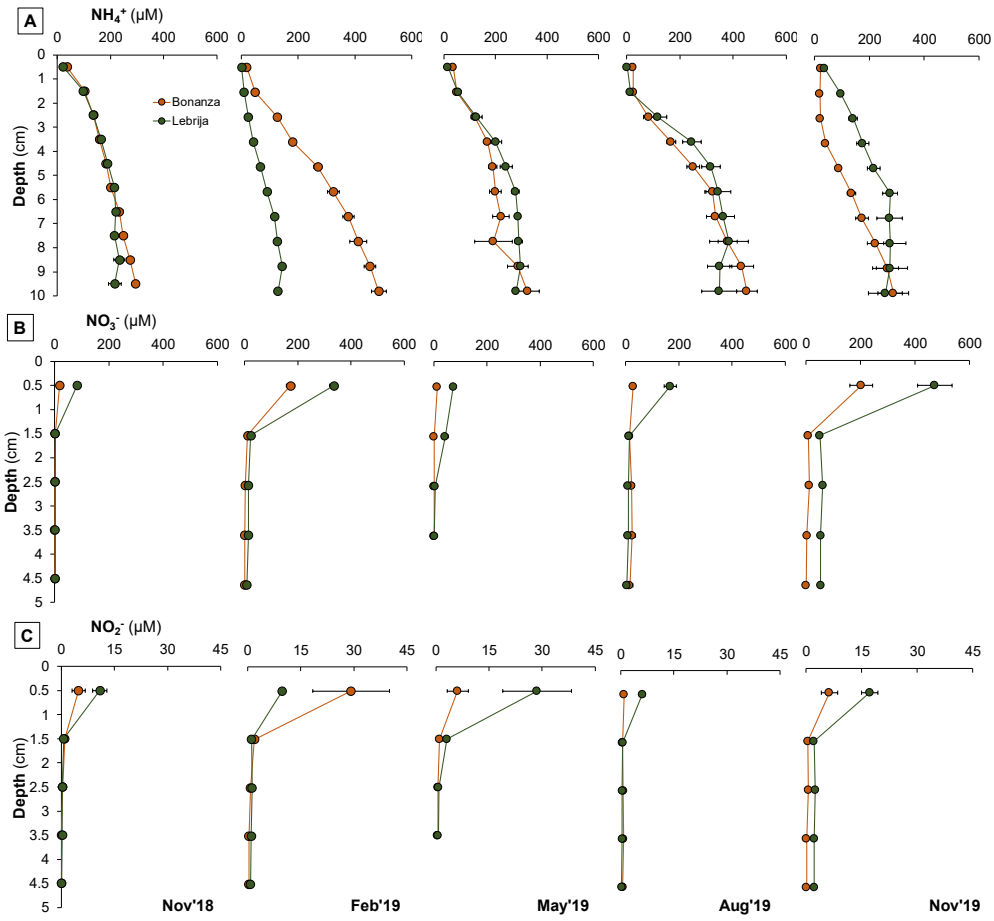


Fig. 5. Seasonal changes in sediment porewater concentrations of (**A**) ammonium (NH_4^+) (**B**) nitrate (NO_3^-) and (**C**) nitrite (NO_2^-) in the first 10 cm in Bonanza (orange dots and lines) and Lebrija (green dots and lines) along the Guadalquivir estuary during the sampling period, from November 2018 to November 2019. Data points represent means ± SE (n=3).

Net NO_3^- fluxes (from -2.55 ± 1.55 to 2.03 ± 1.63 mmol m^{-2} h^{-1}) followed a similar seasonal trend in both sites and were about one order of magnitude higher than those of ammonium (**Fig. 7B**). NO_3^- fluxes, both in light and in darkness, were negative during November 2018 and February 2019, suggesting a nitrate uptake by the sediment, decreasing in May and August to values around zero. This difference was clear in darkness for both sites (post hoc, $p<0.05$; **Table S5**) whereas in light differences over time were found only in Lebrija. In November 2019, there was a considerable scattering in the measured nitrate fluxes, both in absolute values

and in the direction across the sediment-water interface. Net NO_2^- fluxes (from -0.03 to 0.10 mmol m^{-2} h^{-1}) were lower than ammonium and nitrate fluxes. Net NO_2^- fluxes showed a peak of efflux in May showing statistically clear interactions with season and site ($p < 0.0001$; Table S3) (Fig. 7C).

3. 7. Net production rates of DIC, NH_4^+ and Fe^{2+} and net consumption rate of SO_4^{2-} within the sediment

Net production (DIC, NH_4^+ and Fe^{2+}) and consumption rates (SO_4^{2-}) in the sediment were calculated modelling the porewater profiles (Fig. 5, 6) with the PROFILE software (Berg *et al.* 1998). Net DIC production within the sediment ranged from 0.30 ± 0.05 to 1.29 ± 0.14 to mmol m^{-2} h^{-1} in Bonanza, and from 0.36 ± 0.09 to 0.94 ± 0.47 mmol m^{-2} h^{-1} in Lebrija (Fig. S3A). Two relative maxima were found in Bonanza in May and November 2019, while in Lebrija they were found in February and August 2019. Net NH_4^+ production rates in Bonanza ranged from 3.17 µmol m^{-2} h^{-1} in May and November 2019 to 19.37 µmol m^{-2} h^{-1} in November 2018 (Fig. S3B). In Lebrija, two NH_4^+ production rates maxima were found in November 2018 and August 2019 with values up to 35.70 µmol m^{-2} h^{-1} and minimum values of 18.69 µmol m^{-2} h^{-1} in February 2019.

Net production of NO_3^- and NO_2^- could not be estimated using PROFILE because both nutrients were restricted to the upper cm of sediment (Fig. 5). Net Fe^{2+} production rate represents an estimation of iron reduction microbial pathway within the sediment. Fe^{2+} production rates showed very low values between November 2018 to May 2019, increasing in August 2019 up to values of 164.93 and 69.12 µmol m^{-2} h^{-1} at Bonanza and Lebrija, respectively (Fig. S3C). Net SO_4^{2-} consumption rates allow us to estimate sulfate reduction activity within the sediment. These rates showed values between -15.48 and 17.43 µmol m^{-2} h^{-1}, with maximum values in May and November 2019 at Bonanza and Lebrija, respectively (Fig. S3D).

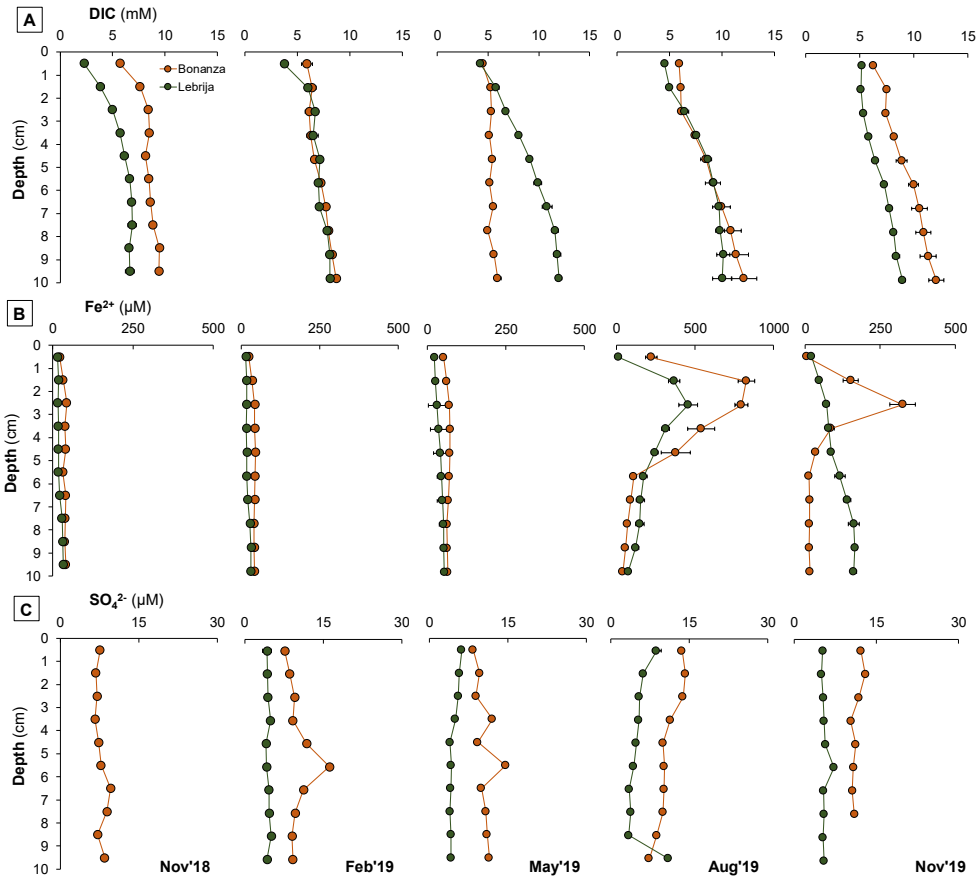


Fig. 6. Seasonal changes in sediment porewater concentrations of (**A**) DIC, (**B**) Fe^{2+} and (**C**) SO_4^{2-} in the first 10 cm in Bonanza (orange dots and lines) and Lebrija (green dots and lines) of the Guadalquivir estuary during the sampling period, from November 2018 to November 2019. Data points represent means ± SE (n=3). November 2018 samples for SO_4^{2-} in Lebrija were lost (white area).

4. Discussion

4. 1. Organic carbon and total nitrogen

The concentrations of organic carbon (C_{org}) and total nitrogen (N_T) in intertidal sediments of the Guadalquivir Estuary were lower than in the nearby intertidal sediments of Cadiz Bay (Bohórquez et al., 2019; Corzo et al., 2009; Haro et al.,

2020), but similar to those observed in its sublittoral sediments (Burgos, Ortega, Bohórquez, et al., 2018) and in other temperate estuaries (Rios-Yunes et al., 2023). The relatively scarce differences in the vertical distribution of C_{org}, N_T and C:N with depth (**Fig. S2**) indicated that sediments are well mixed in the upper 10 cm depth (Canfield et al., 2005). Bonanza exhibits clearly higher C_{org} in some months but similar NT than Lebrija, resulting in higher C:N ratios at the more marine site (**Fig. 2, Fig. S2**). Despite this difference among sites, C:N ratios in the Guadalquivir Estuary were similar to other muddy intertidal environments (Cabrita & Brotas, 2000; Haro et al., 2020; Rios-Yunes et al., 2023). C:N ratio >10 in the sediment surface suggests that, in addition to autochthonous production by MPB or phytoplankton, there is a certain contribution of allochthonous organic matter from the river catchment area (Hedges et al., 1997; Hillebrand & Sommer, 1999). Seasonal differences in C_{org} and N_T were statistically clear in both sites, although they depended on the site, with peaks in November. This seasonal pattern coincided with seasonal changes in Chl *a*, as discussed in the following section. Nonetheless, it was likely affected as well by seasonal changes in the annual precipitation pattern and the management of river flow in the Alcala de Rio dam (**Fig. S1**). Precipitation was high in February and November and might have increased

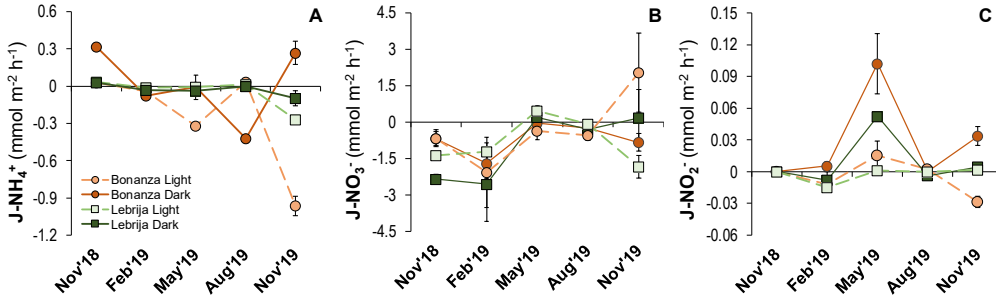


Fig. 7. Seasonal changes in (**A**) NH_4^+, (**B**) NO_3^-, and (**C**) NO_2^- fluxes in light and in darkness across the sediment-water column interface in Bonanza (orange) and Lebrija (green) along the Guadalquivir estuary during the sampling period, from November 2018 to November 2019. Data points represent means ± SE (n=5).

the contribution of allochthonous organic matter to the sediment.

4. 2. Microphytobenthic biomass seasonal dynamics

Microphytobenthos biomass estimated by the Chla concentration decreased exponentially with depth within the sediment as expected (Fig. S2) (Garcia-Robledo et al., 2016; García-Robledo et al., 2010; Macintyre et al., 1996), except in Lebrija in November 2019, when Chla concentration was similar down to 5 cm depth (Fig 2). This unusual sediment Chla vertical profile could be related to a higher sediment accumulation and resuspension following an opening of the Alcalá del Río dam (Fig. S1, S2) (Díez-Minguito et al., 2012). Chla followed a seasonal cycle with highest surface values in winter (February) and in fall (November) and a minimum in summer (August) in both sampling sites. The MPB biomass seasonal pattern in the Guadalquivir Estuary coincides with the MPB seasonal cycles recorded in the inner Bay of Cadiz (Garcia-Robledo et al., 2016; Haro et al., 2020, 2022). Furthermore, the Chla concentration range (3.76-13.50 µg cm^{-3}) was similar to that found in the Bay of Cádiz (Garcia-Robledo et al., 2016; Haro et al., 2020) and other estuarine zones around the world (Cabrita & Brotas, 2000; Kwon et al., 2020; McTigue et al., 2015). The higher values in November of 2019, not observed in 2018, are probably related to changes in the rainfall pattern, with more prolonged but lower intensity rains, providing nutrients to the sediment surface. In fact, among the environmental variables studied, MPB biomass estimated by Chla was only positively correlated with water column NO_3^- ($r = 0.76$, $p<0.05$, $n=9$).

The Chla:Phaeoa ratio can be used as a proxy of the active chlorophyll since phaeopigments form in the water column and sediments due to microbial degradation and grazing (Lee et al., 2000; McTigue et al., 2015). The Chla:Phaeoa ratio in the Guadalquivir Estuary was usually < 1, although in the surface layers in Bonanza the ratio was slightly higher than in Lebrija (Fig. S2, Fig. 2). The maximum of Chla:Phaeoa observed in summer in Bonanza at the sediment surface could be due to higher grazing rate on MPB and microbial degradation rates during summer (Lee et al., 2000; McTigue et al., 2015). However, no such summer maximum was observed in the more riverine sampling point (Fig. 2). In the intertidal sediments of the Guadalquivir River, Chla and Phaeoa concentrations were statistically correlated with N_T content ($r=0.52$ and 0.24, respectively, $p<0.05$, $n=150$), while the correlation with C_{org} was weaker for Chla ($r=0.21$, $p=0.01$, $n=150$) not significant for for Phaeoa ($r= 0.12$, $p=0.16$) Therefore, MPB biomass seems to contribute significantly to the pool of labile organic matter within the sediment, which usually has a higher N content and a higher turnover time.

4. 3. Net metabolism in the Guadalquivir intertidal sediments

Net community primary production in light and respiration rate in darkness measured in this study have to be considered potential rates since they were measured at saturating light conditions or in the dark, respectively, and at constant temperature. These data are the first available on the benthic metabolism of intertidal sediments in the Guadalquivir Estuary. The sediment surface in the area is characterized by a macroscopically evident MPB biofilm dominated by diatoms. In general, NCP and R_{dark} were higher in Bonanza than in Lebrija, with values being similar to those measured in the Cadiz Bay (Burgos, Ortega, & Forja, 2018; Haro et al., 2020) and other temperate estuarine intertidal sediments (Kwon et al., 2020; Macintyre et al., 1996; Underwood & Kromkamp, 1999). One notable contrast between the sites studied was the existence of very low or even negative NCP values in Lebrija, while Bonanza showed positive NCP throughout the year. This contrast was even more evident comparing theirs DNCP, the intertidal sediment community was always net autotrophic in Bonanza and could thus contribute positively to the overall primary production of the estuary along the year; while in Lebrija, positive values of DNCP were only observed in February and August.

The seasonal dynamics of NCP was different in Lebrija and Bonanza; however, R_{dark} followed the same pattern (Fig. 3). We only observed a NCP annual maximum in Bonanza in August, while in Lebrija in addition to the peak in August, the annual maximum occurred in February. The spatiotemporal changes in net community production and respiration did not correlate clearly with any of the environmental variables measured in this study. Seasonal trends in NCP and R_{dark} did not coincide with changes in MPB standing stocks in the Guadalquivir Estuary (Fig. 2). This lack of seasonal coupling was also observed in the sediments of the inner Bay of Cádiz, where the seasonal maximum in MPB biomass occurs in winter whereas MPB primary production peaks in summer (Garcia-Robledo et al., 2016; Haro et al., 2020). The absence of covariation between seasonal changes in MPB biomass and photosynthetic production occurs because each variable can be affected differently by a number of abiotic and biotic ecological factors, such as irradiance, temperature, desiccation, grazing and resuspension (Coelho et al., 2009; Pratt et al., 2015; Savelli et al., 2018; Ubertini et al., 2012), leading to complex site–dependent interactions.

4. 4. Inorganic nitrogen concentration in the water column and sediment

Dissolved inorganic nitrogen (DIN = NO_3^-+ NO_2^- + NH_4^+) in the water column of the Guadalquivir Estuary was dominated by NO_3^-, > 99 % of DIN in February (**Fig. 4; Table 1**). Similarly high concentrations of NO_3^- have been recorded in previous studies in the Guadalquivir Estuary and are likely associated with the nitrification of urban waste and runoff of excess fertilizers from agricultural fields (Flecha et al., 2015; Mendiguchía et al., 2007). Water column NO_3^- followed a seasonal change with maximum concentration in winter and minimum in summer, suggesting a link to the precipitation seasonal changes in the area (**Fig. 4, Fig. S1**) and an important impact of fertilizers runoff from agricultural lands. NO_2^- and NH_4^+ changed clearly along the year but followed only partially the trend of NO_3^-, with low concentrations also observed in winter (**Fig. 4**). The high concentration of water column NO_3^- does not sustain a correspondently high phytoplankton primary production due to light limitation due to the high turbidity (**Fig. S1C**) (Ruiz et al., 2017). Alternatively, PO_4^{3-} limitation could also contribute to explaining the low productivity due to the very high DIN:PO_4^{3-} ratio (**Table 1**). However, MPB biomass estimated by Chla was positively correlated with water column nitrate indicating that intertidal MPB could have a competitive ecological advantage over phytoplankton in turbid tidal estuaries, because at low tide MPB can receive sunlight directly (Underwood & Kromkamp, 1999).

Porewater NH_4^+, NO_3^- and NO_2^- showed seasonal differences in both sampling sites although their time evolution was not always parallel (**Fig. 5**). The range of porewater NH_4^+ and NO_2^- concentrations in the sediments of Guadalquivir Estuary was similar to those of other intertidal environments like the Bay of Cadiz (Garcia-Robledo et al., 2016; Haro et al., 2020), Tagus Estuary (Cabrita & Brotas, 2000) and the Eastern Scheldt (Rios-Yunes et al., 2023). In contrast, NO_3^- concentrations in the Guadalquivir estuary were an order of magnitude higher than those in the Bay of Cadiz and other environments (Cabrita & Brotas, 2000; Garcia-Robledo et al., 2016; Haro et al., 2020; Rios-Yunes et al., 2023), probably caused by the much higher NO_3^-concentration in the water column of the river. Vertical distribution of NH_4^+, NO_3^- and NO_2^- followed the expected pattern in sediments (Berg et al., 1998, 2003). In the anoxic layers of sediment NO_3^- and NO_2^- are used in denitrification and anammox contributing to the mineralization of organic matter under anoxic

conditions (Hensen et al., 2006; Stein & Klotz, 2016). It is interesting to note that both inorganic nitrogen species in the sediment followed similar vertical distributions and seasonal trends ($r = 0.65$, $p<0.05$, $n=100$). In addition, NO_3^- and NO_2^- followed similar patterns in the porewater and the water column, evidencing a clear coupling between both compartments.

Vertical distribution of porewater NH_4^+ showed an inverse pattern to that of oxidised inorganic nitrogen species (Fig. S2, Fig. 5), increasing downward as it is typically observed in marine sediments (Berg et al., 1998, 2003). The accumulation of porewater NH_4^+ is mainly the result of the progressive mineralization of organic matter, resulting in a long term difussive efflux to the water column (Hensen et al., 2006). Nonetheless this NH_4^+ flux to upper sediment layers and to the water column can be intercepted by different microbial communities. MPB can use directly NH_4^+ to fulfill its N-demand for growth, a process energetically more favorable that the uptake of NO_3^- and NO_2^-, which requires further reduction intracellularly (Dortch, 1990; Glibert et al., 2016). In addition, NH_4^+ in the oxic sediment layer serves as a substrate for nitrification and indirectly for coupled nitrification-denitrification (Risgaard-Petersen, 2003). The seasonal trend of porewater NH_4^+ showed a maximum in August in both sampling locations, which might be related to a general stimulation of microbial degradation of organic matter by the higher summer temperatures.

4. 5. Fluxes of inorganic nitrogen at sediment-water interface

Net fluxes of the different DIN species confirmed the important biogeochemical role of NO_3^- in this estuary. NO_3^- fluxes across the sediment-water interface were an order of magnitude higher than those of NH_4^+ and NO_2^-. Although ocassionally a net NO_3^- efflux from the sediment toward the water column was recorded, on an annual average, the sediment was a net NO_3^- sink both in light and dark conditions (-0.70 ± 1.1 mmol NO_3^- m^2 h^{-1}). The magnitude of NO_3^- fluxes in the intertidal sediments of Guadalquivir Estuary were higher than those typically measured in subtidal sediments (Boynton et al., 2018, 2023; Rios-Yunes et al., 2023) and in intertidal sediments of different ecosystems (Bartoli et al., 2003; Rios-Yunes et al., 2023), but did not reach the very high values reported in the Tagus Estuary (Cabrita & Brotas, 2000). Net NH_4^+ fluxes in most of the incubations in both sampling sites along the year were close to zero or negative indicating mainly a net NH_4^+ uptake by the

sediment, same as NO_3^-. The overall maginitude of these NH_4^+ fluxes was similar to those found elsewhere, including intertidal sediments (Bartoli et al., 2003; Cabrita & Brotas, 2000; Rios-Yunes et al., 2023) and subtidal sediments where fluxes are usually positive, releasing NH_4^+ to the water column (Boynton et al., 2018, 2023). In addtion to a dilution effect due to tidal mixing, the uptake of NH_4^+ and mainly NO_3^- by the Guadalquivir Estuary sediments likely contributes to the observed seaward reduction of water column concentrations of these nutrients (Flecha et al., 2015; Mendiguchía et al., 2007). Therefore, sediments have an important role buffering the high load of DIN from the water column and reducing its export to the Gulf of Cádiz.

MPB can consume NO_3^- and NH_4^+ for growth, therefore afecting their net fluxes at sediment water interface. The N-demand of MPB can be estimated from the NCP rate using a photosynthetic quotient (0.9 CO_2:O_2, mol:mol) and the stoichiometric C:N ratio of MPB (119C:17N, mol:mol; (Hillebrand & Sommer, 1999)). The mean NCP rates at Bonanza and Lebrija sites, 5.42 ± 2.02 and 1.60 ± 1.85 mmol O_2 m^{-2} h^{-1}, represent an estimated N-demand of 0.70 ± 0.26 and 0.20 ± 0.24 mmol N m^{-2} h^{-1}, in Bonaza and Lebrija, respectively. Mean annual DIN fluxes ($J\text{-}NO_3^-$ + $J\text{-}NO_2^-$ + $J\text{-}NH_4^+$) at the sediment water interface were -0.62 and -0.93 mmol N m^{-2} h^{-1}, in Bonaza and Lebrija, respectively. This the MPB N-demand could account for the entire sediment DIN uptake in Bonanza and 21% in Lebrija. These calculations point out a relevant role of MPB as a potential N-sink, particularly in Bonaza, affecting the exchange of DIN between the water column and sediments in the Guadalquivir Estuary, as shown elsewhere (Risgaard-Petersen, 2003; Sundbäck et al., 2000).

The differences in the net NO_3^- and NH_4^+ fluxes between light and dark conditions suggest a different role of MPB in the net sediment uptake of these nutrients from the water column. In general, net sediment uptake rate of NH_4^+ was higher in light (-0.25 ± 0.38 and -0.05 ± 0.11 mmol NH_4^+ m^{-2} h^{-1} for Bonanza and Lebrija, respectively) than in darkness (0.01 ± 0.27 and -0.03±0.04 mmol NH_4^+ m^{-2} h^{-1} for Bonaza and Lebrija), whereas no significant differences were found for net NO_3^- fluxes. The higher net NH_4^+ uptake rate in light is consistent with the expected higher N-demand of MPB coupled to the photosynthetic activity and growth during light (Longphuirt et al., 2009) and the preference over NO_3^- during assimilation mentioned earlier. MPB used most likely a higher fraction of NH_4^+ from the water column in Bonanza compared to Lebrija, since the differences in net uptake rate between light and dark conditions and the N- demand were higher in the former.

The observation that the net NO_3^- uptake by the sediment did not change with light does not necessarily mean that MPB did not use water column NO_3^- at all, but rather that other processes, not light-dependent, might account for a larger fraction of the measured net NO_3^- fluxes. In fact, since the sum of the sediment net NH_4^+ uptake plus NH_4^+ production within the sediment are lower than MPB N-demand, the consumption of NO_3^- by MPB, despite being energetically less favourable, seems necessary. As far as the other processes are concerned, a substantial fraction of sediment NO_3^- uptake from the water column is likely due to high rates of denitrification in the anoxic sediment layer. These were probably higher in Lebrija than in Bonanza as suggested by a considerably higher net NO_3^- uptake in Lebrija and the evident excess of uptake compared to the estimated MPB N-demand at this sampling location.

4. 6. Iron and sulfate as alternative electrons acceptors

Porewater concentrations of Fe^{2+} and SO_4^{2-} were measured in the intertidal sediments of the Guadalquivir Estuary as an initial evaluation of the potential role of $Fe^{(III)}$ minerals and SO_4^{2-} as potential e^- acceptors for the microbial degradation of organic matter in anoxic conditions. The reduction of $Fe^{(III)}$ in the sediment releases Fe^{2+} that is soluble in anoxic conditions. Fe^{2+} concentrations in general were in the range of values reported for other estuaries (Pastor et al., 2011) , being clearly higher in the most marine station of Bonanza (**Fig. S2, Fig. 6**). They changed considerably with depth and season, with a characteristic peak at 1.5 - 2.5 cm depth in both sampling stations. The intensity of the subsurface peak changed seasonally, being clearly higher in summer in both sampling sites, coincident with the highest temperature and lowest nitrate concentration in the water column.

Integrated Fe^{2+} production rates, calculated from the porewater profiles, showed a strong increase in August 2019 (**Fig. S3**), and in the range of previously reported values for marine sediments (Canfield et al., 1993). The higher Fe-reduction activity in summer was related most likely to the higher temperatures that would reduce oxygen solubility and increase microbial activity, both aerobic and anaerobic. Sediment Fe^{2+} concentrations were negatively correlated with those of NO_3^- in the water column ($r = -0.83$, $p < 0.05$), suggesting a negative feedback between these two compounds. In August 2019, the decrease in the water column NO_3^- limited or reduced denitrification, most likely, decreasing competition and thus permiting

increased rates of iron respiration. Similarly, the higher Fe^{2+} concentrations measured in Bonanza with respect to Lebrija could also be related to the higher availability of NO_3^- in the upstream zones, favouring its use as an electron acceptor over iron, since it's more favorable energetically.

Sulfate reduction is the dominant microbial process for organic matter mineralization in anoxic marine sediments, where SO_4^{2-} acts as an terminal electron acceptor in anaerobic microbial respiratory chains (Jorgensen & Kasten, 2006). The evaluation of the role of SO_4^{2-} reduction in estuarine sediments is more complex due to differences in SO_4^{2-} concentration along the freshwater – seawater salinity gradient. As expected concentrations were lower in Lebrija than in Bonanza as expected by the differences in salinity (Table S1). In the first 10 cm of the Guadalquivir estuary sediments, the typical decrease in the SO_4^{2-} concentration with depth caused by SO_4^{2-} reduction (Jørgensen et al., 2019; Jorgensen & Kasten, 2006) was not evident. This might indicate that SO_4^{2-} reduction is not a relevant pathway for the oxidation of organic matter in the upper sediment layers of the Guadalquivir estuary.

4. 7. Mineralization of organic matter in the sediment

The mineralization of organic matter in the sediment occurs by aerobic respiration in the oxic upper sediment layer, and a variety of anaerobic metabolic pathways below the oxic penetration depth (Middelburg et al., 1993). Dark respiration rate represents a good estimate of aerobic and anaerobic organic matter mineralization since it encompasses both the O_2 consumption in the direct oxidation of the organic compounds plus the O_2 being consumed in the re-oxidation of reduced inorganic products produced during anaerobic degradation (NH_4^+, H_2S, Fe^{2+}, etc.) (Jorgensen et al., 2022). Thus, dark respiration rates were consistently higher in Bonanza sediments than in Lebrija, 2.38±0.99 and 1.32±0.29 mmol m^{-2} h^{-1}, corresponding to C_{org} mineralization rates of 2.14 ±0.89 and 1.19±0.26 mmol CO_2 m^{-2} h^{-1}, respectively (Table 2), using a respiratory quotient of CO_2:O_2 = 0.90 (Jorgensen et al., 2022).

The shape of DIC profiles indicate the existence of an upward DIC flux, as a result of organic matter mineralization. In light, part of the CO_2 upward flux to the water column can be intercepted by the photosynthetic C-fixation activity of MPB (Sundbäck et al., 2004). Net DIC production ranged from 0.30 ± 0.05 to 1.29 ±

0.14 to mmol m^{-2} h^{-1} in Bonanza, and from 0.36 ± 0.09 to 0.94 ± 0.47 mmol m^{-2} h^{-1} in Lebrija (Fig. S3D; Table 2). These rates, determined by modelling DIC profiles (Berg et al., 1998), were lower (38-69 %) than the C_{org} mineralization rates calculated from the O_2 consumption rates in darkness. Nonetheless, they confirmed a higher annual mean mineralization rate in Bonanza than in Lebrija. Methodological differences inherent to both approaches and the consumption of a fraction of CO_2 produced within the sediment by MPB photosynthetic C-fixation might explain the lower mineralization rates estimated from the steady state DIC profiles.

Table 2. Sediment net community production and organic matter mineralization rates averaged for the period of study (n=5, mean±SD) at each of the two locations studied in the Guadalquivir estuary. Photosynthietic quotient used for NCP in light and respiratory quotient for dark respiration were 0.9 in both cases. Stoichiometric ratios for converting measured rates to C units were: 106C: 424Fe^{2+}; 106C:53SO_4^{2-}; 106C:84.8NO_3^-; 106C:53CH_4 (Froelich et al., 1979). Net NO_3^- reduction (denitrification) was calculated from the net sediment NO_3^- uptake from the water column in darkness. Net CH_4 production rates (methanogenesis) have been taken from Sánchez-Rodríguez et al. (2022). * indicates that there is a statistically clear difference between Bonanza and Lebrija (T-test, statistical significance p-valor<0.05)

	Process rates *(mmol m^{-2} h^{-1})*		*Source of data*	*Estimation of C_{org} fixation and mineralization rates* *(mmol CO_2 m^{-2} h^{-1})*	
	Bonanza	**Lebrija**		**Bonanza**	**Lebrija**
*Net community production (NCP)**	5.42 ± 2.02	1.60 ± 1.85	Core incubations	4.88 ± 1.82	1.44 ± 1.67
Dark Respiration (R_{dark})	2.38 ± 0.99	1.32 ± 0.29	Core incubations	2.14 ± 0.11	1.19 ± 0.26
Net DIC production	0.82 ± 0.36	0.64 ± 0.19	Porewater profiles	0.82 ± 0.36	0.64 ± 0.19
*Net NH_4^+ production**	0.011 ± 0.007	0.026 ± 0.006	Porewater profiles	0.16 ± 0.11	0.32 ± 0.07
Net Fe^{2+} production	0.05 ± 0.06	0.02 ± 0.03	Porewater profiles	0.012 ± 0.015	0.005 ± 0.007
Net SO_4^{2-} reduction	0.005 ± 0.006	0.001 ± 0.001	Porewater profiles	0.010 ± 0.012	0.002 ± 0.002
Net NO_3^- reduction	0.52 ± 1.04	0.89 ± 1.06	Core incubations	0.64 ± 1.30	1.12 ± 1.33
Net CH_4 production	0.0004 - 0.0008	0.002-0.004	Sánchez-Rodríguez et al. (2022)	0.0008 - 0.0016	0.004 - 0.008

Net NH_4^+ mineralization rates were consistently higher in Lebrija than in Bonanza throughout the year, showing in both sites parallel seasonal changes that were not observed in other biogeochemical variables (Fig. S3, Table 2). Using the mean C:N stoichiometry for both sites, 15.4 and 12.2 for Bonanza and Lebrija sediments, respectively, the annual mean NH_4^+ production rates were converted to C_{org} units, resulting in 0.16 ± 0.11 and 0.32 ± 0.07 mmol CO_2 m^{-2} h^{-1}. These rates of organic matter mineralization estimated from NH_4^+ profiles were only 20% and 50 % of those calculated from the DIC profiles for Bonanza and Lebrija respectively. NH_4^+ from mineralization of organic matter can be quickly used for nitrification and as a source of N for MPB (Glibert et al., 2016; Risgaard-Petersen, 2003; Sundbäck et al., 2000), reducing thus the NH_4^+ accumulation within the sediment and resulting in the underestimation of the mineralization rates. In addition, in muddy sediments the adsorption of NH_4^+ to the sediment particles, not measured here, can represent a significant fraction of the total NH_4^+ pool (Mackin & Aller, 1984), likely resulting in further underestimating the NH_4^+ production in the sediment.

The potential contributions of the reduction of iron-oxides (Fe^{III}) and SO_4^{2-} as terminal e^- acceptors for the mineralization of organic matter can be calculated using suitable stoichiometric ratios (Froelich et al., 1979). These calculations for the Guadalquivir Estuary sediments suggest a relatively minor quantitative role for these two anaerobic microbial pathways (Table 2). In both cases, estimated mean annual rates were up to 2 orders of magnitude lower than aerobic rates estimated as oxygen consumption rates. Although not measured in our study, methanogenesis is typically high in estuarine sediments, contributing to the degradation of OM in anoxic conditions (Wells et al., 2020; Zhou et al., 2009). Benthic methane fluxes in subtidal sediments of the Guadalquivir Estuary decreased seaward, with rates of about 0.4 - 0.8 and 2.0 - 4.0 µmol CH_4 m^{-2} h^{-1}, in Bonanza and Lebrija, respectively (Sánchez-Rodríguez et al., 2022) (Table 2). Even taking into account that these release rates likely underestimated the actual CH_4 production rate due to aerobic and anaerobic CH_4 oxidation within the sediment (Abril & Iversen, 2002; Myllykangas et al., 2020), they represent a very small contribution to the oxidation of organic matter in the Guadalquivir Estuary sediments in anoxic conditions, much lower than Fe^{III} reduction and SO_4^{2-} reduction (Table 2). In contrast, denitrification might have a relevant role in the mineralization of organic matter in the Guadalquivir Estuary due to the high NO_3^- content in the water column. The denitrification rate can be estimated from the net NO_3^- uptake rate of the sediment in darkness, producing rates of 0.71±0.57 and 0.97±1.23 mmol NO_3^- m^{-2} h^{-1} in Bonanza and

Lebrija, respectively (Table 2). When denitrification rates were transformed to C units using a suitable stoichiometric ratio for denitrification (Froelich et al., 1979), the results clearly showed a strong contribution of this process, varying between 30-94% of the values for dark O_2 respiration. Denitrification was also more than an order of magnitude higher than the contributions estimated for net Fe^{III} and SO_4^{2-} reduction and methanogenesis in the sediments of the Guadalquivir Estuary (Table 2). These results point out to the potential importance of denitrification in the oxidation of organic matter in the anoxic sediments of the Guadalquivir Estuary.

5. Conclusions

The estuary of the Guadalquivir River, in addition to its high turbidity, is characterized by very high NO_3^- concentrations in the water column. This study shows for the first time that the high NO_3^- concentration and the presence of intertidal MPB as benthic primary producers in the riverbanks condition strongly the C and N biogeochemical cycling at the sediment-water interface. Net community production of intertidal sediments was generally positive due to the MPB photosynthetic activity making the sediment net autotrophic and contributing positively to the overall autochthonous primary production of the estuary. The high NO_3^- concentration in the water column is a very strong determinant of sediment biogeochemistry in this estuary. NO_3^- fluxes dominated the exchange of DIN between the sediment and the water column, with sediments being a net sink of NO_3^- and NH_4^+, therefore reducing the export of DIN to the Gulf of Cádiz. The estimated N-demand of MPB in Bonanza was slightly higher than the total DIN net uptake, whereas in Lebrija it represented 21% of the total. This suggests that the MPB can have a potential strong impact on NO_3^- and NH_4^+ net fluxes between the water column and the sediment. On the one hand, the significantly higher sediment uptake of NH_4^+ in light with respect to dark conditions, a pattern not observed for NO_3^-, seems to suggest that the majority of MPB N-demand is satisfied by the uptake of NH_4^+ from the water column. On the other hand, the high concentration of water column NO_3^-, in addition to supporting partially the MPB N-demand, likely sustained high rates of denitrification within the sediment. Water column-dependent denitrification seems to be the most important anaerobic pathway for the oxidation of organic matter, surpassing Fe-reduction, SO_4^{2-} reduction and methanogenesis by

several orders of magnitude. Direct measurement of these microbial processes and the identification of the microorganisms involved by metagenomics are evident next steps to understand better the biogeochemical cycling of C and N in the Guadalquivir Estuary.

6. Funding

This work has been funded by the project FEDER-UCA18-107225 from the 2014-2020 ERDF Operational Program and by the Department of Economy, Knowledge, Business and University of the Regional Government of Andalusia; the project CTM2017-82274-R from the Ministry of Economy, Industry and Competitiveness of the Government of Spain; and GUADACONECT, PP.FEM.PPA201900.005. Open access fee was co-funded by the QUALIFICA Project (QUAL21-0019, Junta de Andalucía) and the Internal Research Program of the University of Cadiz (Plan Propio - UCA 2023–2024).

References

Abril, G., & Iversen, N. (2002). Methane dynamics in a shallow non-tidal estuary (Randers Fjord, Denmark). *Marine Ecology Progress Series*, *230*, 171-181. https://doi.org/10.3354/meps230171

Anderson, M. J., Gorley, R. N., & Clarke, K. R. (2008). *PERMANOVA + for PRIMER: Guide to Software and Statistical Methods. PRIMER-E: Plymouth, UK*.

Bartoli, M., Nizzoli, D., & Viaroli, P. (2003). Microphytobenthos activity and fluxes at the sediment-water interface: Interactions and spatial variability. *Aquatic Ecology*, *37*(4), 341-349. https://doi.org/10.1023/B:AECO.0000007040.43077.5f

Berg, P., Risgaard-Petersen, N., & Rysgaard, S. (1998). Interpretation of measured concentration profiles in sediment pore water. *Limnol. Oceanogr*, *43(7)*, 1500-1510. https://doi.org/10.4319/lo.1998.43.7.1500

Berg, P., Rysgaard, S., & Thamdrup, B. (2003). Dynamic modeling of early diagenesis and nutrient cycling. A case study in an arctic marine sediment. *American Journal of Science*, *303(10)*(10), 905-955. https://doi.org/10.2475/ajs.303.10.905

Bohórquez, J., Calenti, D., García-Robledo, E., Papaspyrou, S., Jimenez-Arias, J. L., Gómez-Ramírez, E. H., & Corzo, A. (2019). Water column dissolved silica concentration limits microphytobenthic primary production in intertidal sediments. *Journal of Phycology*, *55(3)*(3), 625-636. https://doi.org/10.1111/jpy.12838

Bohórquez, J., McGenity, T. J., Papaspyrou, S., García-Robledo, E., Corzo, A., & Underwood, G. J. C. (2017). Different types of diatom-derived extracellular polymeric substances drive changes in heterotrophic bacterial communities from intertidal sediments. *Frontiers in Microbiology*, *8*(FEB). https://doi.org/10.3389/fmicb.2017.00245

Bower, C. E., & Holm-Hansen, T. (1980). A Salicylate–Hypochlorite Method for Determining Ammonia in Seawater. *Canadian Journal of Fisheries and Aquatic Sciences*, *37*(5), 794-798. https://doi.org/10.1139/f80-106

Boynton, W. R., Ceballos, M. A. C., Bailey, E. M., Hodgkins, C. L. S., Humphrey, J. L., & Testa, J. M. (2018). Oxygen and Nutrient Exchanges at the Sediment-Water Interface: A Global Synthesis and Critique of Estuarine and Coastal Data. En *Estuaries and Coasts* (Vol. 41, Número 2). Estuaries and Coasts. https://doi.org/10.1007/s12237-017-0275-5

Boynton, W. R., Ceballos, M. A. C., Hodgkins, C. L. S., Liang, D., & Testa, J. M. (2023). Large-Scale Spatial and Temporal Patterns and Importance of Sediment–Water Oxygen and Nutrient Fluxes in the Chesapeake Bay Region. *Estuaries and Coasts*, *46*(2), 356-375. https://doi.org/10.1007/s12237-022-01127-0

Burgos, M., Ortega, T., Bohórquez, J., Corzo, A., Rabouille, C., & Forja, J. M. (2018). Seasonal variation of early diagenesis and greenhouse gas production in coastal sediments of Cadiz Bay: Influence of anthropogenic activities. *Estuarine, Coastal and Shelf Science*, *200*, 99-115. https://doi.org/10.1016/j.ecss.2017.10.016

Burgos, M., Ortega, T., & Forja, J. (2018). Carbon Dioxide and Methane Dynamics in Three Coastal Systems of Cadiz Bay (SW Spain). *Estuaries and Coasts*, *41*(4), 1069-1088. https://doi.org/10.1007/s12237-017-0330-2

Cabrita, M. T., & Brotas, V. (2000). Seasonal variation in denitrification and dissolved nitrogen fluxes in intertidal sediments of the Tagus estuary, Portugal. *Marine Ecology Progress Series*, *202*, 51-65. https://doi.org/10.3354/meps202051

Canfield, D. E., Jorgensen, B. B., Fossing, H., Glud, R., Gundersen, J., Ramsing, N. B., Thamdrup, B., Hansen, J. W., Nielsen, L. P., & Hall, P. O. (1993). Pathways of organic carbon oxidation in three continental margin sediments. *Marine geology*, *113(1-2)*(1-2), 27-40. https://doi.org/10.1016/0025-3227(93)90147-N

Canfield, D. E., Kristensen, E., & Thamdrup, B. (2005). *Aquatic Geomicrobiology* (1st Editio). Gulf Professional Publishing. https://doi.org/10.1016/S0065-2881(05)48017-7

Coelho, H., Vieira, S., & Serôdio, J. (2009). Effects of desiccation on the photosynthetic activity of intertidal microphytobenthos biofilms as studied by optical methods. *Journal of Experimental Marine Biology and Ecology*, *381(2)*(2), 98-104. https://doi.org/10.1016/j.jembe.2009.09.013

Corzo, A., Van Bergeijk, S. A., & García-Robledo, E. (2009). Effects of green macroalgal blooms on intertidal sediments: Net metabolism and carbon and nitrogen contents. *Marine Ecology Progress Series*, *380*, 81-93. https://doi.org/10.3354/meps07923

Díez-Minguito, M., Baquerizo, A., Ortega-Sánchez, M., Navarro, G., & Losada, M. A. (2012). Tide transformation in the Guadalquivir estuary (SW Spain) and process-based zonation. *Journal of Geophysical Research: Oceans*, *117(C3)*(3), 1-14. https://doi.org/10.1029/2011JC007344

Díez-Minguito, M., & de Swart, H. E. (2020). Relationships Between Chlorophyll-a and Suspended Sediment Concentration in a High-Nutrient Load Estuary: An Observational and Idealized Modeling Approach. *Journal of Geophysical Research: Oceans*, *125(3)*(3), e2019JC015188. https://doi.org/10.1029/2019JC015188

Donázar-Aramendía, I., Sánchez-Moyano, J. E., García-Asencio, I., Miró, J. M., Megina, C., & García-Gómez, J. C. (2019). Human pressures on two estuaries of the Iberian Peninsula are reflected in food web structure. *Scientific Reports*, *9*(1), 1-10. https://doi.org/10.1038/s41598-019-47793-2

Dortch, Q. (1990). The interaction between ammonium and nitrate uptake in phytoplankton. *Marine Ecology Progress Series*, *61*, 183-201. https://doi.org/10.3354/meps061183

Dushoff, J., Kain, M. P., & Bolker, B. M. (2019). I can see clearly now: Reinterpreting statistical significance. *Methods in Ecology and Evolution*, *10*(6), 756-759. https://doi.org/10.1111/2041-210X.13159

Flecha, S., Huertas, I. E., Navarro, G., Morris, E. P., & Ruiz, J. (2015). Air–Water CO2 Fluxes in a Highly Heterotrophic Estuary. *Estuaries and Coasts*, *38*(6), 2295-2309. https://doi.org/10.1007/s12237-014-9923-1

Froelich, P. N., Klinkhammer, G. P., Bender, M. L., Luedtke, N. A., Heath, G. R., Cullen, D., Dauphin, P., Hammond, D., Hartman, B., & Maynard, V. (1979). Early oxidation of organic matter in pelagic sediments of the eastern equatorial Atlantic: Suboxic diagenesis. *Geochimica et Cosmochimica Acta*, *43(7)*(7), 1075-1090. https://doi.org/10.1016/0016-7037(79)90095-4

Garcia-Robledo, E., Bohorquez, J., Corzo, A., Jimenez-Arias, J. L., & Papaspyrou, S. (2016). Dynamics of inorganic nutrients in intertidal sediments: Porewater, exchangeable, and intracellular pools. *Frontiers in Microbiology*, *7*(MAY), 1-14. https://doi.org/10.3389/fmicb.2016.00761

García-Robledo, E., Corzo, A., & Papaspyrou, S. (2014). A fast and direct spectrophotometric method for the sequential determination of nitrate and nitrite at low concentrations in small volumes. *Marine Chemistry*, *162*, 30-36. https://doi.org/10.1016/j.marchem.2014.03.002

García-Robledo, E., Corzo, A., Papaspyrou, S., Jiménez-Arias, J. L., & Villahermosa, D. (2010). Freeze-lysable inorganic nutrients in intertidal sediments: Dependence on microphytobenthos abundance. *Marine Ecology Progress Series*, *403*, 155-163. https://doi.org/10.3354/meps08470

Glibert, P. M., Wilkerson, F. P., Dugdale, R. C., Raven, J. A., Dupont, C. L., Leavitt, P. R., Parker, A. E., Burkholder, J. M., & Kana, T. M. (2016). Pluses and minuses of ammonium and nitrate uptake and assimilation by phytoplankton and implications for productivity and community composition, with emphasis on nitrogen-enriched conditions. *Limnology and Oceanography*, *61(1)*(1), 165-197. https://doi.org/10.1002/lno.10203

Grasshoff, K., Kremling, K., & Ehrhardt, M. (1999). Methods of seawater analysis. En Toronto. Wiley-VCH, Weinheim, New York, Chiester, Brisbane, Singopore (Ed.), *Marine Chemistry* (3rd ed.). https://doi.org/10.1016/0304-4203(78)90045-2

Haro, S., Bohórquez, J., Lara, M., Garcia-Robledo, E., González, C. J., Crespo, J. M., Papaspyrou, S., & Corzo, A. (2019). Diel patterns of microphytobenthic primary production in intertidal sediments: The role of photoperiod on the vertical migration circadian rhythm. *Scientific Reports*, *9*, 13376. https://doi.org/10.1038/s41598-019-49971-8

Haro, S., Jesus, B., Oiry, S., Papaspyrou, S., Lara, M., González, C. J., & Corzo, A. (2022). Microphytobenthos spatio-temporal dynamics across an intertidal gradient using Random Forest classification and Sentinel-2 imagery. *Science of the Total Environment*, *804*, 149983. https://doi.org/10.1016/j.scitotenv.2021.149983

Haro, S., Lara, M., Laiz, I., González, C. J., Bohórquez, J., Garcia-Robledo, E., Corzo, A., & Papaspyrou, S. (2020). Microbenthic Net Metabolism Along Intertidal Gradients (Cadiz Bay, SW Spain): Spatio-Temporal Patterns and Environmental Factors. *Frontiers in Marine Science*, *7*(February). https://doi.org/10.3389/fmars.2020.00039

Hedges, J. I., Keil, R. G., & Benner, R. (1997). What happens to terrestrial organic matter in the ocean? *Organic Geochemistry*, *27*(5-6), 195-212. https://doi.org/10.1016/S0146-6380(97)00066-1

Hensen, C., Zabel, M., & Schulz, H. N. (2006). Benthic cycling of oxygen, nitrogen and phosphorus. En *Marine Geochemistry* (pp. 207-240). https://doi.org/10.1007/3-540-32144-6_6

Hillebrand, H., & Sommer, U. (1999). The nutrient stoichiometry of benthic microalgal growth: Redfield proportions are optimal. *Limnology and Oceanography*, *44(2)*(2), 440-446. https://doi.org/10.4319/lo.1999.44.2.0440

Høgslund, S., Fossing, H., & Carstensen, J. (2023). Microphytobenthic impact on benthic pelagic nutrient exchange in temperate shallow estuaries. *Estuarine, Coastal and Shelf Science*, *292*, 108475. https://doi.org/10.1016/j.ecss.2023.108475

Huertas, I. E., Flecha, S., Navarro, G., Perez, F. F., & de la Paz, M. (2018). Spatio-temporal variability and controls on methane and nitrous oxide in the Guadalquivir Estuary, Southwestern Europe. *Aquatic Sciences*, *80*(3), 29. https://doi.org/10.1007/s00027-018-0580-5

Jørgensen, B. B., Findlay, A. J., & Pellerin, A. (2019). The biogeochemical sulfur cycle of marine sediments. *Frontiers in Microbiology*, *10*(APR), 1-27. https://doi.org/10.3389/fmicb.2019.00849

Jorgensen, B. B., & Kasten. (2006). Sulfur cycling and methane oxidation. En *Marine Geochemistry* (pp. 371-427). https://doi.org/10.1007/3-540-32144-6_11

Jorgensen, B. B., Wenzhöfer, F., Egger, M., & Glud, R. N. (2022). Sediment oxygen consumption: Role in the global marine carbon cycle. *Earth-Science Reviews*, *228*, 103987. https://doi.org/10.1016/j.earscirev.2022.103987

Kwon, B. O., Kim, H., Noh, J., Lee, S. Y., Nam, J., & Khim, J. S. (2020). Spatiotemporal variability in microphytobenthic primary production across bare intertidal flat, saltmarsh, and mangrove forest of Asia

and Australia. *Marine Pollution Bulletin*, *151*(August 2019), 110707. https://doi.org/10.1016/j.marpolbul.2019.110707

Lee, C., Wakeham, S. G., & I. Hedges, J. (2000). Composition and flux of particulate amino acids and chloropigments in equatorial Pacific seawater and sediments. *Deep-Sea Research Part I: Oceanographic Research Papers*, *47(8)*(8), 1535-1568. https://doi.org/10.1016/S0967-0637(99)00116-8

Li, Y. H., & Gregory, S. (1974). Diffusion of ions in sea water and in deep-sea sediments. Geochim. Cosmochim. Acta. *Geochimica et Cosmochimica Acta*, *38(5)*, 703-714. https://doi.org/10.1016/0016-7037(74)90145-8

Longphuirt, S. N., Lim, J. H., Leynaert, A., Claquin, P., Choy, E. J., Kang, C. K., & An, S. (2009). Dissolved inorganic nitrogen uptake by intertidal microphytobenthos: Nutrient concentrations, light availability and migration. *Marine Ecology Progress Series*, *379*, 33-44. https://doi.org/10.3354/meps07852

Macintyre, H. L., Geider, R. J., & Miller, D. C. (1996). Microphytobenthos: The ecological role of the «secret garden» of unvegetated, shallow-water marine habitats. I. Distribution, abundance and primary production. *Estuaries*, *19*(2), 186-201. https://doi.org/10.2307/1352224

Mackin, J. E., & Aller, R. C. (1984). Ammonium adsorption in marine sediments. *Limnology and Oceanography*, *29(2)*(2), 250-257. https://doi.org/10.4319/lo.1984.29.2.0250

McTigue, N. D., Bucolo, P., Liu, Z., & Dunton, K. H. (2015). Pelagic-benthic coupling, food webs, and organic matter degradation in the Chukchi Sea: Insights from sedimentary pigments and stable carbon isotopes. *Limnology and Oceanography*, *60(2)*(2), 429-445. https://doi.org/10.1002/lno.10038

Megina, C., Donázar-Aramedía, Í., Miró, J. M., García-Lafuente, J., & García-Gómez, J. C. (2023). The hyperturbid mesotidal Guadalquivir estuary during an extreme turbidity event: Identifying potential management strategies. *Ocean and Coastal Management*, *246*(October 2023). https://doi.org/10.1016/j.ocecoaman.2023.106903

Mendiguchía, C., Moreno, C., & García-Vargas, M. (2007). Evaluation of natural and anthropogenic influences on the Guadalquivir River (Spain) by dissolved heavy metals and nutrients. *Chemosphere*, *69(10)*(10), 1509-1517. https://doi.org/10.1016/j.chemosphere.2007.05.082

Middelburg, J. J., Barranguet, C., Boschker, H. T. S., Herman, P. M. J., Moens, T., & Heip, C. H. R. (2000). The fate of intertidal microphytobenthos carbon: An in situ 13C-labeling study. *Limnology and Oceanography*, *45(6)*(6), 1224-1234. https://doi.org/10.4319/lo.2000.45.6.1224

Middelburg, J. J., Vlug, T., & van der Nat, J. W. A. (1993). Organic matter mineralization in marine systems. *Global and Planetary Change*, *8*, 47-58. https://doi.org/10.1016/0921-8181(93)90062-S

Miró, J. M., Megina, C., Donázar-aramendía, I., & García-gómez, J. C. (2022). Effects of maintenance dredging on the macrofauna of the water column in a turbid estuary. *Sciences of Total Environment*, *806*. https://doi.org/10.1016/j.scitotenv.2021.151304

Miró, J. M., Megina, C., Donázar-Aramendía, I., Reyes-Martínez, M. J., Sánchez-Moyano, J. E., & García-Gómez, J. C. (2020). Environmental factors affecting the nursery function for fish in the main estuaries of the Gulf of Cadiz (south-west Iberian Peninsula). *Science of the Total Environment*, *737*, 139614. https://doi.org/10.1016/j.scitotenv.2020.139614

Myllykangas, J. P., Rissanen, A. J., Hietanen, S., & Jilbert, T. (2020). Influence of electron acceptor availability and microbial community structure on sedimentary methane oxidation in a boreal estuary. *Biogeochemistry*, *148*(3), 291-309. https://doi.org/10.1007/s10533-020-00660-z

Navarro, G., Gutiérrez, F. J., Díez-Minguito, M., Losada, M. A., & Ruiz, J. (2011). Temporal and spatial variability in the Guadalquivir estuary: A challenge for real-time telemetry. *Ocean Dynamics*, *61*(6), 753-765. https://doi.org/10.1007/s10236-011-0379-6

Pastor, L., Cathalot, C., Deflandre, B., Viollier, E., Soetaert, K., Meysman, F. J. R., Ulses, C., Metzger, E., & Rabouille, C. (2011). Modeling biogeochemical processes in sediments from the Rhône River prodelta area (NW Mediterranean Sea). *Biogeosciences*, *8*(5), 1351-1366. https://doi.org/10.5194/bg-8-1351-2011

Paterson, D. M. (1989). Short-term changes in the erodibility of intertidal cohesive sediments related to the migratory behavior of epipelic diatoms. *Limnology and Oceanography*, *34(1)*(1), 223-234. https://doi.org/10.4319/lo.1989.34.1.0223

Pratt, D. R., Pilditch, C. A., Lohrer, A. M., Thrush, S. F., & Kraan, C. (2015). Spatial Distributions of Grazing Activity and Microphytobenthos Reveal Scale-Dependent Relationships Across a Sedimentary Gradient. *Estuaries and Coasts*, *38*(3), 722-734. https://doi.org/10.1007/s12237-014-9857-7

Rios-Yunes, D., Tiano, J. C., van Oevelen, D., van Dalen, J., & Soetaert, K. (2023). Annual biogeochemical cycling in intertidal sediments of a restored estuary reveals dependence of N, P, C and Si cycles to temperature and water column properties. *Estuarine, Coastal and Shelf Science*, *282*(January), 108227. https://doi.org/10.1016/j.ecss.2023.108227

Risgaard-Petersen, N. (2003). Coupled nitrification-denitrification in autotrophic and heterotrophic estuarine sediments: On the influence of benthic microalgae. *Limnology and Oceanography*, *48(1)*(1), 93-105. https://doi.org/10.4319/lo.2003.48.1.0093

Ruiz, J., Macías, D., & Navarro, G. (2017). Natural forcings on a transformed territory overshoot thresholds of primary productivity in the Guadalquivir estuary. *Continental Shelf Research*, *148*(March), 199-207. https://doi.org/10.1016/j.csr.2017.09.002

Sánchez-Rodríguez, J., Sierra, A., Jiménez-López, D., Ortega, T., Gómez-Parra, A., & Forja, J. (2022). Dynamic of CO2, CH4 and N2O in the Guadalquivir estuary. *Science of the Total Environment*, *805*, 150193. https://doi.org/10.1016/j.scitotenv.2021.150193

Sarazin, G., Michard, G., & Prevot, F. (1999). A rapid and accurate spectroscopic method for alkalinity measurements in sea water samples. *Water Research*, *33(1)*, 290-294. https://doi.org/10.1016/S0043-1354(98)00168-7

Savelli, R., Dupuy, C., Barillé, L., Lerouxel, A., Guizien, K., Philippe, A., Bocher, P., Polsenaere, P., & Le Fouest, V. (2018). On biotic and abiotic drivers of the microphytobenthos seasonal cycle in a temperate intertidal mudflat: A modelling study. *Biogeosciences*, *15*(23), 7243-7271. https://doi.org/10.5194/bg-15-7243-2018

Schutte, C. A., Ahmerkamp, S., Wu, C. S., Seidel, M., De Beer, D., Cook, P. L. M., & Joye, S. B. (2018). Chapter 12—Biogeochemical dynamics of coastal tidal flats. En *Coastal Wetlands: An Integrated Ecosystem Approach* (Número January, pp. 407-440). https://doi.org/10.1016/B978-0-444-63893-9.00012-5

Soetaert, K., Middelburg, J. J., Heip, C., Meire, P., Van Damme, S., & Maris, T. (2006). Long-term change in dissolved inorganic nutrients in the heterotrophic Scheldt estuary (Belgium, The Netherlands). *Limnology and Oceanography*, *51(1-2)*, 409-423. https://doi.org/10.4319/lo.2006.51.1_part_2.0409

Stal, L. J., van Gemerden, H., & Krumbein, W. E. (1984). The simultaneous assay of chlorophyll and bacteriochlorophyll in natural microbial communities. *Journal of Microbiological Methods*, *2(6)*, 295-306. https://doi.org/10.1016/0167-7012(84)90048-4

Stein, L. Y., & Klotz, M. G. (2016). The nitrogen cycle. *Current Biology*, *26(3)*, R94-R98. https://doi.org/10.1016/j.cub.2015.12.021

Sundbäck, K., Linares, F., Larson, F., Wulff, A., & Engelsen, A. (2004). Benthic nitrogen fluxes along a depth gradient in a microtidal fjord: The role of denitrification and microphytobenthos. *Limnology and Oceanography*, *49(4)*, 1095-1107. https://doi.org/10.4319/lo.2004.49.4.1095

Sundbäck, K., & Miles, A. (2002). Role of microphytobenthos and denitrification for nutrient turnover in embayments with floating macroalgal mats: A spring situation. *Aquatic Microbial Ecology*, *30*(1), 91-101. https://doi.org/10.3354/ame030091

Sundbäck, K., Miles, A., & Göransson, E. (2000). Nitrogen fluxes, denitrification and the role of microphytobenthos in microtidal shallow-water sediments: An annual study. *Marine Ecology Progress Series*, *200*, 59-76. https://doi.org/10.3354/meps200059

Ubertini, M., Lefebvre, S., Gangnery, A., Grangeré, K., Le Gendre, R., & Orvain, F. (2012). Spatial Variability of Benthic-Pelagic Coupling in an Estuary Ecosystem: Consequences for Microphytobenthos Resuspension Phenomenon. *PLoS ONE*, *7(8)*, e44155. https://doi.org/10.1371/journal.pone.0044155

Underwood, & Kromkamp. (1999). Primary Production by Phytoplankton and Microphytobenthos in Estuaries. *Advances in Ecological Research*, *29*, 93-154. https://doi.org/10.1016/s0065-2504(08)60192-0

Viollier, E., Inglett, P. W., Hunter, K., Roychoudhury, A. N., & Cappellen, P. Van. (2000). *The Ferrozine method revisted*. *15(6)*, 785-790. https://doi.org/10.1016/S0883-2927(99)00097-9

Wells, N. S., Chen, J. J., Maher, D. T., Huang, P., Erler, D. V., Hipsey, M., & Eyre, B. D. (2020). Changing sediment and surface water processes increase CH4 emissions from human-impacted estuaries. *Geochimica et Cosmochimica Acta*, *280*, 130-147. https://doi.org/10.1016/j.gca.2020.04.020

Yallop, M. L., De Winder, B., Paterson, D. M., & Stal, L. J. (1994). Comparative structure, primary production and biogenic stabilization of cohesive and non-cohesive marine sediments inhabited by microphytobenthos. *Estuarine, Coastal and Shelf Science*, *39(6)*, 565-582. https://doi.org/10.1016/S0272-7714(06)80010-7

Zhou, H., Yin, X., Yang, Q., Wang, H., Wu, Z., & Bao, S. (2009). Distribution, source and flux of methane in the western Pearl River Estuary and northern South China Sea. *Marine Chemistry*, *117(1-4)*(1-4), 21-31. https://doi.org/10.1016/j.marchem.2009.07.011

Zuur, A. F., Ieno, E. N., & Elphick, C. S. (2010). A protocol for data exploration to avoid common statistical problems. *Methods in Ecology and Evolution*, *1*(1), 3-14. https://doi.org/10.1111/j.2041-210x.2009.00001.x

Supplementary material for:

Benthic metabolism and nutrient dynamics of an hyperturbid and hypernutrified estuary

Valle Perez-Rodriguez[1,2*], Alfonso Corzo[1,2], Sokratis Papaspyrou[1,2], Stefanie Anne van Bergeijk[3], Cesar Vilas[3], Pedro Cañavate[3], Emilio Garcia-Robledo[1,2]

[1]Microbial Ecology and Biogeochemistry laboratory, Department of Biology, Faculty of Marine and Environmental Science, University of Cadiz, Pol. Río San Pedro s/n, Puerto Real, Spain

[2]Instituto Universitario de Investigación Marina (INMAR), Campus Universitario de Puerto Real, 11510, Cadiz, Spain

[3]IFAPA Centro El Toruño Ctra. N IV Madrid-Cádiz, km 654a Camino de Tiro Pichón, 11500 El Puerto de Santa María, Spain

Supplementary results: Table S1-5, Figures S1-3

Supplementary Table 1. In situ water column temperature and salinity. These conditions were kept during the flux determination in the laboratory. Temperature is represented in ºC and salinity in PSU.

Date	*Measured parameter*	*Bonanza*	*Lebrija*
November 2018	Temperature	18	18.4
	Salinity	15	1
February 2019	Temperature	17.2	17.5
	Salinity	12	1
May 2019	Temperature	18	18.5
	Salinity	15	7
August 2019	Temperature	27.7	28.5
	Salinity	23	7
November 2019	Temperature	22.4	22.9
	Salinity	10	3

Supplementary Table S2. Results of main effects of PERMANOVA tests on sediment variables testing for the fixed factors time, site, and depth and core identity introduced as a random factor nested within site and time.

Variable	*Source of Variation*	*df*	*SS*	*MS*	*Pseudo-F*	*P(perm)*	*perms*	*P(MC)*
C_{org}	Date	4	218.67	54.668	2.0924	0.119	999	0.124
	Site	1	365.84	365.84	14.002	0.001	998	0.003
	Depth	9	109.96	12.218	4.3112	0.001	999	0.001
	Site*Date	4	755.54	188.89	7.2296	0.001	996	0.002
	Site*Depth	9	25.197	2.7996	0.98783	0.433	999	0.44
	Core(DaxSi)	20	522.54	26.127	9.2188	0.001	999	0.001
	Res	252	714.19	2.8341				
	Total	299	2711.9					
N_T	Date	4	0.2745	6.86E-02	2.9035	0.046	999	0.037
	Site	1	0.25537	0.25537	10.805	0.006	998	0.003
	Depth	9	1.5138	0.1682	25.485	0.001	998	0.001
	Site*Date	4	1.2813	0.32033	13.553	0.001	999	0.001
	Site*Depth	9	0.29953	3.33E-02	5.0426	0.001	999	0.001
	Core(DaxSi)	20	0.4727	2.36E-02	3.581	0.001	999	0.001
	Res	252	1.6632	6.60E-03				
	Total	299	5.7604					
CN	Date	4	320.75	80.187	2.4355	0.081	999	0.09
	Site	1	762.23	762.23	23.151	0.001	997	0.001
	Depth	9	97.514	10.835	3.3497	0.001	996	0.002
	Site*Date	4	734.19	183.55	5.5748	0.003	999	0.005
	Site*Depth	9	35.528	3.9475	1.2204	0.252	996	0.294
	Core(DaxSi)	20	658.49	32.924	10.179	0.001	996	0.001
	Res	252	815.12	3.2346				
	Total	299	3423.8					
Chla	Date	4	17.96	4.49	49.673	0.001	998	0.001
	Site	1	0.55564	0.55564	6.1471	0.02	996	0.019
	Depth	4	17.385	4.3463	46.623	0.001	998	0.001
	Site*Date	4	3.4908	0.8727	9.6547	0.001	999	0.001
	Site*Depth	4	1.8509	0.46273	4.9637	0.002	999	0.002
	Core(DaxSi)	20	1.8078	9.04E-02	0.96962	0.509	999	0.53
	Res	112	10.441	9.32E-02				
	Total	149	53.491					
Ratio Chla/Phaeoa	Date	4	0.79503	0.19876	63.825	0.001	997	0.001
	Site	1	4.48E-04	4.48E-04	0.14399	0.719	995	0.713
	Depth	4	0.22345	5.59E-02	5.6646	0.001	998	0.002
	Site*Date	4	0.10364	2.59E-02	8.3199	0.001	998	0.001
	Site*Depth	4	7.46E-02	1.87E-02	1.8913	0.103	999	0.105

Core(DaxSi)	20	6.23E-02	3.11E-03	0.31578	0.998	998	0.998
Res	112	1.1045	9.86E-03				
Total	149	2.364					

Supplementary Table S3. Results of main effects of PERMANOVA tests on sediment-water fluxes testing for the fixed factors time and site, in light and in darkness.

	Variable	*Source of Variation*	*df*	*SS*	*MS*	*Pseudo-F*	*P(perm)*	*perms*	*P(MC)*
Light	**NCP**	Date	4	149.14	37.285	26.038	0.001	998	0.001
		Site	1	248.9	248.9	173.82	0.001	995	0.001
		Date ×Site	4	163.8	40.95	28.598	0.001	999	0.001
		Res	40	57.278	1.432				
		Total	49	619.13					
	J-NO_2^-	Date	4	7959.9	1990	15.436	0.001	999	0.001
		Site	1	1621.9	1621.9	12.58	0.001	998	0.001
		Date ×Site	4	5151.4	1287.8	9.9896	0.001	999	0.001
		Res	40	5156.8	128.92				
		Total	49	19890					
	J-NO_3^-	Date	4	2.26E+07	5.65E+06	2.050	0.101	998	0.101
		Site	1	3.07E+06	3.07E+06	1.114	0.301	993	0.285
		Date ×Site	4	3.95E+07	9.87E+06	3.582	0.009	999	0.008
		Res	40	1.10E+08	2.75E+06				
		Total	49	1.75E+08					
	J-NH_4^+	Date	4	2.96E+06	7.41E+05	86.045	0.001	999	0.001
		Site	1	5.46E+05	5.46E+05	63.459	0.001	998	0.001
		Date ×Site	4	9.43E+05	2.36E+05	27.388	0.001	999	0.001
		Res	40	3.44E+05	8608.5				
		Total	49	4.80E+06					
Dark	**R_{dark}**	Date	4	14.535	3.6337	26.143	0.001	998	0.001
		Site	1	12.591	12.591	90.589	0.001	997	0.001
		Date ×Site	4	7.7835	1.9459	14	0.001	997	0.001
		Res	40	5.5597	0.13899				
		Total	49	40.469					
	J-NO_2^-	Date	4	27625	6906.3	13.886	0.001	998	0.001
		Site	1	13440	13440	27.024	0.001	997	0.001
		Date ×Site	4	15741	3935.3	7.9125	0.001	999	0.001
		Res	40	19894	497.35				
		Total	49	76701					
	J-NO_3^-	Date	4	2.18E+07	5.46E+06	3.584	0.009	998	0.015

	Site	1	3683.2	3683.2	0.002	0.966	998	0.96
	Date ×Site	4	1.02E+07	2.55E+06	1.673	0.193	999	0.185
	Res	40	6.09E+07	1.52E+06				
	Total	49	9.29E+07					
J-NH_4^+	Date	4	2.27E+07	5.68E+06	3.7115	0.011	999	0.01
	Site	1	39579	39579	2.59E-02	0.893	999	0.89
	Date ×Site	4	1.12E+07	2.80E+06	1.8283	0.12	998	0.148
	Res	40	6.12E+07	1.53E+06				
	Total	49	9.51E+07					

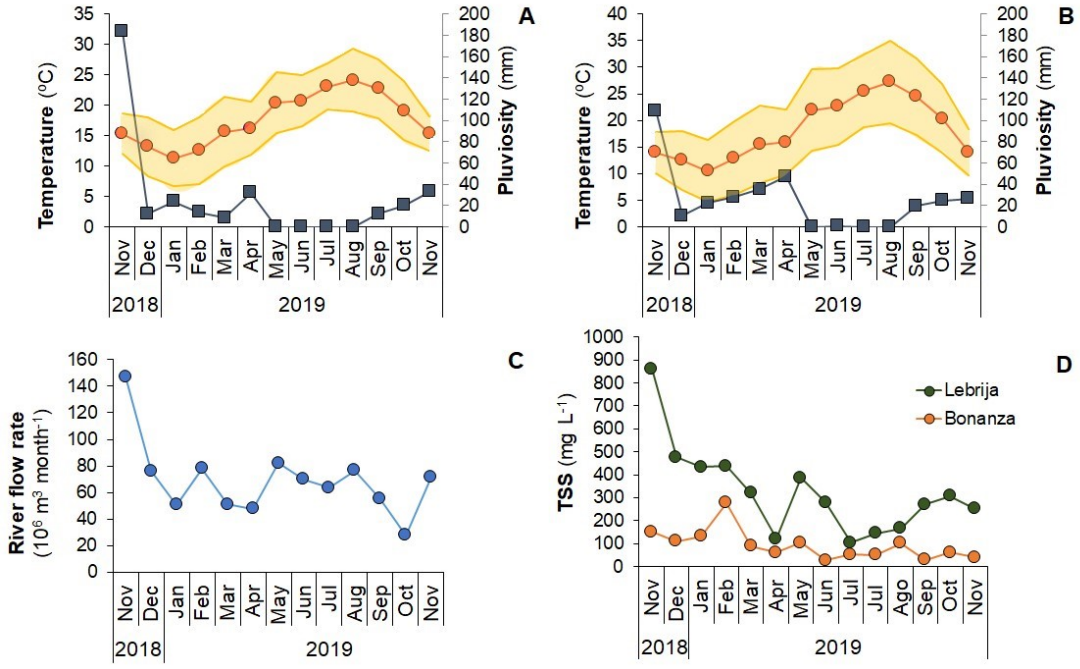
Supplementary Table 4. Results of main effects of PERMANOVA tests on sediment porewater variables testing for the fixed factors time, site, and depth and core identity introduced as a random factor nested within site and time.

Variable	*Source of Variation*	*df*	*SS*	*MS*	*Pseudo-F*	*P(perm)*	*perms*	*P(MC)*
DIC	Date	4	1415	353.74	47.543	0.001	998	0.001
	Site	1	270.14	270.14	36.307	0.001	998	0.001
	Depth	9	873.01	97.001	56.167	0.001	999	0.001
	Site×Date	4	1300	325.01	43.681	0.001	999	0.001
	Site×Depth	9	106.92	11.88	6.8789	0.001	998	0.001
	Core(Da×Si)	20	148.81	7.4404	4.3082	0.001	998	0.001
	Res	252	435.21	1.727				
	Date	299	4549.1					
NH_4^+	Date	4	2.67E+05	66730	3.4072	0.014	999	0.012
	Site	1	33289	33289	1.6997	0.206	996	0.196
	Depth	9	2.91E+06	3.24E+05	115.46	0.001	999	0.001
	Site×Date	4	6.31E+05	1.58E+05	8.0554	0.001	999	0.001
	Site×Depth	9	1.46E+05	16183	5.7735	0.001	997	0.001
	Core(Da×Si)	20	3.92E+05	19585	6.9871	0.001	997	0.001
	Res	252	7.06E+05	2803				
	Date	299	5.09E+06					
Fe^{2+}	Date	4	114.34	28.585	82.241	0.001	999	0.001
	Site	1	1.459	1.459	4.1977	0.056	997	0.064
	Depth	9	27.682	3.0758	9.0969	0.001	999	0.001
	Site×Date	4	31.376	7.8439	22.567	0.001	999	0.001
	Site×Depth	9	21.122	2.3469	6.9412	0.001	998	0.001
	Core(Da×Si)	20	6.9516	0.34758	1.028	0.419	997	0.425
	Res	252	85.205	0.33812				
		299	288.14					
NO_3^-	Date	4	105.45	26.363	26.465	0.001	998	0.001
	Site	1	35.642	35.642	35.78	0.001	994	0.001
	Depth	4	140.8	35.2	25.916	0.001	998	0.001
	Site×Date	4	9.815	2.4537	2.4632	0.072	998	0.093
	Site×Depth	4	2.9426	0.73564	0.54161	0.719	998	0.691
	Core(Da×Si)	20	19.923	0.99616	0.73341	0.768	999	0.792
	Res	112	152.12	1.3582				

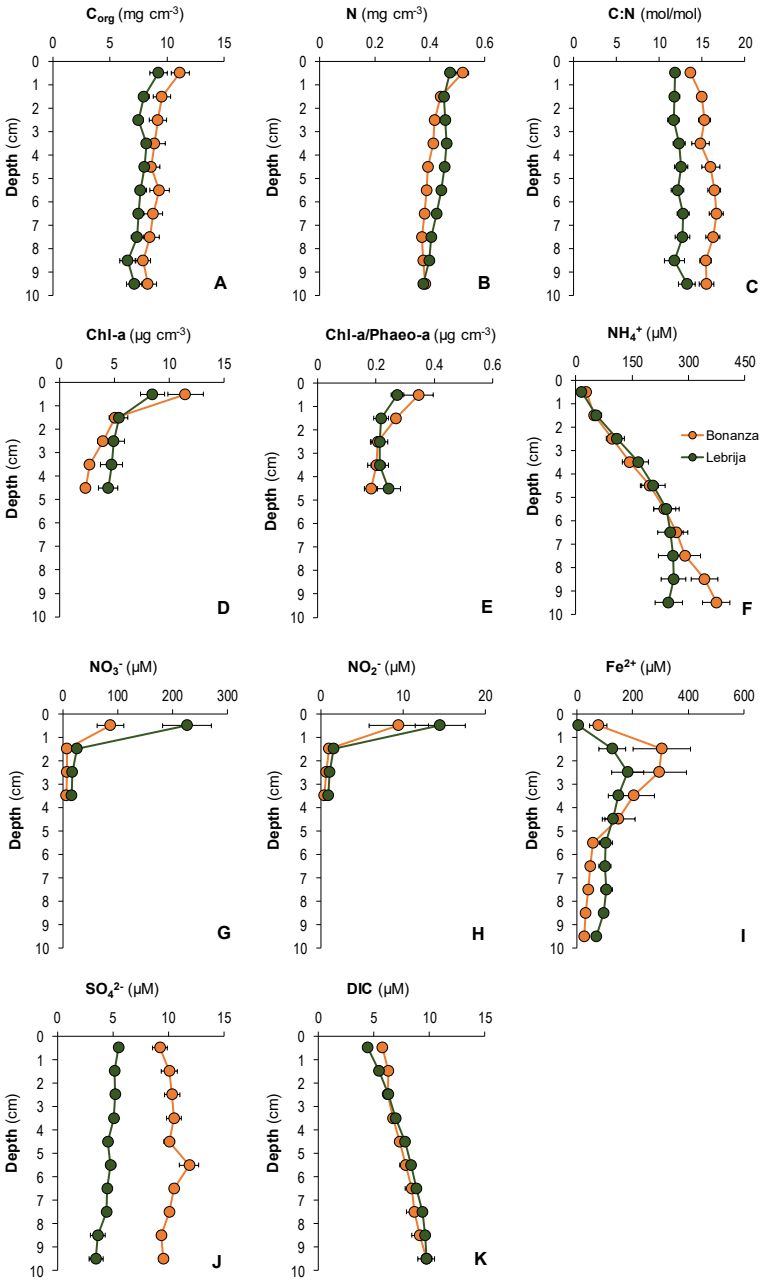
	Date	149	466.7					
NO_2^-	Date	4	46.686	11.672	20.704	0.001	999	0.001
	Site	1	0.57328	0.57328	1.0169	0.374	996	0.33
	Depth	4	59.241	14.81	13.233	0.001	999	0.001
	Site×Date	4	1.9578	0.48945	0.86824	0.527	998	0.505
	Site×Depth	4	5.6582	1.4146	1.2639	0.276	999	0.27
	Core(Da×Si)	20	11.274	0.56372	0.50368	0.965	999	0.966
	Res	112	125.35	1.1192				
	Date	149	250.74					

Supplementary Table S5. Results of main effects of PERMANOVA tests on water column nutrient concentrations testing for the fixed factors time and site, in light and in darkness.

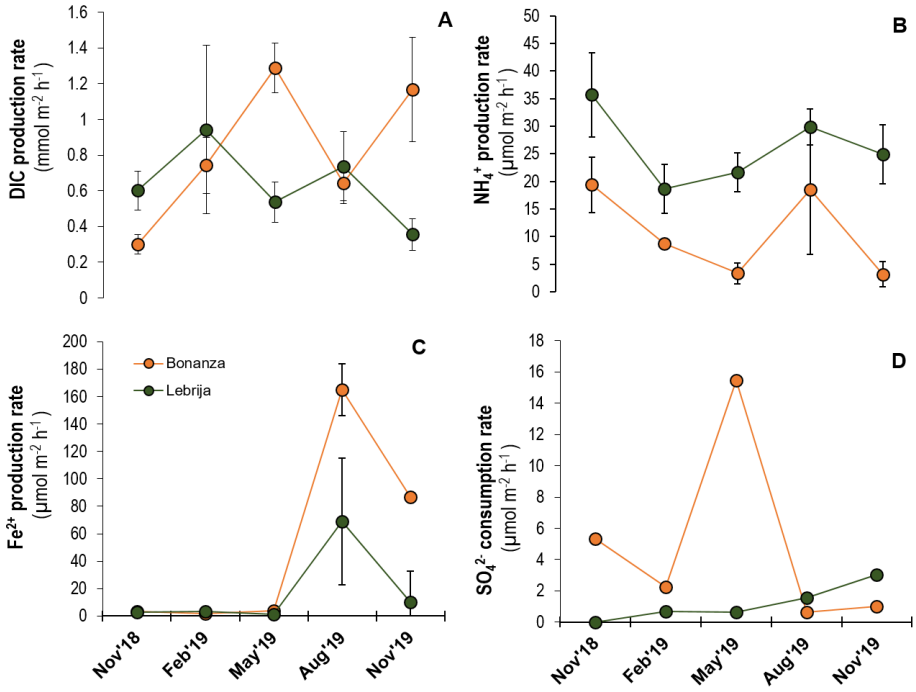
Variable	*Source of Variation*	*df*	*SS*	*MS*	*Pseudo -F*	*P(perm)*	*perms*	*P(MC)*
initial NO_3^- WC	Date	4	5.67E+05	1.42E+05	436.87	0.001	999	0.001
	Site	1	1.37E+05	1.37E+05	421.2	0.001	987	0.001
	Date ×Site	4	37425	9356.3	28.834	0.001	997	0.001
	Res	10	3244.9	324.49				
	Total	4	24.58	0.0002				
initial NH_4^+- WC	Date	4	273.25	68.313	7.6483	0.011	999	0.008
	Site	1	16.26	16.26	1.8205	0.228	997	0.188
	Date ×Site	4	26.212	6.5529	0.73367	0.626	999	0.584
	Res	10	89.317	8.9317				
	Total	19	405.04					



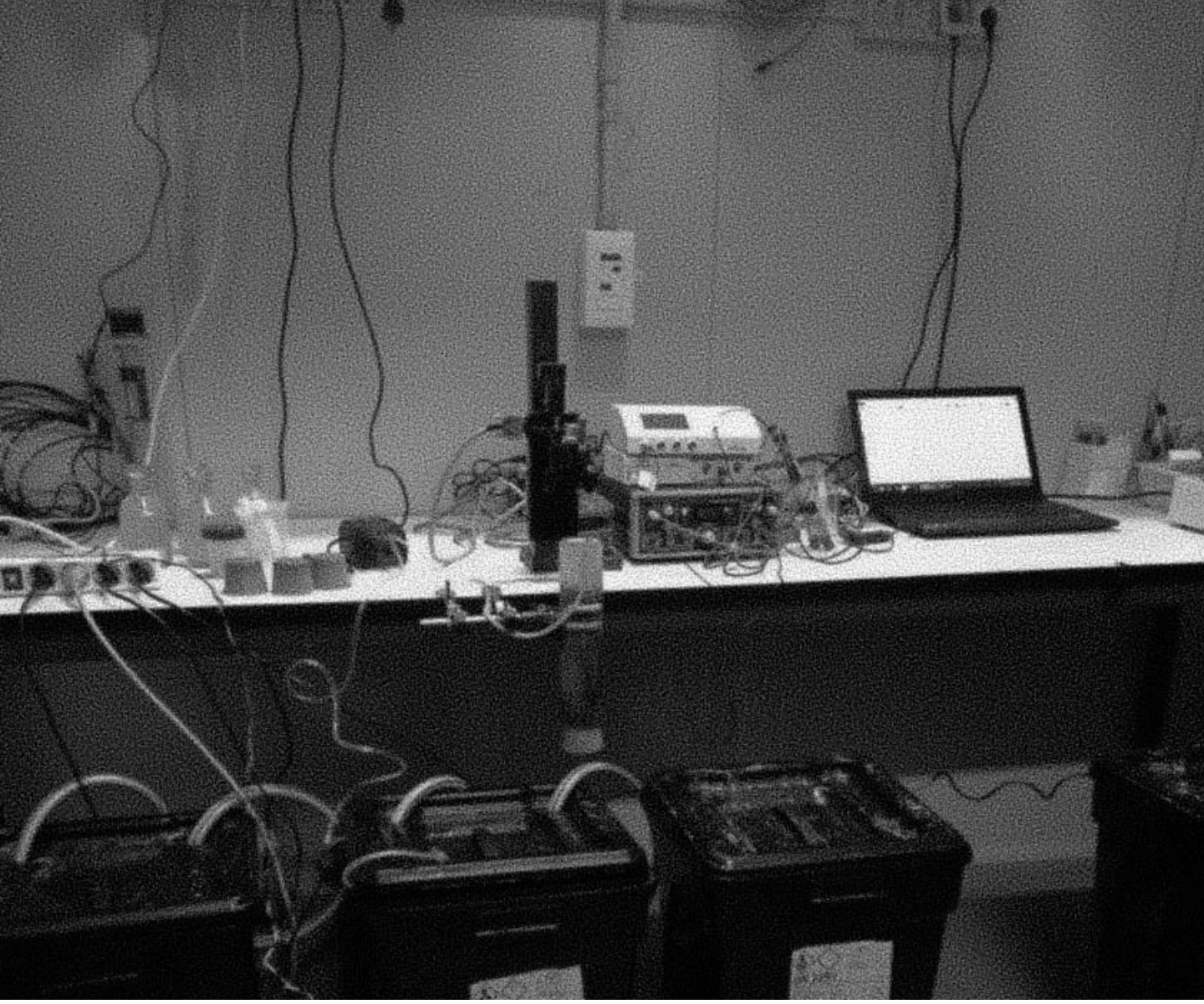
Supplementary Figure 1. (A) Climatic conditions in Chipiona and (B) Las Cabezas de San Juan, (C) Guadalquivir River flow rate at the Alcalá del Río dam, and (D) the concentration of total suspended solids. Chipiona (A) and Las Cabezas de San Juan (B) represent the closest sites from which data could be found.



Supplementary Figure 2. Annual average changes in sediment content of (**A**) C_{org}, (**B**)N_T, (**C**) C:N, (**D**) Chl-a, (**E**) Chla:Phaeoa ratio, and porewater concentrations of (**F**) NH_4^+, (**G**) NO_3^-, (**H**) NO_2^-, (**I**)Fe^{2+}, (**J**) SO_4^{2-} and (**K**) DIC, in Bonanza (orange) and Lebrija (green) along the Guadalquivir estuary during the sampling period, from November 2018 to November 2019.. Data are means ± SE (n=3).

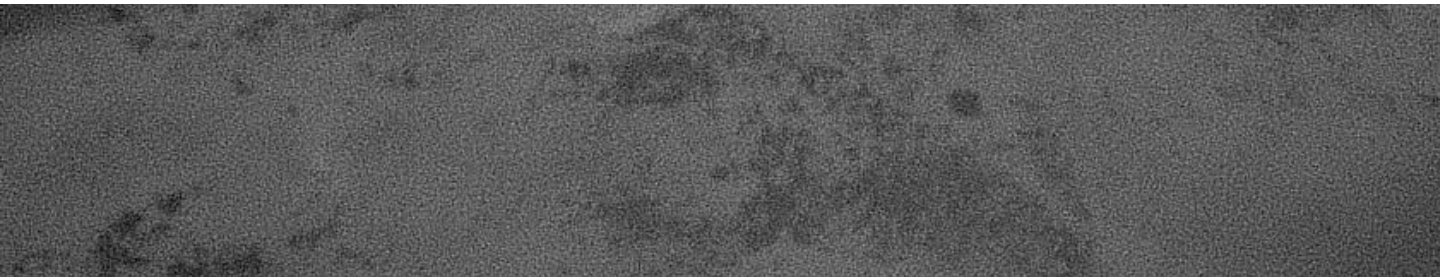


Supplementary Figure 3. Depth integrated (0-10 cm) net production of (**A**) DIC, (**B**) NH_4^+, (**C**) and Fe^{2+}, and (**D**) net consumption of SO_4^{2-} estimated from the porewater profiles using the PROFILE software (Berg et al 1998) in Bonanza (orange) and Lebrija (green) along the Guadalquivir estuary during the sampling period, from November 2018 to November 2019. Data points represent the average of three sediment cores ± SE (n=3) except for SO_4^{2-} where only one replicate was available.



Chapter 3:

Impact of heatwaves on net metabolism, nutrient and greenhouse gases fluxes at the sediment water interphase of a shallow coastal ecosystems



Impact of heatwaves on net metabolism, nutrient and greenhouse gases fluxes at the sediment-water interphase of a shallow coastal ecosystems

Valle Perez-Rodriguez[1], Alfonso Corzo[1], Sokratis Papaspyrou[1], Ana Sierra[2,] Joe D. Taylor[5], Cindy J. Smith[4], Fabien Cholet[4], Emilio Garcia-Robledo[1]

[1]Departamento de Biología, Facultad de Ciencias Marinas y Ambientales, Universidad de Cádiz, Campus Universitario Río San Pedro, 11510 Puerto Real, Cádiz, Spain.

[2] Instituto Universitario de Investigación Marina (INMAR), Campus Universitario de Puerto Real, Universidad de Cádiz, Campus Universitario Río San Pedro, 11510 Puerto Real, Cádiz, Spain.

[3] Dpto. Química-Física, INMAR, Facultad de Ciencias del Mar y Ambientales, Universidad de Cádiz, Campus Universitario Río San Pedro, 11510 Puerto Real, Cádiz, Andalucía, Spain

[4] Advanced Research Centre, Infrastructure and Environment, James Watt School of Engineering, University of Glasgow, 11 Chapel Lane G11 6EW, Glasgow, UK.

[5] UK Centre for Ecology and Hydrology, Wallingford, OX10 8BB, UK

Keywords: Climate change, nutrient fluxes, temperature dependence, Nitrification, denitrification, greenhouse gases

Abstract

Global average temperatures and the frequency of extreme climatic events, such as heat waves, are increasing due to the anthropogenic rise in the emission of greenhouse gases (GHGs). Shallow aquatic areas can potentially buffer some of the anthropogenic alterations, acting as net sinks for nutrients and GHGs, such as CO_2, CH_4 or N_2O. However, these shallow environments are also vulnerable to climate variations with yet unknown consequences in their role as climate buffers. In order to investigate the impact of altered temperatures on the net exchange of GHGs and nutrients, we quantified the variations produced in the net metabolism, dissolved inorganic nitrogen and GHGs fluxes in sediments from the Bay of Cadiz exposed to a wide range of temperatures (from 10 to 42 ºC). During 5 days of laboratory-controlled experiment, sediment-water fluxes were measured by core incubations and oxygen microprofiles, also studying the changes produced in the microbial community. Our results showed a significant enhancement of sediment respiration with temperature, with evidence of respiration inhibition after prolonged exposure to high temperatures, commonly reached during heatwaves (>34ºC). Nitrogen cycling processes were also affected by temperature, although not in a simple way. Moderate warming increased nitrification processes, increasing the net

efflux of nitrite. However, under high temperature conditions, dissimilatory processes such as denitrification and dissimilatory nitrate reduction to ammonium (DNRA) seem to be enhanced. The abundance of key nitrification genes did not increase significantly but the metagenomic analysis of the microbial community showed an enrichment of denitrification pathway genes at the highest temperatures. N_2O release from the sediment increased with temperature up to 26-32°C, but decreased at higher temperatures. N_2O emissions were also higher during the first few days, showing a decoupling of processes that increased the net release from the sediment. Methane release from sediment increased exponentially with temperature, revealing a large impact of short-term temperature increases on emissions of both GHGs from shallow environments. Therefore, increasing the frequency and duration of heat waves could significantly increase the net release of GHGs such as CO_2, CH_4 and N_2O, with unknown feedback consequences on global warming.

1. Introduction

Global warming is considered one of the most serious threats to ecosystems with temperatures of the Earth's surface increasing worldwide, being directly linked to the production and emission of anthropogenic Green House Gases (GHG) (Burkholz et al., 2020; Meehl et al., 2005; Oliver et al., 2019; Parmesan et al., 2022; Perkins-Kirkpatrick & Lewis, 2020). This global warming is additionally increasing the intensity and frequency of episodes of extreme climatic conditions (ECC) (Fischer & Knutti, 2015; Henson et al., 2016; Schutte et al., 2019; Smith et al., 2023; Ummenhofer & Meehl, 2017). The ecosystem response to the extreme temperature changes during heat waves may result in a feedback loop leading to an increase of naturally produced GHG during biogeochemical cycling, therefore reinforcing global warming (Burkholz et al., 2020).

Shallow coastal ecosystems like estuaries and wetlands play a vital role in providing essential ecosystem services. These areas are characterized by high biodiversity, support economically important species, and act as crucial buffers during the exchange of organic matter, nutrients, oxygen, and GHG between land and ocean. Additionally, they receive substantial inputs of organic carbon and nutrients from rivers and runoff, further emphasizing their importance as critical interfaces between land and sea (Froneman, 2005; Hines et al., 2013; Schutte et al., 2019). In these environments, the accumulated organic material in the sediment

undergoes a sequence of microbial processes, where oxygen is rapidly consumed, leading to suboxic and anoxic conditions that further drive organic matter decomposition and nutrient recycling by anaerobic microbial metabolisms (Canfield et al., 1993; Schutte et al., 2019). These processes result in the production of CO_2 but might also generate or consume potent greenhouse gases like N_2O and CH_4. Shallow coastal environments acting as net sources might contribute significantly to global atmospheric emissions and then play a crucial role in the global nitrogen cycle and the destruction of stratospheric ozone (Burgos et al., 2018; Burkholz et al., 2020; Herbert, 1999).

Shallow coastal systems, and particularly intertidal systems, are subjected to a wide range of physical forcings, such as daily and seasonal light cycles, immersion and emersion periods due to tidal changes, and temperature variations. The latter are of particular interest as they are directly affected by global warming. Under standard conditions, intertidal sediments can undergo temperature changes of several degrees (e. g. from 17 to 24º C in northern systems) (Guarini et al., 1997), being even higher in areas with larger temperature variations (Deldicq et al., 2021). As a consequence, biogeochemical processes and fluxes of solutes, including GHG, can vary significantly throughout the day (Haro et al., 2019; Hicks et al., 2018). Variations in temperature due to heatwaves can differentially modify physicochemical processes with opposite effects on solute solubility and diffusion. An increase in temperature can decrease, for example, the availability of oxygen while at the same time increase its diffusion rates thus affecting the rates and depth distribution of biogeochemical processes involved in carbon and nitrogen mineralization (Apple et al., 2006; Hicks et al., 2018; Rios-Yunes et al., 2023; Saad & Conrad, 1993; Thamdrup et al., 1998). Temperature changes can also directly influence enzymatic processes in biogeochemical cycles, leading to varying impacts on metabolic rates and shifting the relative importance of different processes. Typically, higher temperatures are expected to accelerate metabolic activities, but the relative effect can vary depending on the specific process and enzymes involved. For instance, elevated temperatures may enhance nitrification by increasing directly enzyme activity or by a higher availability of ammonium due to increased remineralization rates and simultaneously limit nitrification due to reduced oxygen concentrations.

Monitoring and understanding the effects of rising temperatures on ecosystem components is essential for predicting ecosystem responses (Fischer & Knutti,

2015; Parmesan et al., 2022). However, knowledge about the impacts of extreme climatic events, such as heat waves, remains limited, and few studies have examined their impacts on intertidal communities (Easterling et al., 2000; Perkins-Kirkpatrick & Lewis, 2020; Stott et al., 2004). In the present study, we investigated the impact of maintained temperature variations during a 4-day experiment in the absence of tides and in darkness to limit the confounding factors. The aim was to assess the effects of temperatures surpassing the standard ranges characteristic of the sampled area (the Bay of Cadiz) on the sediment microbial composition and metabolism. Sediment-water oxygen and nutrient exchange, the emission of greenhouse gases and the changes in the bacterial community were assessed during the experiment. Even though the results may not be directly extrapolated to field conditions, they provide valuable insights into how highly exposed systems may respond, how their communities and metabolic processes might be affected, and whether these communities can adapt to such large changes in temperature.

2. Material and Methods

2. 1. Study site and sampling

Sediment cores (n = 24, id. 5.5 cm, 30 cm length) and *in situ* water were collected on May 2018 in a non-vegetated muddy area of the shallow Río San Pedro tidal creek (Cádiz, Spain) (36 ° 34 ' 37.5 "N, 6 ° 11 ' 14.3" W) (**Fig. 1**). The creek has an average depth of 3-6 meters and a semi-diurnal tidal regime. Water temperature varies between 10 and 23ºC in winter and summer, respectively (Ferrón et al., 2009; Tovar et al., 2000).

Cores were transported to the laboratory after collection and distributed among five 40 L tanks filled with aerated *in situ* water (36 ‰). Sediment cores were maintained for 4 days at 18ºC in darkness for acclimation. After this period, four sediment cores were used to measure initial conditions (time 0) as described below. Subsequently, temperature in each of the tanks was progressively modified to reach five different temperatures (10, 18, 26, 34, and 42 º C) by using electrical heaters or cooling units. The final temperatures were reached after approximately 6 hours. The effect of the temperature changes was measured after 12, 36, 60, and 84 hours.

For each temperature and day, three sediment cores were incubated to measure sediment-water fluxes of inorganic nitrogen nutrients (NO_3^-, NO_2^-, NH_4^+), oxygen

(O_2), methane (CH_4) and nitrous oxide (N_2O). One additional sediment core was used to measure oxygen microprofiles, as described below. Additional subsamples were taken for molecular analyses, including DNA extraction, 16S rRNA gene amplification and sequencing, bioinformatic processing, and qPCR, to characterize the microbial community and its functional potential.

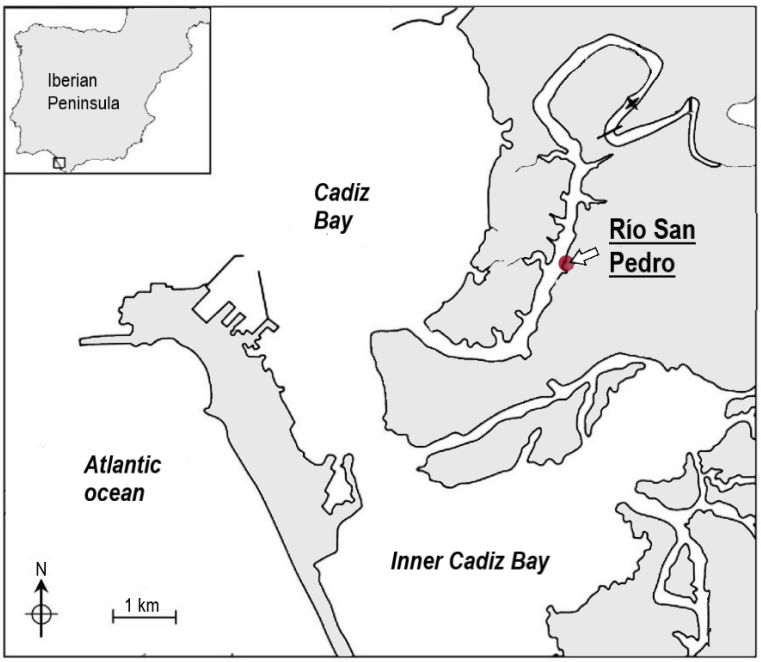


Figure 1. Map of the Bay of Cadiz. Red dot represents the sampling site at Río San Pedro creek.

2. 2. Sediment-water fluxes

Sediment cores (20 cm of sediment and 10 cm of water column) were equipped with magnetic stirrers suspended in the water column and driven by external motors to maintain the turbulence in the water column. Once initial water samples were collected, sediment cores were sealed with rubber stoppers and incubated for 2-10 hours, depending on the temperature. At the end of the incubation period, sediment cores were opened outside the water tank for collecting final samples and cores returned to their corresponding tank.

Water samples (10 mL) for nutrient analyses were filtered (MF300 glass fiber filter, 0.7 µm nominal pore size, FisherBrand) in 12 mL plastic tubes and stored frozenat -24º C until analysis. Nitrate and nitrite were analyzed following the procedure described in Garcia-Robledo et al. (2014), and ammonium according to Bower & Holm-Hansen (1980). Spectrophotometric measurements were performed on a Multiskan™ GO microplate reader (Thermo Scientific™).

Oxygen fluxes for the determination of diffusive oxygen uptake (DOU) at the sediment-water interface were measured by O_2 vertical concentration profiles in darkness with oxygen selective microelectrodes (100 µm tip size, Unisense A/S, Denmark) controlled by a motorized micromanipulator (MS-232), connected to a computer using the Sensor Trace Pro software (Unisense®). The microelectrodes were calibrated in the water column with constant bubbling for the 100% oxygen saturation and in the anoxic zone of the sediment for the 0% saturation. From the profiles, the depth of maximum oxygen penetration (Zox) was identified and the oxygen fluxes were determined at the diffusive boundary layer by applying Fick's first law for diffusion (Jørgensen & Revsbech, 1985; Kühl et al., 1994; Revsbech, 1989)(**Eq 1**):

$$J(O_2) = \varphi D_0 (\partial C / \partial z) \quad (1)$$

where J is the diffusive flux, **φ** is the porosity in the surface layer, D_0 is the molecular diffusion coefficient, and $\partial C/\partial z$ is the concentration gradient at the diffusive boundary layer. D_0 was derived from standard values based on the prevailing salinity and temperature conditions (Soetaert & Petzoldt, 2008).

Samples for the determination of N_2O and CH_4 concentrations were collected in 50 mL serum bottles and preserved with 120 µL of 37% formaldehyde. Concentrations of the dissolved gases were measured using a Bruker® gas chromatograph model 450 GC as described previously by Sierra (2017).

Sediment-water fluxes (mmol m^{-2} h^{-1}) for nutrients, total oxygen uptake (TOU) and GHGs were calculated as a mass balance during the incubation according to the following formula (**Eq. 2**):

$$J = \frac{(C_{final} - C_{initial}) \cdot h}{\Delta t} \quad (2)$$

where, C corresponds to the initial and final concentrations (μmol L^{-1}), h represents the height of the water column (m), and Δt is the incubation time interval (h). Positive flux represents release from the sediment and negative flux uptake by the sediment.

2. 3. Organic matter, DIC and nutrients profiles in the sediment

On the last day of the experiment, one core from each temperature treatment was sliced every cm down to 5 cm depth. Slices were transferred to 50 mL Falcon tubes and homogenized to collect about 1 g of the sediment slurry for DNA extraction as explained below. The rest wascentrifuged at 4700 ×g for 20 min at 4 °C in a Sorvall™ Legend™ X1R centrifuge (Thermo Scientific™) to extract the porewater (PW). Three mL were transferred to Exetainers® (LabCO, UK) and preserved with 50 μL of 32-37% formaldehyde for later analysis of Dissolved Inorganic Carbon (DIC) via the Gran titration method (Mehrbach et al., 1973), and the remaining fraction was transferred to 6 mL plastic vials and kept frozen at -24ºC until later analysis for nutrients concentrations. Centrifuged sediment was frozen, freeze-dried and homogenized. Carbon and N content were analyzed on an elemental analyzer (Leco CHNS 932) at the Central Services of the University of A Coruña, Spain. Organic carbon (C_{org}) was determined as the difference between the total carbon measured in the freeze-dried sediment samples and inorganic carbon measured on a replicate previously combusted at 550°C for 4 h. Total nitrogen was measured in the freeze-dried sediment samples.

Besides, dissolved inorganic carbon (DIC) and dissolved inorganic nitrogen (DIN) fluxes at the sediment-water interface were calculated from the DIC and DIN profiles, using Fick's first law equation applied to the upper 2 cm sediment layer and the diffusion coefficient with the sediment (D_s), hereafter referred as steady state fluxes.

2. 4. Apparent activation energy and Q_{10} calculation

The dependence of the measured microbial processes with temperature was quantified by the calculation of the apparent activation energy (E_a) and the Q_{10} value. For that purpose, the measured rates were adjusted to the Arrhenius equation, and E_a was calculated by eq. 3:

$$E_a = -R \cdot T \cdot \ln\left(\frac{Rate}{A}\right) \quad (3)$$

where, A is a constant, R is the ideal gases constant (J K^{-1} mol^{-1}) and T is the experimental temperature (ºK). E_a was then used to calculate the Q_{10}, following eq. 4 (Glud, 2008; Thamdrup et al., 1998):

$$Q'_{10} = \exp\left(E_a \cdot 10K \cdot \left(R \cdot T \cdot (T + 10K)\right)^{-1}\right) \quad (4)$$

In addition, we also calculated Q_{10} values as the difference in rates between two temperatures following eq. 5:

$$Q_{10} = \left(\frac{R_2}{R_1}\right)^{\frac{10}{(T_2 - T_1)}} \quad (5)$$

2. 5. DNA extraction, PCR and sequencing of 16S rRNA

Prior to the centrifugation to extract PW, a portion of the sediment (~1g) was placed in 1.5 mL microcentrifuge tubes and frozen at -80 °C. DNA extraction was performed according to mechanical-chemical lysis protocol of Griffiths et al (2000). The quality and concentration of the extracted DNA was checked by spectrophotometry using a µdrop Multiskan GO (Thermo-Scientific) and confirmed by Qubit (Thermo-Scientific). The 16S rRNA gene V4 variable region PCR primers 515F-806R (Walters et al., 2016) was amplified using the HotStarTaq Plus Master Mix Kit (Qiagen, USA) with the following cycling conditions: 95°C for 5 minutes, followed by 30 cycles of 95°C for 30 seconds, 53°C for 40 seconds and 72°C for 1 minute, and a final elongation step at 72°C for 10 minutes. PCR products were checked by gel electrophoresis. Samples are multiplexed using unique dual indices and are pooled together in equal proportions based on their molecular weight and DNA concentrations. Pooled samples were purified using calibrated Ampure XP beads. Then the pooled and purified PCR product was used to prepare an Illumina DNA library. Sequencing was performed at MR DNA (www.mrdnalab.com, Shallowater, TX, USA) on a MiSeq following the manufacturer's guidelines.

2. 6. Bioinformatics analysis

Sequences (fastq files) were processed using DADA2 pipeline (Callahan et al., 2016) in R V.4.0 (R Core Team 2021). Forward and reverse reads were trimmed

to 250 and 220 bases, respectively. Filtering settings were maximum number of Ns (maxN) = 0, maximum number of expected errors (maxEE) = (1.1). The primer sequences were removed using trimLeft=c(20.20). Sequences were dereplicated and the DADA2 core sequence variant inference algorithm applied. mergePairs was used to merge sequences and ASV tables were constructed. Chimeric sequences were removed using removeBimeraDenovo default settings. ASVs were taxonomically assigned using assignTaxonomy at default settings against the Silva version 138 database. Samples were rarefied to 150,000 reads per sample for Bacteria before further analysis and singleton ASVs removed, as well as ASVs appearing in less than 2 samples.

The ASV tables and sequences served as input for picrust2 (PICRUSt2; https://github.com/picrust/picrust2; Version 2.2.0), which was executed to obtain copy number corrected predicted metagenomes from the 16S ASVs. Picrust2 provided information on the relative proportion for different Kyoto Encyclopedia of Genes and Genomes (KEGG; http://www.genome.jp/kegg/) pathways which were analysed further to assess whether there was a predicted functional change in the community under each different treatment.

2.7. Quantitative PCR

Genes involved in the nitrogen cycle were quantified by qPCR. All samples were analysed in duplicates. A 1:10 dilution was used to remove inhibitory substances (Tatti et al., 2016). Standard curves constructed by amplifying the gene of interest according to Smith et al., (2006) and no-template controls (NTC) were included in triplicate in each assay. Quantitative PCR was performed using the SYBR Green GoTaq qPCR Master Mix (Promega), and the appropriate primers and cycling conditions in a 20 µl reaction (Table SI). qPCR assays were conducted using a CFX Connect Real-Time PCR Detection System (BioRad). Successful amplification of the desired fragments was assessed by agarose gel electrophoresis, while specificity was checked by melt curve analysis.

2.8. Statistical analysis

The effects of day and temperature on sediment-water fluxes were analyzed using a Linear Mixed Model (LMM). In this model, exposure time (hours) and temperature (ºC) were treated as fixed effects, while core was included as a random effect to account for repeated measurements on the same cores over four days (84 hours). The model allowed us to assess both the main effects and the interaction between day and temperature. When the dataset was insufficient for fitting a Linear Mixed Model (LMM), Kruskal-Wallis tests or 2-way ANOVA were employed instead. All analyses were performed using R version 4.3.1 (R Core Team, 2021). Statistical significance was accepted at $p < 0.05$, and all analyses were performed using R software (lme4 package). Results are reported as mean ± SE unless otherwise indicated.

For DNA sequence analysis. All analyses were performed using R version 4.3.0 (R Core Team, 2021). To visualize the taxonomic composition prokaryotic communities, the phyloseq package (McMurdie & Holmes, 2013) was used for generating bar plots and heatmaps. Bar plots displayed the relative abundance of taxa at different taxonomic levels, while heatmaps provided an overview of taxonomic profiles across samples. Significance in taxa across time and treatment was assessed using ANOVA and DeSeq2 (Love et al., 2014). Alpha diversity metrics were computed using the phyloseq package, and diversity indices such as Shannon and observed species were calculated, comparisons were made using Kruskal-Wallis tests. The microbiome package (Lahti & Shetty, 2017) facilitated the visualization of alpha diversity measures through boxplots and rarefaction curves. Beta diversity analysis was conducted based on Bray-Curtis distance matrices. Non-metric Multidimensional Scaling (nNMDS) plots were generated using the phyloseq package to visualize the dissimilarity between communities. The microbiomeSeq package (Paulson et al., 2013) aided in statistical testing for significant differences in beta diversity between treatment groups. Statistical significance in alpha and beta diversity metrics was assessed using permutational multivariate analysis of variance (PERMANOVA) using the adonis2 function as well as Kruskal Wallis and Dunn tests in the vegan package (Oksanen et al., 2001).

3. Results

3. 1. Diffusive and total oxygen fluxes at the sediment-water interface

Temperature had a clear effect on the measured O_2 microprofiles (Fig. 2). At high temperatures, O_2 was quickly consumed by the sediment resulting in decreased oxygen penetration depth (z_{ox}) (~1.3 mm at 42 °C) while softer, more deeply extended O_2 microprofiles were recorded at lower temperatures (~4 mm at 10 ºC). Both diffusive and total sediment oxygen fluxes (consumption rates) increased with temperature (Fig. 3). Diffusive oxygen fluxes increased linearly with temperature at a rate of 34 µmol O_2 m^{-2} h^{-1} $ºC^{-1}$. The rate was 1.6 times higher at 42 ºC compared to 10 °C after 12 h and 2.8 times after 60h. After 84 h, however, DOU decreased at the two highest temperatures. Volumetric DOU (DOU_{vol}), calculated by dividing the areal DOU rate by the oxic-layer thickness (m), showed more pronounced changes as expected since z_{ox} tended to decrease with temperature (Fig. 3b). Total oxygen uptake (TOU) increased with temperature as well, showing a maximum around 26-34 ºC after 12 h (Fig. 3c). TOU at the highest temperatures of 36-42ºC was double that at 10-18 ºC; however, the increase did not follow a clear linear pattern as in DOU. Significant

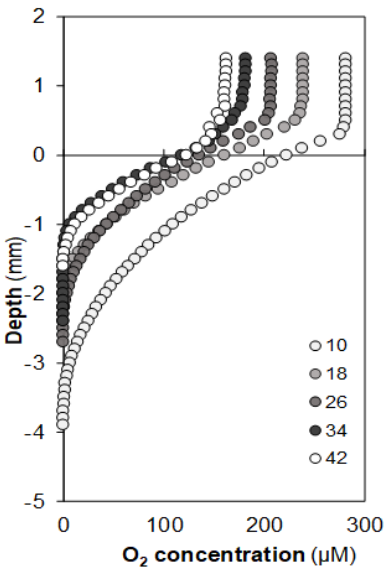


Figure 2. O_2 average micro-profiles measured in the sediment-water interface in sediments exposed to different temperatures for 24 hours.

Table I. E_a and Q_{10} values calculated from areal rates of diffusive oxygen uptake (mmol O_2 m^{-2} h^{-1}) and volumetric rate in the oxic layer (mmol O_2 m^{-3} h^{-1}). Ea was calculated from eq. 2 and Q_{10} from the eq. 3 at 18 ºC. When Q_{10} is calculated by temperature intervals (eq. 5) the mean value for all with rates per surface area is 1.33±0.14 and per volume is 2.47±0.52 (n=16) (Mean ±SE).

	Areal rates		*Volumetric rates*	
Hours	*E_a (KJ/mol)*	*Q_{10}*	*E_a (KJ/mol)*	*Q_{10}*
12	10.50 ± 2.99	1,61 ± 0,83	28.11 ± 7.9	1.47±0.90
36	28.17 ± 3.27	1,44 ± 0,93	59.69±4.10	2.27±0.95
60	28.84 ± 4.78	1,40 ± 0,88	53.49±8.53	2.08±0.89
84	58.19 ± 5.94	1,18 ± 0,93	101.10*	4,01*

*Calculated with the linear part of the curve (between 10-26 ºC)

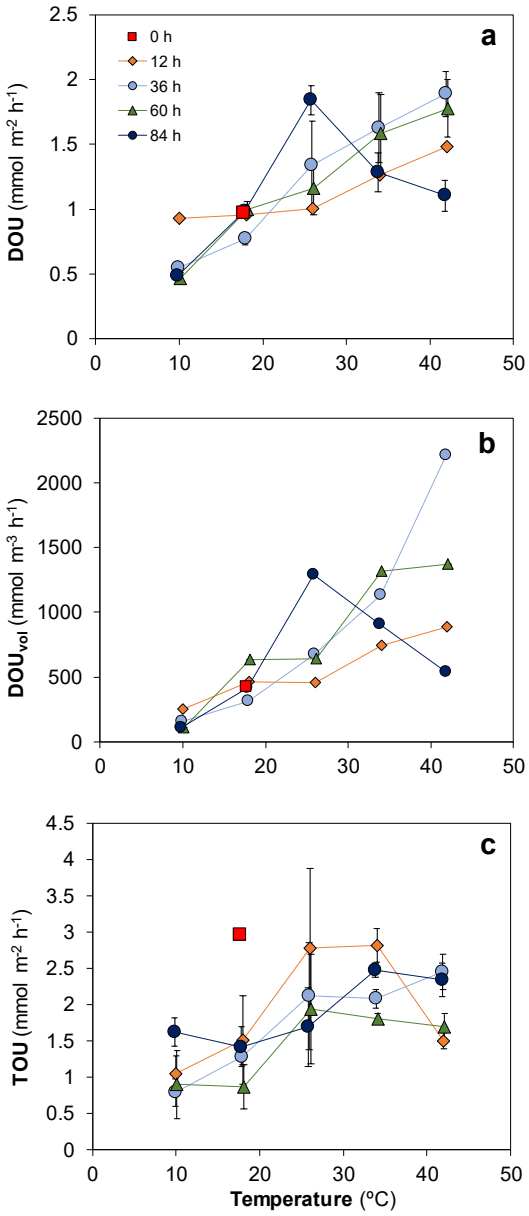


Figure 3. Diffusive oxygen uptake (DOU) expressed in areal rates (**A**) and volumetric rates, considering the oxygen penetration depth, (**B**) and total oxygen uptake (TOU)(**C**) in the sediments exposed at different temperatures during 4 days. Diffusive fluxes were measured by microelectrodes and total O_2 flux was measured by incubations. Data are means ± SE

differences were found in TOU values with respect to both temperature and time (p-value = 0.0310; LMM).

The apparent activation energy (E_a) calculated from areal (mmol O_2 m^{-2} h^{-1}) and volumetric (mmol O_2 m^{-3} h^{-1}) DOU rates increased noticeably over time (**Fig. 4**). However, no significant differences were observed throughout the experiment (p-value = 0.3916; Kruskal-Wallis test). Mean E_a (areal) increased from 10.5 KJ mol^{-1} after 12 hours to 58.2 KJ mol^{-1} after 84 h. (**Table I**) Mean E_a (volumetric) were between 2.7 to 1.7 times bigger than areal rates, after 12 and 84 h, respectively. In contrast, when E_a was calculated for areal TOU rates its value decreased with incubation time from 34.7 to 12.3 kJ mol^{-1}. For comparison with other studies, Q_{10} values were calculated from E_a as well (Eq. 4) (**Table II**). Q_{10} was 1.2 - 2.2 when calculated from E_a (DOU_{areal}), 1.5 – 4.0 from E_a (DOU_{vol}), and 1.6 and 1.2 from Ea (TOU) after 12 and 84 h, respectively.

3. 2. Dissolved inorganic carbon and nitrogen profiles

DIC and NH_4^+ porewater profiles were affected by temperature variations, in particular at higher temperatures. Initial concentration of DIC (18 ºC, 0h) was constant with depth around 4.01 ± 0.13 mM (**Fig. 5a**). At the end of the experiment, sediment cores exposed to temperatures above 18ºC showed a clear accumulation of DIC inside the sediment with a peak at 2-3 cm reaching 9.6 mM at 42º C. As a result, integrated DIC concentration with depth increased linearly with temperature (**Fig. S2**).

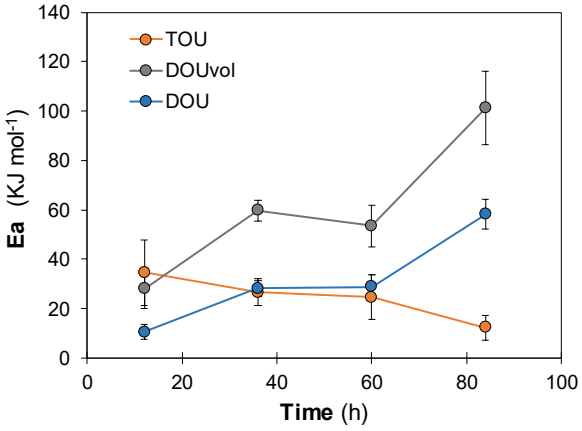


Figure 4. Activation energy (E_a,*(KJ mol^{-1}))* calculated from diffusive oxygen uptake areal (DOU) rates (mmol O_2 m^{-2} h^{-1}) and volumetric rates (DOU_{VOL}) in the oxic layer (mmol O_2 m^{-3} h^{-1}) and total oxygen uptake rates (TOU) (mmol O_2 m^{-2} h^{-1}).

Porewater NH_4^+ increased progressively with depth from 12.3 µM to 102.0 µM at 5 cm at the beginning of the experiment (**Fig. 5b**). After 84 h, concentrations increased in all the treatments. At the three lowest temperatures, values reached 350 µM whereas a much higher built up with depth was observed at 34 and 42ºC, reaching maximum values of 670 and 1050 µM, respectively. Integrated NH_4^+ concentration with depth did not change up to 26ºC but increased linearly with temperature up to 42 ºC (**Fig. S2a**).

In contrast to DIC and NH_4^+, porewater profiles of NO_2^- and NO_3^- in the sediment indicated generally net consumption (**Fig. 6c,d**). NO_2^- and NO_3^- concentrations were very low and very little NO_3^- was measured below the first centimeter. NO_3^- concentrations were higher at lower temperatures both in the water column and sediment. (**Fig. 6c,d**). Integrated NO_2^- and NO_3^- concentrations did not show a trend with temperature; a minimum at 26º C was recorded for both nutrients (**Fig. S2b**).

The ratio between integrated DIC and integrated total dissolved inorganic nitrogen (NH_4^+ (directly from remineralization) + NO_2^- + NO_3^- (produced by nitrification of that

NH_4^+) (DIC:DIN) decreased considerably from initial conditions to those measured after 84 h. DIC:DIN showed its lowest value of 8.3 at 42º C and its highest of 25 at 26º C (Fig. S2c).

3.3 DIC and DIN fluxes at the sediment-water interface

The steady state fluxes at different temperatures indicated an important increase of DIC and NH_4^+ efflux with temperature after 84 h, increasing from values of 60.0 and 10.7 mmol m^{-2} h^{-1} at 18º C to 861. 3 and 257.7 mmol m^{-2} h^{-1} at 42º C for DIC and NH_4^+, respectively (Fig. 6a). DIC and NH_4^+ production rates were linearly correlated (DIC=3.2·NH_4^+, r^2=0,97, p<0.05). NO_3^- flux in the upper sediment layer showed an inverse trend both in direction and change with temperature with rates at least 3 orders of magnitude lower than DIC and NH_4^+ production rates. (Fig. 6b).

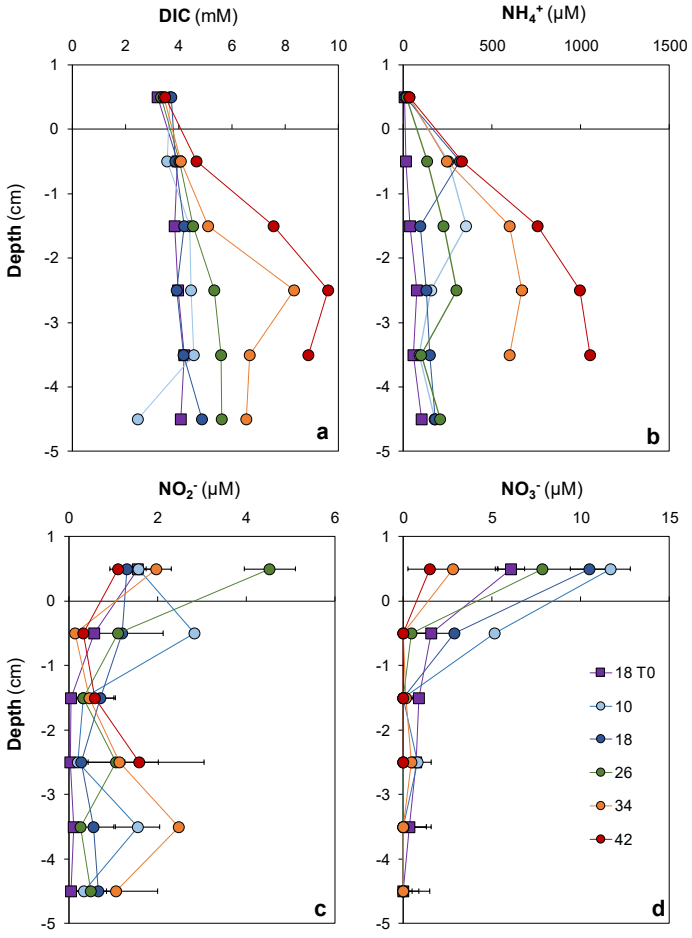


Figure 5. Porewater profiles of DIC (A), NH_4^+ (B), NO_2^- (C) and NO_3^- (D) concentrations measured in sediment cores before the experiment (18ºC, purple square) and after being exposed at different temperatures for 84 h (circles). Data are means ± SE (n = 3) of replicate analyses.

Table II. Compilation of literature data on the temperature dependence of respiration rate of different type of sediment.

RESPIRATION

Ecosystem	*Site*	*T (ºC)*	*Used technique*	Q_{10}	E_a (kJ mol^{-1})	*Exp. duration (h)*	*Rates range*	*Light*	*Type*	*Reference*
West Lawrencetown marsh	Canada	10-20 2-10	*Whole core incubation*	1.0-2.2 1.9-4.1		96-120	0.5-15 mm^{-3} cm^{-2} h^{-1} 3-100 mm^{-3} cm^{-2} h^{-1}	Light	Intertidal high and low sediment	(Duff & Teal, 1965)
Sapelo marshes	Georgia	10-20 2-10	*Whole core incubation*	1.7-1.9 1.3-4.8		96-120	0.7-18 mm^{-3} cm^{-2} h^{-1} 0.7-9 mm^{-3} cm^{-2} h^{-1}	Light	Spartina marshes muddy sediment	(Duff & Teal, 1965)
Norsminde Fjord	Denmark	2-20	*Whole core incubation*	2.7		4	36.6-43.0 mmol m^{-2} d^{-1}	Dark	Homogeneized sediment	(Jørgensen & Sørensen, 1985)
Nova Scotia	Canada	6-14	*Whole core incubation*	6.5 2			0-18 mg O_2 m^{-2} h^{-1} 13-90 mg O_2 m^{-2} h^{-1}	Dark Light	Sandflat upper intertidal sediment	(Grant, 1986)
A-horizon soils		4-28	*Incubation chambers*	1.7-1.9		24h (50-120 days)	0.12-1.6 umol CO_2 g^{-1} d^{-1}	Dark	Ultisol forest surface	(Winkler et al., 1996)
Aahrus Bay sediment	Denmark	4-14	*Whole core incubation + microsensor*	1.9-3.1	51-76	4-11	0-11 umol cm^{-3} d^{-1}	Light	Homogeneized sediment	(Thamdrup, et al., 1998)
Menai Strait	North Wales	7.6-15	*Winkler method*	4.0-9.3		24	25 umol O_2 dm^{-3} d^{-1}	Dark	*Phaeocystis* bloom	(Lefèvre et al., 1994)
Svaldbard fjords *Weser estuary*	Norway Germany	0-10 0-10	*Whole core incubation + Winkler method*	1.7-2.1 2.5-4.9	33-49 59-103	1-10 2-6	0.13-1.50 µmol g d.w.$^{-1}$ h^{-1} 0-8 µmol g d.w.$^{-1}$ h^{-1}		Fine brown silt sediment Fine silt cover by diatoms	(Thamdrup & Fleischer, 1998a)

Hornsund *Storfjorden*	Norway Norway	-2-45	*Whole core incubation + Winkler method*	1.84 1.77		65	15 µmol O_2 cm^{-3} d^{-1} 4.6 µmol O_2 cm^{-3} d^{-1}	Dark	Fine-grained sediment Soft and clayey sediment	(Arnosti et al., 1998a)
Ebro delta	Spain	15-30	*Microelectrodes/ Chambers*	2.35	55	1-1.5	196-630 nmol O_2 cm^{-3} min^{-1}	Light	Intertidal/salterns	(Epping & Kühl, 2000)
Niva Bay *Trondheimsfjord* *Adventfjord*	Denmark Norway Norway	5-15	*Whole core incubation + microsensor*	2.2-5.2 1.7-2.6 2.4-3.2	51-105 34-62 55-75	24	0-0.05 nmol O_2 cm^{-2} s^{-1} 0-0.08 nmol O_2 cm^{-2} s^{-1} 0-0.03 nmol O_2 cm^{-2} s^{-1}	12:12 Dark/ Light	Subtidal sediment from semi-enclosed bays	(Hancke & Glud, 2004b)
Cadiz Bay intertidal sediment	Spain	10-34	*Whole core incubation + microsensor*	1.18 - 1.61	10.50 - 58.19	84	0.5-3 mmol O_2 m^{-2} h^{-1}	Dark	Intertidal creek non-vegetated sediment	*This study*

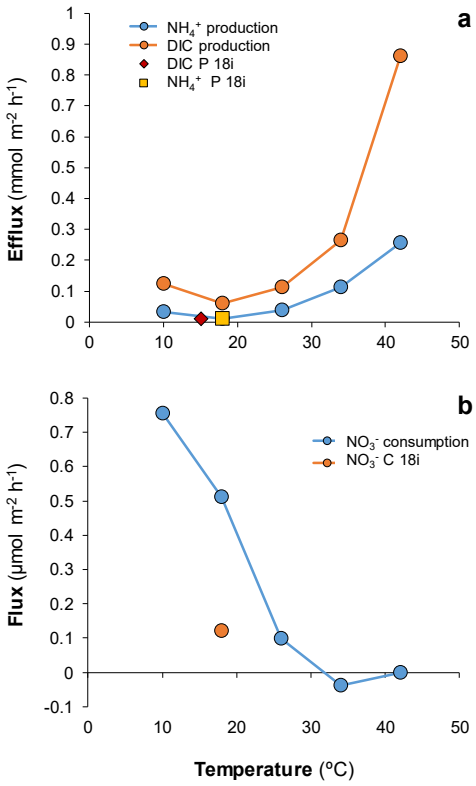


Figure 6. DIC and NH_4^+ production (**A**) and NO_3^- consumption fluxes (**B**) at the sediment water interphase estimated using the upper 2 cm sediment layer of their respective steady state vertical profiles as a function of temperature. 18_i represents initial data and the other values are values taken at 84h exposure.

Core incubations indicated that increasing temperature produced a significant increase in the NH_4^+ influx to the sediment, showing significant differences at at 34ºC (p-value = 6.56e-07) and 42º C (p-value = 0.0003); LMM), being linear with temperature in most of the cases and reaching a maximum value of -1000 µmol m^{-2} h^{-1} (**Fig. 7a**). The magnitude of the flux decreased progressively with time, even shifting to positive fluxes for the lowest temperatures after 36 h. The rate of flux change with temperature was highest after 12 h of exposure (-22.7 ± 5.8 µmol m^{-2} h^{-1} $ºC^{-1}$) and progressively decreased with time to reach values of -12.6 ± 3.2 µmol m^{-2} h^{-1} $ºC^{-1}$ after 84h.

NO_2^- was mainly exported to the water column from the sediment, with positive fluxes measured over the course of the experiment at temperatures below 42ºC (**Fig. 7b**). Temperature increased the net NO_2^- efflux, showing highest positive values at 34ºC after 12h and at 26ºC for the rest of the experiment; however, fluxes were mostly negative at 42ºC. Nitrite fluxes did not change significantly over time at any temperature, except within the range of 26-34ºC (p-values = 0.0032 and 0.0002 for 26ºC and 34ºC, respectively; LMM).

NO_3^- fluxes did not show a clear pattern with temperature or with times. NO_3^- flux differences over time were smaller at the lowest, mostly showing efflux, and highest temperatures, mostly showing influx. In contrast, they varied from +100 to -110 µmol m^{-2} h^{-1} with no clear temporal trend at 26ºC (**Fig. 7c**). NO_3^- fluxes showed no

dependence on time or temperature, except at 26ºC compared to initial 18ºC (p-values = 0.0298, 0.0008, and 0.0424 at 36, 60, and 84 hours of heat exposure, respectively; LMM).

The sensitivity of NH_4^+ and NO_2^- fluxes to temperature was estimated by E_a and Q_{10}. Ea for NH_4^+ increased with time throughout the experiment from 31.0 ± 7.4 to 82.0 ± 31.4 kJ mol^{-1}, corresponding to a Q_{10} of 1.5 and 3.1, after 12 and 84 h respectively. In contrast, E_a for NO_2^- fluxes decreased considerably after 84h (**Table SII**).

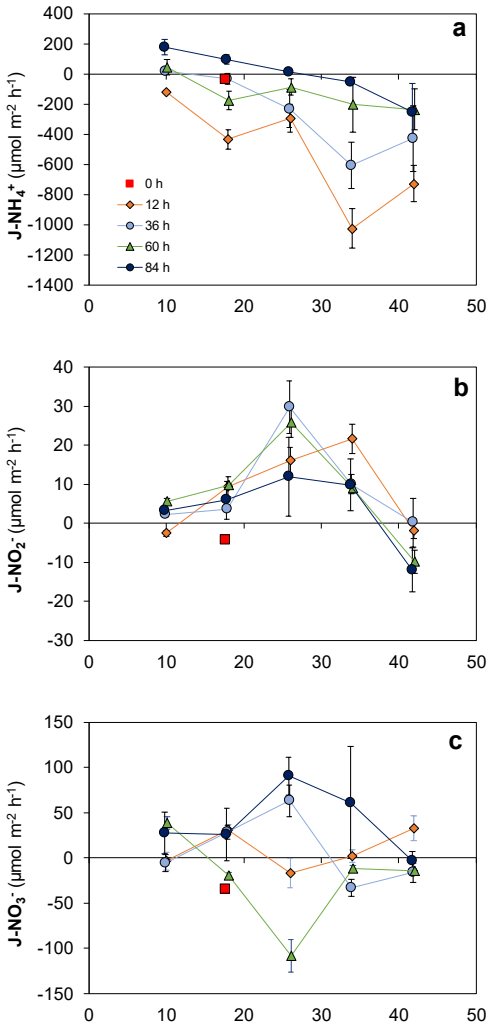


Figure 7. Sediment-water fluxes of inorganic nutrients (NH_4^+ (**A**), NO_2^- (**B**) and NO_3^- (**C**) measured in sediment cores exposed to altered temperatures (days 1-4), from an average in situ temperature of 18ºC measured at day 0. Data are means ± SE (n = 3).

3. 4. N_2O and CH_4 fluxes

Nitrous oxide and methane were always released from the sediment throughout the experiment (**Fig. 8**). N_2O fluxes showed significant differences with temperature at 42 ºC (p-value=0.0006; LMM) (**Fig. 8a**). Just after 12 h, N_2O flux increased exponentially with temperature. Net release decreased progressively with time i.e. the peak at 42 °C was observed at 12 h, at 34 °C at 36 h and at 26 °C at 60 h. Although differences were not clear statistically, highest values at the lowest temperatures (10 and 18 °C) were observed after 84 h. The values of E_a and Q_{10} for N_2O fluxes were lower than other solutes, 13.2 kJ mol^{-1} and 1.2 respectively, and tended to decrease over time (**Table SII**).

CH_4 fluxes increased exponentially with temperature during the entire experiment (Fig. 8b) and showed significant differences with 42 ºC (p-value=8.43e-05; LMM). At the lowest temperatures (10-18ºC), fluxes were similar to the initial ones and ranged from 0.39 to 1.30 nmol m^{-2} h^{-1}. At 34 ºC and 42 °C, the release of methane increased one and two order of magnitude, respectively. E_a and Q_{10} values for CH_4 production by the sediment were among the highest measured in this study, 85.5±10.9 kJ mol^{-1} and 3.3 ± 0.5, respectively (Table SII).

3. 5. Organic carbon and total nitrogen content

Initial concentration of organic carbon content (C_{org}) and total nitrogen content (N_{total}) in the upper 5 cm were 20.8 ± 3.2 and 1.4 ± 0.3 mg g dw^{-1}, respectively, resulting in a C:N (mol:mol) of 18.5 ± 5.4 (Fig. S1). After 84h, we observed no clear changes in the vertical profiles of C_{org} at higher temperature range (26-42 ºC), whereas we observed a decrease in the upper sediment layer (up to 4 cm) at 10 and 18 ºC with respect to initial concentration. The final N_{total} concentration in the upper 0-3 cm sediment layer was lower than the initial one after 84 h of temperature exposure in all assayed temperatures. The different response of C_{org} and N_{total} contents to temperature resulted in an increase in C:N ratio in the upper 2 cm at 26-42 ºC with respect to initial conditions at 18ºC.

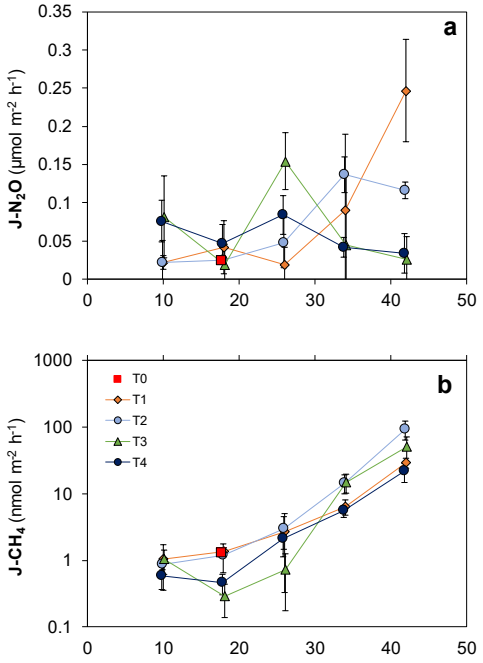


Figure 8. Sediment-water fluxes of nitrous oxide (**A**) and methane (**B**) measured in sediment cores exposed to altered temperatures (days 1-4), from an average in situ temperature of 18ºC measured at day 0. CH_4 flux is represented in log_{10}. Data are means ± SE (n = 3).

3.6. Quantitative PCR

The gene abundance of the different enzymes involved in the nitrogen cycle showed a general pattern of higher content at the middle temperatures of 18 and 26 °C (Fig 9). The abundance of the different genes varied several orders of magnitude with nirS and nrfA showing the highest abundances and Arch amoA and nrxB the lowest. Differences at the end of the experiment between treatments did not show any clear differences ($p>0.05$) with the exception of nrxB, where 10 and 42 °C were different from the initial and 18 °C. Normalizing the abundances to total 16s rDNA copy numbers resulted in relatively similar patterns with highest numbers at 18 to 26 °C with the exception of Arch amoA and nosZ that showed the highest ratio at 42 °C (Fig 9). For Bac amoA, CoAmmox, nxrb, and nrfA, the initial ratio was clearly different than the rest (Fig. 9, right side).

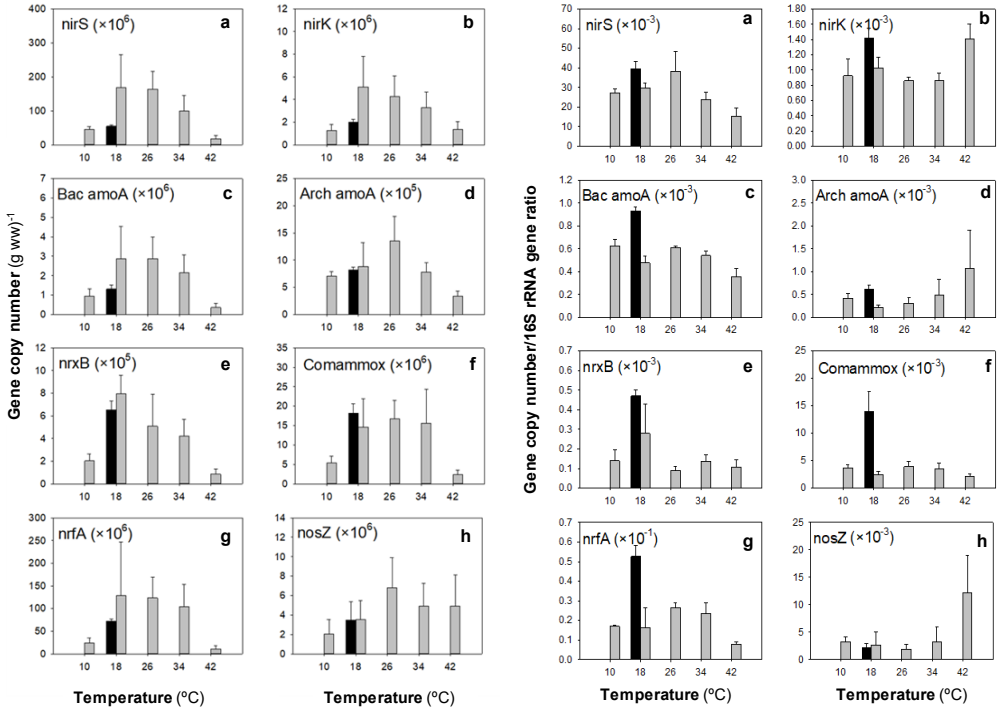


Fig 9. Functional gene copy numbers in sediment across five temperatures (10, 18, 26, 34, 42 °C). On the left without normalizing by 16S rRNA, and on the right normalized data. Mean ± SE (n = 3) are shown for: (**a**) nirS, (**b**) nirK, (**c**) bacterial amoA, (**d**) archaeal amoA, (**e**) nxrB, (**f**) comammox, (**g**) nrfA, and (**h**) nosZ. Black bars = start (0 h); gray bars = 84 h.

3.7. Taxonomic responses of Archaea and Bacteria to heat treatments

The Archaeal data set contained 846 ASVs from 30,288 sequenced with Archaea accounting for on average <0.6% of the total sequence reads. The Bacteria data 5,796,536 across 7983 ASVs. The most abundant phylum greater than 3% relative abundance in samples were Proteobacteria accounting for 47.9% on average of the total sequence reads in each sample, followed by Desulfobacterota (10.3%), Bacteroidota (9.3%), Chloroflexi (4.8%), Planctomycetes (3.9%), Gemmatimonadota (3.9%), Verrucomicrobiota (3.6%) & Myxococcota (3.5%) (Fig 10a). There were little differences in the relative abundance of main groups between Initial, 10 °C, 18 °C, 26 °C, 34 °C (Kruskal wallis, $p>0.05$). A significant increase in the relative abundance for Chloroflexi (Anaerolineales) and Firmicutes (Peptostreptococcales, Tissierellales) (Kruskal wallis, $p<0.05$) and a decrease for Myxococcota and Verrucomicrobiota (Kruskal wallis, $p<0.05$) was found though when comparing the initial conditions with the 42 °C treatment (Dunn's $p<0.05$). The low abundance of Archaea in some samples prevented a further detailed analysis. However, a clear increase in Methanosarciniales was observed from the Initial to the 42 °C treatment (Fig 10b). Looking at the Proteobacteria in more detail (Fig. S3) the Alphaproteobacteria; Rhodospirillales showed an 18-fold increase (Dunn $p<0.05$) from 0.1% in the initial to 1.8 % in the 42°C treatment and Alphaproteobacteria; Caulobacterales a 10-fold increase (Dunn $p<0.05$) from 0.1% in the initial to 1.1% 42°C treatment. The Gammaproteobacteria; Pseudomonadales showed an increase from a mean of 10% in the initials to a mean of 13% in the 42°C treatment (Dunn $p<0.05$). The Gammaproteobacteria; Steroidobacterales showed an increase in 18°C treatment and 26°C treatment but this then decreased in the 42°C treatment (Kruskal Wallis, $p<0.05$, Dunn test $p<0.01$).

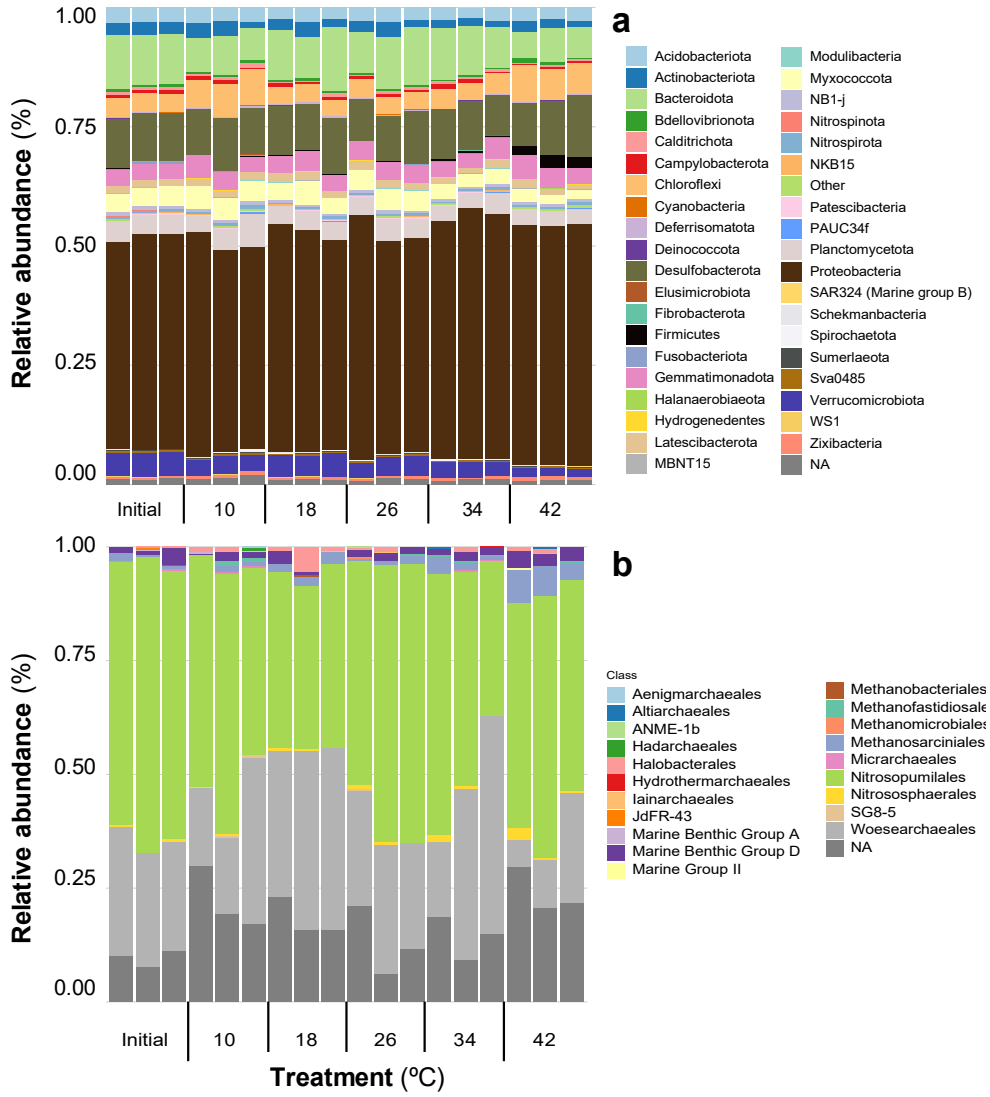


Figure 10. Relative abundance of microbial taxa (classes) in sediment across temperature treatments (Initial, 10, 18, 26, 34, 42 °C) at initial conditions and after 84h. Stacked bars show mean proportions of (**a**) phyla and (**b**) archaeal classes. Only taxa representing ≥1 % of the community in at least one sample are colored; remaining groups are pooled as "Other" or "NA."

3. 8. Richness, diversity and community responses of Bacteria to heat treatments

Richness of ASVs was variable between replicates but there was two-fold difference between each treatment with a decreasing trend in richness with increasing temperature (Fig. 11). The changes in the relative abundance of several groups were also reflected in the diversity with a decreasing trend in diversity although this was statistically clear only between initial and 34 °C (Kruskal wallis $p<0.01$) and initial and 42 °C (Kruskal Wallis $p<0.01$). The community composition based on both Bray-Curtis and Jaccard dissimilarity matrices showed a significant difference only between the initial and 42 °C treatment (PERMANOVA, $p<0.05$) (Fig. 12).

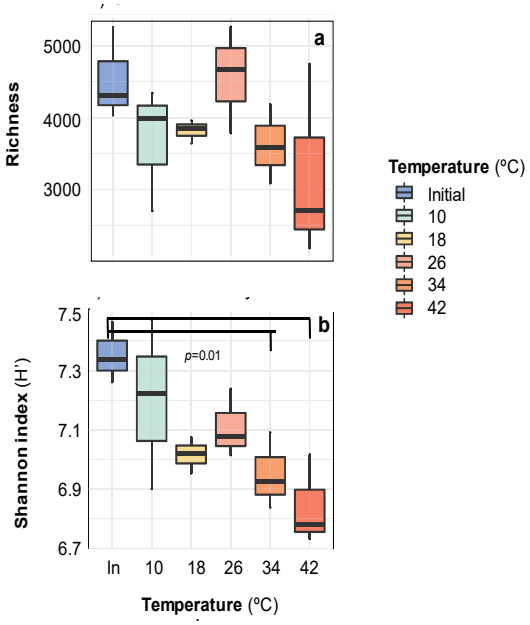


Figure 11. Sediment microbial α-diversity across temperature treatments. Boxplots show (**a**) observed richness and (**b**) Shannon diversity (H′) for Initial (In), 10, 18, 26, 34, and 42 °C (n = 3 per treatment).

3. 9. Reconstructed functional analysis using PiCrust2

ASVs were used as inputs for predicting metagenomes. The PCA plot based on relative abundances of different KEGG pathways between the various treatments showed a clear separation between initial, 34 °C and 42 °C indicating functional differences of the taxa present. For example, the denitrification pathway showed a higher proportion of sequence reads at 42 °C compared to Initial. Other pathways that were more abundant were those of the TCA cycle VII (PWY-7254) corresponding to acetate-producers, as well as ectoine biosynthesis, an osmolyte to deal with

increased salinity (P101-PWY) (Fig. S4). On the other hand, neither methanotrophic nor methanogenic metabolism pathways showed any clear differences.

4. Discussion

4. 1. Effect of temperature increase on total sediment metabolism

Sediment metabolism was strongly affected by temperature enhancing heterotrophic microbial metabolism and organic matter degradation rates (Hancke & Glud, 2004a). Oxygen consumption rates (DOU, TOU areal and DOU volumetric rates) increased linearly with temperature (Table I), whereas DIC and NH_4^+ concentrations within the sediment also increased with temperature (Fig. 5a). The increase in total metabolism observed here is consistent with earlier studies on temperature effects on benthic communities (Hancke & Glud, 2004; Wieland & Kühl, 2000). Despite the variability in exposure times in the different experiments (Table II) and across the wide range of temperatures all resulted in a sustained rise in sediment O_2 demand. However, the effect varies several folds between different temperatures.

The impact of heat waves on sediment oxygen consumption is complex, as temperature influences several interdependent physicochemical and biological processes (Hancke & Glud, 2004a; Jørgensen & Revsbech, 1985; Wieland & Kühl, 2000). Higher temperatures reduce O_2 solubility, being the concentration in equilibrium with the atmosphere is 0.58 times lower at 42º with respect to 10 ºC. In addition, an increase in T would reduce the apparent diffusive boundary layer (DBL) thickness. The apparent DBL, estimated from eq. 1 in Jørgensen and Revsbech (1985), at 42º was 0. 69 times the value at 10ºC. Finally, higher T increases the molecular diffusion coefficient, D_o is 2.27 times higher at 42º vs. 10º C. While the reduced DBL thickness and increased diffusion could elevate DOU, the lower oxygen solubility may offset this effect. Accurately assessing these temperature-dependent changes is challenging due to the simultaneous interplay of these variables (Jørgensen & Revsbech, 1985; Millero & Poisson, 1981; Wieland & Kühl, 2000). Our calculations, following Rasmussen and Jørgensen (1992) (Eq 2 and 17), to obtain the concentration of O_2 at the sediment surface and the oxygen flux, respectively, suggest that sediment oxygen demand (DOU) increases with

temperature by 20% (1.2 times) from 10ºC to 42ºC, driven by physicochemical only temperature-dependent effects. This is a minor effect compared to the 178% increase observed on average (2.78-fold) in DOU across the same temperature range during the experiment. In addition, factors like wind and tidal-induced turbulence likely play a more significant role than the physicochemical changes in O_2 solubility and diffusivity in the control of oxygen fluxes *in situ*.

Although both DOU and TOU increased with temperature, the effect was clearer for DOU, showing a clear progressive increase in DOU with temperature and time in the first 60h, indicating greater temperature sensitivity, likely due to microbial acclimation or changes in community composition. Following the increase in rates, a decrease was clearly observed at the two highest temperatures that could indicate inhibition of microbial respiration from prolonged heat exposure (Fig. 3). However, the bacterial community at the end of the experiment showed a change in the community of bacteria and a decrease in the diversity of the taxa with temperature, statistically clear at the highest temperatures (Fig. 10a). In addition, the functional profile of the community also showed a clear separation between the initial, 34 ºC and 42 ºC, indicating a functional adaptation. For example, Verrucomicrobiota and Mycococcota that include aerobic bacteria decreased in abundance, whereas Firmicutes and Chloroflexi that contain high temperature tolerant members increased in relative abundance (Fig. 10a). The decrease in oxygen consumption rates was then most likely due to the depletion of labile organic substrates (Arnosti et al., 1998; Glud, 2008; Hansen & Kristensen, 1998; Papaspyrou et al., 2004), as the community seemed to adapt to the temperature changes.

TOU rates, influenced by both diffusive and advective fluxes, showed a less clear temperature dependence, likely due to differences in the abundance and type of micro and meiofauna affecting the overall temperature changes. Consequently, TOU did not show a clear decrease at the highest temperatures but it was maximum, remaining highest at the highest temperatures (34-42°C), The contribution of DOU to TOU increased from about 30% at 18°C to 60-80% across the temperature range, suggesting a potential negative effects to the infauna under higher temperature or at least a higher contribution of microorganisms to the O_2 fluxes at higher temperature. Regardless, the DOU/TOU ratios observed were consistent with those reported in intertidal and subtidal sediments (Musat et al., 2006; Rabouille et al., 2003).

The sensitivity of DOU to temperature, measured by E_a and Q_{10}, increased over time (Fig. 4), indicating that microbial communities acclimate quickly to rising temperatures. After 12 to 84 hours of exposure, mean E_a (areal) for DOU increased from 10.5 to 58.2 KJ mol^{-1} (Q_{10} from 1.15 to 2.22), whereas mean E_a (volumetric) was 2.7 to 1.7 times higher, respectively. These findings, which align with previous research using O_2 in short-term incubation experiments with different tidal and subtidal sediment communities from different geographic locations, including experiment with sediment slurries (Table II), suggest that prolonged heat waves have a more pronounced impact on sediment oxygen demand than previously observed in short-term studies. In contrast to DOU, Ea for TOU rates decreased from 34.7 to 12.3 kJ mol^{-1} over time (Q_{10} from 1.61 to 1.18). These values are lower than those reported in short-term studies at higher latitudes for whole core incubations but at lower temperature ranges (Q_{10}=2.4 - 3.3, Hancke & Glud (2004)). This suggests that the effect of temperature increase seems to be higher at lower temperatures. The decline in Ea for TOU likely reflects the harmful effects on infauna due to prolonged exposure to increased temperatures and the reduced oxygen availability. This suggests that the duration and intensity of temperatures increase, such as heat waves, can significantly affect both sediment biochemistry and trophic webs.

4. 2. Nitrogen cycling processes

The effect of temperature on the nitrogen cycle varied both in time and with temperature. NH_4^+ fluxes revealed a linear change with temperature whose intensity, however, changed over time (Fig. 7a). Initially, after 12 hours, the sediment acted as a net sink for NH_4^+, with uptake rates being 7.5 times higher at 34 - 42 ºC with respect to 10 ºC. Since the experiment was conducted in the dark to exclude the effect of assimilation by benthic microalgae, this demand likely stemmed from a stimulation of the nitrification and bacterial assimilation (Dalsgaard & Thamdrup, 2002; Rosales Villa et al., 2019; Schutte et al., 2019). Sediment NH_4^+ was another source contributing to the bacterial demand. In fact, production rates of NH_4^+ calculated from the steady profiles at the end of the experiment increased exponentially with temperature (Fig. 6). These rates were similar to values previously reported for Cadiz Bay sediments (Burgos et al., 2018) and other temperate regions (Berg et al., 1998; Hansen & Kristensen, 1998; Leote & Epping, 2015; Papaspyrou et al., 2007). Although, the sediment was a net source of NH_4^+

at lower temperatures, at 34ºC and 42ºC, the sediment continued to uptake NH_4^+ from the water column over time, albeit at lower rates (Fig. 7a), suggesting a stimulation of nitrification rates.

Although NO_3^- profiles indicated a consumption of this solute in the sediment, increasing with temperature, suggesting temperature-stimulated denitrification (Canion et al., 2014) (Fig. 5d), they did not have the sufficient resolution to discern the fine depth changes occurring at the few upper mm. In fact, NO_2^- and NO_3^- fluxes were mostly positive, supporting an increase in nitrification rates. NO_2^- rates exhibited a more consistent pattern with NO_2^- efflux increasing with temperature up to 34 ºC, but an influx at 42 ºC, whereas those of NO_3^- varied unpredictably with fluxes alternating between consumption and release within a day, most notable at 26 ºC (Fig. 7b,c). The exception was the fluxes at 42 ºC that like NO_2^- were negative although very close to undetectable levels.

Nitrifying microorganisms exhibit broad thermal tolerance, with optimal activity typically between 25 and 35 °C in temperate coastal sediments (Herbert, 1999). Yet, whole-core measurements often record lower nitrification rates in summer than in winter, an effect attributed to the thermal reduction of the oxic layer, and thus O_2 availability-alongside intensified competition for NH_4^+ by fast-growing heterotrophs (Hansen et al., 1981). In our study, sediment O_2 demand increased markedly with temperature, causing oxygen penetration depth to shrink from roughly 4 mm to 1.3 mm (Fig. 2). Such narrowing of the oxic zone shifts the balance toward anaerobic processes and can uncouple nitrification–denitrification coupling, ultimately dampening the net stimulation of nitrification at the highest temperatures (Thamdrup & Fleischer, 1998). However, despite pronounced functional shifts, we observed no significant change in the absolute abundance of key nitrification genes (bacterial and archaeal amoA, nxrB), except for a relative enrichment of archaeal amoA at 42 °C (Fig. 9c,d,e). This decoupling between gene abundance and process rates likely reflects the inherently slow growth and high activation energies of nitrifiers, whose biomass responds more slowly to temperature changes than enzyme-mediated reaction rates (Reay et al., 1999). Concurrently, the net fluxes of NO_2^- and NO_3^- revealed non-linear responses: effluxes rose with warming up to 34 °C but shifted toward a slight uptake at 42 °C (Fig. 7b,c). Such behavior suggests that dissimilatory nitrate reduction processes (denitrification and DNRA) increasingly outpace downstream NO_2^- oxidation at extreme temperatures. Indeed, DNRA is known to intensify under warming and low-O_2 conditions, competing

effectively with denitrification (Dawson & Murphy, 1972; Nizzoli et al., 2010). Furthermore, temperature-mediated enhancements of denitrification and anammox rates have been reported in saline sediments, with differing thermal optima among pathways (Brin et al., 2017). By the end of the experiment (84 h), the cumulative effect of heat stress drove a shift in NO_2^- dynamics that underscores the dual importance of heat-wave intensity and duration in situ (Tan et al., 2020). Metagenomic evidence further corroborated this functional shift: reads associated with the denitrification pathway increased significantly at 42 °C, alongside enrichments in archaeal acetate-producing pathways (PWY-7254) and ectoine biosynthesis (P101-PWY), markers of osmotic and thermal stress (**Fig. S4**). Incorporating the effect of episodic thermal anomalies on the nitrogen cycle into predictive models is essential for accurately forecasting nutrient fluxes and greenhouse-gas emissions from intertidal and coastal wetland systems under future climate scenarios.

4. 3. Production of greenhouse gases

Estuaries can act as either sources or sinks for N_2O depending on conditions and timing (Lamontagne et al., 2003). In the San Pedro River, N_2O fluxes ranged from -0.11 and 0.38 μmol m^{-2} h^{-1} (-2.64 – 9.12 μmol m^{-2} d^{-1}) (**Fig. 8**), these net emission rates aligns with previously reported values in the area (Ferrón et al., 2009). Our results did not show a clear effect of temperature, despite that increased temperatures may enhance denitrification by expanding anoxic conditions, potentially leading to greater N_2O production. However, this might trigger contrary effects, for instance, the thinner oxic zone might limit nitrification, reducing NO_x^- availability for N_2O production. In addition, DNRA or Anammox might becom more important at 42ºC, consuming NO_3^- without generating N_2O. Moreover, metagenomics results indicate stronger expression of *nosZ*, suggesting enhanced reduction of the N_2O produced in earlier steps.

Methane (CH_4) in coastal systems primarily originates from estuarine inputs or benthic production linked to organic matter mineralization. Its production mainly results from methanogenesis, which involves anaerobic processes such as acetate fermentation or CO_2 reduction (Faber et al., 2012; Ferrón et al., 2009) although recent discoveries also revealed the relevance of other processes going on in the sediment surface and even at oxic marine environments (Repeta et al., 2016; Xiao

et al., 2017, 2018). Methane concentration in the water column is influenced by both aerobic and anaerobic oxidation processes. While methane oxidation can continue under hypoxic-anoxic conditions as oxygen levels decrease, its dynamics are complex due to the interplay between physicochemical processes and biological aerobic and anaerobic processes (Abril et al., 2002; Bastviken et al., 2008; Gudasz et al., 2010). Higher temperatures enhance the production of methane carried out by microorganisms and increase the diffusive flux from the deeper parts of the sediment to the water column. However, the methane that diffuses upwards is also consumed by microbial oxidation processes, also favored at higher temperatures (Abril & Iversen, 2002; Herbert, 1999; Stocker, 2014). Both production of CH_4 and emission from the sediment show a remarkable temperature dependence for wide range of ecosystems and microbial communities. Nevertheless, a relative increase of the emissions at higher temperatures it is commonly observed, then suggesting a decoupling between production and consumption processes (Yvon-Durocher et al., 2014). In our experiment, we also observed that methane released from the sediment increased with temperature, reaching a peak of 93.4 nmol m^2 h^{-1} (2.24 µmol m^2 d^{-1}) at 42 ºC (Fig. 8). The range of fluxes measured are higher than previous data reported in the Río San Pedro, but they are similar to those reported in coastal basins of the Mexico's Western Margin (Abril et al., 2002; Bastviken et al., 2008; Ferrón et al., 2009; Sansone et al., 2004).

The metagenomic data showed that warming to 42 °C notably shifted the key methanogenic players. Methanosarciniales, archaeal methanogens that tolerate higher temperatures and rely on acetate, became significantly more abundant than at the experiment's outset. At the same time, Rhodospirillales, a group of purple non-sulfur bacteria that ferment organic substrates into acetate, also increased ($p < 0.01$). This tandem rise suggests a simple but effective partnership: Rhodospirillales produce acetate, which Methanosarciniales then convert to methane (Fig. 10a). In contrast, the broader Pi2 Crust bacterial community showed no clear change in methanogenic or methanotrophic genes, indicating that these two groups drive the temperature-induced spike in CH_4 production.

The results obtained during the laboratory simulation of a short-term heatwave on intertidal sediments from the Río San Pedro creek revealed a quick and significant impact on the biogeochemical processes and microbial community structure. The increase in oxygen consumption, coupled with relevant changes in nitrogen cycling pathways towards denitrification at higher temperatures, revealed the vulnerability of shallow coastal areas to short-term alterations of temperatures caused by

extreme climate events. The rise in the methane efflux at high temperatures, driven by alterations in the archaeal and bacterial communities involved in methanogenesis, highlights the potential for increased greenhouse gas emissions from coastal sediments under future climate scenarios. Although we have used a simplified system for simulating the impacts of heatwaves, further research is needed to better understand the impacts of the increased intensity and duration of heatwave events in the response of shallow coastal ecosystems to global warming.

Acknowledgements

We would like to thank Ana Tamayo, Marta Najarro and Jose Calderon Caro for assistance in the laboratory. This work has been co-financed by the 2014-2020 ERDF Operational Program and by the Department of Economy, Knowledge, Business and University of the Regional Government of Andalusia (Project reference: FEDER-UCA18-107225). This publication is part of the R&D projects CTM2017-82271-R (Microbahia II) & PID2020-112488RB-I00 (Extreme-FUN), & MULTIFLUX funded by MCIN/AEI/10.13039/501100011033.

References

Abril, G., & Iversen, N. (2002). Methane dynamics in a shallow non-tidal estuary (Randers Fjord, Denmark). *Marine Ecology Progress Series*, *230*, 171-181. https://doi.org/10.3354/meps230171

Abril, G., Nogueira, M., Etcheber, H., Cabeçadas, G., Lemaire, E., & Brogueira, M. J. (2002). Behaviour of Organic Carbon in Nine Contrasting European Estuaries. *Estuarine, Coastal and Shelf Science*, *54*(2), 241-262. https://doi.org/10.1006/ecss.2001.0844

Apple, J., Del Giorgio, P., & Kemp, W. (2006). Temperature regulation of bacterial production, respiration, and growth efficiency in a temperate salt-marsh estuary. *Aquatic Microbial Ecology*, *43*, 243-254. https://doi.org/10.3354/ame043243

Arnosti, C., Jørgensen, B. B., Sagemann, J., & Thamdrup, B. (1998a). Temperature dependence of microbial degradation of organic matter in marine sediments: Polysaccharide hydrolysis, oxygen consumption, and sulfate reduction. *Marine Ecology Progress Series*, *165*(May), 59-70. https://doi.org/10.3354/meps165059

Arnosti, C., Jørgensen, B., Sagemann, J., & Thamdrup, B. (1998b). Temperature dependence of microbial degradation of organic matter in marine sediments:polysaccharide hydrolysis, oxygen consumption, and sulfate reduction. *Marine Ecology Progress Series*, *165*, 59-70. https://doi.org/10.3354/meps165059

Bastviken, D., Cole, J. J., Pace, M. L., & Van De Bogert, M. C. (2008). Fates of methane from different lake habitats: Connecting whole-lake budgets and CH $_4$ emissions. *Journal of Geophysical Research: Biogeosciences*, *113*(G2), 2007JG000608. https://doi.org/10.1029/2007JG000608

Berg, P., Risgaard-Petersen, N., & Rysgaard, S. (1998). Interpretation of measured concentration profiles in sediment pore water. *Limnology and Oceanography*, *43*(7), 1500-1510. https://doi.org/10.4319/lo.1998.43.7.1500

Bower, C. E., & Holm-Hansen, T. (1980). A Salicylate–Hypochlorite Method for Determining Ammonia in Seawater. *Canadian Journal of Fisheries and Aquatic Sciences*, *37*(5), 794-798. https://doi.org/10.1139/f80-106

Brin, L. D., Giblin, A. E., & Rich, J. J. (2017). Similar temperature responses suggest future climate warming will not alter partitioning between denitrification and anammox in temperate marine sediments. *Global Change Biology*, *23*(1), 331-340. https://doi.org/10.1111/gcb.13370

Burgos, M., Ortega, T., Bohórquez, J., Corzo, A., Rabouille, C., & Forja, J. M. (2018). Seasonal variation of early diagenesis and greenhouse gas production in coastal sediments of Cadiz Bay: Influence of anthropogenic activities. *Estuarine, Coastal and Shelf Science*, *200*, 99-115. https://doi.org/10.1016/j.ecss.2017.10.016

Burgos, M., Ortega, T., & Forja, J. (2018). Carbon Dioxide and Methane Dynamics in Three Coastal Systems of Cadiz Bay (SW Spain). *Estuaries and Coasts*, *41*(4), 1069-1088. https://doi.org/10.1007/s12237-017-0330-2

Burkholz, C., Garcias-Bonet, N., & Duarte, C. M. (2020). Warming enhances carbon dioxide and methane fluxes from Red Sea seagrass (<i>Halophila stipulacea</i>) sediments. *Biogeosciences*, *17*(7), 1717-1730. https://doi.org/10.5194/bg-17-1717-2020

Callahan, B. J., McMurdie, P. J., Rosen, M. J., Han, A. W., Johnson, A. J. A., & Holmes, S. P. (2016). DADA2: High-resolution sample inference from Illumina amplicon data. *Nature Methods*, *13*(7), 581-583. https://doi.org/10.1038/nmeth.3869

Canfield, D. E., Jørgensen, B. B., Fossing, H., Glud, R., Gundersen, J., Ramsing, N. B., Thamdrup, B., Hansen, J. W., Nielsen, L. P., & Hall, P. O. J. (1993). Pathways of organic carbon oxidation in three continental margin sediments. *Marine Geology*, *113*(1-2), 27-40. https://doi.org/10.1016/0025-3227(93)90147-N

Canion, A., Kostka, J. E., Gihring, T. M., Huettel, M., Van Beusekom, J. E. E., Gao, H., Lavik, G., & Kuypers, M. M. M. (2014). Temperature response of denitrification and anammox reveals the adaptation of microbial communities to in situ temperatures in permeable marine sediments that span 50° in latitude. *Biogeosciences*, *11*(2), 309-320. https://doi.org/10.5194/bg-11-309-2014

Dalsgaard, T., & Thamdrup, B. (2002). Factors Controlling Anaerobic Ammonium Oxidation with Nitrite in Marine Sediments. *Applied and Environmental Microbiology*, *68*(8), 3802-3808. https://doi.org/10.1128/AEM.68.8.3802-3808.2002

Dawson, R. N., & Murphy, K. L. (1972). The temperature dependency of biological denitrification. *Water Research*, *6*(1), 71-83. https://doi.org/10.1016/0043-1354(72)90174-1

Deldicq, N., Langlet, D., Delaeter, C., Beaugrand, G., Seuront, L., & Bouchet, V. M. P. (2021). Effects of temperature on the behaviour and metabolism of an intertidal foraminifera and consequences for benthic ecosystem functioning. *Scientific Reports*, *11*(1), 4013. https://doi.org/10.1038/s41598-021-83311-z

Duff, S., & Teal, J. M. (1965). *Temperature change and gas exchange in Nova Scotia and Georgia salt-marsh muds*.

Easterling, D. R., Meehl, G. A., Parmesan, C., Changnon, S. A., Karl, T. R., & Mearns, L. O. (2000). Climate Extremes: Observations, Modeling, and Impacts. *Science*, *289*(5487), 2068-2074. https://doi.org/10.1126/science.289.5487.2068

Epping, E., & Kühl, M. (2000). The responses of photosynthesis and oxygen consumption to short-term changes in temperature and irradiance in a cyanobacterial mat (Ebro Delta, Spain). *Environmental Microbiology*, *2*(4), 465-474. https://doi.org/10.1046/j.1462-2920.2000.00129.x

Faber, P. A., Kessler, A. J., Bull, J. K., McKelvie, I. D., Meysman, F. J. R., & Cook, P. L. M. (2012). The role of alkalinity generation in controlling the fluxes of CO₂ during exposure and inundation on tidal flats. *Biogeosciences*, *9*(10), 4087-4097. https://doi.org/10.5194/bg-9-4087-2012

Feng, G., Sun, W., Zhang, F., Karthik, L., & Li, Z. (2016). Inhabitancy of active Nitrosopumilus-like ammonia-oxidizing archaea and Nitrospira nitrite-oxidizing bacteria in the sponge Theonella swinhoei. *Scientific Reports*, *6*(1), 24966. https://doi.org/10.1038/srep24966

Ferrón, Alonso-Pérez, Anfuso, E., Murillo, F., Ortega, T., Castro, C., & Forja, J. (2009). Benthic nutrient recycling on the northeastern shelf of the Gulf of Cádiz (SW Iberian Peninsula). *Marine Ecology Progress Series*, *390*, 79-95. https://doi.org/10.3354/meps08199

Ferrón, Ortega, & Forja. (2009). Benthic fluxes in a tidal salt marsh creek affected by fish farm activities: Río San Pedro (Bay of Cádiz, SW Spain). *Marine Chemistry*, *113*(1-2), 50-62. https://doi.org/10.1016/j.marchem.2008.12.002

Fischer, E. M., & Knutti, R. (2015). Anthropogenic contribution to global occurrence of heavy-precipitation and high-temperature extremes. *Nature Climate Change*, *5*(6), 560-564. https://doi.org/10.1038/nclimate2617

Fowler, S. J., Palomo, A., Dechesne, A., Mines, P. D., & Smets, B. F. (2018). Comammox *Nitrospira* are abundant ammonia oxidizers in diverse groundwater-fed rapid sand filter communities. *Environmental Microbiology*, *20*(3), 1002-1015. https://doi.org/10.1111/1462-2920.14033

Froneman, P. W. (2005). Biogeochemistry of Marine Systems. *African Journal of Aquatic Science*, *30*(1), 91-91. https://doi.org/10.2989/16085910509503840

García-Robledo, E., Corzo, A., & Papaspyrou, S. (2014). A fast and direct spectrophotometric method for the sequential determination of nitrate and nitrite at low concentrations in small volumes. *Marine Chemistry*, *162*, 30-36. https://doi.org/10.1016/j.marchem.2014.03.002

Glud, R. N. (2008). Oxygen dynamics of marine sediments. *Marine Biology Research*, *4*(4), 243-289. https://doi.org/10.1080/17451000801888726

Grant, J. (1986). Sensitivity of benthic community respiration and primary production to changes in temperature and light. *Marine Biology*, *90*(2), 299-306. https://doi.org/10.1007/BF00569142

Guarini, J., Blanchard, G., Gros, P., & Harrison, S. (1997). Modelling the mud surface temperature on intertidal flats to investigate the spatio-temporal dynamics of the benthic microalgal photosynthetic capacity. *Marine Ecology Progress Series*, *153*, 25-36. https://doi.org/10.3354/meps153025

Gudasz, C., Bastviken, D., Steger, K., Premke, K., Sobek, S., & Tranvik, L. J. (2010). Erratum: Temperature-controlled organic carbon mineralization in lake sediments. *Nature*, *466*(7310), 1134-1134. https://doi.org/10.1038/nature09383

Hallin, S., & Lindgren, P.-E. (1999). PCR Detection of Genes Encoding Nitrite Reductase in Denitrifying Bacteria. *Applied and Environmental Microbiology*, *65*(4), 1652-1657. https://doi.org/10.1128/AEM.65.4.1652-1657.1999

Hancke, K., & Glud, R. (2004a). Temperature effects on respiration and photosynthesis in three diatom-dominated benthic communities. *Aquatic Microbial Ecology*, *37*, 265-281. https://doi.org/10.3354/ame037265

Hancke, K., & Glud, R. N. (2004b). Temperature effects on respiration and photosynthesis in three diatom-dominated benthic communities. *Aquatic Microbial Ecology*, *37*(3), 265-281. https://doi.org/10.3354/ame037265

Hansen, Henriksen, K., & Blackburn, T. (1981). Seasonal distribution of nitrifying bacteria and rates of nitrification in coastal marine sediments. *Microbial Ecology*, *7*(4), 297-304. https://doi.org/10.1007/BF02341424

Hansen, K., & Kristensen, E. (1998). The impact of the polychaete Nereis diversicolor and enrichment with macroalgal (Chaetomorpha linum) detritus on benthic metabolism and nutrient dynamics in organic-poor and organic-rich sediment. *Journal of Experimental Marine Biology and Ecology*, *231*(2), 201-223. https://doi.org/10.1016/S0022-0981(98)00070-7

Haro, S., Bohórquez, J., Lara, M., Garcia-Robledo, E., González, C. J., Crespo, J. M., Papaspyrou, S., & Corzo, A. (2019). Diel patterns of microphytobenthic primary production in intertidal sediments: The role of photoperiod on the vertical migration circadian rhythm. *Scientific Reports*, *9*(1), 13376. https://doi.org/10.1038/s41598-019-49971-8

Henson, S. A., Beaulieu, C., & Lampitt, R. (2016). Observing climate change trends in ocean biogeochemistry: When and where. *Global Change Biology*, *22*(4), 1561-1571. https://doi.org/10.1111/gcb.13152

Herbert, R. A. (1999). Nitrogen cycling in coastal marine ecosystems. *FEMS Microbiology Reviews*.

Hicks, N., Liu, X., Gregory, R., Kenny, J., Lucaci, A., Lenzi, L., Paterson, D. M., & Duncan, K. R. (2018). Temperature Driven Changes in Benthic Bacterial Diversity Influences Biogeochemical Cycling in Coastal Sediments. *Frontiers in Microbiology*, *9*, 1730. https://doi.org/10.3389/fmicb.2018.01730

Hines, J., Hammrich, A., Steiner, D., & Gessner, M. O. (2013). A field facility to simulate climate warming and increased nutrient supply in shallow aquatic ecosystems. *Oecologia*, *173*(4), 1169-1178. https://doi.org/10.1007/s00442-013-2720-x

Hornek, R., Pommerening-Röser, A., Koops, H.-P., Farnleitner, A. H., Kreuzinger, N., Kirschner, A., & Mach, R. L. (2006). Primers containing universal bases reduce multiple amoA gene specific DGGE band patterns when analysing the diversity of beta-ammonia oxidizers in the environment. *Journal of Microbiological Methods*, *66*(1), 147-155. https://doi.org/10.1016/j.mimet.2005.11.001

Jørgensen, B. B., & Revsbech, N. P. (1985). Diffusive boundary layers and the oxygen uptake of sediments and detritus1. *Limnology and Oceanography*, *30*(1), 111-122. https://doi.org/10.4319/lo.1985.30.1.0111

Jørgensen, B., & Sørensen, J. (1985). Seasonal cycles of 02, N03- and S042- reduction in estuarine sediments: The significance of an N03- reduction maximum in spring. *Marine Ecology Progress Series*, *24*(January 1985), 65-74. https://doi.org/10.3354/meps024065

Kühl, M., Lassen, C., & Jorgensen, B. (1994). Light penetration and light intensity in sandy marine sediments measured with irradiance and scalar irradiance fiber-optic microprobes. *Marine Ecology Progress Series*, *105*, 139-148. https://doi.org/10.3354/meps105139

Lahti & Shetty. (2017). *Microbiome R package* [Software]. Bioconductor. https://doi.org/10.18129/B9.BIOC.MICROBIOME

Lamontagne, M., Duran, R., & Valiela, I. (2003). Nitrous oxide sources and sinks in coastal aquifers and coupled estuarine receiving waters. *The Science of The Total Environment*, *309*(1-3), 139-149. https://doi.org/10.1016/S0048-9697(02)00614-9

Lefèvre, D., Bentley, T. L., Robinson, C., Blight, S. P., & Williams, P. J. le B. (1994). The temperature response of gross and net community production and respiration in time-varying assemblages of temperate marine micro-plankton. *Journal of Experimental Marine Biology and Ecology*, *184*(2), 201-215. https://doi.org/10.1016/0022-0981(94)90005-1

Leote, C., & Epping, E. H. G. (2015). Sediment–water exchange of nutrients in the Marsdiep basin, western Wadden Sea: Phosphorus limitation induced by a controlled release? *Continental Shelf Research*, *92*, 44-58. https://doi.org/10.1016/j.csr.2014.11.007

Levy-Booth, D. J., & Winder, R. S. (2010). Quantification of Nitrogen Reductase and Nitrite Reductase Genes in Soil of Thinned and Clear-Cut Douglas-Fir Stands by Using Real-Time PCR. *Applied and Environmental Microbiology*, *76*(21), 7116-7125. https://doi.org/10.1128/AEM.02188-09

Love, M. I., Huber, W., & Anders, S. (2014). Moderated estimation of fold change and dispersion for RNA-seq data with DESeq2. *Genome Biology*, *15*(12), 550. https://doi.org/10.1186/s13059-014-0550-8

McMurdie, P. J., & Holmes, S. (2013). phyloseq: An R Package for Reproducible Interactive Analysis and Graphics of Microbiome Census Data. *PLOS ONE*, *8*(4).

Meehl, G. A., Washington, W. M., Collins, W. D., Arblaster, J. M., Hu, A., Buja, L. E., Strand, W. G., & Teng, H. (2005). How Much More Global Warming and Sea Level Rise? *Science*, *307*(5716), 1769-1772. https://doi.org/10.1126/science.1106663

Mehrbach, C., Culberson, C. H., Hawley, J. E., & Pytkowicx, R. M. (1973). Measurement of the Apparent Dissociation Constants of Carbonic Acid in Seawater At Atmospheric Pressure. *Limnology and Oceanography*, *18*(6), 897-907. https://doi.org/10.4319/lo.1973.18.6.0897

Millero, F. J., & Poisson, A. (1981). International one-atmosphere equation of state of seawater. *Deep Sea Research Part A. Oceanographic Research Papers*, *28*(6), 625-629. https://doi.org/10.1016/0198-0149(81)90122-9

Musat, N., Werner, U., Knittel, K., Kolb, S., Dodenhof, T., Van Beusekom, J. E. E., De Beer, D., Dubilier, N., & Amann, R. (2006). Microbial community structure of sandy intertidal sediments in the North Sea, Sylt-Rømø Basin, Wadden Sea. *Systematic and Applied Microbiology*, *29*(4), 333-348. https://doi.org/10.1016/j.syapm.2005.12.006

Nizzoli, D., Carraro, E., Nigro, V., & Viaroli, P. (2010). Effect of organic enrichment and thermal regime on denitrification and dissimilatory nitrate reduction to ammonium (DNRA) in hypolimnetic sediments of two lowland lakes. *Water Research*, *44*(9), 2715-2724. https://doi.org/10.1016/j.watres.2010.02.002

Oksanen, J., Simpson, G. L., Blanchet, F. G., Kindt, R., Legendre, P., Minchin, P. R., O'Hara, R. B., Solymos, P., Stevens, M. H. H., Szoecs, E., Wagner, H., Barbour, M., Bedward, M., Bolker, B., Borcard, D., Carvalho, G., Chirico, M., De Caceres, M., Durand, S., … Borman, T. (2001). *vegan: Community Ecology Package* (p. 2.6-10) [Dataset]. https://doi.org/10.32614/CRAN.package.vegan

Oliver, E. C. J., Burrows, M. T., Donat, M. G., Sen Gupta, A., Alexander, L. V., Perkins-Kirkpatrick, S. E., Benthuysen, J. A., Hobday, A. J., Holbrook, N. J., Moore, P. J., Thomsen, M. S., Wernberg, T., & Smale, D. A. (2019). Projected Marine Heatwaves in the 21st Century and the Potential for Ecological Impact. *Frontiers in Marine Science*, *6*, 734. https://doi.org/10.3389/fmars.2019.00734

Papaspyrou, S., Kristensen, E., & Christensen, B. (2007). Arenicola marina (Polychaeta) and organic matter mineralisation in sandy marine sediments: In situ and microcosm comparison. *Estuarine, Coastal and Shelf Science*, *72*(1-2), 213-222. https://doi.org/10.1016/j.ecss.2006.10.020

Papaspyrou, S., Thessalou-Legaki, M., & Kristensen, E. (2004). Impact of Pestarella tyrrhena on benthic metabolism in sediment microcosms enriched with seagrass and macroalgal detritus. *Marine Ecology Progress Series*, *281*, 165-179. https://doi.org/10.3354/meps281165

Parmesan, C., Morecroft, M. D., & Trisurat, Y. (2022). *Climate Change 2022:Impacts, Adaptation and Vulnerability*.

Paulson, J. N., Stine, O. C., Bravo, H. C., & Pop, M. (2013). *Differential abundance analysis for microbial marker-gene surveys*.

Perkins-Kirkpatrick, S. E., & Lewis, S. C. (2020). Increasing trends in regional heatwaves. *Nature Communications*, *11*(1), 3357. https://doi.org/10.1038/s41467-020-16970-7

Rabouille, C., Denis, L., Dedieu, K., Stora, G., Lansard, B., & Grenz, C. (2003). Oxygen demand in coastal marine sediments: Comparing in situ microelectrodes and laboratory core incubations. *Journal of Experimental Marine Biology and Ecology*, *285-286*, 49-69. https://doi.org/10.1016/S0022-0981(02)00519-1

Rasmussen, H., & Jorgensen, B. (1992). Microelectrode studies of seasonal oxygen uptake in a coastal sediment: Role of molecular diffusion. *Marine Ecology Progress Series*, *81*, 289-303. https://doi.org/10.3354/meps081289

Reay, D. S., Nedwell, D. B., Priddle, J., & Ellis-Evans, J. C. (1999). Temperature Dependence of Inorganic Nitrogen Uptake: Reduced Affinity for Nitrate at Suboptimal Temperatures in Both Algae and Bacteria.

Applied and Environmental Microbiology, *65*(6), 2577-2584. https://doi.org/10.1128/AEM.65.6.2577-2584.1999

Repeta, D. J., Ferrón, S., Sosa, O. A., Johnson, C. G., Repeta, L. D., Acker, M., DeLong, E. F., & Karl, D. M. (2016). Marine methane paradox explained by bacterial degradation of dissolved organic matter. *Nature Geoscience*, *9*(12), 884-887. https://doi.org/10.1038/ngeo2837

Revsbech, N. P. (1989). An oxygen microsensor with a guard cathode. *Limnology and Oceanography*, *34*(2), 474-478. https://doi.org/10.4319/lo.1989.34.2.0474

Rios-Yunes, D., Tiano, J. C., Van Oevelen, D., Van Dalen, J., & Soetaert, K. (2023). Annual biogeochemical cycling in intertidal sediments of a restored estuary reveals dependence of N, P, C and Si cycles to temperature and water column properties. *Estuarine, Coastal and Shelf Science*, *282*, 108227. https://doi.org/10.1016/j.ecss.2023.108227

Rosales Villa, A. R., Jickells, T. D., Sivyer, D. B., Parker, E. R., & Thamdrup, B. (2019). Benthic nitrogen cycling in the North Sea. *Continental Shelf Research*, *185*, 31-36. https://doi.org/10.1016/j.csr.2018.05.005

Saad, O. A. L. O., & Conrad, R. (1993). Temperature dependence of nitrification, denitrification, and turnover of nitric oxide in different soils. *Biology and Fertility of Soils*, *15*(1), 21-27. https://doi.org/10.1007/BF00336283

Sansone, F. J., Graham, A. W., & Berelson, W. M. (2004). Methane along the western Mexican margin. *Limnology and Oceanography*, *49*(6), 2242-2255. https://doi.org/10.4319/lo.2004.49.6.2242

Scala, D. J., & Kerkhof, L. J. (1998). Nitrous oxide reductase (*nosZ*) gene-specific PCR primers for detection of denitrifiers and three *nosZ* genes from marine sediments. *FEMS Microbiology Letters*, *162*(1), 61-68. https://doi.org/10.1111/j.1574-6968.1998.tb12979.x

Schutte, C. A., Ahmerkamp, S., Wu, C. S., Seidel, M., De Beer, D., Cook, P. L. M., & Joye, S. B. (2019). Biogeochemical Dynamics of Coastal Tidal Flats. En *Coastal Wetlands* (pp. 407-440). Elsevier. https://doi.org/10.1016/B978-0-444-63893-9.00012-5

Sierra, A., Jiménez-López, D., Ortega, T., Ponce, R., Bellanco, M. J., Sánchez-Leal, R., Gómez-Parra, A., & Forja, J. (2017). Spatial and seasonal variability of CH 4 in the eastern Gulf of Cadiz (SW Iberian Peninsula). *Science of The Total Environment*, *590-591*, 695-707. https://doi.org/10.1016/j.scitotenv.2017.03.030

Smith, K. E., Burrows, M. T., Hobday, A. J., King, N. G., Moore, P. J., Sen Gupta, A., Thomsen, M. S., Wernberg, T., & Smale, D. A. (2023). Biological Impacts of Marine Heatwaves. *Annual Review of Marine Science*, *15*(1), 119-145. https://doi.org/10.1146/annurev-marine-032122-121437

Soetaert, K., & Petzoldt, T. (2008). *marelac: Tools for Aquatic Sciences* (p. 2.1.11) [Dataset]. https://doi.org/10.32614/CRAN.package.marelac

Stocker, T. F. (2014). Climate Change 2013: The Physical Science Basis. Contribution of Working Group I to the Fifth Assessment Report of the Intergovernmental Panel on Climate Change. *Environmental Research Letters*, *9*(8), 13pp.

Stott, P. A., Stone, D. A., & Allen, M. R. (2004). Human contribution to the European heatwave of 2003. *Nature*, *432*(7017), 610-614. https://doi.org/10.1038/nature03089

Suzuki, M. T., Taylor, L. T., & DeLong, E. F. (2000). Quantitative Analysis of Small-Subunit rRNA Genes in Mixed Microbial Populations via 5′-Nuclease Assays. *Applied and Environmental Microbiology*, *66*(11), 4605-4614. https://doi.org/10.1128/AEM.66.11.4605-4614.2000

Tan, E., Zou, W., Zheng, Z., Yan, X., Du, M., Hsu, T.-C., Tian, L., Middelburg, J. J., Trull, T. W., & Kao, S. (2020). Warming stimulates sediment denitrification at the expense of anaerobic ammonium oxidation. *Nature Climate Change*, *10*(4), 349-355. https://doi.org/10.1038/s41558-020-0723-2

Tatti, E., McKew, B. A., Whitby, C., & Smith, C. J. (2016). Simultaneous DNA-RNA Extraction from Coastal Sediments and Quantification of 16S rRNA Genes and Transcripts by Real-time PCR. *Journal of Visualized Experiments*, *112*, 54067. https://doi.org/10.3791/54067

Thamdrup, B., & Fleischer, S. (1998). Temperature dependence of oxygen respiration, nitrogen mineralization, and nitrification in Arctic sediments. *Aquatic Microbial Ecology*, *15*, 191-199. https://doi.org/10.3354/ame015191

Thamdrup, B., Hansen, J. W., & Jørgensen, B. B. (1998). Temperature dependence of aerobic respiration in a coastal sediment. *FEMS Microbiology Ecology*, *25*(2), 189-200. https://doi.org/10.1016/S0168-6496(97)00095-0

Tovar, A., Moreno, C., Mánuel-Vez, M. P., & García-Vargas, M. (2000). Environmental impacts of intensive aquaculture in marine waters. *Water Research*, *34*(1), 334-342. https://doi.org/10.1016/S0043-1354(99)00102-5

Ummenhofer, C. C., & Meehl, G. A. (2017). Extreme weather and climate events with ecological relevance: A review. *Philosophical Transactions of the Royal Society B: Biological Sciences*, *372*(1723), 20160135. https://doi.org/10.1098/rstb.2016.0135

Walters, W., Hyde, E. R., Berg-Lyons, D., Ackermann, G., Humphrey, G., Parada, A., Gilbert, J. A., Jansson, J. K., Caporaso, J. G., Fuhrman, J. A., Apprill, A., & Knight, R. (2016). Improved Bacterial 16S rRNA Gene (V4 and V4-5) and Fungal Internal Transcribed Spacer Marker Gene Primers for Microbial Community Surveys. *mSystems*, *1*(1), e00009-15. https://doi.org/10.1128/mSystems.00009-15

Welsh, A., Chee-Sanford, J. C., Connor, L. M., Löffler, F. E., & Sanford, R. A. (2014). Refined NrfA Phylogeny Improves PCR-Based *nrfA* Gene Detection. *Applied and Environmental Microbiology*, *80*(7), 2110-2119. https://doi.org/10.1128/AEM.03443-13

Wieland, A., & Kühl, M. (2000). Irradiance and temperature regulation of oxygenic photosynthesis and O 2 consumption in a hypersaline cyanobacterial mat (Solar Lake, Egypt). *Marine Biology*, *137*(1), 71-85. https://doi.org/10.1007/s002270000331

Winkler, J. P., Cherry, R. S., & Schlesinger, W. H. (1996). The Q10 relationship of microbial respiration in a temperate forest soil. *Soil Biology and Biochemistry*, *28*(8), 1067-1072. https://doi.org/10.1016/0038-0717(96)00076-4

Wuchter, C., Abbas, B., Coolen, M. J. L., Herfort, L., Van Bleijswijk, J., Timmers, P., Strous, M., Teira, E., Herndl, G. J., Middelburg, J. J., Schouten, S., & Sinninghe Damsté, J. S. (2006). Archaeal nitrification in the ocean. *Proceedings of the National Academy of Sciences*, *103*(33), 12317-12322. https://doi.org/10.1073/pnas.0600756103

Xiao, Beulig, F., Kjeldsen, K. U., Jørgensen, B. B., & Risgaard-Petersen, N. (2017). Concurrent Methane Production and Oxidation in Surface Sediment from Aarhus Bay, Denmark. *Frontiers in Microbiology*, *8*, 1198. https://doi.org/10.3389/fmicb.2017.01198

Xiao, Beulig, F., Røy, H., Jørgensen, B. B., & Risgaard-Petersen, N. (2018). Methylotrophic methanogenesis fuels cryptic methane cycling in marine surface sediment. *Limnology and Oceanography*, *63*(4), 1519-1527. https://doi.org/10.1002/lno.10788

Yvon-Durocher, G., Allen, A. P., Bastviken, D., Conrad, R., Gudasz, C., St-Pierre, A., Thanh-Duc, N., & Del Giorgio, P. A. (2014). Methane fluxes show consistent temperature dependence across microbial to ecosystem scales. *Nature*, *507*(7493), 488-491. https://doi.org/10.1038/nature13164

Impact of heatwaves on net metabolism, nutrient and greenhouse gases fluxes at the sediment-water interphase of a shallow coastal ecosystems

Valle Perez-Rodriguez[1], Alfonso Corzo[1], Sokratis Papaspyrou[1], Ana Sierra[2,] Joe D. Taylor[5], Cindy J. Smith[4], Fabien Cholet[4], Emilio Garcia-Robledo[1]

[1]Departamento de Biología, Facultad de Ciencias Marinas y Ambientales, Universidad de Cádiz, Campus Universitario Río San Pedro, 11510 Puerto Real, Cádiz, Spain.

[2] Instituto Universitario de Investigación Marina (INMAR), Campus Universitario de Puerto Real, Universidad de Cádiz, Campus Universitario Río San Pedro, 11510 Puerto Real, Cádiz, Spain.

[3] Dpto. Química-Física, INMAR, Facultad de Ciencias del Mar y Ambientales, Universidad de Cádiz, Campus Universitario Río San Pedro, 11510 Puerto Real, Cádiz, Andalucía, Spain

[4] Advanced Research Centre, Infrastructure and Environment, James Watt School of Engineering, University of Glasgow, 11 Chapel Lane G11 6EW, Glasgow, UK.

[5] UK Centre for Ecology and Hydrology, Wallingford, OX10 8BB, UK

Supplementary results: Table SI-II, Figures S1-4

Table S1. Primer sets and qPCR conditions used for the various genes targeted involved in the nitrogen cycle and standard curve characteristics.

Process		Target gene	Primer set	Sequence	q-PCR conditions used	Reference	Efficiency (%)	Slope	R^2
		16S rDNA	Bact1369F Prok1492R	CGGTGAATACGTTCYCGG GGWTACCTTGTTAC GACTT	95°C-15min; 40x (95ºC-10sec; 59ºC-15sec; 72ºC-20sec)	Suzuki et al., (2000)	92.4	-3.518	0.998
Denitrification	Copper containing nitrite reductases	**nirK**	**nirK FlaCu** **nirK R3Cu**	ATCATGGTSCTGCCGCG GCCTCGATCAGRTTGTGGTT	95°C-15min; 40x (95ºC-15sec; 57ºC-20sec; 72ºC-1min)	Hallin and Lindgren, (1999)	92.0	-3.530	0.997
	Haem contaiing nitrite reductases	**nirS**	**nirS1F** **nirS 3R**	CCTAYTGGCCGGCRCART GCCGCCGTCRTGVAGGAA	95°C-15min; 40x (95ºC-15sec; 57ºC-20sec; 72ºC-1min)	Levy-Booth and Winder, (2010)	99.3	-3.338	0.997
	nitrous oxide reductase	**nosZ**	**nosZ-1527F-q** **nosZ-1773R-q**	CGCTGTTCHTCGACAGYCA ATRTCGATCARCTGBTCGTT	95°C-15 min; 40x (95°C-15 seg; 56°C-15 seg; 72°C-30 seg)	Modified Scala & Kerkhoff (1998)	83.4	-3.796	0.996

Nitrification	nitrite oxidoreductase	**nxrB**	**nxrBqF** **nxrBqR**	TGTGGTGGAACAACGTGGAA CCCGGCATCGAAAATGGTCA	95°C-15min; 40x (95ºC-20sec; 56ºC-20sec; 72ºC-30sec)	Feng et al., (2016)	94.9	-3.450	0.999
Dissimilatory nitrate reduction to ammonium	dissimilatory periplasmic cytochrome c nitrite reductase	**nrfA**	**nrfAF2aw** **nrfAR1**	CARTGYCAYGTBGARTA TWNGGCATRTGRCARTC	95°C-15min; 40x (94°C-30sec; 48°C-30sec; 72°C-1min)	Welsh et al., (2014)	87.2	-3.671	0.994
Ammonia oxidation	ammonia monooxygenase	**AmoA**	**BacamoA-1F** **BacamoA-2R**	GGGGHTTYTACTGGTGGT CCCCTCBGSAAAVCCTTCTTC	95°C-15min; 40x (95°C-30 sec, 47°C-30 sec, 72°C-1 min)	Hornek et al., (2006)	90.7	-3.566	1.000
Ammonia oxidation		**amoA**	**Arch-amoWAF** **Arch-amoWAR**	CTGAYTGGGCYTGGACATC TTCTTCTTTGTTGCCCAGTA	95°C-15min; 40x (95°C-30sec; 58°C-40sec, 72°C-1min)	Wuchter et al., (2006)	105.7	-3.192	0.997
Ammonia oxidation (Comammox)		**amoA**	**Ntsp-amoA 162F** **NtspamoA 359R**	GGATTTCTGGNTSGATTGGA WAGTTNGACCACCASTACCA	95°C-15min; 40x (94°C-30sec; 48°C-30sec; 72°C-1min)	Fowler et al., (2018)	87.2	-3.672	0.997

Table SII. E_a and Q_{10} values calculated from areal E_a was calculated from eq. 2 and Q_{10} from the eq. 3 at 18 ºC.

	Day	*E_a*	*E_a SE*	*Q_{10}*	*Q_{10} SE*
NO_2^-	1	25,46	3,76	1,39	1,05
	2	34,50	8,09	1,61	1,11
	3	25,30	4,05	1,41	1,05
	4	6,83	7,94	1,10	1,11
NH_4^+	1	31,04	7,37	1,53	1,10
	2	38,54	7,54	1,70	1,10
	3	17,34	10,63	1,27	1,15
	4	82,00	31,44	3,08	1,51
N_2O	1	13,16	5,45	1,19	1,07
	2	12,27	4,09	1,18	1,05
	3	4,00	6,94	1,06	1,09
	4	3,20	2,58	1,04	1,03
CH_4	1	73,57	15,39	2,74	1,22
	2	99,87	15,22	3,94	1,22
	3	92,01	31,28	3,53	1,50
	4	76,46	11,72	2,85	1,16

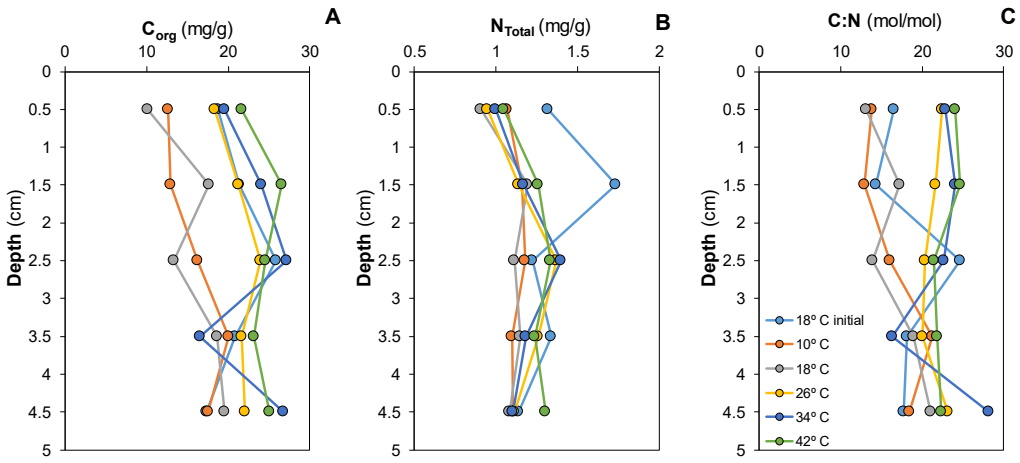


Fig. S1. Organic carbon (C_{org}) content, total nitrogen (N_{Total}) content and carbon/nitrogen ratio (C:N) in the the first 5 cm depth PW at the first day (initial) and the last day of study.

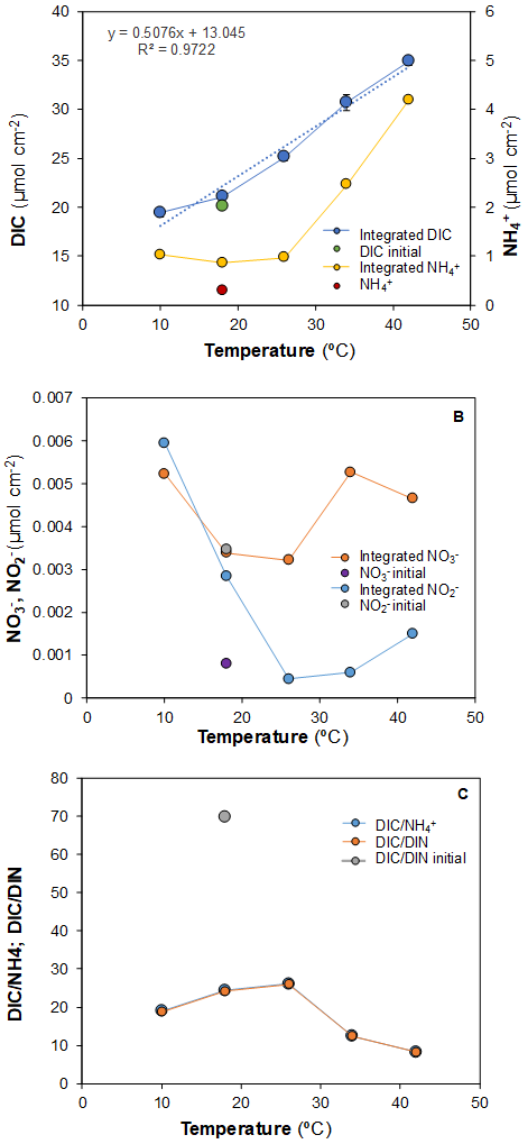


Fig. S2. Integrated concentration of DIC and NH_4^+ within the sediment (upper 5cm). The DIC concentration at the 4-5 cm layer (sample lost) of cores incubated at 42 ºC was assumed equal to that of 3-4 cm layer for correct integration at the same depth. Similarly, NH_4^+ samples from 4-5 cm at 34º C and 42º C incubations were unavailable and were considered equal to their respective concentrations at the 3-4 cm layers for integration.

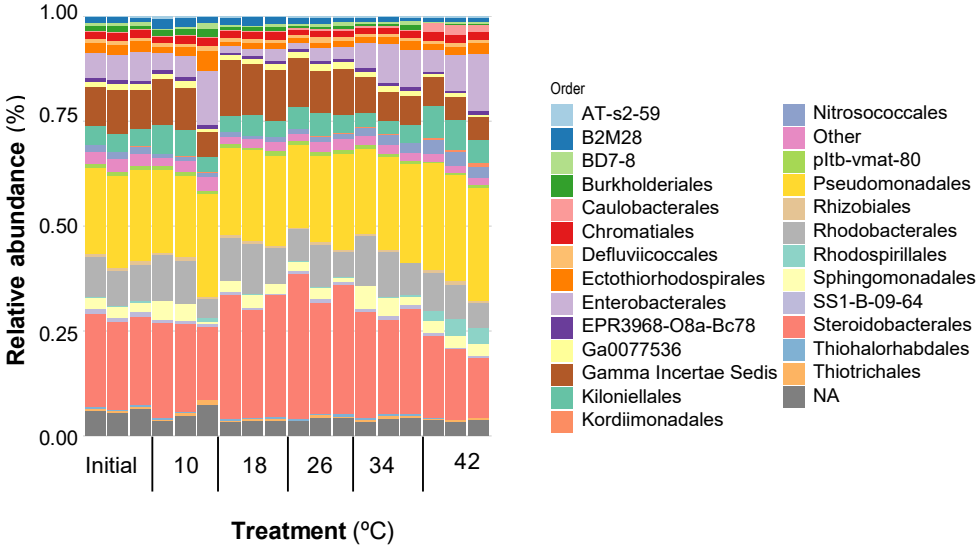


Fig. S3. Proteobacteria composition at order level in sediment across temperature treatments (Initial, 10, 18, 26, 34, 42 °C) at initial conditions and after 84h. Stacked bars show means. Only taxa representing ≥1 % of the community in at least one sample are colored; remaining groups are pooled as "NA."

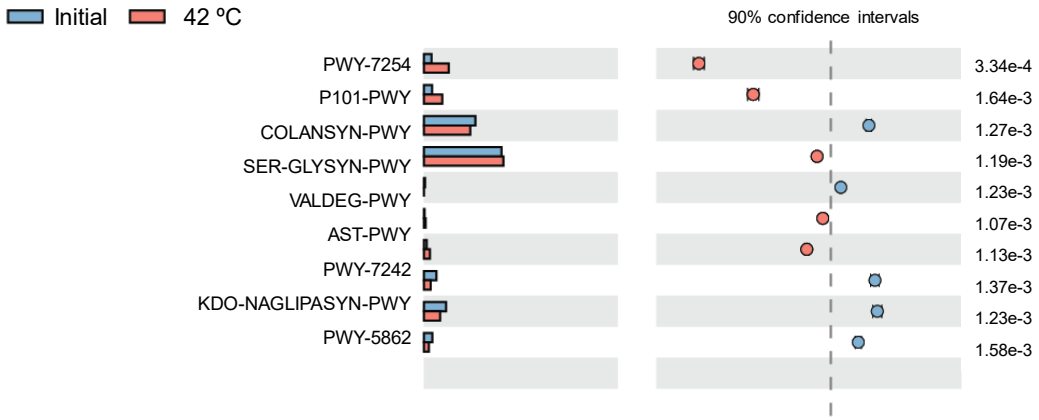
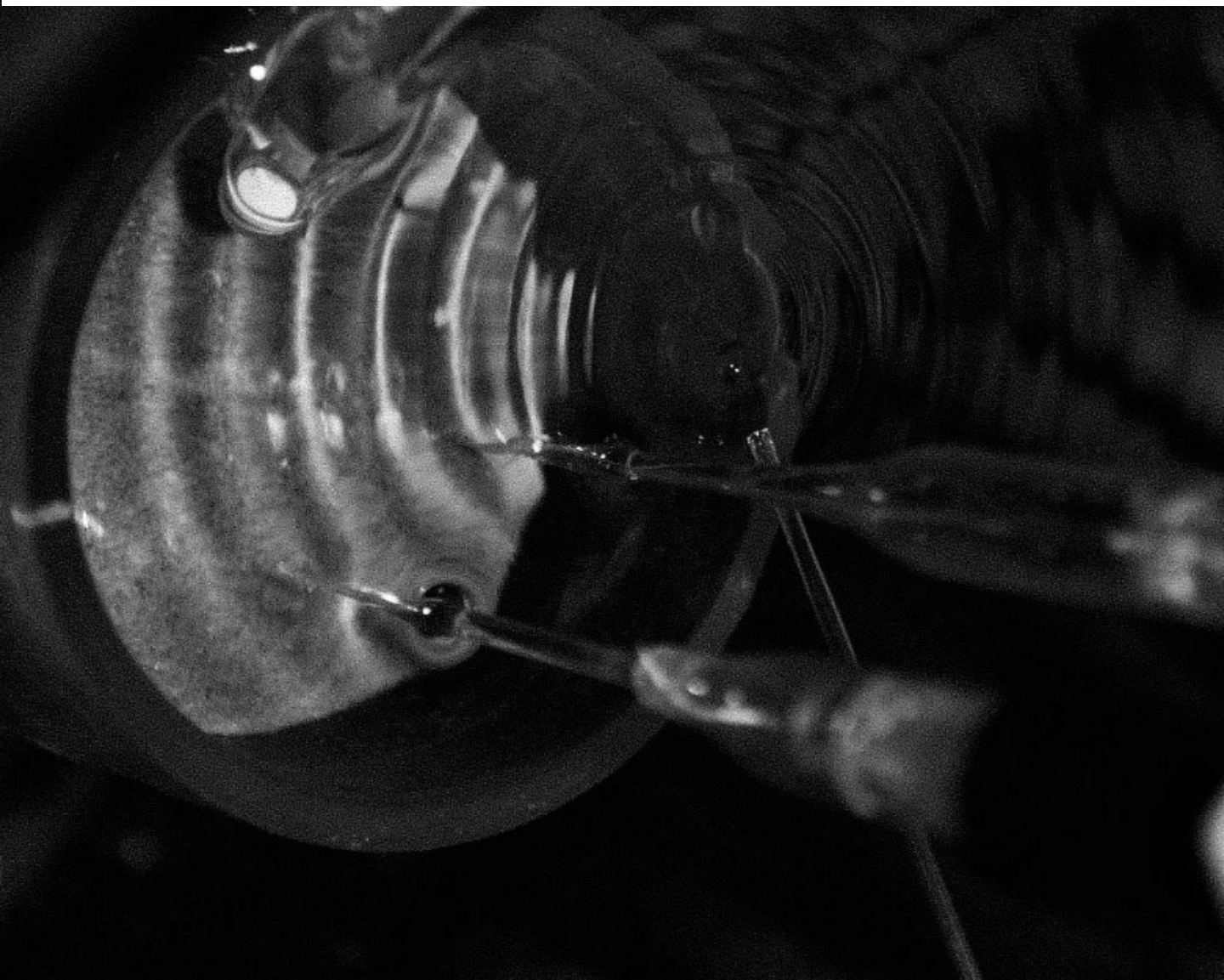


Fig S4. Differential abundance of selected metabolic pathways in sediment microbial communities at Initial (blue) and 42 °C (red). Horizontal bars on the left show mean pathway abundances; points on the right indicate $\log_2$ fold-changes with 90 % confidence intervals (dashed line at zero). Pathway IDs (left) and corresponding p-values (right). Colors on the right denote pathways enriched under each condition. IDs correspond to: PWY-7254 (Tricarboxylic acid [TCA] cycle VII - acetate-producers), P101-PWY (Ectoine biosynthesis), COLANSYN-PWY (Colanic acid building blocks biosynthesis), SER-GLYSYN-PWY (L-serine and glycine biosynthesis), VALDEG-PWY (L-valine degradation I), AST-PWY (L-aspartate superpathway), PWY-7242 (Superpathway of histidine, purine, and pyrimidine degradation), KDO-NAGLIPASYN-PWY (Kdo N-acetyl-lipid A biosynthesis), PWY-5862 (Menaquinol-7 [vitamin K_2] biosynthesis).

Chapter 4

Wind storms increase benthic-pelagic coupling and nutrient outwelling from shallow coastal wetlands



Windstorms increase benthic-pelagic coupling and nutrient outwelling from shallow coastal wetlands

Alfonso Corzo[1], Valle Perez-Rodriguez[1], Sara Haro[2], Sokratis Papaspyrou[1], Sandra Rizzo-Calderón[1], Mª Dolores Jimenez-Lopez[1], Emilio Garcia-Robledo[1]

[1]Department of Biology, Faculty of Marine and Environmental Science, University of Cadiz, Pol. Río San Pedro s/n, Puerto Real, Spain

[2] Department of Ecology and Geology, Faculty of Sciences, University of Málaga, Málaga, Spain

Keywords: Windstorms, Nutrient content, Microphytobenthos, Shallow coast, Climate change, Net community production

Abstract: The increase in the intensity and frequency of extreme climatic events as consequence of climate change is likely to affect considerably coastal shallow areas, which hold some of the most productive ecosystem in earth. We analyse the impact of a windstorm event (WSE) on relevant biogeochemical characteristics in the water column and intertidal sediments of the inner Cadiz Bay (Spain), as a model for shallow coastal environments. Samples were collected before, during and after a WSE in two sampling points with different sediment characteristics, sandy and muddy, located in opposed sides of the inner bay to cover maximum variability. Total suspended solids (TSS), chlorophyll a (Chla) and most dissolved inorganic nutrients (NH_4^+, NO_2^-, NO_3^-, PO_4^{3-} and SiO_4^{4-}) increased transiently in the water column during WSE, showing an evident transfer of matter from the sediment. TSS and Chla in water column were linearly related among them and with wind speed, while concentration of inorganic nutrients was not. This difference suggests that the concentration of inorganic nutrients in the water column are not the direct result of the release during resuspension but that further biogeochemical processing occurs in the water column. TSS and Chla estimated by Sentinel-2 imagery before, during and after the WSE confirmed the impact on the water column, but also a considerable degree of spatial heterogeneity, being maximum changes located in the North and North-East zones of the bay. The effect of WSE on the biogeochemical properties of sediment surface like O_2 vertical distribution, measured with microsensors, net metabolism, content of Chla, organic carbon, total nitrogen and pore water NH_4^+ and PO_4^{3-} differed between two sampling points. Therefore, differences in sediment characteristics, hydrodynamics conditions and

the horizontal transport within the basin and with the sea are important to determine the effect of WSE in shallow environments. WSE affect considerably the environmental conditions in the sediment and water column within the inner bay but also the export of TSS plus organic and inorganic nutrients to the sea with tides increased up to 3.6 times. Overall, the effect of WSE in shallow coastal environments would increase considerably the outwelling from the continent, affecting as well coastal primary production and higher trophic levels.

1. Introduction

Coastal and estuarine shallow areas are some of the most productive areas worldwide, providing multiple ecosystems services. However, these areas are vulnerable to the effects of climate change (Mieszkowska et al., 2020; Schutte et al., 2019). The ongoing climate change is increasing the frequency and the magnitude of extreme climatic events (ECE), such as heatwaves and wind-storms event (WSE) (Meehl & Tebaldi, 2004; Schutte et al., 2019; Smith et al., 2023). ECEs can affect considerably the biological communities and biogeochemical cycling in these areas (Hicks et al., 2018; Parmesan et al., 2022). Intertidal sediments and photic sediments in shallow coastal zones are inhabited by a community of microbial primary producers, being dominated by diatoms and cyanobacteria (microphytobenthos, MPB)(Haro et al., 2019; Sundbäck & Miles, 2002; Underwood & Kromkamp, 1999). MPB has a significant ecological and biogeochemical role, being for example the main benthic primary producers in bare intertidal sediments and contributing more than 50% of the total primary production in some estuarine environments (Chen & Lee, 2022; Frankenbach et al., 2020; Haro et al., 2020, 2022; Underwood & Kromkamp, 1999). MPB is also an important food source, directly for marine meiofauna and macrofauna (Middelburg et al., 2000), and indirectly for heterotrophic bacteria due to the production of exopolymers (Bohórquez et al., 2017). Furthermore, MPB exopolymers promote sediment cohesion, decrease resuspension rates, and, therefore, improve water quality (Paterson, 1989; Yallop et al., 1994). Finally, MPB photosynthetic activity significantly influences daily oxygen availability in the upper sediment layer and consequently the rate and pathways of organic matter mineralization and nutrient recycling (Høgslund et al., 2023; Rios-Yunes et al., 2023; Risgaard-Petersen, 2003; Schutte et al., 2019; Soetaert et al., 2006). These ecological functions of MPB can

be potentially impacted by ECE and then, the increase in the intensity and frequency of diverse types of ECE could lead to relevant ecosystem alterations.

In shallow coastal environments, extreme wind events increase shear stress during immersion due to the wind induced waves disrupting the sediment – water interface, leading to the resuspension of the upper sediment layer. This results in an increase of the exchange of dissolved nutrients, sediment, and MPB cells with the water column (Hope et al., 2020). However, during emersion, strong winds are likely to enhance desiccation of the intertidal sediment surface (Coelho et al., 2009). Therefore, windstorms could negatively affect in different ways the MPB biomass, primary production, and net metabolism of the microbial community that inhabit the sediment surface. In contrast, the higher availability of nutrients and the increase in diatom abundance, despite the higher turbidity and lower light availability, might increase the primary production in the water column. At the same time, strong wind events likely contribute to the horizontal transport and relocation of the organic and inorganic fraction of sediment within the system (Jiménez-Arias et al., 2020), including resuspended MPB cells, and even enhancing their export to neighbouring ecosystems (Ha et al., 2020; Zhang & Blomquist, 2018).

In this work, the effect of a windstorm on the water column and intertidal sediment of a model shallow coastal environment, the inner Cadiz Bay, was studied using *in situ* field measurements and remote sensing techniques before, during and after a strong wind event. Sediment physicochemical variables and metabolic rates were measured using sediment cores. In parallel, water column samples were also collected for studying the impact on water column photosynthetic pigments and total suspended soils (TSS). In addition, changes in key water column variables were analysed at the scale of the entire inner bay using Sentinel-2 imagery. As a result of the sediment resuspension during the windstorms, we hypothesized that significant increases in the Chla and TSS concentration in the water column during and after the windstorm, in parallel to a decrease of Chla in the sediment surface, a possible decrease of MPB primary production and the transfer of inorganic nutrients from the sediment to the water column. This work provides a comprehensive data set to quantitatively evaluate the specific effects of strong wind events, whose frequency are increasing because of global warming, on key ecological and biogeochemical variables of the intertidal sediments and the water column in shallow coastal estuarine zones.

2. Material and methods

2.1. Study site description and sampling

The inner section of the Bay of Cadiz, located in the southwest of the Iberian Peninsula, is a model site to study the effect of windstorm events on shallow coastal environments (Fig. 1) as several previous studies about MPB and its contribution are already available in the region. The Bay is a shallow water body, with an average depth of less than 3 m at high tide and a large intertidal area, > 13 km^2 (~60% of its surface). The Bay is affected by semidiurnal tides that oscillate between a maximum tidal height of 1.75 m and a minimum of -1.5 m relative to the local mean sea level (MSL). MPB covers at least 62% of the intertidal sediment's surface (Haro et al., 2022).

The *in situ* sampling was carried out between June and July of 2021 (see more details below), in two different locations, selected to represent as much as possible the variability in the characteristics of the intertidal zone in inner Cadiz Bay. The first was located in the western part of the Bay, (Cadiz) (36°29'24.8"N; 6°15'51.9"W), a site more susceptible to possible changes during windstorms due to its proximity to the main mouth of the bay connecting it to the ocean and its reduced surface area, with sandy sediment partially covered by seagrass meadows, i.e., *Nanozostera noltei* and *Cymodocea nodosa*, macroalgae (*Caulerpa prolifera*, and small patches of *Ulva* spp.,) and MPB. The second was located in the northeastern part of the bay (Puerto Real) (36°31'38.9"N; 6°11'53.7"W), being less exposed, with muddy sediment covered mainly by MPB.

Five sediment cores (4.5 Ø, 30 cm length) and seawater (20 L) were collected at both sampling sites before, during a windstorm event (WSE) (from the 23rd to the 27th June). Samples were taken on the 3rd and 22th June (20 days and 1 day before the ECE), 24th and 25th June (during the ECE), and 29th June and 6th July 2021 (just after and 1 week after the windstorm). Sediment samples were collected in the intertidal zone at low tide, in areas of bare sediment colonized by MPB (visual observation), avoiding aquatic plant fragments or leaves in the collected samples. Water samples were collected as close as possible to the sediment core locations. Both, sediment cores and seawater were transported immediately to the laboratory. Cores from each site were placed in a separate 12 L aquarium filled with *in situ* seawater and maintained in a temperature-controlled room at 18 ºC. Sediment

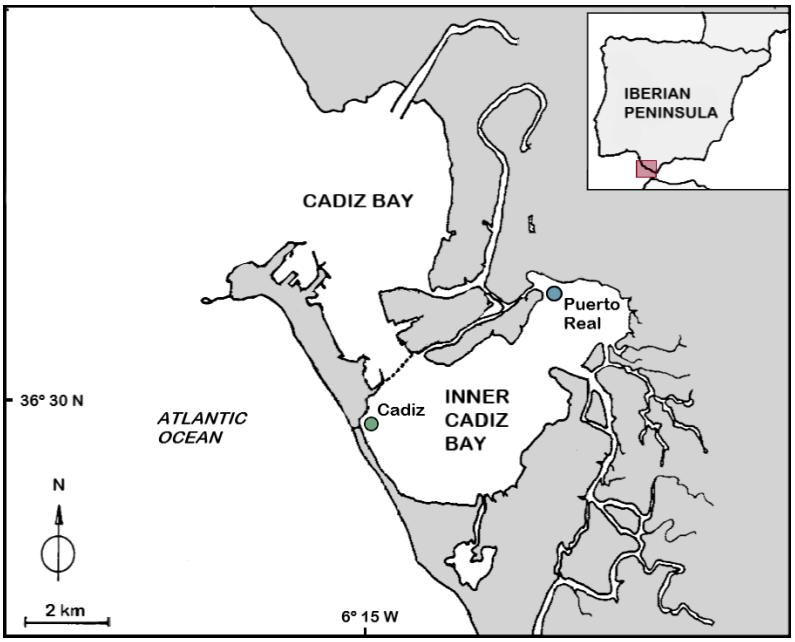


Fig. 1. Location of the sampling and the study zone. The blue pin represents the location of the Puerto Real sampling point (muddier sediment in the northeast of inner Cadiz Bay), whereas the green pin shows the Cadiz point (sandier sediment in the western inner Cadiz Bay).

cores were illuminated during the full light incubations with LED lamps (Lince 6M Verso, Light Environment Control S. L.) at saturating irradiance (1360 µmol photon m^{-2} s^{-1} on average).

Wind speed (m/s) and direction (sexagesimal degrees) during the study period were obtained from the meteorological station of Cadiz (36° 29' 59" N; 6° 15' 28" W) of the *Spanish Meteorological Agency* (AEMET).

2.2. Oxygen microprofiles and net metabolism at the sediment water interface

Vertical microprofiles of oxygen concentration were determined at the sediment-water interface in the collected cores in light and in darkness, using O_2 microsensors (50 µm tip size, Unisense®, Denmark) moved by a motorised micromanipulator (MS-232), controlled with the Sensor Trace Pro software

(Unisense®). Microsensors were calibrated by measuring O_2 in a well-aerated water column (100% saturation) and the anoxic part of the sediment (0% saturation). Diffusive O_2 fluxes at the sediment-water interface were calculated in the diffusive boundary layer by applying Fick's first law of diffusion (Revsbech, 1989; Corzo et al., 2005). Net community production rate in light (NCP) was equal to the diffusive oxygen fluxes in light, and dark respiration rate (R_{dark}) was equal to the to the diffusive oxygen fluxes in dark conditions.

2.3. Total suspended solids, photosynthetic pigments and nutrients content in the water column

For the determination of total suspended solids (TSS) and photosynthetic pigments, 15 L of *in situ* water were brought to the laboratory within an hour. A known volume of water was filtered through previously weighted GF/F filters. Filters were stored frozen (-30 ºC) until further processing. TSS was calculated as the weight difference of the filter before and after freeze-drying in the darkness (Labconco FreeZone Legacy 2.5L, CROMTEK) to prevent photosynthetic pigments degradation and corrected for the filtered volume.

Photosynthetic pigments were extracted from the same freeze-dried filters in 3 mL 100% ethanol and stored in darkness for 18 h. Then, absorbance spectra of the extracts were measured on a microplate reader (Multiskan GO; Thermo Scientific). Chlorophyll-a (Chla) and chlorophyll-c (Chlc) were estimated according to Ritchie *et al.* (2008).

Inorganic nutrients: ammonium (NH_4^+), nitrate (NO_3^-), nitrite (NO_2^-), phosphate (PO_4^{3-}) and silicate (SiO_4^{4-}) were measured in water samples taken *in situ* with 20 mL plastic syringes and filtered through a GF/F filter (n=5). Samples were stored on ice and frozen once in the laboratory (-30ºC) until analysis. Inorganic nutrients concentration was measured by colorimetric methods on a microplate reader (Multiskan GO; Thermo Scientific): ammonium (NH_4^+) following Bower and Holm-Hansen (1980), nitrate (NO_3^-) and nitrite (NO_2^-) following Garcia-Robledo (2014), phosphate (PO_4^{3-}) according to Koroleff (1999) and silicate (SiO_4^{4-}) following Grasshoff *et al.* (1999).

2.4. Organic matter, nutrients and chlorophyll content in sediment

Once the O_2 microprofiling was finished, sediment cores were immediately sectioned in 1-cm thick slices. Sediment samples were centrifuged at 4700 × g for 20 min at 4ºC, and the supernatant was kept at −20ºC for porewater nutrient analyses as previosuly described. Sediment pellets were subsequently frozen, freeze-dried and kept in dark conditions until further processing. A portion (circa 1.5 g for muddy sediment and circa 2.5 g for sandy sediment) was used to determine photosynthetic pigments as described above. Organic matter was measured by loss on ignition at 550 ºC for 4 h (Heiri et al., 2001). Organic carbon (C_{org}) was determined as the difference between total carbon measured in a portion of sediment and inorganic carbon measured on the previously combusted sample. Total nitrogen in the sediment (N_T) was determined in the untreated sample. Samples for C and N were analyzed on an elemental analyzer (LECO CHNS 932) at the Central Services of the University of A Coruña. Bulk dry density for Cadiz and Puerto Real sediments were 1.53 g cm^{-3} and 0.71 g cm^{-3}, respectively, based on the dry weight of a known volume of sediment.

2.5. Chlorophyll-a and suspended particulate matter using Sentinel-2 imagery

To explore with more detail how the ECE could impact the Chla and TSS concentrations at the water surface, cloud-free Level 1C Sentinel-2 images will be downloaded from the Copernicus Open Access, Hub websites (https://scihub.copernicus.eu) for the 20th June (before of storm event), the 25th June (during) and the 30th June (after) 2021. Sentinel-2 bands at different resolutions (10-20-60 m) were resampled (bilinear resampling method) to a 10 m spatial resolution. The atmospheric correction processor Case 2 Regional Coast Colour (C2RCC) was applied using the Sentinel Application Platform (SNAP; https://step.esa.int/main/download/snap-download/), to map Chla and TSS concentrations, and Z90 (i.e., the depth at which 90% of the irradiance is attenuated) (Brockmann et al., 2016; Soriano-González et al., 2022). We selected the C2RCC, based on neural network, over other processors for two reasons. First, this processor was developed for optically complex waters in coastal environments such as those in the present study, where an increase of Chla and TSS concentrations was expected as consequence of the ECE. Second, the C2RCC

processors provide the Z90 product which can be used as a proxy of the light attenuation coefficient (K_d, K_d =1/Z90, Morel et al., 2007; Saulquin et al., 2013), thus permitting to discuss whereas the decrease of light attenuation in water column during windstorms might have an effect on net community primary production.

2.6. Statistical analysis

The effects of date, depth and location in nutrients (water column and porewater) and fluxes at the sediment-water interface were tested by ANOVA. Statistical analyses were performed using R software (version 4.3.3) using the car package. When data did not fulfil ANOVA requirements, differences were determined using the Kruskal-Wallis test (package stats). Statistical clear differences were accepted at the $p<0.05$ level. All the results were expressed as mean ± SE unless stated otherwise. Biogeochemical variables (excluding meteorological ones) were normalized to eliminate differences in scales. Resemblance between sites and sampling dates based on the environmental variables was then estimated calculating the Euclidean distance. Non-metric multidimensional scaling analysis (nMDS) was used to visualize the ordination of the samplings on the n-dimensional space. The Pearson correlations of the variables with the first two axis was then projected on the 2D plot.

3. Results

3.1. Meteorological conditions during the studied windstorm

Daily average temperature during the windstorm event (WSE) ranged between 20.1 ± 2.1 ºC and 26.3 ± 2.1 ºC. During the days previous to the studied WSE, the daily average wind speed ranged from 2.5 to 10.4 m s^{-1}, with the mean daily wind speed remaining below 5 m s^{-1}. The daily average direction shifted from 291.67º (west-northwest, WNW) to 94.96 (E) and back again to WNW winds (Fig. 2a, b). During the WSE, the mean wind speed increased from below 5 m s^{-1} to about 10 m s^{-1} with wind gusts up to 23 m s^{-1}. The WSE studied in this work could be described as moderate in intensity, as it resulted in a 57% increase in average wind speed, a 23% increase in maximum temperature and a 33% increase in maximum wind gusts compared to the average data observed in 2021 (Fig. S1).

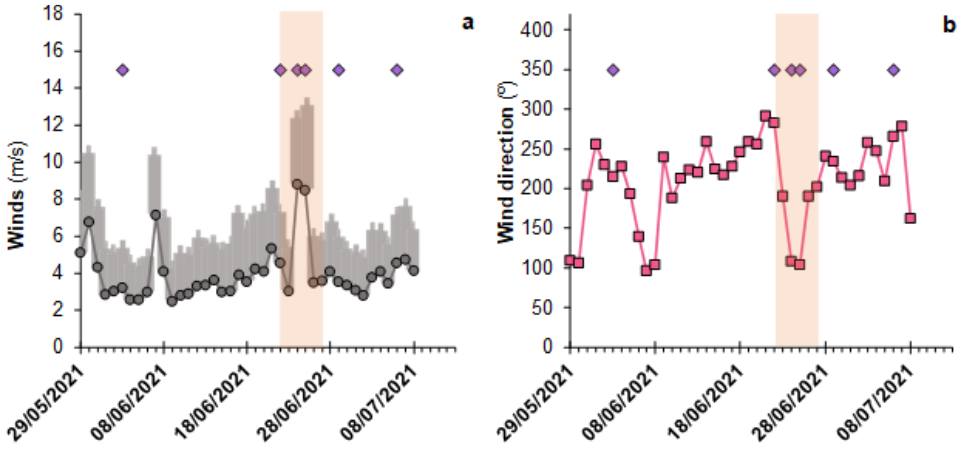


Fig. 2. Changes in winds velocities (a) and wind direction (b) throughout the experiment. Purple diamonds represent the days in which samples were taken. Data are daily means ± SE (n=24). Orange shaded area represents the duration of the windstorm.

3.2. *In situ* total suspended solids and chlorophyll-a in the water column

TSS in the water column during the standard wind conditions measured before the WSE was 13.24 ± 0.60 and 28.67 ± 1.22 g m^{-3} in Cadiz and Puerto Real respectively. TSS were significantly higher in the muddy sediment area of Puerto

Real compared with the sandy sediment of Cadiz sampling site at standard wind conditions. During the windstorm, TSS increased to values higher than 124 g m^{-3} in both sites (Fig. 3a).

Chla concentrations in the water column were higher in Puerto Real than in Cadiz in standard wind conditions (2.71 ± 0.99 mg m^{-3} in Puerto Real, versus 1.64 ± 2.19 mg m^{-3} in Cadiz). During the WSE, Chla increased in both places, up to 6.69 ± 1.10 mg m^{-3} and 11.53± 2.88 mg m^{-3} in Cadiz and Puerto Real respectively, decreasing one week later to values similar to those measured before the WSE in both sites (Fig. 3b). Chla and TSS in the water column were strongly correlated between themselves and with wind speed. However, these correlations were different for Cadiz and Puerto Real suggesting spatial heterogeneity between both sampling sites (Fig. 4).

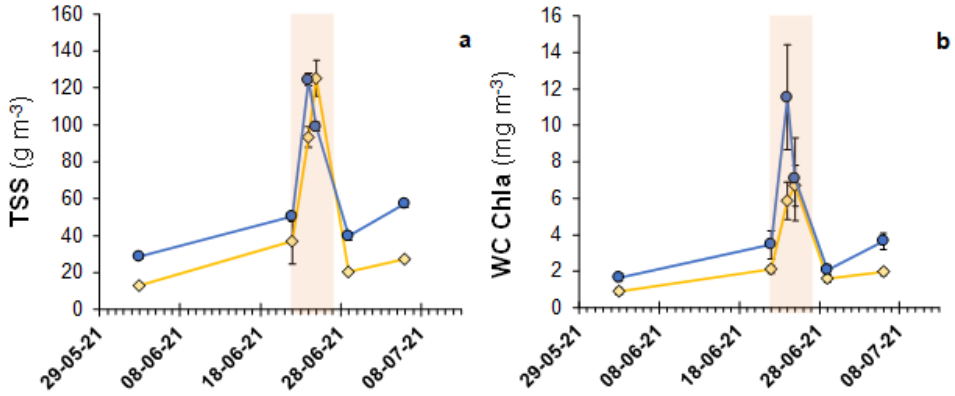


Fig. 3. (a) Total suspended solids (TSS) and (b) chlorophyll (Chla) concentrations in the water column. Blue dots and lines represent Puerto Real (muddy sediment) and yellow rhombs and lines represent Cadiz (sandy sediment). Data are means ± SE (n=5). Orange shaded area represents the duration of the windstorm.

3.3. Remote sensing of chlorophyll and suspended particulate matter

Chla concentrations in the water column, estimated from satellite images, before, during, and after the WSE, were in general lower in Cadiz, located in the western inner bay, than in Puerto Real, in northeastern section of the bay (Fig. 5a-c). Satellite images clearly show a general increase in water column Chla in the entire inner bay

during the WSE, with a considerable spatial heterogeneity, with highest values in the north to east section. The spatial distribution of TSS followed a pattern similar to that of Chla before, during, and after the WSE, reaching up to 30 g m^{-3} in the north -east sections (Fig. 5d-f).

Z90, an indicator of light attenuation, decreased from 1.8±0.4 (K_d=0.55 m^{-1}) to 0.6±0.1 m (K_d=1.66 m^{-1}) in Cadiz and from 1.1±0.2 (K_d=0.9 m^{-1}) to 0.5±0.02 m (K_d=2 m^{-1}) in Puerto Real during the WSE, which amount to a K_d increase of 3 and 2.2 times for Cadiz and Puerto Real, respectively (Fig. 5g-i).

3.4 Chlorophyll-a, organic carbon and total nitrogen in the sediment

Chla concentration in the sediment was initially higher in Puerto Real than in Cadiz (37.41 ± 0.58 and 24.27 ± 2.87 mg Chla m^{-2}, respectively) (Fig. 6a). Chla decreased during the WSE in Puerto Real and increased slightly in Cadiz. After the WSE, Chla levels in the sediment

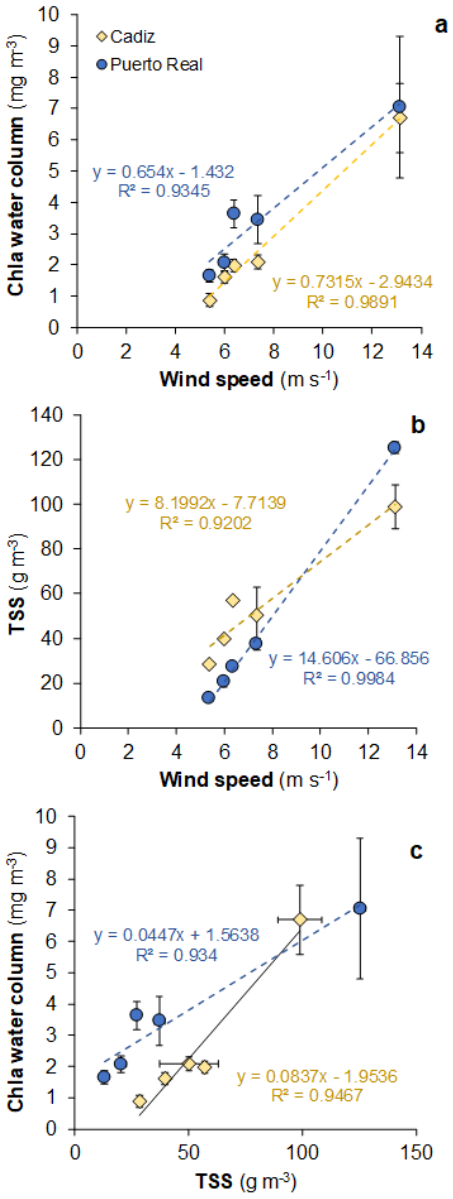


Fig. 4. Relationship between mean wind speed and water column (**a**) chlorophyll and (**b**) total suspended solids (TSS) concentrations. (**c**) Relationship between TSS and Chla at the two sampling location of Cadiz and Puerto Real. Data are means ± SE (n=5).

further decreased for Puerto Real while returning to pre-WSE level in Cadiz.

Sediment C_{org} content was about 4.5 times higher in Puerto Real than in Cadiz (**Fig. 6b**), with average values of 324.5 ± 21.6 and 73.3±14.7 g C m^{-2}, respectively. During the WSE, C_{org} decreased in Puerto Real and increased slightly in Cadiz. After the WSE, in Puerto Real, C_{org} returned to previous levels, whereas in Cadiz it slightly decreased further. Total Nitrogen (N_T) content in Puerto Real was 3 times higher than in Cadiz (27.7±2.4 vs 9.9±2.5 g N_T m^{-2}) (**Fig. 6c**). Changes in N_T in response to the WSE followed the same trend than C_{org} with minimal deviations. The Corg: NT ratio (C:N) was higher in Puerto Real than in Cadiz, (13.4 ± 0.7 vs 9.81 ± 2.1). The WSE did not affect significantly C:N ratio in Puerto Real while it seemed to induce a very high increase in Cadiz. The minimum C:N value was found right before de WSE and the maximum was found after the WSE.

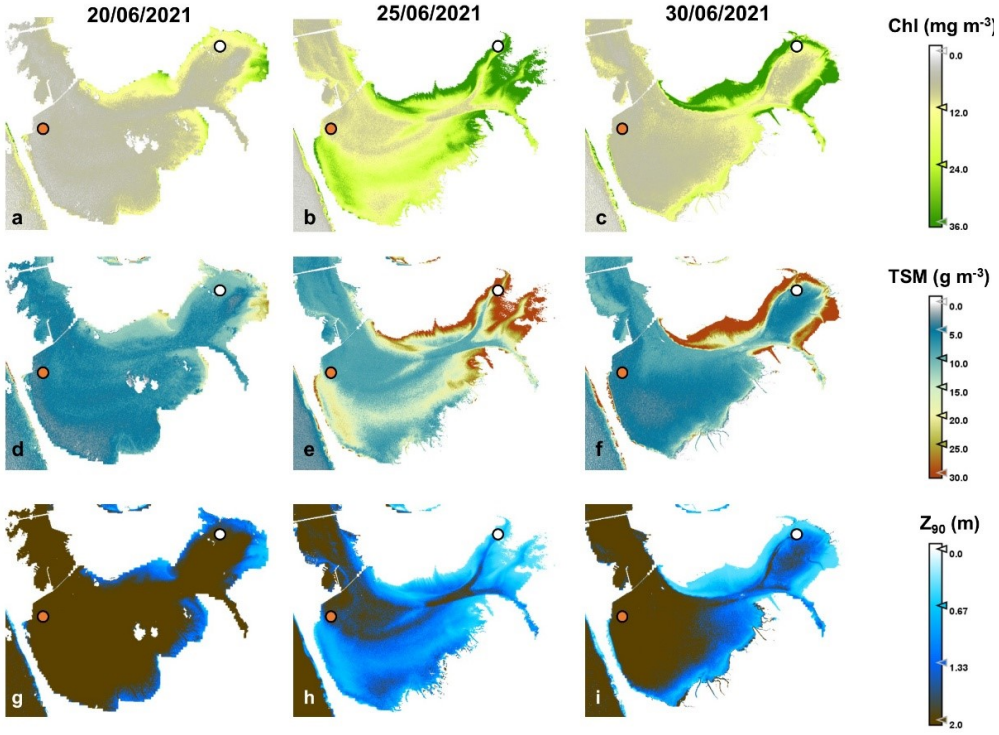


Fig. 5. (**a-c**) Chlorophyll concentration (Chl, mg m^{-3}), (**d-f**) suspended particulate matter (SPM, g m^{-3}) and (**g-i**) the depth of the water column from which 90% of the water-leaving irradiance (Z90, m) in inner Cadiz Bay for the 20th of June (before of windstorm event), the 25th of June (during) and the 30th of June (after) of 2021 estimated from Sentinel-2 imagery using C2RCC processor. White and orange dots represent the sampling sites in Puerto Real and Cadiz, respectively.

3. 5. Oxygen profiles at the sediment surface and net production and respiration rates

The oxygen distribution in the sediment-water interface was different in Cadiz and Puerto Real (Fig. 7). In Puerto Real, a small peak at about 0.3 - 0.4 mm depth was recorded in light, whereas a more pronounced peak was observed in Cadiz. The O_2 penetration depth (z_{ox}) was roughly two times higher in Cadiz than in Puerto Real both in light and in darkness (Fig. S2). During the WSE, O_2 concentration within the sediment decreased in Cadiz, whereas in Puerto Real both O_2 concentration and z_{ox} were higher.

NCP and R_{dark} followed the same pattern in response to the WSE in each site (Fig. 8). However, fluxes increased in Puerto Real and decreased in Cadiz, showing differences with time and site (2-way ANOVA, p-value<0.05). NCP was 3-fold higher in Cadiz than in Puerto Real, showing maximum values of 4.9 ± 0.5 mmol m^{-2} h^{-1} in Cadiz and 1.6 ± 0.3 mmol m^{-2} h^{-1} in Puerto Real. When normalised by the sediment Chla content, the difference increased to 7-fold (74.2 and 9.7 µmol O_2 mg $Chla^{-1}$ h^{-1} for Cadiz and Puerto Real, respectively). R_{dark} showed the same patterns than NCP in both sites and presented a similar range, (0.54 - 1.17 mmol O_2 m^{-2} h^{-1} in Cadiz and 0.64 - 0.95mmol O_2 m^{-2} h^{-1} in Puerto Real (Fig. 8b).

3.6. Nutrient concentrations in the water column and sediment

Ammonium concentration in the water column before the WSE showed a maximum value of 2.5 µM, with higher values in Puerto Real (Fig. 9a). During the WSE, it increased initially in Cadiz, up to 5.2 ± 1.9 µM NH_4^+, but decreased in Puerto Real to 0.6 ± 0.3 µM NH_4^+ (Kruskal-wallis, p-valor <0.05). After the WSE, NH_4^+ increased in both sampling sites, reaching values higher than those pre-WSE in Cadiz.

Nitrate concentrations showed a similar pattern to that of NH_4^+. Concentrations before, during, and after the WSE, were higher in Cadiz than in Puerto Real, ranging between 2.1 ± 0.1 µM and 4.0 ± 0.1 µM (Cadiz) and from 1.5 ± 0.6 µM to 2.5 ± 0.1 µM (Puerto Real). During the WSE, NO_3^- decrease in both places although the differences with the initial values were only clearly different in Cadiz (1-way ANOVA, Site as factor, p-value<0.05; Tukey HSD). After the WSE, NO_3^- concentration did not recover to previous values. Water column NO_2^- was very low in both sites, ranging from 0.17 to 0.40 µM (**Fig. 9c**). It increased initially during the WSE in both sites and maintained values higher than pre-WSE, but differences were not statistically clear (Kruskal-Wallis, p-value >0.05).

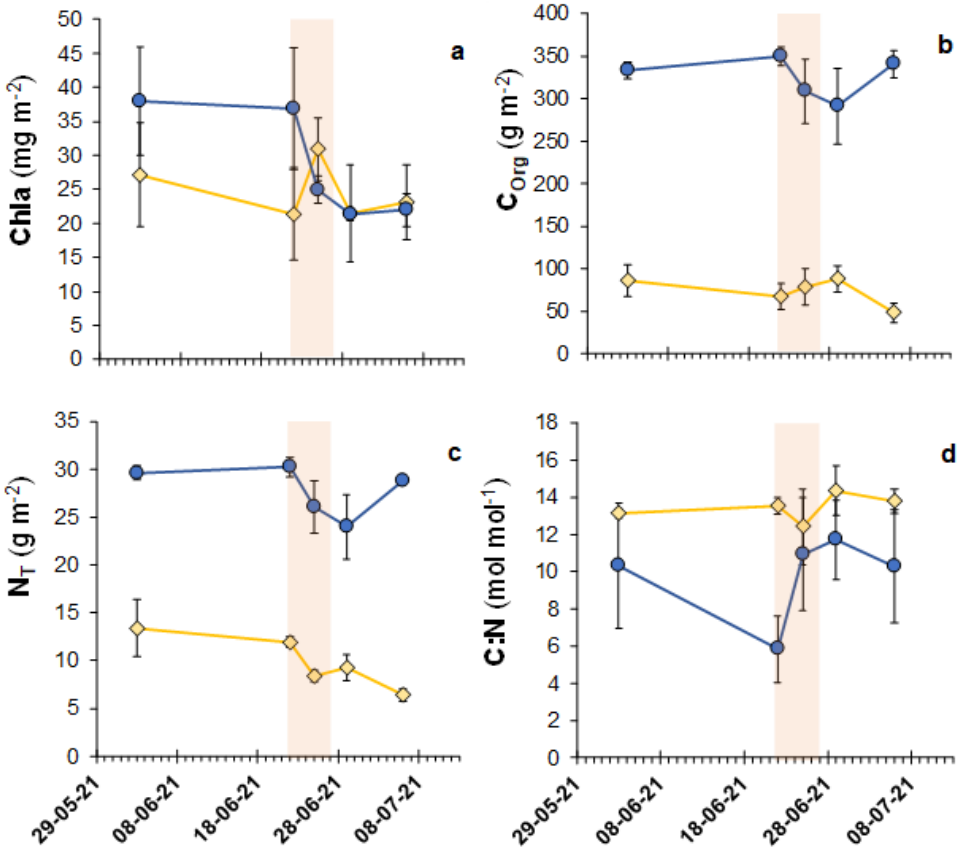


Fig. 6. Changes in chlorophyll-a (**a**), organic carbon (C_{Org}) (**b**), total nitrogen (N_T) (**c**) and carbon:nitrogen ratio (**d**) content in the upper layer of the sediment. Blue dots and lines represent Puerto Real and yellow rhombs and lines represent Cadiz values. Data are means ± SE (n=5). Orange shaded area represents the duration of the wind-storm.

Phosphate (PO_4^{3-}) concentration in the water column was generally low (< 0.5 µM). During pre-WSE, concentrations were around 0.1 µM. During the WSE, PO_4^{3-} concentrations increased transitorily up to 0.16 and 0.38 µM in Puerto Real and Cadiz, respectively, decreasing quickly to the pre-WSE values afterwards (**Fig. 9d**). Silicate (SiO_4^{4-}) concentration in the water column showed roughly similar patterns to the rest of the nutrients increasing from an average of around 5 µM pre-WSE up to 4 times in Cádiz (to (7.1 ± 1.1 µM and 20.2 ± 0.5 µM, in Puerto Real and Cadiz, respectively). It is interesting to note that SiO_4^{4-} is the only nutrient that did not increase immediately after the start of the WSE. SiO_4^{4-} decreased post WSE to values similar to the pre-WSE ones (**Fig. 9e**).

Porewater NH_4^+ concentrations increased significantly with depth within the sediment from about 2-10 µM at the sediment surface up to 110-130 µM at 5.5 cm depth (**Fig. S3**) and were affected also by site and time (3-way ANOVA, site, time and depth as factors, p- value <0.05). Porewater NH_4^+ concentrations were generally higher in the muddy sediment of Puerto Real compared to the sandy sediment of Cadiz before, during and after the WSE. NH_4^+ concentrations in the upper sediment layer were lowest during the WSE in both sampling sites (2.4 ± 0.7 µM and 10.4 ± 3.0 µM in Cadiz and Puerto Real, respectively). The concave shape of the profile in the upper layer indicates increased mixing in the upper sediment layer. After the WSE, NH_4^+ recovered to values similar to the initial ones in both sampling sites. Porewater PO_4^{3-} concentration was similar in Cadiz and Puerto Real, ranging from 0.5 to 3 µM, with no clear pattern with depth or due to the WSE (**Fig. S3**).

3.7 Multivariate analysis

nMDS analysis of the biogeochemical variability, based on the sediment and water column environmental variables studied, clearly separated the two sites, mainly along the first axis (**Fig. 10**). Axis 1 of the nMDS ordination plot correlated strongly (>|0.7|) with sediment organic matter, sediment NH_4^+ and water column SiO_4^{4-} and PO_4^{3-}, whereas axis 2 correlated most notably (>|0.6|) with TSS, Chla and water column ammonium. The trajectory of changes clearly shows that for both sites the WSE had a significant effect on the pre-WSE state of the system, whilst after the WSE, the system returned to the initial conditions, more closely for Cadiz.

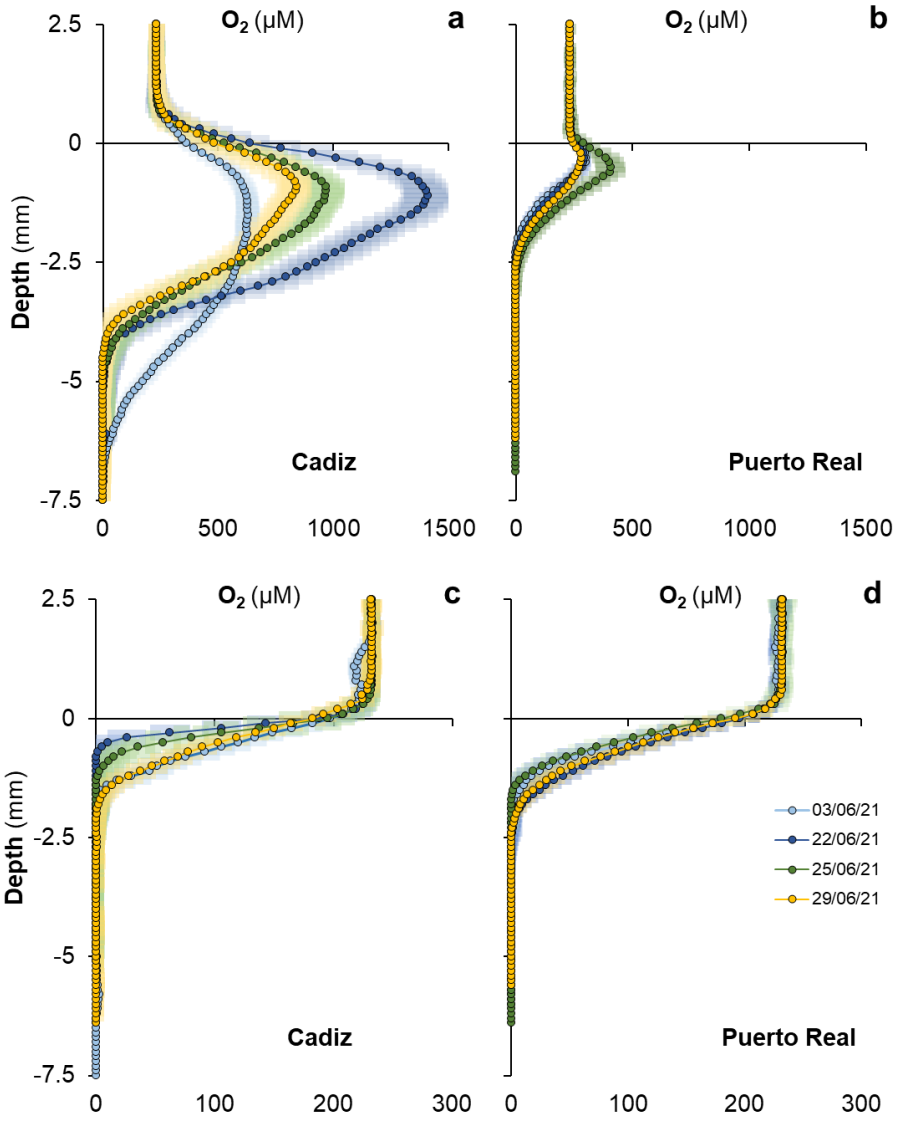


Fig. 7. Changes in the mean ± SD vertical oxygen concentration profiles in light (**a, b**) and dark (**c, d**) conditions across the sediment-water interface, before (June 3th and June 22th), during (June 25th) and after (June 29th) the WSE for Cadiz (a, **c**) and for Puerto Real (**b, d**). Standard deviations are plotted as bars for each average profile.

4. Discussion

4.1. Sediment and MPB resuspension induced by a windstorm event

The inner Cadiz Bay is a shallow coastal system, where wind speed strongly correlates with water column turbidity (Garcia-San Miguel, 2010) due to the resuspension of the upper sediment layer. This resuspension transfers inorganic and organic sediment particles, MPB cells, and releases porewater nutrients from the anoxic sediment to the water column (Fig. 3-6, Fig. 9) as indicated by the significant linear correlation between water column TSS and Chla concentration with wind velocity (Fig. 4). These positive correlations depended on the sampling site but remained always statistically clear. The remote sensing data indicate the considerable spatial heterogeneity in the distribution of TSS and Chla within the inner bay, with concentrations being higher in Puerto Real compared to Cadiz (Fig. 5). Local differences in wind speed and the degree of exposure and as a result of the generated turbulence due to the local geomorphology have been shown to affect the correlations between Chla, TSS, and wind speed elsewhere (de Jorge & van Beusekom, 1995; Redzuan & Underwood, 2021). Differences in sediment grain size also contribute to local differences in water column concentrations; sediment in Puerto Real is muddy and thus potentially more easily resuspended. In fact, previous experimental work in aerodimeter flumes showed that grain size was the main variable affecting MPB resuspension (Ubertini et al., 2015).

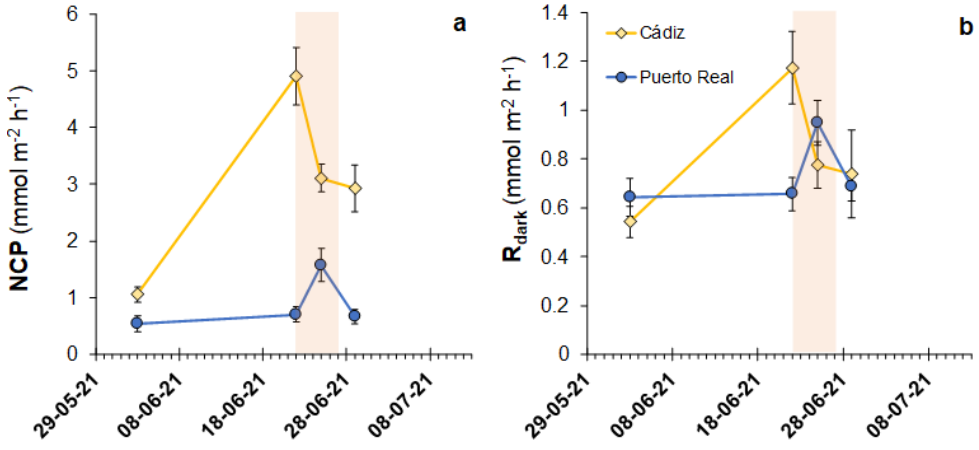


Fig. 8. Changes in the interface water column-sediment oxygen fluxes throughout the experiment showed as net community production (NCP) (**a**) and darkness respiration (R_{dark}) (**b**). Yellow rhombs and lines represent Cadiz and blue dots and lines represent Puerto Real values. Data are means ± SE (n=5). Orange shaded area represents the duration of the windstorm.

The high correlations between water column Chla, TSS, and wind speed observed in the Bay suggest that Chla in the water column originated from resuspended MPB biomass, as previously shown in other shallow aquatic environments(de Jorge & van Beusekom, 1995). Although not studied here, tidal currents might play an additional role affecting MPB resuspension in this shallow environment, like the adjacent Guadalquivir estuary, where tidal currents resuspend MPB and largely control water column Chla (Díez-Minguito & De Swart, 2020). Regardless of the driving force, resuspended MPB might be a very important food source for suspension-feeders, with phytoplankton, usually in lower abundance, playing a minor role (Ubertini et al., 2015).

4.2 Influence of the WSE in the sediment chlorophyll, organic carbon and nitrogen

The resuspension of TSS and Chla during the WSE had clear effects on the sediment variables. The sediment surface, during and after the WSE, was likely the result of the exposure of deeper sediment layers, initially anoxic, during resuspension and the sedimentation of resuspended solids of different origins and locations, which have been mixed and transported horizontally during the WSE. These processes alter the biogeochemical characteristics of the sediment like the Chla, C_{org} and N_T contents (Fig. 6), likely remineralization rates, and contribute to the cycling of OM across habitats. Previous work using stable isotopes in the area indicated that the characteristics of the organic matter accumulated in the sediment along a tidal gradient were similar, resulting from a well-mixed combination of material from subtidal, intertidal and high-marsh plant communities (Jiménez-Arias et al., 2020). Therefore, the strong hydrodynamics conditions during a WSE would favor this ecological and biogeochemical connectivity within the inner bay and must be taken into account when analyzing the changes in the sediment surface and its relation with the water column.

Chla concentration in the sediment was higher in the muddy sediment of Puerto Real (~ 37 mg Chla m^{-2}) than in the sandy sediment of Cadiz (~ 25 mg Chla m^{-2}) as it is frequently observed in other tidal flats when comparing areas of different grain size distribution (Cahoon et al., 2012; Middelburg et al., 2000). These Chla values

are within the range reported previously in the inner Cadiz Bay and the tidal banks of the Guadalquivir estuary (Garcia-Robledo et al., 2016; Haro et al., 2020; Papaspyrou et al., 2013; Perez-Rodriguez et al., 2024), as well as other temperate tidal flats (Cahoon et al., 2012; Kwon et al., 2020; Middelburg et al., 2000; Redzuan & Underwood, 2021). The WSE induced erosion of the upper sediment layer, where most of the MPB Chla is concentrated (Garcia-Robledo et al., 2010, 2016). In Puerto Real, it clearly reduced the Chla content at the sediment surface to almost half of its initial value during and after the WSE. In contrast, we observed a slight increase in the Chla in Cadiz. This could be attributed to the net transport and sedimentation of SPM and Chla to the western area of the bay as will be discussed later.

The net rate of resuspension and sedimentation can be roughly estimated from the difference in sediment Chla content from the day before and during the WSE (June 23^{th} - 25^{th}), which amounted to a loss of -5.9 mg Chla m^{-2} d^{-1} for Puerto Real and a net gain of +4.75 mg Chla m^{-2} d^{-1} for Cadiz. The higher net resuspension/sedimentation rate in Puerto Real compared to Cadiz agrees with the higher water column Chla observed at this site (**Fig. 3, 5**), and was likely due to the smaller size of sediment particles in this area. The increase in the water column Chla concentration at both sites can also give an indication of the degree of resuspension, 4.05 and 1.88 mg Chla m^{-3} d^{-1} for Puerto Real and Cadiz, respectively. These values are in the same order of magnitude than those calculated from changes in the sediment (assuming a standard 1 m depth water column) and suggest a net transfer from the sediment to the water column even in the Cadiz area (**Fig. 3**). This discrepancy suggests a redistribution of resuspended Chla and TSS most likely due to local differences in the geomorphology resulting in mesoscale differences in water turbulence during the WSE. This mesoscale heterogeneity in the water column TSS and Chla concentrations is evident in the satellite images studied (**Fig. 5**).

Following the WSE, the concentration of TSM decreased very quickly (**Fig. 3, 5**), leading probably to a burial of the MPB community remaining at the sediment surface. However, in muddy sediments, compared to sandy ones, epipelic diatom, which are able to migrate vertically, dominate (Cartaxana et al., 2011; Haro et al., 2019; Ribeiro et al., 2013). Therefore, this capacity should in principle foster the recolonization of the sediment surface. However, our results do not show any clear

recovery or increase of MPB biomass, estimated by Chla, one week after the WSE (Fig. 6).

Contents of C_{org} and N_T and C:N ratio measured before, during and after the WSE were in the same range of those measured in previous studies in inner Bay of Cadiz (Haro et al., 2020; Papaspyrou et al., 2013). Changes in sediment C_{org} and N_T followed a general trend rather similar to that of Chla, particularly in Puerto Real, which seems to suggest a strong coupling between these variables (Fig. 6, Fig. S4). The higher sediment C:N ratio in Puerto Real is consistent with the generally higher content of refractory C_{org} in muddy sediments compared with sandy ones (Fig. 6d). Overall, the C:N ratio seemed to increase slightly after the WSE, probably due to the sedimentation of TSS.

4.3. Effects of WSE on net metabolism at the sediment-water interface

The benthic microbial community's response to the WSE was investigated through a detailed analysis of changes of O_2 dynamics at the sediment-water interface. The presence of a subsurface O_2 peak within the sediment in light indicated clearly the photosynthetic activity of the MPB, which was higher Cadiz, as indicated by its higher height, width and O_2 penetration depth (Fig 7. Fig. 8, Fig. S2). This difference is likely due to the higher sand content and as a result a higher permeability and lower organic matter content (Billerbeck et al., 2006). Light availability, grain size, active MPB biomass, organic matter content, and hydrodynamic conditions are key factors controlling O_2 dynamics (Billerbeck et al., 2006; Fenchel & Glud, 2000; Glud, 2008; Meysman et al., 2010) and can be altered during WSE in different ways, affecting in turn the community net metabolism at the sediment surface.

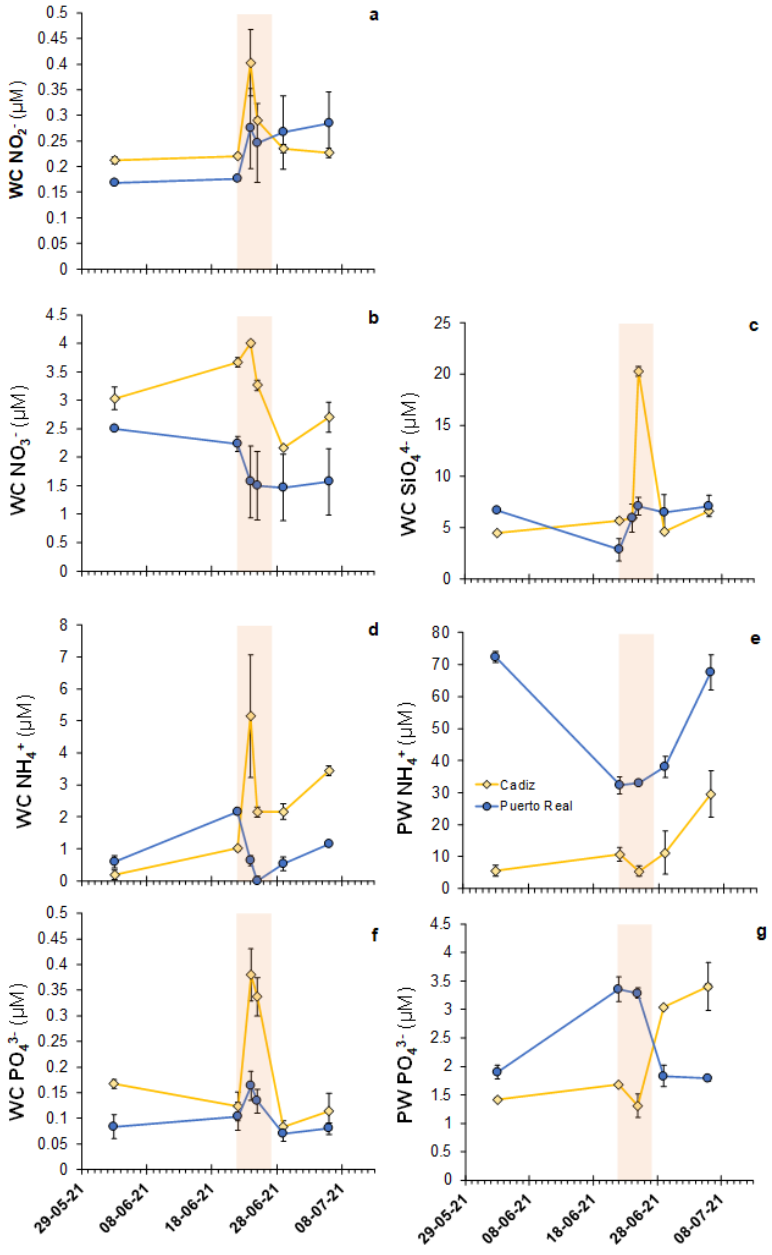


Fig. 9. Changes in the nutrient content in Puerto Real and Cadiz in the water column: NO_3^- (**a**), NO_2^- (**b**), SiO_4^{4-} (**c**), NH_4^+ (**d**) and PO_4^{3-} (**f**) in pore water of upper sediment layer (2cm): NH_4^+ (**e**) and PO_4^{3-} (g). Blue dots and lines represent Puerto Real and yellow rhombs and lines represent Cadiz values. Data are means ± SE (n=5). Orange shaded area represents the duration of the wind-storm.

Net community production and dark respiration rates measured before, during, and after the WSE were similar to previous observations in different tidal flats of the inner Cadiz Bay and in the Guadalquivir Estuary (Haro et al., 2020; Perez-Rodriguez et al., 2024) and elsewhere in Europe, America and Asia (Kwon et al., 2020; MacIntyre et al., 1996; Méléder, 2020; Underwood & Kromkamp, 1999). Between sites, rates were higher in Cadiz than in Puerto Real (**Fig 8**). The ratio NCP:R_{dark}, a proxy of net metabolism, was always higher in Cadiz (1.9- 4.2) compared to Puerto Real (0.8 – 1.7) and higher than 1. This suggests the existence of a highly net autotrophic microbial community in the former. Normalizing primary production rate by Chla also supported a higher productivity of MPB in Cadiz compared to Puerto Real, 53.23 ± 20.32 and 5.35 ± 2.57 µmol O_2 mg $Chla^{-1}$ h^{-1}, respectively. Sandy sediments typically support higher primary production per unit of Chla and a higher turnover rate (Huettel et al., 2014; MacIntyre et al., 1996; Middelburg et al., 2000). In addition, differences in the geomorphological-hydrodynamic settings between sampling sites, affect net resuspension and sedimentation rates and ultimately benthic metabolism, which can explain the different response of the MPB community to the WSE in Puerto Real and Cadiz. It is interesting to note that NCP and R_{dark} followed parallel trends within a sampling site throughout the study, but were clearly different among sites (a decrease in Cadiz and an increase in Puerto Real) (**Fig. 8**).

NCP and R_{dark} covaried tightly in Cadiz and Puerto Real ($r^2 > 0.94$), showing site-specific relations (**Fig. S4**). They also correlated positively with temperature and wind speed and with several water column properties, that were directly affected by the WSE, like TSS and Chla concentrations (**Fig.4, Fig. S4**). This is counterintuitive as higher values of TSS and Chla will increase turbidity and decrease the light availability and photic depth, affecting *in situ* MPB photosynthetic rates negatively. However, on the one hand, in this study NCP and R_{dark} rates were measured in collected cores in laboratory conditions with no light limitations. In addition, despite the turbulence induced, this was not sufficient to maintain the sediment in resuspension as probably was during in situ conditions. Therefore, metabolic rates must be considered potential, particularly for NCP. On the other hand, the WSE may have had a real positive effect on metabolic rates. Higher water turbulence and the shallowness of the inner bay increased the exchange of dissolved and particulate matter between the sediment and water column on the vertical axis, in addition to a considerable horizontal mixing within the inner bay basin. Therefore,

the fertilizing effect of higher availability of inorganic and organic nutrients, along with higher exchange rates, seemed to favor the net metabolic activity of MPB. *In situ*, MPB primary production will be limited by strong turbidity during the WSE, but since TSS settled down quickly after the WSE, MPB primary production and growth will recover not long after, being able to fully utilize the nutrients released in previous phases of strong winds.

4.4. Exchange of nutrients between the sediment and the water column

The range of concentrations for the different dissolved inorganic nutrients (NH_4^+, NO_3^-, NO_2^-, PO_4^{3-} and SiO_4^{4-}) observed during the study, both in the water column and sediment, were within the typical spatial and seasonal variability found in the inner Cadiz Bay (Corzo et al., 2009; Garcia-Robledo et al., 2010, 2016; Haro et al., 2020). The effect of WSE was evident (Fig 9) resulting in a clear increase in all nutrients. PO_4^{3-} and SiO_4^{4-} showed a net release to the water column in both Cadiz and Puerto Real because of the WSE, although of different magnitudes (Table I). For NH_4^+, assuming a 1 m depth water column, we recorded an increase in Cadiz (2.07 ± 0.95 mmol m^{-2} d^{-1}) suggesting a net resuspension and a decrease in Puerto Real (-0.77±0.09 mmol m^{-2} d^{-1}) suggesting an increase in the sediment and therefore net sedimentation. Similarly, using the sediment porewater data, WSE induced a loss of NH_4^+ from the sediment in Cadiz (0.035±0.008 mmol m^{-2} d^{-1}), whereas in Puerto Real, on average, changes were very small and more variable (-0.005 ± 0.014 mmol m^{-2} d^{-1}).

The changes detected in the water column for NH_4^+ and PO_4^{3-}compared to those measured in the sediment are more than two orders of magnitude lower (Table I). This difference may be the sum of various factors. The resuspension of the upper sediment layer favors the release of dissolved and particulate nutrients to the water column (Christiansen et al., 1997; Couceiro et al., 2013; Wengrove, 2015), where they can support phytoplankton primary production (Cowan et al., 1996; Warnken et al., 2000). The vertical flux of nutrients across the sediment water interphase is largely dependent on hydrodynamic conditions affecting the sediment boundary layer, the concentration gradients between the sediment and the water column and on the sediment erosion threshold (Couceiro et al., 2013; Kleeberg & Herzog, 2014; Lorke et al., 2003; Van Duren & Middelburg, 2001). When shear stress exceeds the erosion threshold, the resuspension of sediment and porewater release become the

dominant mechanism of nutrient flux (Kalnejais et al., 2010; Kleeberg & Herzog, 2014). This was probably the case here as indicated by the increase in TSS and Chla during the WSE (Fig.3). Horizontal transport within the inner bay, particularly the highly developed network of tidal creeks, also likely contribute significantly to the TSS and nutrients concentrations within the inner bay.

The observed differences between the two sites may in part be due also to the different grain size distribution, of sandy sediment in Cadiz and muddy sediment in Puerto Real. Since muddy sediments are dominant in the inner Cadiz Bay, the resuspension and exchange rates measured in Puerto Real are likely more representative of the system. In addition, the exchange rates, calculated from changes in the well mixed water column, likely integrates the higher spatial heterogeneity of benthic communities and represents better the effect on the system than rates calculated from changes in the sediment. Nonetheless, since there is no information on the spatial distribution of inorganic nutrients in the inner bay water column, we averaged rates in Cadiz and Puerto Real to provide rough estimations for the whole system (Table I). These calculations indicated an WSE induced increase in inner bay water column of about 0.65 ± 1.42 mmol NH_4^+ m^{-3} d^{-1}, 0.84 ± 0.71 mmol SiO_4^{4-} m^{-3} d^{-1}, 0.08 ± 0.05 mmol PO_4^{3-} m^{-3} d^{-1}, 0.07 ± 0.02 mmol NO_2^- m^{-3} d^{-1} and a decrease of 0.08 ± 0.25 mmol NO_3^- m^{-3} d^{-1}. Primary producers can rapidly take advantage of this flux of nutrients to the water column from the sediment. However, the N:P, N:Si and Si:P stoichiometric ratio of these net enrichments (7.7, 0.7 and 11.1 respectively) suggest that growth of phytoplankton and MPB, would be limited by N and Si (Brzezinski, 1985; Redfield, 1958). The general increase of water column dissolved and particulate nutrients likely affect phytoplankton, MPB and other major primary producers of the inner bay as macroalgae and seagrasses (Haro et al., 2020, 2022), although at the same turbidity increases light attenuation, which is likely to limit primary production during WSE. Therefore, more field work is needed to evaluate the effect of WSE on the different communities of primary producers during WSE and afterward.

4.5. WSE-induced shift in ecosystem state and outwelling to coastal waters

Transient shifts of biological communities and ecosystems in response to perturbations, such as a WSE, have been largely studied in terrestrial ecosystems but less in coastal wetland environments (Folke et al., 2004; Sardanyés, 2024). An analysis of the evolution of the inner bay's ecosystem in a more integrative way using a multivariate approach clearly highlighted not only the differences between Cadiz and Puerto Real, but also the shift in the system's state in the n-dimensional space and a clear and very rapid return to the initial position (Fig. 10). This highlights the strong transient impact that WSE have on shallow coastal wetlands. More frequent and intense WSE, due to climate change, might have a more persistent effect on the microbial community and biogeochemistry of the inner bay as observed in other systems under high intensity perturbations (Cordero, 2023).

Table I. Net resuspension or release rates for calculated from changes in the water column between 22 and 24 of June and from changes in the sediment between 22 and 25 of June. Positive values indicate transfer from the sediment to the water column. Standard errors (SE) were calculated based on error propagation theory with the expression $SE_R=((SE_i^2-SE_f^2)^{0.5})/t$, where SE_R is the standard error of calculated rate, SE_i is the standard error of initial measurement, previous to WSE, SE_f is the standard error during the WSE and t is the time interval in days between i and f. Sediment data are expressed by surface units integrating the upper 2 cm of measured profiles.

WATER	Cadiz	SE	Puerto Real	SE	Average	SE
TSS, g m^{-3} d^{-1}	27.99	6.95	37.12	2.12	32.55	4.56
Chl a, mg m^{-3} d^{-1}	1.89	0.52	4.04	1.49	2.96	1.08
NH_4^+, mmol m^{-3} d^{-1}	2.07	0.95	-0.77	0.09	0.65	1.42
NO_2^-, mmol m^{-3} d^{-1}	0.09	0.03	0.05	0.04	0.07	0.02
NO_3^-, mmol m^{-3} d^{-1}	0.17	0.05	-0.33	0.32	-0.08	0.25
PO_4^{3-}, mmol m^{-3} d^{-1}	0.13	0.03	0.03	0.02	0.08	0.05
SiO_4^{4-}, mmol m^{-3} d^{-1}	0.13	0.11	1.55	0.87	0.84	0.71
SEDIMENT						
Chl a, mg m^{-2} d^{-1}	27.99	6.95	37.12	2.12	32.55	4.56
C_{org} , g m^{-2} d^{-1}	1.89	0.52	4.04	1.49	2.96	1.08
N_T , g m^{-2} d^{-1}	2.07	0.95	-0.77	0.09	0.65	1.42
NH_4^+, µmol m^{-2} d^{-1}	0.09	0.03	0.05	0.04	0.07	0.02
PO_4^{3-}, µmol m^{-2} d^{-1}	0.17	0.05	-0.33	0.32	-0.08	0.25

Since the inner bay is connected to the outer Cadiz bay, a substantial volume of water is exchanged between both twice t a day due to tides. The volume of water exchanged between the two basins is considerable, up to 55.1 hm^3 for the maximum tidal prism, which represents 36.6 % of its maximum volume (150.5 hm^3). The WSE can increase considerably tidal export with respect to standard weather conditions, as it is generally highly dependent on wind speed and direction. During the WSE studied here, $3.59x10^6$ Kg TSS d^{-1}, $3.26x10^2$ Kg Chla d^{-1}, $9.27x10^4$ mol SiO_4^{4-} d^{-1}, $7.94x10^4$ mol (NH_4^+ + NO_2^-) d^{-1} and $8.72x10^3$ mol PO_4^{3-} d^{-1} were exported from the inner bay based on the net resuspension rates determined from the average water column increases (**Table I**). The outwelling rates, between standard wind speed (SW) conditions, occurring before and after the WSE, and those during WSE conditions, increased between 1.1 and 3.6 times for NO_3^- and Chla respectively (**Table II**). It is interesting to note that both approaches to estimate outwelling rates produced similar results. Therefore, the export of water enriched with dissolved nutrients, Chla, and TSS, might represent a considerably source of nutrients to the outer bay and the coastal waters of Gulf of Cadiz, likely affecting coastal primary production.

Table II. Average outwelling rates ± standard error of TSS, Chla and inorganic nutrients calculated for the inner bay from average concentration in the water column during standard wind conditions (SW) (average of pre- and post WSE) and during the windstorm event (WSE). Data were scaled up to whole inner bay taking into account the maximum volume of water exchanged with maximum tidal prism. The increase in the outwelling rate is given by the ratio between the windstorm and the standard conditions (WSE:SW).

WATER	SW	WSE	WSE:SW
TSS, Kg d^{-1}	$3.8 \times 10^6 \pm 0.5 \times 10^6$	$12.2 \times 10^6 \pm 1.6 \times 10^6$	3.2
Chl a, Kg d^{-1}	$2.4 \times 10^2 \pm 0.3 \times 10^2$	$8.7 \times 10^2 \pm 2.4 \times 10^2$	3.6
NH_4^+, mol d^{-1}	$1.5 \times 10^5 \pm 0.4 \times 10^5$	$2.9 \times 10^5 \pm 2.1 \times 10^5$	1.9
NO_2^-, mol d^{-1}	$2.5 \times 10^4 \pm 0.1 \times 10^4$	$3.3 \times 10^4 \pm 0.6 \times 10^4$	1.4
NO_3^-, mol d^{-1}	$2.7 \times 10^5 \pm 0.3 \times 10^5$	$2.8 \times 10^5 \pm 1.2 \times 10^5$	1.1
PO_4^{3-}, mol d^{-1}	$1.1 \times 10^4 \pm 0.1 \times 10^4$	$2.8 \times 10^4 \pm 1.2 \times 10^4$	2.5
SiO_4^{4-}, mol d^{-1}	$6.1 \times 10^5 \pm 0.5 \times 10^5$	$10.8 \times 10^5 \pm 6.7 \times 10^5$	1.8

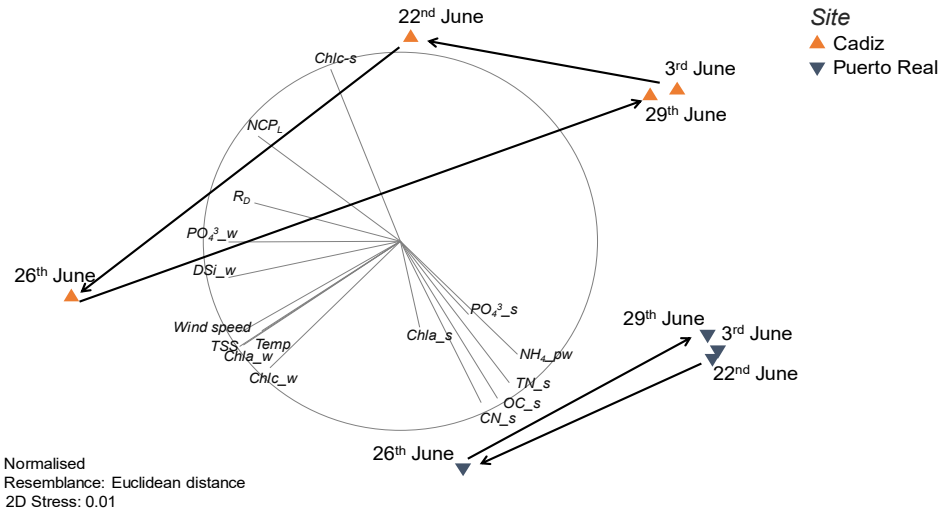


Fig. 10. Multidimensional scaling analysis (n-MDS) based on Euclidean distance between the values of the different climatological (wind speed and T), water column (TSS, Chla, NH_4^+, NO_2^-, NO_3^-, PO_4^{3-}, SiO_4^{4-}) and sediment (Chla, C_{org}, N_T, NH_4^+, PO_4^{3-}, NCP in light and R_{dark}) variables characterizing the Cadiz (yellow rhomb) and Puerto Real (blue triangle) systems in the different sampling dates. Arrows indicate the time evolution of both systems.

5. Conclusions

Our results show that wind velocity had a strong impact on the biogeochemical properties of the water column and intertidal sediments in the shallow inner Cadiz Bay. We observed a transient increase in TSS and Chla in the water column during WSE, correlating with wind speed, supporting the transfer of matter from the sediment due to the resuspension of upper sediment layer and the exposure of the underlying anoxic sediment. Most dissolved inorganic nutrients in the water column, also increased during the WSE. However, their concentration did not correlate clearly with wind speed suggesting that the effect of WSE on nutrient dynamics in the water column is complex. In addition to the direct release, the resuspended particulate and dissolved matter suffers dramatic changes in the redox conditions, which likely stimulate biogeochemical cycling contributing to changes in nutrients concentrations in the water column. Further experimental work is needed to

investigate directly the biogeochemical processing of the resuspended matter in the water column. The considerable spatial heterogeneity in water column Chla and TSS observed from the satellite images also suggest that sediment characteristics, hydrodynamics conditions and the horizontal transport within the basin are important factors determining the effect of WSE in shallow environments, both in the sediment surface and in the water column. The analysis of the whole system response to WSE in the inner Cadiz Bay using n-dimensional techniques clearly showed how WSE represents a perturbation that shift the state of the system transiently from an initial position, but also how this kind of shallow ecosystems return back to the initial state rather quickly. The recovering time likely depends to some degree on the intensity of the perturbation and therefore the effects of more frequent WSE and of different intensities should be monitored, as due to climate change these are expected to increase. Tidal exchange of inorganic and organic matter with the sea likely increases during WSE, affecting biogeochemical and ecological processes within the bay but also the adjacent coastal ecosystems, thus fertilizing local-regional coastal sea and finally fueling coastal primary production and higher trophic levels.

Acknowledgements

This work has been co-financed by the 2014-2020 ERDF Operational Program and by the Department of Economy, Knowledge, Business and University of the Regional Government of Andalusia (Project reference: FEDER-UCA18-107225). This publication is part of the R&D projects CTM2017-82271-R (Microbahia II) & PID2020-112488RB-I00 (Extreme-FUN), & MULTIFLUX funded by MCIN/AEI/10.13039/501100011033.

References

Billerbeck, M., Werner, U., Polerecky, L., Walpersdorf, E., deBeer, D., & Huettel, M. (2006). Surficial and deep pore water circulation governs spatial and temporal scales of nutrient recycling in intertidal sand flat sediment. *Marine Ecology Progress Series*, *326*, 61-76. https://doi.org/10.3354/meps326061

Bohórquez, J., McGenity, T. J., Papaspyrou, S., García-Robledo, E., Corzo, A., & Underwood, G. J. C. (2017). Different types of diatom-derived extracellular polymeric substances drive changes in heterotrophic bacterial communities from intertidal sediments. *Frontiers in Microbiology*, *8*(FEB). https://doi.org/10.3389/fmicb.2017.00245

Bower, C. E., & Holm-Hansen, T. (1980). A Salicylate–Hypochlorite Method for Determining Ammonia in Seawater. *Canadian Journal of Fisheries and Aquatic Sciences*, *37*(5), 794-798. https://doi.org/10.1139/f80-106

Brockmann, C., Doerffer, R., Peters, M., Kerstin, S., Embacher, S., Ruescas, A., Brockmann, C., Doerffer, R., Peters, M., Kerstin, S., Embacher, S., & Ruescas, A. (2016). Evolution of the C2RCC Neural Network for Sentinel 2 and 3 for the Retrieval of Ocean Colour Products in Normal and Extreme Optically Complex Waters. *ESASP*, *740*, 54.

Brzezinski, M. A. (1985). THE Si:C:N RATIO OF MARINE DIATOMS: INTERSPECIFIC VARIABILITY AND THE EFFECT OF SOME ENVIRONMENTAL VARIABLES[1]. *Journal of Phycology*, *21*(3), 347-357. https://doi.org/10.1111/j.0022-3646.1985.00347.x

Cahoon, L. B., Carey, E. S., & Blum, J. E. (2012). Benthic Microalgal Biomass on Ocean Beaches: Effects of Sediment Grain Size and Beach Renourishment. *Journal of Coastal Research*, *283*, 853-859. https://doi.org/10.2112/JCOASTRES-D-10-00178.1

Cartaxana, P., Ruivo, M., Hubas, C., Davidson, I., Serôdio, J., & Jesus, B. (2011). Physiological versus behavioral photoprotection in intertidal epipelic and epipsammic benthic diatom communities. *Journal of Experimental Marine Biology and Ecology*, *405*(1-2), 120-127. https://doi.org/10.1016/j.jembe.2011.05.027

Chen, Z. L., & Lee, S. Y. (2022). Tidal Flats as a Significant Carbon Reservoir in Global Coastal Ecosystems. *Frontiers in Marine Science*, *9*, 900896. https://doi.org/10.3389/fmars.2022.900896

Christiansen, C., Gertz, F., Laima, M. J. C., Lund-Hansen, L. C., Vang, T., & Jürgensen, C. (1997). Nutrient (P, N) dynamics in the Southwestern Kattegat, Scandinavia: Sedimentation and resuspension effects. *Environmental Geology*, *29*(1-2), 66-77. https://doi.org/10.1007/s002540050105

Coelho, H., Vieira, S., & Serôdio, J. (2009). Effects of desiccation on the photosynthetic activity of intertidal microphytobenthos biofilms as studied by optical methods. *Journal of Experimental Marine Biology and Ecology*, *381*(2), 98-104. https://doi.org/10.1016/j.jembe.2009.09.013

Cordero, I. (2023). High intensity perturbations induce an abrupt shift in soil microbial state. *The ISME Journal*.

Corzo, A., Luzon, A., Mayayo, M. J., Van Bergeijk, S. A., Mata, P., & García De Lomas, J. (2005). Carbonate Mineralogy Along a Biogeochemical Gradient in Recent Lacustrine Sediments of Gallocanta Lake (Spain). *Geomicrobiology Journal*, *22*(6), 283-298. https://doi.org/10.1080/01490450500183654

Corzo, A., Van Bergeijk, S., & García-Robledo, E. (2009). Effects of green macroalgal blooms on intertidal sediments: Net metabolism and carbon and nitrogen contents. *Marine Ecology Progress Series*, *380*, 81-93. https://doi.org/10.3354/meps07923

Couceiro, F., Fones, G. R., Thompson, C. E. L., Statham, P. J., Sivyer, D. B., Parker, R., Kelly-Gerreyn, B. A., & Amos, C. L. (2013). Impact of resuspension of cohesive sediments at the Oyster Grounds (North Sea) on nutrient exchange across the sediment–water interface. *Biogeochemistry*, *113*(1-3), 37-52. https://doi.org/10.1007/s10533-012-9710-7

Cowan, J., Pennock, J., & Boynton, W. (1996). Seasonal and interannual patterns of sediment-water nutrient and oxygen fluxes in Mobile Bay, Alabama (USA):regulating factors and ecological significance. *Marine Ecology Progress Series*, *141*, 229-245. https://doi.org/10.3354/meps141229

de Jorge, V. N., & van Beusekom, J. E. E. (1995). Wind- and tide-induced resuspension of sediment and microphytobenthos from tidal flats in the Ems estuary. *Limnology and Oceanography*, *40*(4), 776-778. https://doi.org/10.4319/lo.1995.40.4.0776

Díez-Minguito, M., & De Swart, H. E. (2020). Relationships Between Chlorophyll-a and Suspended Sediment Concentration in a High-Nutrient Load Estuary: An Observational and Idealized Modeling Approach. *Journal of Geophysical Research: Oceans*, *125*(3), e2019JC015188. https://doi.org/10.1029/2019JC015188

Fenchel, T., & Glud, R. N. (2000). Benthic primary production and O_2 -CO_2 dynamics in a shallow-water sediment: Spatial and temporal heterogeneity. *Ophelia*, *53*(2), 159-171. https://doi.org/10.1080/00785236.2000.10409446

Folke, C., Carpenter, S., Walker, B., Scheffer, M., Elmqvist, T., Gunderson, L., & Holling, C. S. (2004). *Regime shifts, resilience, and biodiversity in ecosystem management*.

Frankenbach, S., Ezequiel, J., Plecha, S., Goessling, J. W., Vaz, L., Kühl, M., Dias, J. M., Vaz, N., & Serôdio, J. (2020). Synoptic Spatio-Temporal Variability of the Photosynthetic Productivity of Microphytobenthos and Phytoplankton in a Tidal Estuary. *Frontiers in Marine Science*, *7*, 170. https://doi.org/10.3389/fmars.2020.00170

Garcia-Robledo, E., Bohorquez, J., Corzo, A., Jimenez-Arias, J. L., & Papaspyrou, S. (2016). Dynamics of Inorganic Nutrients in Intertidal Sediments: Porewater, Exchangeable, and Intracellular Pools. *Frontiers in Microbiology*, *7*. https://doi.org/10.3389/fmicb.2016.00761

García-Robledo, E., Corzo, A., & Papaspyrou, S. (2014). A fast and direct spectrophotometric method for the sequential determination of nitrate and nitrite at low concentrations in small volumes. *Marine Chemistry*, *162*, 30-36. https://doi.org/10.1016/j.marchem.2014.03.002

Garcia-Robledo, E., Corzo, A., Papaspyrou, S., Jiménez-Arias, J., & Villahermosa, D. (2010). Freeze-lysable inorganic nutrients in intertidal sediments: Dependence on microphytobenthos abundance. *Marine Ecology Progress Series*, *403*, 155-163. https://doi.org/10.3354/meps08470

Garcia-San Miguel, C. (2010). *EFECTO DEL VIENTO EN EL COEFICIENTE DE ATENUACIÓN DE LA LUZ EN EL AGUA PARA EL SACO INTERNO DE LA BAHIA DE CADIZ*.

Glud, R. N. (2008). Oxygen dynamics of marine sediments. *Marine Biology Research*, *4*(4), 243-289. https://doi.org/10.1080/17451000801888726

Grasshoff, K., Kremlingl, K., & Ehrhardt, M. (1999). *Methods of Seawater Analysis, Third, Completely Revised and Extended Edition*.

Ha, H. J., Kim, H., Kwon, B.-O., Khim, J. S., & Ha, H. K. (2020). Influence of tidal forcings on microphytobenthic resuspension dynamics and sediment fluxes in a disturbed coastal environment. *Environment International*, *139*, 105743. https://doi.org/10.1016/j.envint.2020.105743

Hansen, H. P., & Koroleff, F. (1999). Determination of nutrients. En K. Grasshoff, K. Kremling, & M. Ehrhardt (Eds.), *Methods of Seawater Analysis* (1.ª ed., pp. 159-228). Wiley. https://doi.org/10.1002/9783527613984.ch10

Haro, S., Bohórquez, J., Lara, M., Garcia-Robledo, E., González, C. J., Crespo, J. M., Papaspyrou, S., & Corzo, A. (2019). Diel patterns of microphytobenthic primary production in intertidal sediments: The role of photoperiod on the vertical migration circadian rhythm. *Scientific Reports*, *9*(1), 13376. https://doi.org/10.1038/s41598-019-49971-8

Haro, S., Jesus, B., Oiry, S., Papaspyrou, S., Lara, M., González, C. J., & Corzo, A. (2022). Microphytobenthos spatio-temporal dynamics across an intertidal gradient using Random Forest classification and Sentinel-2 imagery. *Science of the Total Environment*, *804*, 149983. https://doi.org/10.1016/j.scitotenv.2021.149983

Haro, S., Lara, M., Laiz, I., González, C. J., Bohórquez, J., Garcia-Robledo, E., Corzo, A., & Papaspyrou, S. (2020). Microbenthic Net Metabolism Along Intertidal Gradients (Cadiz Bay, SW Spain): Spatio-Temporal Patterns and Environmental Factors. *Frontiers in Marine Science*, *7*(February). https://doi.org/10.3389/fmars.2020.00039

Heiri, O., Lotter, A. F., & Lemcke, G. (2001). Loss on ignition as a method for estimating organic and carbonate content in sediments: Reproducibility and comparability of results. *Journal of Paleolimnology*, *25*(1), 101-110. https://doi.org/10.1023/A:1008119611481

Hicks, N., Liu, X., Gregory, R., Kenny, J., Lucaci, A., Lenzi, L., Paterson, D. M., & Duncan, K. R. (2018). Temperature Driven Changes in Benthic Bacterial Diversity Influences Biogeochemical Cycling in Coastal Sediments. *Frontiers in Microbiology*, *9*, 1730. https://doi.org/10.3389/fmicb.2018.01730

Høgslund, S., Fossing, H., & Carstensen, J. (2023). Microphytobenthic impact on benthic pelagic nutrient exchange in temperate shallow estuaries. *Estuarine, Coastal and Shelf Science*, *292*, 108475. https://doi.org/10.1016/j.ecss.2023.108475

Hope, J. A., Paterson, D. M., & Thrush, S. F. (2020). The role of microphytobenthos in soft-sediment ecological networks and their contribution to the delivery of multiple ecosystem services. *Journal of Ecology*, *108*(3), 815-830. https://doi.org/10.1111/1365-2745.13322

Huettel, M., Berg, P., & Kostka, J. E. (2014). Benthic Exchange and Biogeochemical Cycling in Permeable Sediments. *Annual Review of Marine Science*, *6*(1), 23-51. https://doi.org/10.1146/annurev-marine-051413-012706

Jiménez-Arias, J. L., Morris, E., Rubio-de-Inglés, M. J., Peralta, G., García-Robledo, E., Corzo, A., & Papaspyrou, S. (2020). Tidal elevation is the key factor modulating burial rates and composition of organic matter in a coastal wetland with multiple habitats. *Science of The Total Environment*, *724*, 138205. https://doi.org/10.1016/j.scitotenv.2020.138205

Kalnejais, L. H., Martin, W. R., & Bothner, M. H. (2010). The release of dissolved nutrients and metals from coastal sediments due to resuspension. *Marine Chemistry*, *121*(1-4), 224-235. https://doi.org/10.1016/j.marchem.2010.05.002

Kleeberg, A., & Herzog, C. (2014). Sediment microstructure and resuspension behavior depend on each other. *Biogeochemistry*, *119*(1-3), 199-213. https://doi.org/10.1007/s10533-014-9959-0

Kwon, B.-O., Kim, H., Noh, J., Lee, S. Y., Nam, J., & Khim, J. S. (2020). Spatiotemporal variability in microphytobenthic primary production across bare intertidal flat, saltmarsh, and mangrove forest of Asia and Australia. *Marine Pollution Bulletin*, *151*, 110707. https://doi.org/10.1016/j.marpolbul.2019.110707

Lorke, A., Müller, B., Maerki, M., & Wüest, A. (2003). Breathing sediments: The control of diffusive transport across the sediment—water interface by periodic boundary-layer turbulence. *Limnology and Oceanography*, *48*(6), 2077-2085. https://doi.org/10.4319/lo.2003.48.6.2077

MacIntyre, H. L., Geider, R. J., & Miller, D. C. (1996). Microphytobenthos: The Ecological Role of the «Secret Garden» of Unvegetated, Shallow-Water Marine Habitats. I. Distribution, Abundance and Primary Production. *Estuaries*, *19*(2), 186. https://doi.org/10.2307/1352224

Meehl, G. A., & Tebaldi, C. (2004). More Intense, More Frequent, and Longer Lasting Heat Waves in the 21st Century. *Science*, *305*(5686), 994-997. https://doi.org/10.1126/science.1098704

Méléder, V. (2020). Mapping the Intertidal Microphytobenthos Gross Primary Production Part I: Coupling Multispectral Remote Sensing and Physical Modeling. *Frontiers in Marine Science*, *7*.

Meysman, F. J. R., Galaktionov, O. S., Glud, R. N., & Middelburg, J. J. (2010). Oxygen penetration around burrows and roots in aquatic sediments. *Journal of Marine Research*, *68*(2). https://doi.org/10.1357/002224010793721406

Middelburg, J. J., Barranguet, C., Boschker, H. T. S., Herman, P. M. J., Moens, T., & Heip, C. H. R. (2000). The fate of intertidal microphytobenthos carbon: An in situ 13C-labeling study. *Limnology and Oceanography*, *45*(6), 1224-1234. https://doi.org/10.4319/lo.2000.45.6.1224

Mieszkowska, N., Burrows, M., & Sugden, H. (2020). Impacts of climate change on intertidal habitats, relevent to the coastal and marine environment around the UK [Pdf]. *MCCIP Science Review 2020*, 16 pages. https://doi.org/10.14465/2020.ARC12.ITH

Morel, A., Huot, Y., Gentili, B., Werdell, P. J., Hooker, S. B., & Franz, B. A. (2007). Examining the consistency of products derived from various ocean color sensors in open ocean (Case 1) waters in the perspective of a multi-sensor approach. *Remote Sensing of Environment*, *111*(1), 69-88. https://doi.org/10.1016/j.rse.2007.03.012

Papaspyrou, S., Diz, P., García-Robledo, E., Corzo, A., & Jimenez-Arias, J. (2013). Benthic foraminiferal community changes and their relationship to environmental dynamics in intertidal muddy sediments (Bay of Cádiz, SW Spain). *Marine Ecology Progress Series*, *490*, 121-135. https://doi.org/10.3354/meps10447

Parmesan, C., Morecroft, M. D., & Trisurat, Y. (2022). *Climate Change 2022:Impacts, Adaptation and Vulnerability*.

Paterson, D. M. (1989). Short-term changes in the erodibility of intertidal cohesive sediments related to the migratory behavior of epipelic diatoms. En *Limnology and Oceanography* (Vol. 34, Número 1, pp. 223-234). https://doi.org/10.4319/lo.1989.34.1.0223

Perez-Rodriguez, V., Corzo, A., Papaspyrou, S., Van Bergeijk, S. A., Vilas, C., Cañavate, J. P., & Garcia-Robledo, E. (2024). Benthic metabolism and nutrient dynamics of a hyperturbid and hypernutrified estuary. *Frontiers in Marine Science*, *11*, 1389673. https://doi.org/10.3389/fmars.2024.1389673

Redfield, A. C. (1958). The biological control of chemical factors in the environment. *American Scientist*, *46*(3), 205-221.

Redzuan, N. S., & Underwood, G. J. C. (2021). The importance of weather and tides on the resuspension and deposition of microphytobenthos (MPB) on intertidal mudflats. *Estuarine, Coastal and Shelf Science*, *251*, 107190. https://doi.org/10.1016/j.ecss.2021.107190

Revsbech, N. P. (1989). An oxygen microsensor with a guard cathode. *Limnology and Oceanography*, *34*(2), 474-478. https://doi.org/10.4319/lo.1989.34.2.0474

Ribeiro, L., Brotas, V., Rincé, Y., & Jesus, B. (2013). Structure and diversity of intertidal benthic diatom assemblages in contrasting shores: A case study from the Tagus estuary[1]. *Journal of Phycology*, *49*(2), 258-270. https://doi.org/10.1111/jpy.12031

Rios-Yunes, D., Tiano, J. C., Van Oevelen, D., Van Dalen, J., & Soetaert, K. (2023). Annual biogeochemical cycling in intertidal sediments of a restored estuary reveals dependence of N, P, C and Si cycles to temperature and water column properties. *Estuarine, Coastal and Shelf Science*, *282*, 108227. https://doi.org/10.1016/j.ecss.2023.108227

Risgaard-Petersen, N. (2003). Coupled nitrification-denitrification in autotrophic and heterotrophic estuarine sediments: On the influence of benthic microalgae. *Limnology and Oceanography*, *48*(1), 93-105. https://doi.org/10.4319/lo.2003.48.1.0093

Ritchie, R. J. (2008). *Ritchie Universal chlorophyll equations for estimating chlorophylls a, b, c, and d.pdf*. *46*(1), 115-126.

Sardanyés, J. (2024). Identifying regime shifts, transients and late warning signals for proactive ecosystem management. *Biological Conservation*.

Saulquin, B., Hamdi, A., Gohin, F., Populus, J., Mangin, A., & d'Andon, O. F. (2013). Estimation of the diffuse attenuation coefficient KdPAR using MERIS and application to seabed habitat mapping. *Remote Sensing of Environment*, *128*, 224-233. https://doi.org/10.1016/j.rse.2012.10.002

Schutte, C. A., Ahmerkamp, S., Wu, C. S., Seidel, M., De Beer, D., Cook, P. L. M., & Joye, S. B. (2019). Biogeochemical Dynamics of Coastal Tidal Flats. En *Coastal Wetlands* (pp. 407-440). Elsevier. https://doi.org/10.1016/B978-0-444-63893-9.00012-5

Smith, K. E., Burrows, M. T., Hobday, A. J., King, N. G., Moore, P. J., Sen Gupta, A., Thomsen, M. S., Wernberg, T., & Smale, D. A. (2023). Biological Impacts of Marine Heatwaves. *Annual Review of Marine Science*, *15*(1), 119-145. https://doi.org/10.1146/annurev-marine-032122-121437

Soetaert, K., Middelburg, J. J., Heip, C., Meire, P., Van Damme, S., & Maris, T. (2006). Long-term change in dissolved inorganic nutrients in the heterotrophic Scheldt estuary (Belgium, The Netherlands). *Limnology and Oceanography*, *51*(1part2), 409-423. https://doi.org/10.4319/lo.2006.51.1_part_2.0409

Soriano-González, J., Urrego, E. P., Sòria-Perpinyà, X., Angelats, E., Alcaraz, C., Delegido, J., Ruíz-Verdú, A., Tenjo, C., Vicente, E., & Moreno, J. (2022). Towards the Combination of C2RCC Processors for Improving Water Quality Retrieval in Inland and Coastal Areas. *Remote Sensing 2022, Vol. 14, Page 1124*, *14*(5), 1124. https://doi.org/10.3390/RS14051124

Sundbäck, K., & Miles, A. (2002). Role of microphytobenthos and denitrification for nutrient turnover in embayments with floating macroalgal mats: A spring situation. *Aquatic Microbial Ecology*, *30*, 91-101. https://doi.org/10.3354/ame030091

Ubertini, M., Lefebvre, S., Rakotomalala, C., & Orvain, F. (2015). Impact of sediment grain-size and biofilm age on epipelic microphytobenthos resuspension. *Journal of Experimental Marine Biology and Ecology*, *467*, 52-64. https://doi.org/10.1016/j.jembe.2015.02.007

Underwood, G. J. C., & Kromkamp, J. (1999). Primary Production by Phytoplankton and Microphytobenthos in Estuaries. En *Advances in Ecological Research* (Vol. 29, pp. 93-153). Elsevier. https://doi.org/10.1016/S0065-2504(08)60192-0

Van Duren, L. A., & Middelburg, J. J. (2001). The Benthic Boundary Layer: Transport Processes and Biogeochemistry. *Eos, Transactions American Geophysical Union*, *82*(52), 658-659. https://doi.org/10.1029/01EO00381

Warnken, K., Gill, G. A., Santschi, P., & Griffin, L. L. (2000). *Benthic exchange of nutrients in Galveston Bay, Texas*. *23*(5), 647-661. https://doi.org/10.2307/1352891

Wengrove, M. E. (2015). *Field and laboratory observations of bed stress and associated nutrient release in a tidal estuary*.

Yallop, M. L., De Winder, B., Paterson, D. M., & Stal, L. J. (1994). Comparative structure, primary production and biogenic stabilization of cohesive and non-cohesive marine sediments inhabited by microphytobenthos. *Estuarine, Coastal and Shelf Science*, *39*(6), 565-582. https://doi.org/10.1016/S0272-7714(06)80010-7

Zhang, Q., & Blomquist, J. D. (2018). Watershed export of fine sediment, organic carbon, and chlorophyll-a to Chesapeake Bay: Spatial and temporal patterns in 1984–2016. *Science of The Total Environment*, *619-620*, 1066-1078. https://doi.org/10.1016/j.scitotenv.2017.10.279

Supplementary material for:

Windstorms increase benthic-pelagic coupling and nutrient outwelling from shallow coastal wetlands

Alfonso Corzo[1], Valle Perez-Rodriguez[1], Sara Haro[2], Sokratis Papaspyrou[1], Sandra Rizzo-Calderón[1], Mª Dolores Jimenez-Lopez[1], Emilio Garcia-Robledo[1]

[1]Department of Biology, Faculty of Marine and Environmental Science, University of Cadiz, Pol. Río San Pedro s/n, Puerto Real, Spain

[2] Department of Ecology and Geology, Faculty of Sciences, University of Málaga, Málaga, Spain

Supplementary results: Figures S1-4

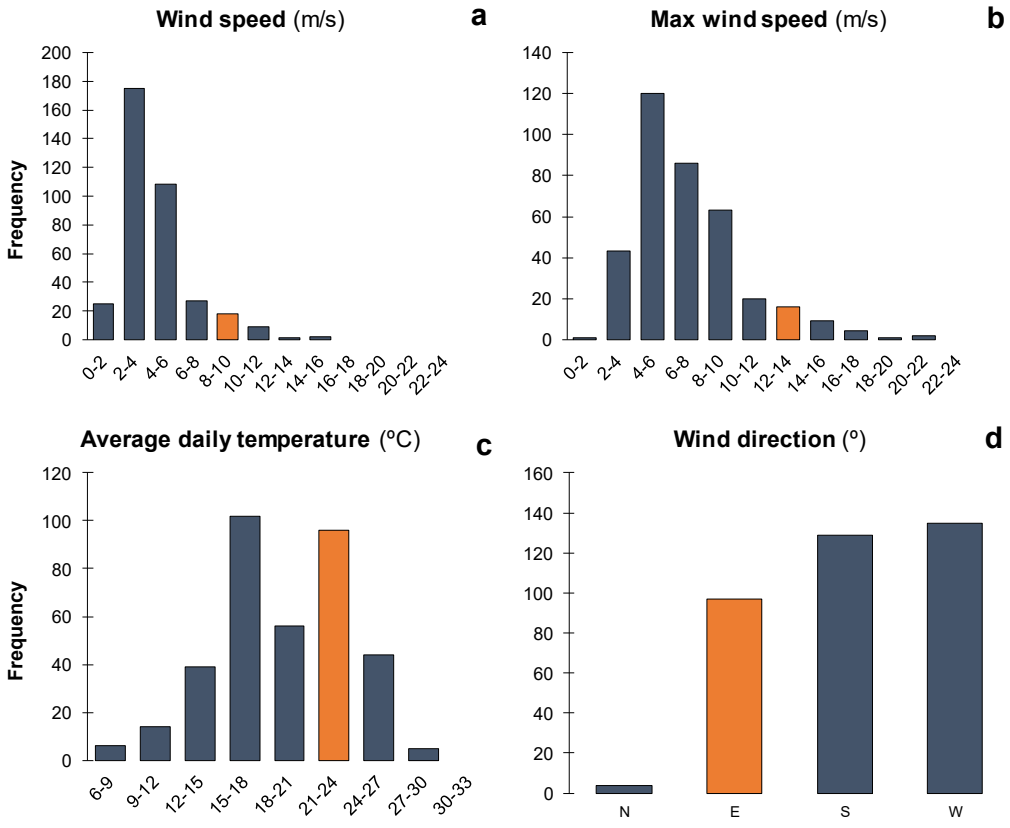


Fig. S1. Frequency distribution of annual mean daily wind speed (**a**), daily maximum wind speed, including gusts (**b**), mean daily temperature (**c**), and mean daily wind direction (**d**) during the sampling year (2021). The range of values for the aforementioned variables during the investigated WSE is indicated by orange bars.

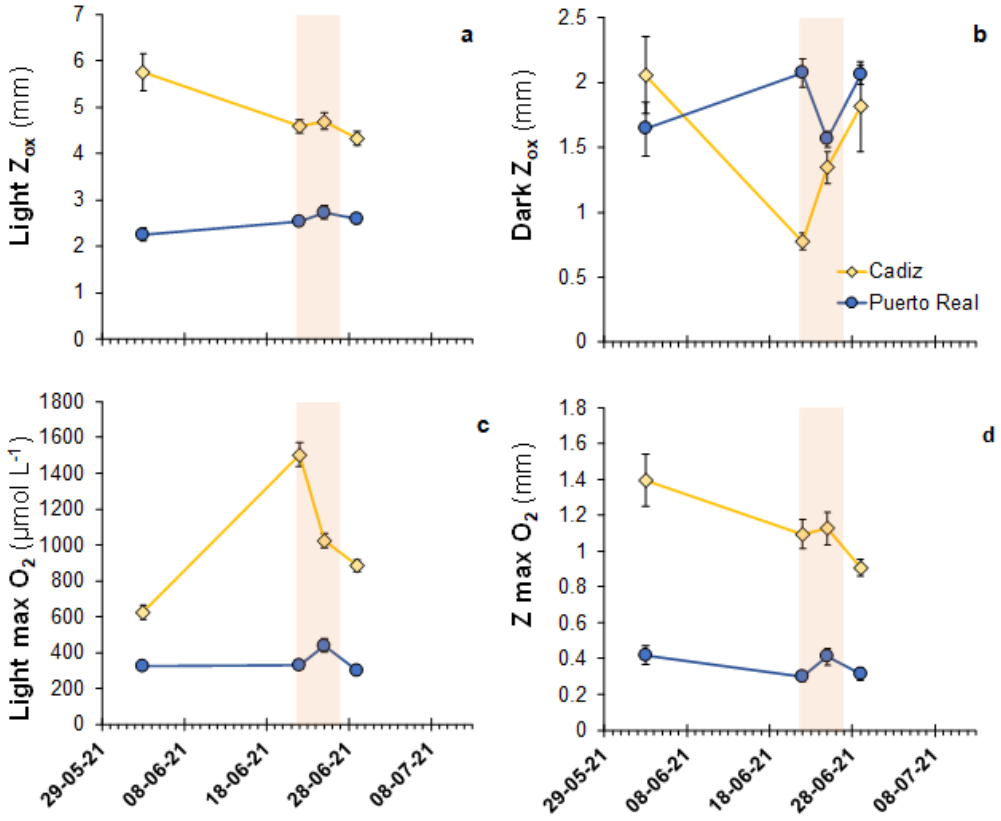


Fig. S2. Changes in oxygen penetration depth in the sediment (z_{ox}) in light and dark conditions (**a, b**), peak of maximum O_2 in light (C_{max})(**c**) and depth at which the maximum O_2 concentration occurred (z_{Cmax})(**d**). Blue dots and lines represent Puerto Real and yellow rhombs and lines represent Cadiz values. Data are means ± SE (n=5). Orange shaded area represents the duration of the wind-storm.

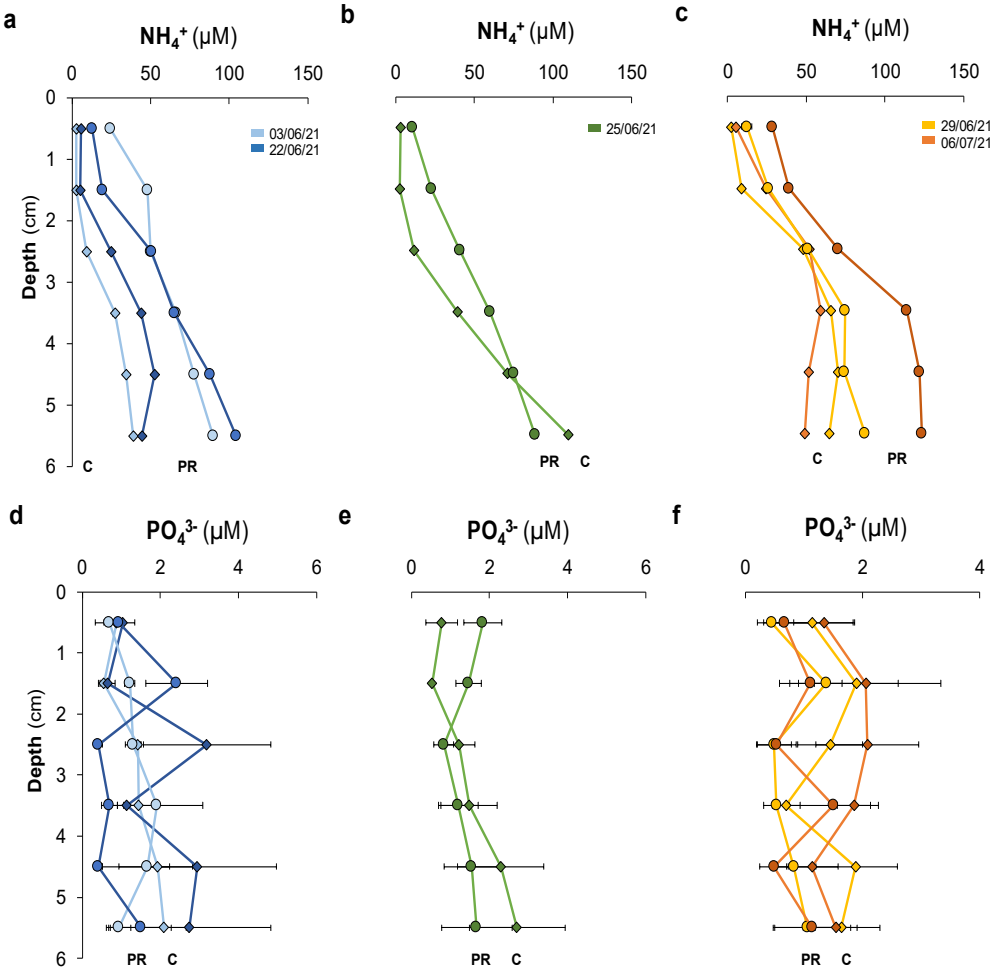


Fig. S3. Concentration profiles within the sediment of NH_4^+ (**a, b, c**) and PO_4^{3-} (**d, e, f**). Left panels (blue) represent the data before the WSE, middle ones (green) the data during WSE and, right panels (orange), values found after the WSE. Rhombs represent data from Cadiz (indicated by a 'C') and circles represent Puerto Real (indicated as 'PR'). Data are means and SE (n=3)

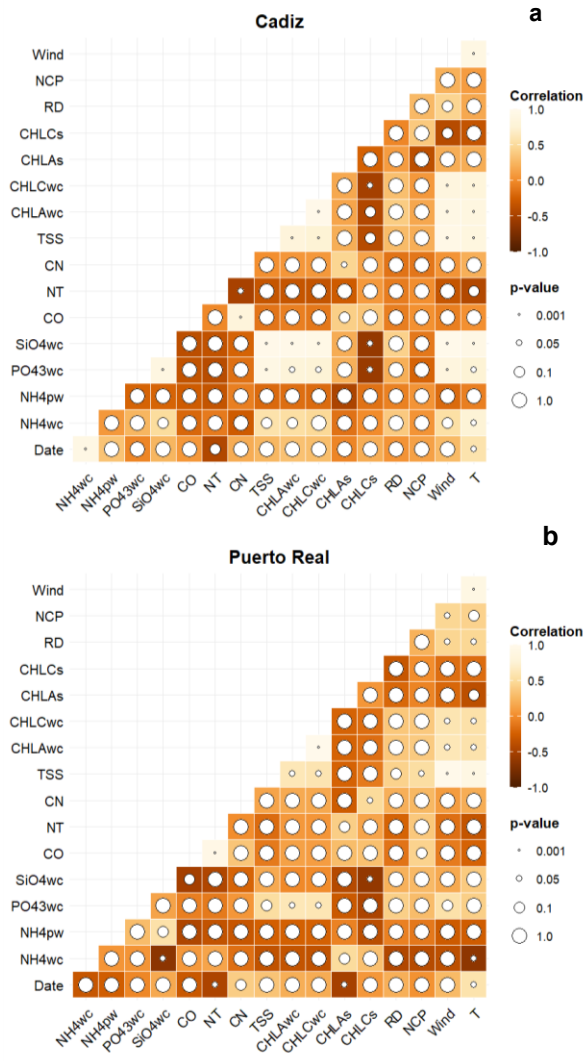


Figure S4. Correlation matrix of all studied parameters during the windstorm event: Ammonium content (in the water column (NH4wc) and in the pore-water (NH4pw), phosphate content in the water column (PO43wc), silica content in the water column (SiO4), organic carbon content (CO), total nitrogen content (NT), carbon:nitrogen ratio (CN), TSS, Chlorophyll content in the water column (CHLAwc and CHLCwc) and in the sediment (CHLAs and CHLCs), dark respiration (RD), net community production (NCP), wind speed (Wind) and temperature (T). (**a**) Correlation values for Cadiz and (**b**) correlation values for Puerto Real, highlighting site-specific interactions. Stronger correlations are represented by more intense colors, indicating significant interdependencies between the measured variables across both locations.



Chapter 5:

General discussion and conclusions



This chapter brings together the results and conclusions of the previous studies (Chapters 2-4) to provide a broader perspective on the impact of environmental variability on shallow aquatic ecosystems. These studies provide insight into how shallow coastal ecosystems respond to and recover from the influence of extreme weather events and estuarine dynamics.

1.1. Contribution of microphytobenthos to sediment biogeochemistry in the Guadalquivir Estuary

Estuaries and intertidal mudflats are key elements in the functioning of coastal systems by facilitating nutrient recycling, sediment stabilization, and the storage of organic matter and other solutes (French, 2019). The microphytobenthic (MPB) community plays an important role in these processes by promoting carbon fixation and primary production, and influencing the structure and dynamics of sediment communities (MacIntyre et al., 1996; Underwood & Kromkamp, 1999). However, their presence and activity are not constant. MPB are limited by and highly sensitive to changes in basic environmental conditions such as light availability, sediment resuspension, or water dynamics (Cartaxana et al., 2016; Haro et al., 2019; Kromkamp, 2006; Pivato et al., 2019; Redzuan & Underwood, 2021).

In the Guadalquivir Estuary, MPB communities maintained their activity throughout the year despite possible light limitation caused by persistent turbidity and clearly contributed to overall estuarine primary production. Seasonal monitoring revealed that sediments generally sustained positive net community production, with the highest values recorded in Bonanza during the summer, reaching approximately 5.4 mmol O_2 m^{-2} h^{-1}. This seasonality, presenting higher production in summer, was also observed in other turbid systems such as the Scheldt Estuary (Kromkamp et al., 1995; Soetaert et al., 2006). Compared to nearby estuarine areas like the Bay of Cádiz, the sediments of the Guadalquivir Estuary showed lower organic carbon and nitrogen contents (Corzo et al., 2009; Haro et al., 2020). The relatively high C:N ratios, above 10, pointed to a mixed origin of the organic matter, combining local production and allochthonous inputs from the terrestrial basin (Cabrita & Brotas, 2000; Rios-Yunes et al., 2023).

MPB biomass, estimated by the sediment content of Chla, changed seasonally and along the estuary, being the range of values similar to that found in the tidal flats of Cadiz Bay (Garcia-Robledo et al., 2016; Haro et al., 2020) and similar ecosystems world-wide (Cabrita and Brotas, 2000; McTigue et al., 2015; Kwon et al., 2020). Seasonal variations in MPB biomass and mineralization rates appeared to be linked to external drivers such as dam operations and rainfall events, which are known to regulate estuarine inputs of nutrients and organic matter (Rodríguez-Ramírez et al., 2019; Ruiz et al., 2017). In terms of organic matter mineralization, aerobic respiration dominated the upper sediment layer, up to the oxygen penetration depth. However, under anoxic conditions, denitrification stood out as the main anaerobic pathway, likely due to the very high nitrate concentrations in the water column, with rates far exceeding those of iron and sulfate reduction (Burgos et al., 2018; Jørgensen & Kasten, 2006). Our calculations suggest that methane production was very limited, which is consistent with the inhibitory effect of high nitrate concentrations on methanogenesis (Abril & Iversen, 2002).

Sediments at both study sites in the Guadalquivir Estuary, regardless of their location, functioned as net sinks for nitrate and ammonia across all seasons. The annual average NO_3^- uptake rates (-0.70 ± 1.1 m^{-2} h^{-1}) were higher than the uptake of NH_4^+ by an order of magnitude. These fluxes highlight the role of intertidal sediment in mitigating coastal eutrophication by intercepting water column DIN loads before they are exported to the Gulf of Cádiz (Alonso-Pérez & Castro, 2014). Our results clearly suggest that both the N-demand of MPB for growth and the consumption of NO_3^- in denitrification were the main responsible pathways for the nitrogen filtration capacity of Guadalquivir Estuary tidal flats. Seasonal variability significantly influences nitrogen cycling, especially in relation to the effects of light on ammonium and nitrate uptake. Net ammonium assimilation was substantially higher under illuminated conditions, with rates in Bonanza reaching up to five times those observed in Lebrija during dark incubations. This pattern underscores the key role of light availability in regulating nitrogen dynamics in these environments. The enhanced photosynthetic activity of MPB during daylight hours, which increases the demand for inorganic nitrogen to sustain carbon fixation and biomass production (Longphuirt et al., 2009), likely explains the effect of light availability on ammonium net uptake by the sediment. In contrast, NO_3^- fluxes showed no significant differences between light and dark conditions, indicating that nitrate removal is mainly governed by light-independent processes, such as denitrification.

This study provides new evidence about biogeochemical dynamics and primary production in the Guadalquivir Estuary, highlighting the importance of considering the MPB compartment. These results emphasize the central role of MPB and other microbial metabolisms in maintaining primary production and controlling nutrient cycling. Their ability to intercept and transform nitrogen before it reaches coastal waters underscores the need to incorporate benthic processes into estuarine management, especially under growing anthropogenic pressures and changing climate conditions (Garcia-Robledo et al., 2016; Pivato et al., 2019). Future studies should aim to quantify more precisely the spatial and temporal variability of MPB contributions and assess the resilience of these communities under shifting environmental scenarios.

1.2. Effect of heat waves on intertidal sediment biogeochemical processes

Rising greenhouse gas emissions are intensifying climate change, leading to more frequent and severe extreme weather events, such as windstorms or heatwaves. While many studies have examined how temperature can affect several aspects of biogeochemical cycling in intertidal zones in temperate regions (Apple et al., 2006; Hancke & Glud, 2004; Hicks et al., 2018; Rios-Yunes et al., 2023), no data were previously available for the Bay of Cadiz.

Thermal increase during four days, simulating a heat wave, in dark conditions favored heterotrophic microbial metabolism, accelerating OM degradation, as reflected in the linear increase of O_2 consumption (both diffusive and total) and in the rates of DIC and NH_4^+ production. The magnitude of effects varies depending on initial temperature, but DOU increased around 150% between 10 and 42 ºC, indicating that biological activity is driving the thermal response more than changes associated to physicochemical processes such as O_2 solubility, diffusivity, or DBL width (Jørgensen & Revsbech, 1985; Millero & Poisson, 1981). DOU thermal sensibility (quantifyed by E_a and Q_{10}) increased with time suggesting microbial fast aclimatation or community changes, whereas TOU decrease, showing possible effects or even damages in the local infauna by the long exposure to the heat and de depletion of oxygen (Hancke & Glud, 2004; Musat et al., 2006). The increase in the DOU/TOU ratio highlights greater increases in microbial activity compared to

infaunal contributions at higher temperatures (34-42 ºC), as suggested by previous studies from different intertidal areas (Rabouille et al., 2003).

The microbial community of the sediment seems to adapt to the higher temperature during the heat wave. A progressive rise in sediment oxygen demand was observed during the first 60 hours that it was associated with changes in the taxonomic structure of the microbial community. Aerobic microbial groups, such as Verrucomicrobiota and Myxococcota declined at higher temperatures, while heat-tolerant groups like Firmicutes and Chloroflexi became dominant. This shift in the microbial community composition might have been driven by the depletion of labile organic substrates in addition to their different thermal sensitivity (Arnosti et al., 1998; Glud, 2008; Papaspyrou et al., 2004).

Greenhouse gas net fluxes also clearly responded to thermal stress during the heat waves. Observed N_2O fluxes in the San Pedro River (-0.11 to 0.38 µmol m^{-2} h^{-1}) were higher than previously reported, suggesting that global warming might amplify N_2O production by expanding anoxic zones and favoring denitrification (Li et al., 2013; Smith et al., 2012). However, the temperature-emission relationship for N_2O was not linear, as processes like N_2 reduction or substrate competition might modulate net emissions (Lamontagne et al., 2003). For CH_4, the relationship was linear, increasing emissions with temperature, peaking at 42 ºC, and matching values previously reported in coastal margins (Sansone et al., 2004). Discrepancies with other shallow systems (Abril et al., 2002; Bastviken et al., 2008) might result from methodological differences or changes in the microbial community and its capacity to adapt to new temperature conditions. In our experiemntal set up, the increased presence of Methanosarcinales (thermotolerant methanogens) and Rhodospirillales (acetate producers) at 42 ºC favors methanogenesis via acetate (Herbert, 1999; Yvon-Durocher et al., 2014). Additionally, intensified aerobic/anaerobic methane oxidation at higher temperatures partially limited net emissions (Stocker, 2014).

Nitrogen-fluxes at the sediment-water interface changes with temperature and with time during the experiment. Initially, sediments from Rio San Pedro acted as net sinks for NH_4^+, with net uptake rates at the highest temperatures, 7.5 times greater than at 10 ºC, linked to stimulated nitrification, bacterial assimilation or Anammox (Dalsgaard & Thamdrup, 2002; Rosales Villa et al., 2019). Despite this, NH_4^+ production rose exponentially with temperature, similar to previous observations in

the Bay of Cadiz and other temperate regions (Berg et al., 1998; Burgos et al., 2018; Leote & Epping, 2015). Although sediments acted as NH_4^+ sources at low temperatures, little absorption persisted between 34-42 ºC despite no significant change in nitrification gene abundance (e.g., Bac amoA, Arch amoA).

Anaerobic processes were favored and the coupling of nitrification-denitrification was altered by the increased oxigen demand that decrease the oxic layer. Nitrogen oxides fluxes were mainly positive, with nitrite increasing the flux untill reaching 34ºC and then decreasing at 42ºC, and with nitrate presenting diary variability. This might suggest denitrification limitation or even NO_2^- competition between metabolic pathways (Dawson & Murphy, 1972; Nizzoli et al., 2010). At 42 °C, denitrification-related gene sequences became more abundant, and this shift was accompanied by greater activity in acetate-producing (PWY-7254) and osmolyte synthesis (P101-PWY) pathways—evidence of microbial adaptations to both heat and salinity. Yet the modified NO_2^- flux observed at 42 °C revealed a non-linear community response that points to DNRA prevailing over conventional NO_2^- reduction. Anammox could still play a part, but its lower thermal tolerance (Brin et al., 2017; Canion et al., 2014) and the time-dependent nature of community adjustments (Herbert, 1999; Hines et al., 2013) underscore how the length and intensity of heat-wave events can reconfigure biogeochemical cycling in coastal sediments.

Based on these results, it can be concluded that heatwaves cause significant changes in the biogeochemical processes of intertidal sediments, affecting microbial activity, oxygen consumption and greenhouse gases emission. As described above, the thermal stress responses are complex and not always linear, so both intensity and duration of thermal stress has to be consider to properly understand its effects in these systems and its climatic implications.

1.3. Windstorm-generated turbulence affects the dynamics of shallow coastal ecosystems

Shallow coastal areas are particularly vulnerable to physical disturbances that impact their ecological dynamics. Light availability is essential for the growth of microphytobenthos (MPB) in the upper layers of the sediment (Irigoien & Castel, 1997; Kromkamp, 2006; Kühl et al., 1994; Perkins et al., 2001). Consequently,

these systems are highly sensitive to increases in turbidity, characterized by elevated concentrations of total suspended solids (TSS) in the water column. In the Guadalquivir Estuary, turbidity remains persistently high due to its morphology, channel structure, land uses in the catchment, and continuous upstream-downstream water exchange. This permanently high turbidity in the Guadalquivir estuary contrasts with the Bay of Cádiz, where turbidity is less permanent and mainly associated to wind strength. Both natural hydrodynamics and external factors, such as wind storm events (WSE), can alter sediment dynamics, organic matter transport, and nutrient cycling (Davis et al., 2004; Díez-Minguito et al., 2014; Fagherazzi & Wiberg, 2009; Pivato et al., 2019).

In the inner Bay of Cádiz, geomorphological differences between different areas like Puerto Real and Cádiz modulate the response to WSE (Haro et al., 2020). Due to its shallow depth, the Bay is particularly susceptible to wind-induced sediment resuspension, which releases inorganic particles, organic matter, MPB cells, and dissolved nutrients into the water column. This process differed between sites: Puerto Real, with muddy sediment, experienced stronger erosion, while Cádiz, with sandier sediment, showed more deposition. The correlation between wind speed, TSS, and chlorophyll-a (Chla) in the water column, supported by satellite imagery, confirmed that WSEs drive spatial heterogeneity in suspended material (Redzuan & Underwood, 2020). WSE affected sediment Chla concentrations in distinct ways depending on local hydrodynamic conditions and sediment properties (Garcia-Robledo et al., 2016; Haro et al., 2020). In Puerto Real, surface Chla decreased by about 50%, consistent with sediment erosion, while in Cádiz, Chla slightly increased, suggesting sedimentation of TSS driven southwest by the wind. Furthermore, the net transfer of Chla into the water column, and its redistribution across the system, indicates that WSE can act as resource pulses for suspension-feeding organisms (Ubertini et al., 2012)

Sediment resuspension during WSEs also modified organic carbon (C_{org}) and total nitrogen (T_N) contents. Particularly in Puerto Real, an increase in the C:N ratio after the event suggests additional inputs of detrital material from marshes. One week after the WSE, Chla content had not recovered to initial levels, indicating the burial of microbial communities and a disturbance in sedimentary biogeochemical processes (Cartaxana et al., 2011; Haro et al., 2020; Ribeiro et al., 2013). Differences in organic content and sediment permeability between Cádiz and Puerto Real were reflected in oxygen dynamics at the sediment–water interface. In

Cádiz, oxygen penetration was about 2.5 times deeper than in Puerto Real, with a more pronounced subsurface oxygen peak. Consequently, primary production normalized to Chla was ten times higher in Cadiz (53.23 ± 20.32 µmol O_2 mgChla^{-1} h^{-1}) than in Puerto Real (5.35 ± 2.57 µmol O_2 mgChla^{-1} h^{-1}), reflecting a turbulence-adapted and active microphytobenthic community (Huettel et al., 2014; MacIntyre et al., 1996).

Although sandy sediments are generally associated with higher productivity and faster turnover rates (Huettel et al., 2014; MacIntyre et al., 1996; Middelburg et al., 2000), respiration rates recorded during the WSE were comparable to previous observations for the Bay of Cadiz (Haro et al., 2020) and similar coastal areas (Kwon et al., 2020). Meanwhile, increased turbidity during the WSE significantly limited light penetration, affecting MPB photosynthetic activity (Kromkamp et al., 1995; Pivato et al., 2019). Nevertheless, resuspended MPB cells in the water column could contribute to enhancing secondary production by making them more accessible to suspension feeders (Hope et al., 2020). The ratio between net community production (NCP) and dark respiration (R_{dark}) provided insights into the metabolic balance of the system. In Cádiz, the NCP:R_{dark} ratio reflected net autotrophy, while in Puerto Real, it suggested a metabolism closer to heterotrophy, consistent with the higher retention of organic matter in muddy sediments.

WSEs also caused major shifts in dissolved inorganic nutrient concentrations (NH_4^+, NO_3^-, NO_2^-, PO_4^{3-}, SiO_4^{4-}) showing opposite behaviors between sandy and muddy areas. In Cádiz, net release of ammonium was recorded (0.035 ± 0.008 mmol m^{-2} d^{-1}), identifying sandy sediments as a source, while in Puerto Real, ammonium uptake occurred (-0.005 ± 0.014 mmol m^{-2} d^{-1}). Net integrated increases in ammonium, phosphate, and silicate concentrations were observed during the WSE, although the resulting N:P and N:Si molar ratios (7.7 and 0.7, respectively) suggested nitrogen and silicate limitation for algal growth (Brzezinski, 1985; Redfield, 1958). Despite these shifts, a rapid short-term resilience of the benthic community was suggested by multivariate nMDS analysis (Chapter 4).

Beyond local effects, WSEs enhanced the export of organic and inorganic matter to the coastal zone. The event transported an estimated 3.6 × 10^6 kg of TSS and 3.3x10^2 kg of Chla per day from the inner Bay of Cádiz to the Gulf of Cádiz, enriching adjacent ecosystems but also potentially generating nutrient imbalances and food web alterations. As the frequency and intensity of windstorms are expected to increase under climate change scenarios, a deeper understanding of their impacts

on MPB resilience, microbial community structure, and biogeochemical cycles is crucial for anticipating the future dynamics of coastal ecosystems.

References

Abril, G., & Iversen, N. (2002). Methane dynamics in a shallow non-tidal estuary (Randers Fjord, Denmark). *Marine Ecology Progress Series*, *230*, 171-181. https://doi.org/10.3354/meps230171

Abril, G., Nogueira, M., Etcheber, H., Cabeçadas, G., Lemaire, E., & Brogueira, M. J. (2002). Behaviour of Organic Carbon in Nine Contrasting European Estuaries. *Estuarine, Coastal and Shelf Science*, *54*(2), 241-262. https://doi.org/10.1006/ecss.2001.0844

Alonso-Pérez, F., & Castro, C. (2014). Benthic oxygen and nutrient fluxes in a coastal upwelling system (Ria de Vigo, NW Iberian Peninsula): Seasonal trends and regulating factors. *Marine Ecology Progress Series*, *511*, 17-32. https://doi.org/10.3354/meps10915

Apple, J., Del Giorgio, P., & Kemp, W. (2006). Temperature regulation of bacterial production, respiration, and growth efficiency in a temperate salt-marsh estuary. *Aquatic Microbial Ecology*, *43*, 243-254. https://doi.org/10.3354/ame043243

Arnosti, C., Jørgensen, B., Sagemann, J., & Thamdrup, B. (1998). Temperature dependence of microbial degradation of organic matter in marine sediments:polysaccharide hydrolysis, oxygen consumption, and sulfate reduction. *Marine Ecology Progress Series*, *165*, 59-70. https://doi.org/10.3354/meps165059

Bastviken, D., Cole, J. J., Pace, M. L., & Van De Bogert, M. C. (2008). Fates of methane from different lake habitats: Connecting whole-lake budgets and CH_4 emissions. *Journal of Geophysical Research: Biogeosciences*, *113*(G2), 2007JG000608. https://doi.org/10.1029/2007JG000608

Berg, P., Risgaard-Petersen, N., & Rysgaard, S. (1998). Interpretation of measured concentration profiles in sediment pore water. *Limnology and Oceanography*, *43*(7), 1500-1510. https://doi.org/10.4319/lo.1998.43.7.1500

Brin, L. D., Giblin, A. E., & Rich, J. J. (2017). Similar temperature responses suggest future climate warming will not alter partitioning between denitrification and anammox in temperate marine sediments. *Global Change Biology*, *23*(1), 331-340. https://doi.org/10.1111/gcb.13370

Brzezinski, M. A. (1985). THE Si:C:N RATIO OF MARINE DIATOMS: INTERSPECIFIC VARIABILITY AND THE EFFECT OF SOME ENVIRONMENTAL VARIABLES[1]. *Journal of Phycology*, *21*(3), 347-357. https://doi.org/10.1111/j.0022-3646.1985.00347.x

Burgos, M., Ortega, T., & Forja, J. (2018). Carbon Dioxide and Methane Dynamics in Three Coastal Systems of Cadiz Bay (SW Spain). *Estuaries and Coasts*, *41*(4), 1069-1088. https://doi.org/10.1007/s12237-017-0330-2

Cabrita, M., & Brotas, V. (2000). Seasonal variation in denitrification and dissolved nitrogen fluxes in intertidal sediments of the Tagus estuary, Portugal. *Marine Ecology Progress Series*, *202*, 51-65. https://doi.org/10.3354/meps202051

Canion, A., Kostka, J. E., Gihring, T. M., Huettel, M., Van Beusekom, J. E. E., Gao, H., Lavik, G., & Kuypers, M. M. M. (2014). Temperature response of denitrification and anammox reveals the adaptation of microbial communities to in situ temperatures in permeable marine sediments that span 50° in latitude. *Biogeosciences*, *11*(2), 309-320. https://doi.org/10.5194/bg-11-309-2014

Cartaxana, P., Cruz, S., Gameiro, C., & Kühl, M. (2016). Regulation of Intertidal Microphytobenthos Photosynthesis Over a Diel Emersion Period Is Strongly Affected by Diatom Migration Patterns. *Frontiers in Microbiology*, *7*. https://doi.org/10.3389/fmicb.2016.00872

Cartaxana, P., Ruivo, M., Hubas, C., Davidson, I., Serôdio, J., & Jesus, B. (2011). Physiological versus behavioral photoprotection in intertidal epipelic and epipsammic benthic diatom communities. *Journal of Experimental Marine Biology and Ecology*, *405*(1-2), 120-127. https://doi.org/10.1016/j.jembe.2011.05.027

Corzo, A., Van Bergeijk, S., & García-Robledo, E. (2009). Effects of green macroalgal blooms on intertidal sediments: Net metabolism and carbon and nitrogen contents. *Marine Ecology Progress Series*, *380*, 81-93. https://doi.org/10.3354/meps07923

Dalsgaard, T., & Thamdrup, B. (2002). Factors Controlling Anaerobic Ammonium Oxidation with Nitrite in Marine Sediments. *Applied and Environmental Microbiology*, *68*(8), 3802-3808. https://doi.org/10.1128/AEM.68.8.3802-3808.2002

Davis, S. E., Cable, J. E., Childers, D. L., Coronado-Molina, C., Day, J. W., Hittle, C. D., Madden, C. J., Reyes, E., Rudnick, D., & Sklar, F. (2004). Importance of Storm Events in Controlling Ecosystem Structure and Function in a Florida Gulf Coast Estuary. *Journal of Coastal Research*, *204*, 1198-1208. https://doi.org/10.2112/03-0072R.1

Dawson, R. N., & Murphy, K. L. (1972). The temperature dependency of biological denitrification. *Water Research*, *6*(1), 71-83. https://doi.org/10.1016/0043-1354(72)90174-1

Díez-Minguito, M., Baquerizo, A., De Swart, H. E., & Losada, M. A. (2014). Structure of the turbidity field in the G uadalquivir estuary: Analysis of observations and a box model approach. *Journal of Geophysical Research: Oceans*, *119*(10), 7190-7204. https://doi.org/10.1002/2014JC010210

Fagherazzi, S., & Wiberg, P. L. (2009). Importance of wind conditions, fetch, and water levels on wave-generated shear stresses in shallow intertidal basins. *Journal of Geophysical Research: Earth Surface*, *114*(F3), 2008JF001139. https://doi.org/10.1029/2008JF001139

French, J. (2019). Tidal Salt Marshes. En *Coastal Wetlands* (pp. 479-517). Elsevier. https://doi.org/10.1016/B978-0-444-63893-9.00014-9

Garcia-Robledo, E., Bohorquez, J., Corzo, A., Jimenez-Arias, J. L., & Papaspyrou, S. (2016). Dynamics of Inorganic Nutrients in Intertidal Sediments: Porewater, Exchangeable, and Intracellular Pools. *Frontiers in Microbiology*, *7*. https://doi.org/10.3389/fmicb.2016.00761

Glud, R. N. (2008). Oxygen dynamics of marine sediments. *Marine Biology Research*, *4*(4), 243-289. https://doi.org/10.1080/17451000801888726

Hancke, K., & Glud, R. (2004). Temperature effects on respiration and photosynthesis in three diatom-dominated benthic communities. *Aquatic Microbial Ecology*, *37*, 265-281. https://doi.org/10.3354/ame037265

Haro, S., Bohórquez, J., Lara, M., Garcia-Robledo, E., González, C. J., Crespo, J. M., Papaspyrou, S., & Corzo, A. (2019). Diel patterns of microphytobenthic primary production in intertidal sediments: The role of photoperiod on the vertical migration circadian rhythm. *Scientific Reports*, *9*(1), 13376. https://doi.org/10.1038/s41598-019-49971-8

Haro, S., Lara, M., Laiz, I., González, C. J., Bohórquez, J., Garcia-Robledo, E., Corzo, A., & Papaspyrou, S. (2020). Microbenthic Net Metabolism Along Intertidal Gradients (Cadiz Bay, SW Spain): Spatio-Temporal Patterns and Environmental Factors. *Frontiers in Marine Science*, *7*, 39. https://doi.org/10.3389/fmars.2020.00039

Herbert, R. A. (1999). Nitrogen cycling in coastal marine ecosystems. *FEMS Microbiology Reviews*.

Hicks, N., Liu, X., Gregory, R., Kenny, J., Lucaci, A., Lenzi, L., Paterson, D. M., & Duncan, K. R. (2018). Temperature Driven Changes in Benthic Bacterial Diversity Influences Biogeochemical Cycling in Coastal Sediments. *Frontiers in Microbiology*, *9*, 1730. https://doi.org/10.3389/fmicb.2018.01730

Hines, J., Hammrich, A., Steiner, D., & Gessner, M. O. (2013). A field facility to simulate climate warming and increased nutrient supply in shallow aquatic ecosystems. *Oecologia*, *173*(4), 1169-1178. https://doi.org/10.1007/s00442-013-2720-x

Hope, J. A., Paterson, D. M., & Thrush, S. F. (2020). The role of microphytobenthos in soft-sediment ecological networks and their contribution to the delivery of multiple ecosystem services. *Journal of Ecology*, *108*(3), 815-830. https://doi.org/10.1111/1365-2745.13322

Huettel, M., Berg, P., & Kostka, J. E. (2014). Benthic Exchange and Biogeochemical Cycling in Permeable Sediments. *Annual Review of Marine Science*, *6*(1), 23-51. https://doi.org/10.1146/annurev-marine-051413-012706

Irigoien, X., & Castel, J. (1997). Light Limitation and Distribution of Chlorophyll Pigments in a Highly Turbid Estuary: The Gironde (SW France). *Estuarine, Coastal and Shelf Science*, *44*, 507-517.

Jørgensen, B. B., & Kasten, S. (2006). Sulfur Cycling and Methane Oxidation. En H. D. Schulz & M. Zabel (Eds.), *Marine Geochemistry* (pp. 271-309). Springer-Verlag. https://doi.org/10.1007/3-540-32144-6_8

Jørgensen, B. B., & Revsbech, N. P. (1985). Diffusive boundary layers and the oxygen uptake of sediments and detritus1. *Limnology and Oceanography*, *30*(1), 111-122. https://doi.org/10.4319/lo.1985.30.1.0111

Kromkamp, J. (Ed.). (2006). *Functioning of microphytobenthos in estuaries*. Royal Netherlands Academy of Arts and Sciences.

Kromkamp, J., Peene, J., van Rijswijk, P., Sandee, A., & Goosen, N. (1995). *Nutrients, light and primary production by phytoplankton and microphytobenthos in the eutrophic, turbid Westerschelde estuary (The Netherlands)*.

Kühl, M., Lassen, C., & Jorgensen, B. (1994). Light penetration and light intensity in sandy marine sediments measured with irradiance and scalar irradiance fiber-optic microprobes. *Marine Ecology Progress Series*, *105*, 139-148. https://doi.org/10.3354/meps105139

Kwon, B.-O., Kim, H., Noh, J., Lee, S. Y., Nam, J., & Khim, J. S. (2020). Spatiotemporal variability in microphytobenthic primary production across bare intertidal flat, saltmarsh, and mangrove forest of Asia and Australia. *Marine Pollution Bulletin*, *151*, 110707. https://doi.org/10.1016/j.marpolbul.2019.110707

Lamontagne, M., Duran, R., & Valiela, I. (2003). Nitrous oxide sources and sinks in coastal aquifers and coupled estuarine receiving waters. *The Science of The Total Environment*, *309*(1-3), 139-149. https://doi.org/10.1016/S0048-9697(02)00614-9

Leote, C., & Epping, E. H. G. (2015). Sediment–water exchange of nutrients in the Marsdiep basin, western Wadden Sea: Phosphorus limitation induced by a controlled release? *Continental Shelf Research*, *92*, 44-58. https://doi.org/10.1016/j.csr.2014.11.007

Li, Hu, F., Bowman, D., & Shi, W. (2013). Nitrous oxide production in turfgrass systems: Effects of soil properties and grass clipping recycling. *Applied Soil Ecology*, *67*, 61-69. https://doi.org/10.1016/j.apsoil.2013.03.002

Longphuirt, S. N., Ragueneau, O., Chauvaud, L., Martin, S., Jean, F., Thouzeau, G., & Leynaert, A. (2009). Diurnal heterogeneity in silicic acid fluxes in shallow coastal sites: Causes and implications. *Estuarine, Coastal and Shelf Science*, *82*(3), 495-502. https://doi.org/10.1016/j.ecss.2009.02.014

MacIntyre, H. L., Geider, R. J., & Miller, D. C. (1996). Microphytobenthos: The Ecological Role of the «Secret Garden» of Unvegetated, Shallow-Water Marine Habitats. I. Distribution, Abundance and Primary Production. *Estuaries*, *19*(2), 186. https://doi.org/10.2307/1352224

Middelburg, J. J., Barranguet, C., Boschker, H. T. S., Herman, P. M. J., Moens, T., & Heip, C. H. R. (2000). The fate of intertidal microphytobenthos carbon: An in situ ^{13}C-labeling study. *Limnology and Oceanography*, *45*(6), 1224-1234. https://doi.org/10.4319/lo.2000.45.6.1224

Middelburg, J. J., Soetaert, K., Herman, P. M. J., & Heip, C. H. R. (1996). Denitrification in marine sediments: A model study. *Global Biogeochemical Cycles*, *10*(4), 661-673. https://doi.org/10.1029/96GB02562

Millero, F. J., & Poisson, A. (1981). International one-atmosphere equation of state of seawater. *Deep Sea Research Part A. Oceanographic Research Papers*, *28*(6), 625-629. https://doi.org/10.1016/0198-0149(81)90122-9

Musat, N., Werner, U., Knittel, K., Kolb, S., Dodenhof, T., Van Beusekom, J. E. E., De Beer, D., Dubilier, N., & Amann, R. (2006). Microbial community structure of sandy intertidal sediments in the North Sea, Sylt-Rømø Basin, Wadden Sea. *Systematic and Applied Microbiology*, *29*(4), 333-348. https://doi.org/10.1016/j.syapm.2005.12.006

Nizzoli, D., Carraro, E., Nigro, V., & Viaroli, P. (2010). Effect of organic enrichment and thermal regime on denitrification and dissimilatory nitrate reduction to ammonium (DNRA) in hypolimnetic sediments of two lowland lakes. *Water Research*, *44*(9), 2715-2724. https://doi.org/10.1016/j.watres.2010.02.002

Papaspyrou, S., Thessalou-Legaki, M., & Kristensen, E. (2004). Impact of Pestarella tyrrhena on benthic metabolism in sediment microcosms enriched with seagrass and macroalgal detritus. *Marine Ecology Progress Series*, *281*, 165-179. https://doi.org/10.3354/meps281165

Perkins, R., Underwood, G., Brotas, V., Snow, G., Jesus, B., & Ribeiro, L. (2001). Responses of microphytobenthos to light: Primary production and carbohydrate allocation over an emersion period. *Marine Ecology Progress Series*, *223*, 101-112. https://doi.org/10.3354/meps223101

Pivato, M., Carniello, L., Moro, I., & D'Odorico, P. (2019). On the feedback between water turbidity and microphytobenthos growth in shallow tidal environments. *Earth Surface Processes and Landforms*, *44*(5), 1192-1206. https://doi.org/10.1002/esp.4567

Rabouille, C., Denis, L., Dedieu, K., Stora, G., Lansard, B., & Grenz, C. (2003). Oxygen demand in coastal marine sediments: Comparing in situ microelectrodes and laboratory core incubations. *Journal of Experimental Marine Biology and Ecology*, *285-286*, 49-69. https://doi.org/10.1016/S0022-0981(02)00519-1

Redfield, A. C. (1958). The biological control of chemical factors in the environment. *American Scientist*, *46*(3), 205-221.

Redzuan, N. S., & Underwood, G. J. C. (2020). Movement of Microphytobenthos and Sediment Between Mudflats and Salt Marsh During Spring Tides. *Frontiers in Marine Science*, *7*, 496. https://doi.org/10.3389/fmars.2020.00496

Redzuan, N. S., & Underwood, G. J. C. (2021). The importance of weather and tides on the resuspension and deposition of microphytobenthos (MPB) on intertidal mudflats. *Estuarine, Coastal and Shelf Science*, *251*, 107190. https://doi.org/10.1016/j.ecss.2021.107190

Ribeiro, L., Brotas, V., Rincé, Y., & Jesus, B. (2013). Structure and diversity of intertidal benthic diatom assemblages in contrasting shores: A case study from the Tagus estuary[1]. *Journal of Phycology*, *49*(2), 258-270. https://doi.org/10.1111/jpy.12031

Rios-Yunes, D., Tiano, J. C., Van Oevelen, D., Van Dalen, J., & Soetaert, K. (2023). Annual biogeochemical cycling in intertidal sediments of a restored estuary reveals dependence of N, P, C and Si cycles to temperature and water column properties. *Estuarine, Coastal and Shelf Science*, *282*, 108227. https://doi.org/10.1016/j.ecss.2023.108227

Rodríguez-Ramírez, A., Villarías-Robles, J. J. R., Pérez-Asensio, J. N., & Celestino-Pérez, S. (2019). The Guadalquivir Estuary: Spits and Marshes. En J. A. Morales (Ed.), *The Spanish Coastal Systems* (pp. 517-541). Springer International Publishing. https://doi.org/10.1007/978-3-319-93169-2_22

Rosales Villa, A. R., Jickells, T. D., Sivyer, D. B., Parker, E. R., & Thamdrup, B. (2019). Benthic nitrogen cycling in the North Sea. *Continental Shelf Research*, *185*, 31-36. https://doi.org/10.1016/j.csr.2018.05.005

Ruiz, J., Macías, D., & Navarro, G. (2017). Natural forcings on a transformed territory overshoot thresholds of primary productivity in the Guadalquivir estuary. *Continental Shelf Research*, *148*, 199-207. https://doi.org/10.1016/j.csr.2017.09.002

Sansone, F. J., Graham, A. W., & Berelson, W. M. (2004). Methane along the western Mexican margin. *Limnology and Oceanography*, *49*(6), 2242-2255. https://doi.org/10.4319/lo.2004.49.6.2242

Smith, Mosier, A. R., Crutzen, P. J., & Winiwarter, W. (2012). The role of N $_2$ O derived from crop-based biofuels, and from agriculture in general, in Earth's climate. *Philosophical Transactions of the Royal Society B: Biological Sciences*, *367*(1593), 1169-1174. https://doi.org/10.1098/rstb.2011.0313

Soetaert, K., Middelburg, J. J., Heip, C., Meire, P., Van Damme, S., & Maris, T. (2006). Long-term change in dissolved inorganic nutrients in the heterotrophic Scheldt estuary (Belgium, The Netherlands). *Limnology and Oceanography*, *51*(1part2), 409-423. https://doi.org/10.4319/lo.2006.51.1_part_2.0409

Stocker, T. F. (2014). Climate Change 2013: The Physical Science Basis. Contribution of Working Group I to the Fifth Assessment Report of the Intergovernmental Panel on Climate Change. *Environmental Research Letters*, *9*(8), 13pp.

Ubertini, M., Lefebvre, S., Gangnery, A., Grangeré, K., Le Gendre, R., & Orvain, F. (2012). Spatial Variability of Benthic-Pelagic Coupling in an Estuary Ecosystem: Consequences for Microphytobenthos Resuspension Phenomenon. *PLoS ONE*, *7*(8), e44155. https://doi.org/10.1371/journal.pone.0044155

Underwood, G. J. C., & Kromkamp, J. (1999). Primary Production by Phytoplankton and Microphytobenthos in Estuaries. En *Advances in Ecological Research* (Vol. 29, pp. 93-153). Elsevier. https://doi.org/10.1016/S0065-2504(08)60192-0

Yvon-Durocher, G., Allen, A. P., Bastviken, D., Conrad, R., Gudasz, C., St-Pierre, A., Thanh-Duc, N., & Del Giorgio, P. A. (2014). Methane fluxes show consistent temperature dependence across microbial to ecosystem scales. *Nature*, *507*(7493), 488-491. https://doi.org/10.1038/nature13164

1.4. General conclusions:

1. The photosynthetic activity of microphytobenthos in the intertidal sediments of the Guadalquivir Estuary sustained a net autotrophic system for most of the year, with higher microalgae biomass in areas closer to the river mouth in Bonanza, contributing more significantly to the productivity of the estuary.

2. The intertidal sediments of Guadalquivir estuary acted as net sinks for both nitrate and ammonia, thus reducing the net export of dissolved inorganic nitrogen to the Gulf of Cádiz and highlighting the regulatory function of sediments in controlling nutrient dynamics in coastal assemblages.

3. The differential MPB activity along Guadalquivir estuary induced spatial and seasonal differences in the nitrogen demand of MPB and nutrient fluxes between Bonanza and Lebrija, reflecting a dynamic and heterogeneous control of the biogeochemical processes in the intertidal sediment.

4. In the sediments of Río San Pedro, prolonged temperature increases led to a significant rise in oxygen consumption, linked to enhanced organic matter degradation and microbial activity, indicating that heatwaves can intensify respiration and mineralization processes in shallow environments. However, prolonged exposure at high temperatures reduced the oxygen consumption rates, indicating a negative effect of persistent climate alterations.

5. Temperature rise affected nitrogen cycling in the intertidal sediments of Río San Pedro, favoring nitrification and ammonia assimilation at moderate temperatures, but promoting anaerobic processes such as denitrification and dissimilatory nitrate reduction to ammonium (DNRA) at higher temperatures.

6. Methane emissions from sediments to the water column increased exponentially with temperature, also increasing the abundance of thermotolerant methanogenic archaea and acetate-producing fermentative bacteria, suggesting that warming favors methanogenesis over methane oxidation.

7. Extreme temperatures associated with heatwaves caused both structural and functional shifts in the microbial communities of Río San Pedro sediments, with a decline in aerobic taxa such as Verrucomicrobiota or Mycococcota, and an increase in anaerobic and thermotolerant groups such as Firmicutes, Chloroflexi, and Methanosarciniales.

8. Windstorms in the Bay of Cádiz caused strong resuspension of surface sediments, leading to temporary increases in total suspended solids and chlorophyll-a concentrations in the water column, resulting in temporal alterations of the net production of the sediment.

9. Dissolved inorganic nutrient concentrations increased during the wind event, although not in the proportion found in the sediments, suggesting that biogeochemical processes in the water column played a role following sediment resuspension.

10. Satellite imagery revealed a heterogeneous response to the wind event in the Bay of Cádiz, being influenced by sediment characteristics, local hydrodynamics, and horizontal transport within the bay, resulting in stronger impacts observed in the northern and northwestern areas.

11. Windstorms acted as intense but short-lived disturbances capable of temporarily altering the system's state, with a relatively quick recovery. However, a large fraction of the resuspended particulate and dissolved organic and inorganic matter was exported to the sea during the windstorm. The increase in the frequency and/or intensity of such events could affect the annual outwelling rates to Gulf of Cadiz and therefore the coastal production and the long-term stability of such ecosystems.

1.4. Conclusiones generales:

1. La actividad fotosintética del microfitobentos en los sedimentos intermareales del estuario del Guadalquivir mantuvo un sistema netamente autotrófico durante la mayor parte del año, con mayor biomasa de microalgas en áreas cercanas a la desembocadura en Bonanza, contribuyendo de forma más significativa a la productividad del estuario.

2. Los sedimentos intermareales del estuario del Guadalquivir actuaron como sumideros netos tanto de nitrato como de amonio, reduciendo así la exportación neta de nitrógeno inorgánico disuelto al Golfo de Cádiz y destacando la función reguladora de los sedimentos en el control de la dinámica de nutrientes en los ensamblajes costeros.

3. La actividad diferencial del MPB a lo largo del estuario del Guadalquivir indujo diferencias espaciales y estacionales en la demanda de nitrógeno del MPB y en los flujos de nutrientes entre Bonanza y Lebrija, reflejando un control dinámico y heterogéneo de los procesos biogeoquímicos en el sedimento intermareal.

4. En los sedimentos del río San Pedro, los aumentos prolongados de temperatura condujeron a un aumento significativo del consumo de oxígeno, vinculado a una mayor degradación de materia orgánica y actividad microbiana, indicando que las olas de calor pueden intensificar los procesos de respiración y mineralización en ambientes someros. Sin embargo, la exposición prolongada a altas temperaturas redujo las tasas de consumo de oxígeno, lo que indica un efecto negativo de las alteraciones climáticas persistentes.

5. El aumento de temperatura afectó el ciclo del nitrógeno en los sedimentos intermareales del río San Pedro, favoreciendo la nitrificación y la asimilación de amonio a temperaturas moderadas, pero promoviendo procesos anaerobios como la desnitrificación y la reducción disimilatoria de nitrato a amonio (DNRA) a temperaturas más altas.

6. Las emisiones de metano desde los sedimentos hacia la columna de agua aumentaron de forma exponencial con la temperatura, incrementando también la abundancia de arqueas metanógenas termotolerantes y bacterias

fermentativas productoras de acetato, lo que sugiere que el calentamiento favorece la metanogénesis sobre la oxidación del metano.

7. Las temperaturas extremas asociadas a las olas de calor causaron cambios tanto estructurales como funcionales en las comunidades microbianas de los sedimentos del río San Pedro, con un declive de taxones aeróbicos como Verrucomicrobiota o Myxococcota, y un aumento de grupos anaerobios y termotolerantes como Firmicutes, Chloroflexi y Methanosarciniales.

8. Los temporales de viento en la Bahía de Cádiz provocaron una fuerte resuspensión de los sedimentos superficiales, llevando a aumentos temporales de sólidos totales en suspensión y de concentraciones de clorofila-a en la columna de agua, lo que resultó en alteraciones temporales de la producción neta del sedimento.

9. Las concentraciones de nutrientes inorgánicos disueltos aumentaron durante el evento de viento, aunque no en la proporción hallada en los sedimentos, lo que sugiere que procesos biogeoquímicos en la columna de agua jugaron un papel tras la resuspensión sedimentaria.

10. Las imágenes de satélite revelaron una respuesta heterogénea al evento de viento en la Bahía de Cádiz, influida por las características del sedimento, la hidrodinámica local y el transporte horizontal dentro de la bahía, resultando en impactos más fuertes observados en las zonas norte y noroeste.

11. Los temporales de viento actuaron como perturbaciones intensas, pero de corta duración capaces de alterar temporalmente el estado del sistema, con una recuperación relativamente rápida. Sin embargo, una gran parte de la materia particulada y orgánica e inorgánica disuelta resuspendida fue exportada al mar durante el temporal. El aumento en la frecuencia y/o intensidad de tales eventos podría afectar las tasas anuales de desembalse al Golfo de Cádiz y, por tanto, la producción costera y la estabilidad a largo plazo de dichos ecosistemas.